Functional Characterization of the DExH-Box Helicase DHX9

Teresa Lee

Department of Biochemistry
McGill University
Montréal, Québec, Canada

October 2016

A thesis submitted to McGill University in partial fulfillment
of the requirement of the degree of
Doctor of Philosophy

TABLE OF CONTENTS

LIST OF FIGURES

LIST OF TABLES

ABSTRACT

DHX9 is an NTP-dependent DExH-box helicase protein capable of unwinding both RNA and DNA duplexes. It is a multi-domain, multifunctional protein, with regulatory roles in DNA replication, transcription, translation, RNA processing and transport, microRNA processing, and maintenance of genomic stability. Our lab initially uncovered DHX9 as a synthetic lethal hit from an shRNA screen for modifiers of sensitivity to ABT-737 (an inhibitor of BCL-2 family anti-apoptotic factors). Using *Arf*$^{-/-}$Eμ-*Myc*/Bcl-2 mouse lymphoma cells, which overexpress MYC and BCL-2 and are resistant to ABT-737, it was demonstrated that DHX9 suppression overcame ABT-737 resistance by triggering a p53-dependent apoptotic response. The aim of my research was to further characterize the relationship between DHX9 and p53, as well as to investigate the therapeutic potential of targeting DHX9.

To gain further insight into the mechanism by which suppression of DHX9 activates a p53 response, we knocked down DHX9 via shRNAs in primary human diploid fibroblasts whereupon a premature senescence response was observed, characterized by morphological defects, elevated senescence-associated β-galactosidase levels, and cell cycle arrest. This effect was p53-dependent and was accompanied by a gene expression signature closely resembling that of replicative (telomere-dependent) senescent cells. The DHX9-mediated senescence response was attributed to inhibition of DNA replication, which activated a p53 stress response. Our results demonstrated an important role for DHX9 in DNA replication and normal cell cycle progression.

Further studies were carried out to assess the consequences of DHX9 suppression in tumor cells. We extended previous results in the *Arf*$^{-/-}$Eμ-*Myc*/Bcl-2 lymphomas by suppressing DHX9 on its own in various human cancer cell lines, whereupon we documented increased cell death in the majority of cancer cells examined. This was recapitulated in murine *Tsc2*$^{+/-}$Eμ-*Myc* lymphomas, both *ex vivo* and *in vivo*. We next assessed the effect of systemic DHX9 suppression at the organismal level by generating a doxycycline-inducible shDHX9 transgenic mouse model. Despite having detrimental effects on the cellular fitness of tumor cells, sustained and prolonged suppression of DHX9 did not result in any deleterious effects in adult mice. This indicates a

robust tolerance for systemic DHX9 suppression *in vivo* and supports the targeting of DHX9 as an effective and specific chemotherapeutic approach**.**

Having shown that the senescence phenotype induced by loss of DHX9 is dependent on a functional p53 pathway, it was also observed that some human cancer cell lines which were susceptible to DHX9 suppression were deficient in p53. In the final chapter of our work, we investigated the consequences of DHX9 inhibition in cells lacking functional p53. Loss of DHX9 resulted in either increased cell death or cell cycle arrest in p53-deficient mouse lymphomas, HCT116 human colon cancer cells, and mouse embryonic fibroblasts. A subset of classic p53 targets in the p53-deficient cells was activated upon DHX9 knockdown. This implies an alternative, p53-independent mechanism of DHX9-mediated activation of cell death and cell cycle arrest in p53-deficient cells and supports the feasibility of targeting DHX9 in p53-deficient tumors.

RESUMÉ

La DHX9 est une protéine hélicase à boîte DExH qui utilise le NTP pour dérouler à la fois les duplex d'ARN et d'ADN, ainsi que les structures de polynucléotides aberrantes. C'est une protéine multifonctionnelle et multidomaine jouant un rôle de régulateur dans la réplication de l'ADN, la transcription, la traduction, le traitement et le transport de l'ARN, le traitement des micro-ARN et le maintien de la stabilité génomique. Notre laboratoire a initialement découvert la DHX9 comme une cible létale synthétique à partir d'un criblage d'une librairie de shRNA sur les modificateurs de la sensibilité à l'ABT-737 (un inhibiteur de la famille BCL-2 des facteurs anti-apoptotiques). Chez les cellules de lymphome de souris *Arf*$^{-/-}$Eμ-*Myc*/Bcl-2, surexprimant MYC et BCL-2 et résistantes à l'ABT-737, il a été démontré que la suppression de DHX9 renverse la résistance à l'ABT-737 en déclenchant une réponse apoptotique dépendante de p53.
L'objectif de mes recherches était de mieux caractériser la relation entre DHX9 et p53 ainsi qu'étudier le potentiel thérapeutique du ciblage de DHX9.

À cette fin, nous avons réduit l'expression de DHX9 avec des shRNAs dans des fibroblastes diploïdes humains primaires, après quoi une réponse de sénescence prématurée a été observée, caractérisée par des changements morphologiques, une coloration positive pour la sénescence-associée à la β-galactosidase, et l'arrêt du cycle cellulaire. Cet effet était dépendant de la p53 et s'accompagnait d'une signature de l'expression génique ressemblant à celle de cellules sénescentes réplicatives (télomère-dépendantes). La sénescence induite par DHX9 était attribuée à l'inhibition de la réplication de l'ADN, ce qui a activé une réaction de stress de p53. Nos résultats ont démontré un rôle important de DHX9 dans la réplication de l'ADN et la progression du cycle cellulaire normal.

D'autres études ont été réalisées afin d'évaluer les conséquences de la suppression de DHX9 dans les cellules tumorales. Nous avons étendu les résultats antérieurs dans les lymphomes *Arf*$^{-/-}$Eμ-*Myc*/Bcl-2 en supprimant DHX9 seulement dans diverses lignées de cellules cancéreuses humaines et avons observé un accroissement de la mortalité cellulaire dans la majorité des cellules cancéreuses examinées. Ce résultat a été récapitulé dans les lymphomes murins *Tsc2*$^{+/-}$Eμ-*Myc*, à la fois *ex vivo* et *in vivo*. Nous avons ensuite évalué l'effet de la

suppression systémique de DHX9 au niveau de l'organisme en générant un modèle de souris transgénique où la suppression de DHX9 (avec un shRNA) est induite grâce à la doxycycline. Malgré les effets néfastes observés sur la survie des cellules tumorales, une suppression de DHX9 soutenue et prolongée n'a pas d'effet délétère chez les souris adultes. Ceci indique une tolérance robuste à la suppression systémique de cette protéine *in vivo* et appuie le ciblage de la DHX9 comme pouvant être une approche chimiothérapique efficace et spécifique.

Nous avons observé que certaines lignées humaines de cellules cancéreuses qui étaient sensibles à la suppression de DHX9 étaient déficientes en termes d'expression de p53. Dans le dernier chapitre de notre travail, nous avons étudié les conséquences de l'inhibition de DHX9 dans des cellules dépourvues de p53 fonctionnelle. La perte de DHX9 a entraîné une augmentation de la mortalité cellulaire ou de l'arrêt du cycle cellulaire dans trois lignées cellulaires déficientes en p53: les lymphomes de souris, les cellules de cancer du côlon humain HCT116, et les fibroblastes embryonnaires de souris. Un sous-ensemble de cibles classiques de p53 dans les cellules déficientes en p53 était activé à cause de la suppression de DHX9, malgré l'absence de p53 fonctionnelle. Ceci implique que la suppression de DHX9 peut induire un mécanisme alternatif indépendant de p53 pour causer la mort cellulaire et l'arrêt du cycle cellulaire dans des cellules déficientes en p53, et appuie la faisabilité de cibler DHX9 dans les cellules tumorales déficientes en p53.

PREFACE

This is a manuscript-based thesis which consists of two published research articles (presented in Chapters 2 and 3) and one research article under review (presented in Chapter 4), for which I am first author. Portions of Chapter 1 are adapted from a published review article for which I am first author.

Chapter 1:

Lee T and Pelletier J. (2016). The Biology of DHX9 and its Potential as a Therapeutic Target. *Oncotarget* **7(27)**:42716-42739.

Chapter 2:

Lee T, Di Paola D, Malina A, Mills JR, Kreps A, Grosse F, Tang H, Zannis-Hadjopoulos M, Larsson O, and Pelletier J. (2014). Suppression of the DHX9 Helicase Induces Premature Senescence in Human Diploid Fibroblasts in a p53-Dependent Manner. *J Biol Chem* **289(33):**22798-22814.

Chapter 3:

Lee T, Paquet M, Larsson O, and Pelletier J. (2016). Tumor Cell Survival Dependence on the DHX9 DExH-Box Helicase. *Oncogene* **35(39)**:5093-5105.

Chapter 4:

Lee T and Pelletier J. (2016). Dependence of p53-deficient cells on the DHX9 DExH-box helicase. *Oncotarget.* Under revision.

CONTRIBUTION OF AUTHORS

Chapter 2:

I performed all experiments and data analyses under the supervision of Dr. Jerry Pelletier, with the following exceptions: Domenic Di Paola and Amina Kreps performed the genomic and nascent DNA isolation and quantitation and ChIP assays under the guidance of Dr. Maria Zannis-Hadjopoulos. Drs. Frank Grosse and Hengli Tang contributed the wildtype and mutant DHX9 cDNA constructs to the study. Abba Malina and John Mills contributed to the conception and design of some of the experiments. Microarrays were performed at Genome Quebec and Dr. Ola Larsson analyzed the gene expression data.

Chapter 3:

I performed all experiments and data analyses under the supervision of Dr. Jerry Pelletier, with the following exceptions: Francis Robert performed the tail-vein injections of lymphoma cells into mice. The DHX9 shRNA mice were generated by Mirimus (Cold Spring Harbor, NY, USA). Dr. Marilène Paquet provided the histopathological analysis of tissue sections. Microarrays were performed at Genome Quebec and Dr. Ola Larsson analyzed the gene expression data.

Chapter 4:

I performed all experiments and data analyses under the supervision of Dr. Jerry Pelletier.

ORIGINAL CONTRIBUTION TO KNOWLEDGE

Chapter 2: Suppression of the DHX9 Helicase Induces Premature Senescence in Human Diploid Fibroblasts in a p53-Dependent Manner

- Discovered that DHX9 suppression in primary human diploid fibroblasts results in premature senescence, as evidenced by morphological defects, increased senescence-associated β-galactosidase staining, cell cycle arrest, and a gene expression signature resembling that of replicative (telomere-based) senescence.
- Showed that premature senescence resulting from DHX9 knockdown activates p53 signaling and that functional p53 is essential for this process.
- DHX9 is associated with origins of replication and DNA replication is inhibited upon DHX9 knockdown.
- Proposed a model where under normal cellular conditions, DHX9 facilitates DNA replication at origins of replication and loss of DHX9 leads to inhibition of DNA replication. This activates a p53 stress response, leading to cell cycle arrest and senescence.
- Demonstrated an important role for DHX9 in DNA replication and normal cell cycle progression using an *ex vivo* biological system, supporting previous *in vitro* studies implicating DHX9 in replication.

Chapter 3: Tumor Cell Survival Dependence on the DHX9 DExH-Box Helicase

- DHX9 suppression reduces the fitness of several human cancer cell lines derived from multiple myeloma, osteosarcoma, breast, lung and cervical cancers.
- DHX9 suppression is lethal in murine *Tsc2*$^{+/-}$Eμ-*Myc* lymphomas both *ex vivo* and *in vivo* and extends the survival of mice harboring these tumors.
- Generated a doxycycline-inducible shDHX9 transgenic mouse model and used it to show that systemic long-term (6 months) DHX9 suppression does not result in any deleterious effects in adult mice.
- These results provide support for the targeting of DHX9 as an effective chemotherapeutic

approach.

Chapter 4: Dependence of p53-deficient cells on the DHX9 DExH-box helicase

- DHX9 suppression results in increased cell death in p53-null mouse lymphomas and HCT116 cells, and cell cycle arrest in p53-null mouse embryonic fibroblasts.
- A subset of known p53 targets are activated upon DHX9 suppression in the p53-null mouse lymphomas and HCT116 cells despite the absence of functional p53.
- The study indicates the existence of a p53-independent pathway of DHX9-mediated cell death and cell cycle arrest in p53-deficient cells, and opens up the possibility of targeting DHX9 as a therapeutic approach in p53-deficient settings.

ACKNOWLEDGEMENTS

I would like to thank my supervisor, Dr. Jerry Pelletier, for giving me the opportunity to work in his research group. Thank you for giving me a chance. I wish to acknowledge members of the Pelletier lab, past and present, particularly Drs. John Mills and Abba Malina for starting the DHX9 project on which my own research was based, and for their collaboration on this project, Dr. Francis Robert for performing tail-vein injections in experiments featured in Chapter 3, Patrick Sénéchal for his role in procuring needed reagents, and Sophia Moraitis for tips and glassware. I extend my appreciation to my RAC members, Drs. Michel Tremblay, Jose Teodoro, and Uri Saragovi, for their time and scientific advice. I am grateful to my collaborators, Domenic di Paola of Dr. Maria Zannis-Hadjopoulos' lab (McGill University), Dr. Ola Larsson of the Karolinska Institute, and Dr. Marilène Paquette of the Université de Montréal for their invaluable contributions to my research. In addition, I would like to thank Dr. Scott Lowe's research group (Memorial Sloan Kettering Cancer Center) for the sharing of shRNA reagents and their collaboration with respect to technology development for the shRNA mouse model used in this thesis.

My research was partially funded by the Maysie MacSporran graduate studentship and fellowships from the CIHR-sponsored Chemical Biology and Systems Biology Training Programs.

On a more personal note, I would like to acknowledge the various hosts who - along with their featured acts - kept me company during those countless hours in the lab. Quite a few have become favorites, of whom I will always be a fan. To all my heroes out there, thank you for inspiring me to always fight on, no matter what the odds.

LIST OF ABBREVIATIONS

Ago	Argonaute protein
AMP	Adenine monophosphate
ARF	Alternate Reading Frame of CDKN2A tumor suppressor
ATP	Adenosine triphosphate
BAK	BCL-2 homologous antagonist killer
BAX	BCL-2-associated X protein
BCL	B-cell lymphoma, or BCL-2 like
BCM	B-cell media
bp	Basepair
BID	BH3-interacting domain death agonist
BIM	BCL-2 interacting mediator of cell death
BLM	Bloom syndrome helicase
BRCA	Breast cancer susceptibility protein
BSA	Bovine serum albumin
CBP	CREB-binding protein Cap-binding protein
CDC	Cell division cycle
CDK	Cyclin-dependent kinase
CREB	cAMP response element-binding protein
cDNA	Complementary DNA
ChIP	Chromatin Immunoprecipitation
CHK	Checkpoint kinase
CKI	Cyclin-dependent kinase inhibitor
Col1A1	Collagen type 1 alpha 1

DExD (DDX)	Aspartate-glutamine-x-aspartate-box helicase
DExH (DHX)	Aspartate-glutamine-x-histidine-box helicase
DMEM	Dulbecco's Modified Essential Media
DMSO	Dimethyl sulfoxide
DNA	Deoxyribonucleic acid
DNA-PK	DNA-dependent protein kinase
dNTP	Deoxyribonucleotide triphosphate
DOX	Doxycycline
dsRBD	double-stranded RNA-binding domain
DTT	Dithiothreitol
ECL	Enhanced chemiluminescence
eIF	Eukaryotic translation initiation factor
eEF	Eukaryotic translation elongation factor
EGFR	Epidermal growth factor receptor
FACS	Fluorescence activated cell sorting
FBS	Fetal bovine serum
FDR	False discovery rate
FLuc	Firefly luciferase
GAPDH	Glyceraldehyde 3-phosphate dehydrogenase
GFP	Green fluorescent protein
GTP	Guanosine triphosphate
HCl	Hydrogen chloride
HCV	Hepatitis C virus
HIV	Human immunodeficiency virus

hnRNP	Heterogeneous nuclear ribonucleoprotein
HTLV	Human T-lymphotropic virus
INK4A	Inhibitor of Kinase 4
IRES	Internal ribosome entry site
MCL-1	Myeloid cell leukemia-1
MCM	Mini-chromosome maintenance
MDM	Mouse double minute protein
MEF	Mouse embryonic fibroblast
$MgCl_2$	Magnesium chloride
miRNA	microRNA
MLE	Maleless
MOMP	Mitochondrial outer membrane permeabilization
mRNA	messenger RNA
MSCV	Murine Stem Cell Virus
mTOR	Mammalian target of rapamycin
MTAD	Minimal transactivation domain
MYC	Myelocytomatosis viral oncogene
NES	Nuclear export signal
NHEJ	Non-homologous end joining
NLS	Nuclear localization signal
nt	Nucleotide
NTP	Nucleotide triphosphate
OB-fold	Oligonucleotide/oligosaccharide-binding fold
ORC	Origin recognition complex

p53	Tumor protein 53
PAGE	Polyacrylamide gel electrophoresis
PBS	Phosphate buffered saline
PCNA	Proliferating cell nuclear antigen
PCR	Polymerase Chain Reaction
PI	Propidium iodide
PI3K	Phosphoinositide 3 Kinase
PML	Promyelocytic leukemia
PolII	RNA polymerase II
Pre-RC	Pre-replicative complex
Pre-IC	Pre-initiation complex
PTEN	Phosphatase and tensin homolog
PUMA	p53 upregulated modulator of apoptosis
PVDF	Polyvinylidene fluoride
Ras	Rat sarcoma
RB1	Retinoblastoma protein
RIPA	Radio immunoprecipitation assay
RISC	RNA-induced silencing complex
RMA	Robust multichip averaging
RLuc	Renilla luciferase
RNA	Ribonucleic acid
RNAi	RNA interference
rRNA	Ribosomal RNA
RT	Reverse transcriptase

rtTA	Reverse tetracycline-controlled transactivator
RVM	Random variance model
SA-β-gal	Senescence-associated β-galactosidase
SD	Standard deviation
SDS	Sodium dodecyl sulfate
SEM	Standard error of the mean
shRNA	Short-hairpin RNA
TSC	Tuberous sclerosis complex
TUNEL	Terminal deoxynucloetidyl transferase dUTP nick end labeling
UTR	Untranslated region
VEGF	Vascular endothelial growth factor
WRN	Werner syndrome ATP-dependent helicase
WT	Wildtype

CHAPTER 1: GENERAL INTRODUCTION

Portions adapted from:

Lee T and Pelletier J. (2016). The Biology of DHX9 and its Potential as a Therapeutic Target. *Oncotarget* **7(27)**:42716-42739.

1.1 Introduction to DHX9 and DExD/H-box helicases

DHX9 (also known as Nuclear DNA Helicase II (NDH II) and RNA Helicase A (RHA)) is an NTP-dependent helicase protein capable of unwinding both RNA and DNA[1], as well as aberrant polynucleotide structures[2]. It is a member of the DExH-box family of helicases, so-named for the conserved Asp-Glu-Ile-His (DEIH) sequence in its helicase core domain, and is part of the larger superfamily (SF) 2 category of helicases, which comprise both DExH and DExD helicases. DHX9 is a multi-domain, multi-functional protein, with regulatory roles in DNA replication, transcription, translation, RNA processing and transport, microRNA processing, and maintenance of genomic stability. Homologues have been characterized in human, bovine, mouse, *Drosophila*, *C. elegans*, and *Arabidopsis*, although the majority of the research has focused on human DHX9. Many of the biological processes in which DHX9 participates are deregulated during oncogenesis, or are hijacked by viruses to promote their own replication. A wealth of recent studies have implicated DHX9 in human diseases such as various cancers and viral infections, and there is evidence supporting the targeting of DHX9 in disease intervention. This chapter will provide an overview of the structural, biochemical and biological properties of DHX9 as well as its implications in disease.

Helicases are enzymes which catalyze the energy-dependent remodeling of nucleic acids. They utilize the free energy of binding and hydrolysis of nucleotide triphosphates to unwind nucleic acid duplexes or dissociate ribonucleoprotein complexes[3, 4]. Helicases are categorized into six superfamilies (SF1 - SF6) according to their amino acid sequence and structure[3, 5]. SF1 and SF2 helicases are structurally similar, consisting of two globular RecA-like domains in their core helicase region, each comprised of 5 β-strands surrounded by 5 α-helices, and act as monomers or dimers. SF3–SF6 family members contain only one RecA-like domain and form hexameric rings[3, 5]. Members of the largest superfamily, SF2, contain a signature helicase domain consisting of 7-9 evolutionarily conserved motifs, and are further subdivided into 2 main subfamilies based on the consensus sequence in motif II, the major site of NTP-binding and hydrolysis: the DExD-box (DDX) family, which contains the conserved sequence Asp-Glu-x-Asp (where x is any amino acid), and the DExH-box (DHX) family, which is defined by the sequence Asp-Glu-x-His[6]. The DExD/H box interacts with the β and γ phosphates of the NTP

via Mg^{2+} (Figure 1.1A). Structural and biochemical evidence suggests that in addition to motif II, motifs I, VI, and the Q-motif also participate in NTP-binding and hydrolysis. Motif III is responsible for coupling NTP hydrolysis to nucleic acid unwinding, and motifs Ia, Ib, IV, and V are involved in nucleic acid binding (Figure 1.1A)[7]. Despite their overall structural similarities, DDX and DHX family members exhibit significant differences in key residues within the conserved motifs. DHX helicases are also distinct from DDX members in that the former can hydrolyze different NTPs whereas the latter is generally specific for ATP. This is attributed to the Q-motif, which is present in DDX but not DHX helicases, and makes contact with the adenine base[6-8]. The helicase motifs are organized into two RecA-like domains and NTP-binding occurs at the cleft between the two domains[3].

Helicases play a role in a wide variety of cellular processes. Different family members possess the ability to unwind duplexes of DNA or RNA, as well as heteroduplexes and more complex polynucleotide structures (e.g. triple-stranded DNA). Other helicases may act as RNA clamps or chaperones to aid in RNA folding. These functions have made them important players in nucleic acid unwinding and remodeling during replication, transcription, translation, DNA repair, RNA splicing and editing, ribosome biogenesis, RNA transport, and RNA decay[7, 8]. They have been implicated in normal development and the cellular antiviral response, and helicase defects have been associated with genetic disorders and cancers[9-15].

1.2 Biochemical and structural characterization of DHX9

1.2.1 Discovery of DHX9

Mammalian DHX9 was first purified from the nuclear fraction of calf thymus and designated Nuclear DNA Helicase II (NDHII)[16]. The human homolog, known as RNA helicase A (RHA), was isolated shortly afterwards from nuclear extracts of HeLa cells[17]. Initial helicase assays demonstrated double-stranded DNA unwinding activity in bovine DHX9 and RNA unwinding activity with the human orthologue; however, subsequent studies showed that DHX9 from both species could unwind both DNA and RNA in an NTP-dependent manner[1]. cDNA clones for bovine and human DHX9 were obtained by immunoscreening cDNA libraries, and molecular cloning revealed that they were homologous to the *Drosophila* melanogaster protein Maleless (MLE)[18, 19]. MLE was first discovered in *Drosophila* as a gene which when mutated caused

lethality in male zygotes, and was found to play a role in X-chromosome dosage compensation in males[20, 21]. Subsequent work characterized DHX9 homologs in mouse[22], *C. elegans*[23], and *Arabidopsis*[24].

1.2.2 DHX9 functional domains and structure

The human DHX9 gene maps to the prostate cancer susceptibility locus on chromosome 1q25, with a pseudogene, DHX9P, mapping to chromosome 13q22[25]. The active gene is comprised of 29 exons and encodes a 1270 amino acid, 140-kDa protein[26]. In the mouse, DHX9 maps to chromosome 1[22]. In common with other DHX family members, sequence analysis revealed that DHX9 contains a helicase core domain consisting of 8 motifs (Figure 1.1B). As with other SF2 helicases, the core region is subdivided into two RecA-like domains, with motifs I-III residing in domain 1 and motifs IV-VI in domain 2. In addition to the helicase core domain (which spans amino acid (aa) residues 380 to 830 in humans), DHX9 contains 2 double stranded RNA-binding domains (dsRBDs) at its N-terminus[26]. The minimal transactivation domain (MTAD), the site of RNA polymerase II (PolII) interaction (see ***1.4.2 Transcriptional regulation***), is situated between dsRBDII and motif I of the helicase core domain. A helicase-associated domain 2 (HA2) is present adjacent to the C-terminal end of the helicase core domain[27]. At the C-terminus of DHX9 lies an oligonucleotide/oligosaccharide-binding fold (OB-fold)[28], overlapping nuclear localization/export signals[29], and a glycine-rich RGG-box capable of binding single-stranded nucleic acids[26] (Figures 1.1B and 1.2).

Sequence alignment showed a high degree of homology amongst DHX9 from various species. Human DHX9 exhibits 93% identity to the bovine homolog, 90% identity to the murine homolog, and 50%, 42%, and 27% identity to the *D. melanogaster*, *C. elegans*, and *Arabidopsis* homologs respectively (Figure 1.2). The helicase core region is highly conserved amongst all species, whereas the N- and C-terminal regions exhibit more variation. Notably, the RGG-box at the C-terminus of murine DHX9 is significantly more extended than that of DHX9 in other species[30] (Figure 1.2).

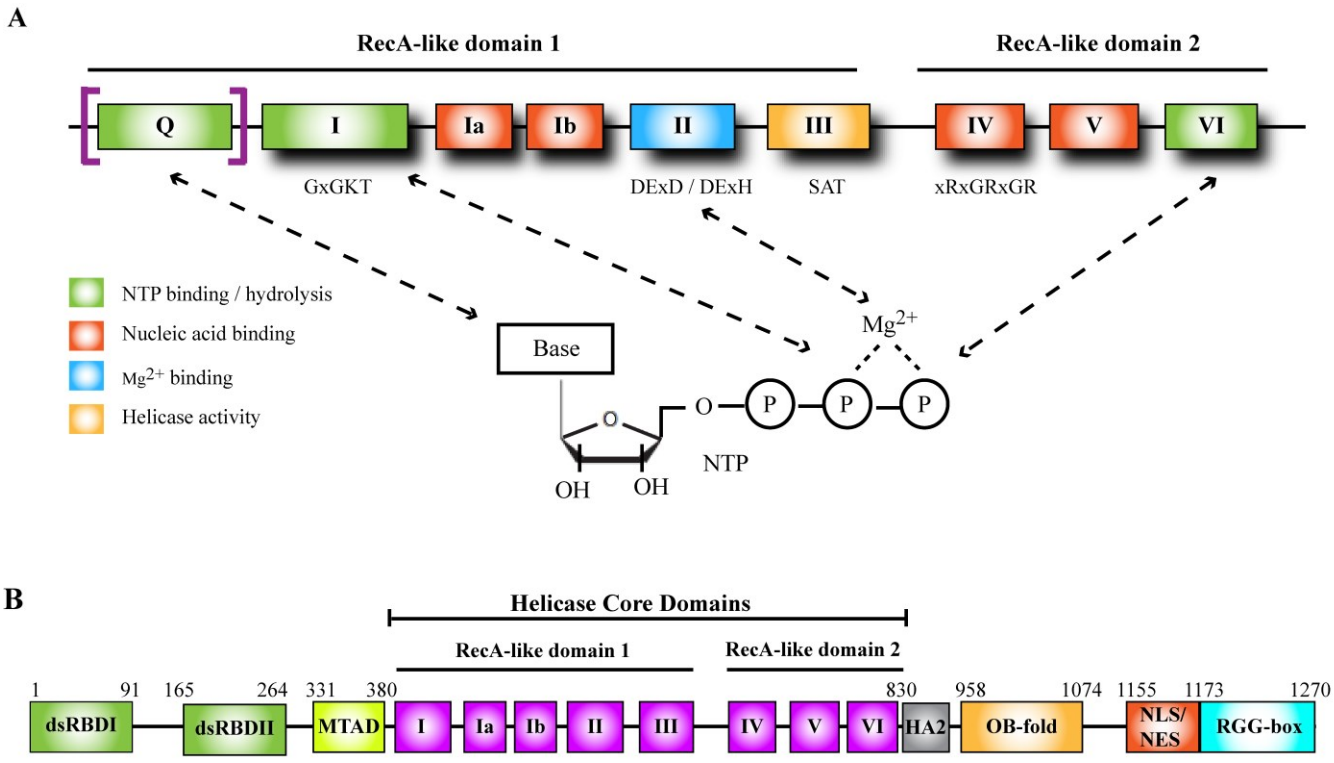

Figure 1.1 Helicase domain of DExD/H-box helicases and functional domains in DHX9.

(A) Conserved sequence motifs in the helicase core domain of DDX and DHX helicases. Consensus sequences are shown below some of the motifs. "x" represents any amino acid. The Q-motif is present in DDX but not DHX box helicases (including DHX9) and confers specificity for ATP binding. (**B**) Schematic representation of DHX9 functional domains. Numbers indicate amino acid positions in human DHX9. dsRBD, double-stranded RNA binding domain; MTAD, minimal transactivation domain; HA2, helicase-associated domain 2; OB-fold, oligonucleotide/oligosaccharide-binding fold; NLS, nuclear localization signal; NES, nuclear export signal.

Figure 1.2 Conservation of DHX9 across various species. Figure legend on following page.

Figure 1.2 Conservation of DHX9 across various species

Multiple sequence alignment of DHX9 homologs from human (*H. sapiens*) (NCBI accession # NP_001348), bovine (*B. taurus*) (NP_776461), mouse (*M. musculus*) (NP_031868), *Drosophila* (*D. melanogaster*) (NP_476641), *C. elegans* (NP_495890), and *Arabidopsis* (*A. thaliana*) (NP_850154). Red text indicates residues that are identical in all species. Blue text indicates residues with high similarity amongst species. The sequence alignment was generated using T-Coffee and visualized with BoxShade.

The structure of DHX9 has been partially solved. X-ray crystallography was used to determine the structure of domain 1 of human DHX9's helicase core in the presence of ADP and Mn^{2+}. This region spans residues 325 to 563 and includes motifs I to III as well as the 90 amino-acid region immediately upstream of motif I, the first 30 residues of which form part of the MTAD[31]. Motifs I-III form a RecA-like α/β core consisting of 5 parallel β-strands alternating with 5 α-helices, a structure which is conserved amongst DExD/H helicases (Figure 1.3A). The conserved motifs are in close proximity to each other, allowing them to cooperatively form nucleotide and nucleic acid binding sites. Binding to the NTP is accomplished via stacking interactions between the base of the nucleotide and an arginine residue (R456 in human DHX9) in motif Ia, and interactions between the phosphates and motif I. The aspartic and glutamic acid residues (D511 and E512) of the DEIH-box bind to the divalent cation, which serves to further coordinate the NTP (Figure 1.3B). The conserved residues S543-A544-T545 in motif III connects motifs I and II. The structural data shows that the Q-motif, which confers nucleotide specificity (to ATP) in DExD helicases, is not present in DHX9 and that DHX9 lacks base-selective contacts, thereby enabling it to utilize all four NTPS (ATP, GTP, CTP, and UTP) for its energy requirements. The region immediately preceding motifs I-III consists of 3 α-helices arranged perpendicular to each other on the surface of the α/β core, while the MTAD region consists of 2 short β-strands which lie in a hydrophobic groove on the surface of the helicase core (Figure 1.3A)[31].

The structure of the two dsRBD domains has also been elucidated. Both dsRBDI and dsRBDII are arranged into a core α–β–β–β–α fold, with the two α-helices lying on one surface of the three-stranded antiparallel β-sheets, and both domains were able to co-crystallize with dsRNA (Figure 1.3C and 1.3D). Interaction with dsRNA is mediated primarily by surface-exposed residues which tend to be highly conserved amongst dsRBDs of various proteins[32]. Despite the structural similarities, dsRBDI and dsRBDII only share 21% sequence similarity, a fact that may confer selectivity in terms of unique RNA or protein interactions. The structures of dsRBDI and dsRBDII in murine DHX9 have been determined by NMR spectroscopy and shown to be very similar to their human counterparts[33, 34].

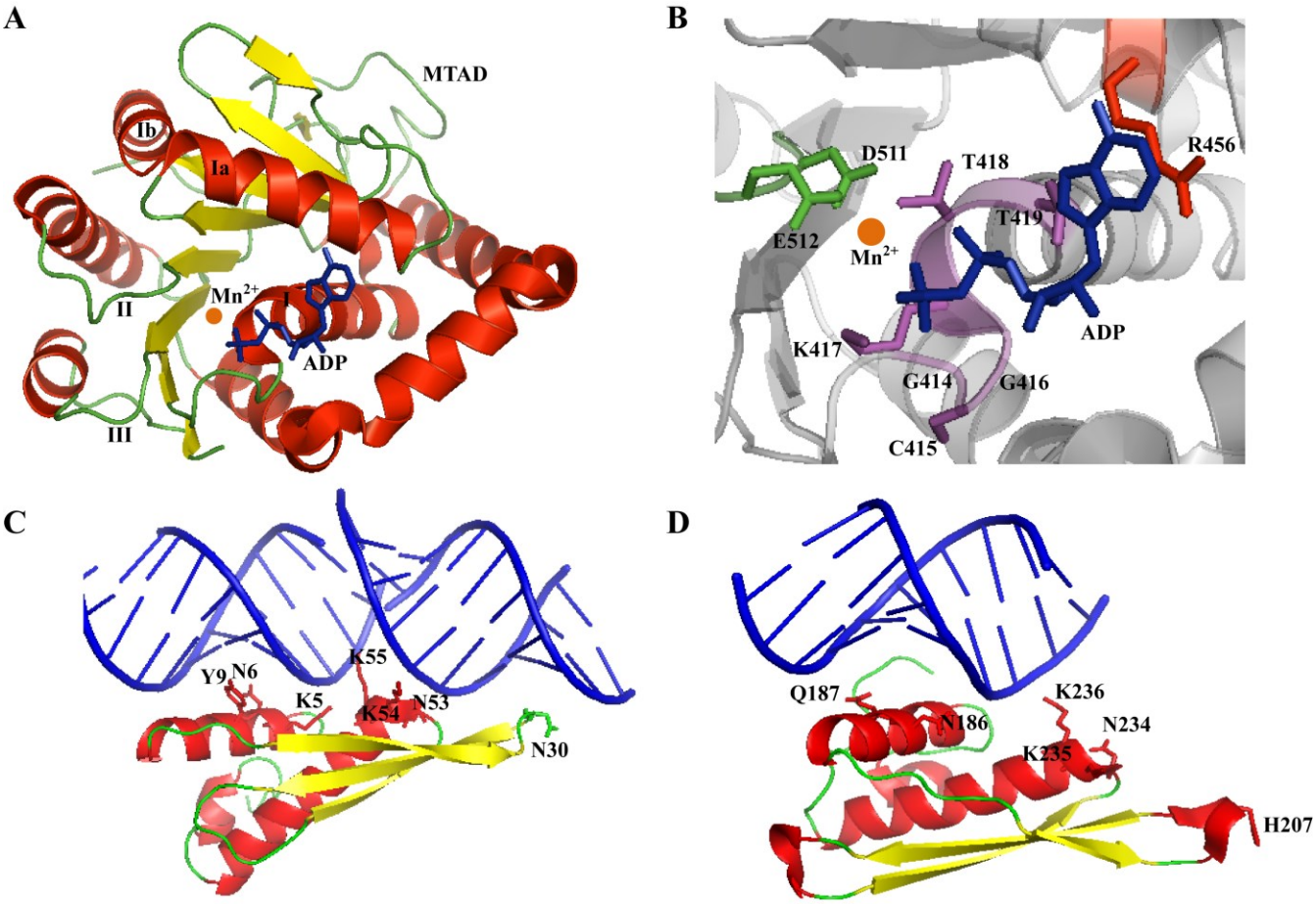

Figure 1.3 Structure of DHX9.

(A) Structure of motifs I-III of the helicase core domain of human DHX9, in complex with ADP and Mn^{2+}. α-helices are shown in red, β-strands in yellow, loops in green and the ADP in blue. Individual motifs are labeled. Structure is derived from Ref. [31]. **(B)** Key residues from (A) that are involved in NTP binding and hydrolysis. Residues D511 and E512 (motif II; green) coordinate binding to the Mn^{2+}. The ADP (blue) is bound by residues R456 (motif Ia; red) and G414 - T419 (motif I; purple). (**C**) and **(D)** Structure of **(C)** dsRBDI and **(D)** dsRBDII from human DHX9. Amino acid residues involved in dsRNA binding are labeled. α-helices are shown in red, β-strands in yellow, loops in green and the dsRNA in blue. Structures of dsRBDI and dsRBDII are derived from Ref. [32]. All structures were generated using PyMOL.

1.2.3 In vitro characterization of DHX9

In vitro studies using human, bovine, and *Drosophila* DHX9 demonstrated that all three homologs are able to bind both DNA and RNA[1, 17, 35]. DHX9 unwinds double-stranded (ds) DNA and RNA, as well as DNA/RNA hybrids, with RNA-containing duplexes being unwound more efficiently than dsDNA[36]. It exhibits a preference for substrates with a short single-stranded non-complementary 3' tail – a feature which is commonly found at replication forks (Figure 1.4). DHX9 translocates in the 3' to 5' direction and is able to utilize all dNTPs and rNTPs for its unwinding activity, with similar K_M values, in concordance with the lack of NTP selectivity (due to the absent Q-motif) demonstrated by structural data[1, 17, 31, 35, 37]. *In vitro* experiments have shown that human DHX9 also unwinds DNA or RNA forks composed of either partially complementary DNA duplexes or DNA/RNA hybrids respectively[38] (Figure 1.4). Related to fork assembly are DNA displacement loops (D-loops), which are formed when single-stranded DNA "invades" a complementary duplex, displacing one strand while forming Watson-Crick base pairs with the complementary strand, and which are found during initiation of homologous recombination[39-41]. Similarly, RNA displacement loops (R-loops) are created when single-stranded RNA invades a DNA duplex, an event that can impede both replication and transcription[42-45]. DHX9 unwinds D- and R-loops approximately 5-7-fold more efficiently than corresponding DNA and RNA forks[38]. DNA and RNA-based G-quadruplexes containing 3' single-stranded tails are also substrates for DHX9 activity (Figure 1.4). Under similar conditions, DHX9 unwinds RNA G-quadruplexes most efficiently, followed by R-loops, DNA G-quadruplexes, D-loops, RNA forks, and DNA forks, in descending order of helicase activity[38]. Another non-canonical structure is triplex DNA, which is composed of three DNA strands with the third strand bound to the duplex via Hoogsteen base pairing[46-48] (Figure 1.4). DHX9 is able to resolve triplex DNA structures, displacing the third strand in a 3' to 5' polarity, and displaying preference for triplexes having a 3' single-stranded overhang on the third strand[2]. DHX9 has far greater helicase activity when presented with this substrate compared to blunt triplexes, triplexes with 5'-overhangs, duplexes (either with blunt ends or overhangs), and forked duplexes[2]. In sum, these data demonstrate that irrespective of the substrate, efficient DHX9 helicase activity requires a 3' single-stranded tail, which may serve as an anchor for enzyme binding. In terms of substrate, it appears that DHX9 is a structure-specific helicase, with

a higher propensity for unwinding RNA-containing substrates, and with a preference for more complex, multi-stranded nucleic acid structures.

The biochemical properties of DHX9 are similar to those of SV40 large T-antigen, a viral DNA/RNA helicase with a 3' to 5' polarity and low selectivity for dNTPs/rNTPs[49]. DHX9 shares many similarities with the RecQ helicases WRN and BLM, which play important roles in the maintenance of genomic stability. WRN and BLM are structure-specific helicases that unwind triplex DNA structures[50], D-loops, and R-loops, with the same 3' to 5' polarity as DHX9[38, 51-54]. DHX9 and WRN both preferentially unwind DNA:RNA heteroduplexes with greater efficiency compared to DNA:DNA homoduplexes[36]. However, there are notable differences amongst these enzymes as well: whereas WRN and BLM can resolve Holliday junctions (another intermediate in homologous recombination), DHX9 cannot[38, 55, 56]. DHX9 can use both DNA- and RNA-based G-quadruplexes as substrates, while WRN and BLM can only resolve DNA G-quadruplexes[38, 57, 58]. DHX9 and the DHX36 helicase are the only enzymes thus far reported to unwind both DNA and RNA G-quadruplexes[59, 60].

Molecular cloning of the various domains and mutational analysis revealed that the two dsRBD domains at the N-terminus and the OB-fold and RGG-box at the C-terminus are dispensable for the NTPase and helicase activities of DHX9, and suggests that a minimal functional helicase likely consists of residues 313-1160 (Figure 1.1B)[26, 27]. The helicase-associated domain 2 (HA2) was found to be necessary for DHX9's unwinding activity[27]. A point mutation in Motif I (GCG**K**T to GCG**R**T) effectively abrogated ATP binding and ATPase activity, supporting sequence and structure data indicating this to be the site of NTP binding[61]. The two dsRBDs show specificity for binding to dsRNA, with optimal binding occurring when both dsRBDs are present. Although not required for unwinding, they enhance the catalytic activity by promoting binding of DHX9 to substrate RNA[27]. The RGG-box, on the other hand, binds specifically to ssDNA, with a lower affinity for ssRNA[26]. While the structure of full-length DHX9 has not been elucidated, it is thought that the N-terminal, helicase core, and C-terminal domains may be in close spatial proximity to each other and that the dsRBDs and RGG domains may help regulate or modulate the helicase activity[26]. For example, the dsRBDs and

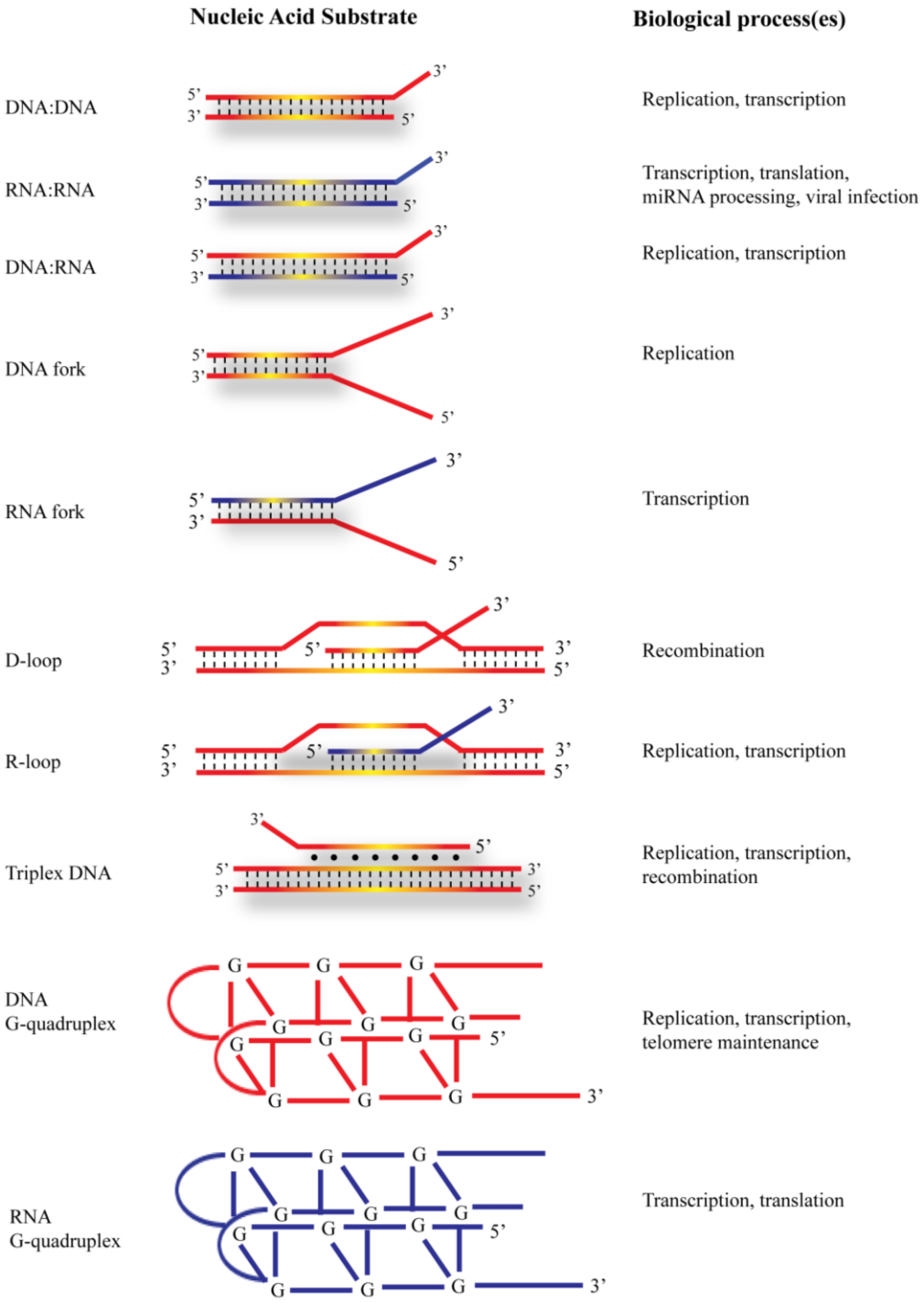

Figure 1.4 Nucleic acid substrates unwound by DHX9.

Schematic representation of nucleic acid substrates that can be remodeled by DHX9. DNA strands are colored in red and RNA strands in blue. The biological processes in which the substrates occur are indicated. Substrates are arranged from top to bottom in approximate order of increasing complexity. See text for a detailed description.

RGG domains may initiate binding to nucleic acids, and may cooperatively recognize single-stranded/double-stranded junctions. This binding may effect an allosteric change to activate the NTPase/helicase activity of DHX9, a situation which is observed in other dsRBD-containing proteins such as the double-stranded RNA-activated protein kinase DAI and the double-stranded RNA adenosine deaminase DRADA[62, 63].

1.3 Biological characterization of DHX9

1.3.1 Cellular localization of DHX9

Although DHX9 is predominantly a nuclear protein, it is able to shuttle to the cytoplasm to carry out some of its functions in translational regulation and miRNA processing[19]. It also migrates into the cytoplasm as a consequence of transcriptional inhibition and during mitosis[64]. During mitosis, release into the cytoplasm starts in prophase, which is marked by chromosomal condensation and breakdown of the nuclear envelope. Exclusion from the nucleus reaches a maximum during metaphase, where the condensed chromosomes align at the center of the cell, and DHX9 reenters the nucleus during telophase, where the nuclear envelope reforms[64, 65]. Shuttling is dependent on a nuclear localization signal (NLS) and a nuclear export signal (NES), both located at the C-terminal region (Figure 1.1B), and nuclear import is mediated by the classical importin-α/β dependent pathway[29, 66]. Nuclear translocation also requires methylation of arginine residues in the NLS by the protein arginine methyltransferase PRMT1[67]. In addition, there is evidence that nuclear localization is mediated by the neuronal kinesin KIF1Bβ and its binding partner exportin-2 (XPO-2)[68]. The nuclear export pathway utilized by DHX9 remains to be elucidated, but it has been determined to be insensitive to leptomycin B, a drug that specifically blocks the CRM-1-dependent nuclear export pathway[66, 69, 70]. Aside from the NLS and NES region, subcellular localization may also depend on other functional domains. For example, a fragment of DHX9 containing dsRBDI and dsRBDII was found to localize to the cytoplasm, and mutation of the RNA PolII-binding MTAD resulted in nuclear localization defects[71].

Localization within the nucleus is dynamic and dependent on species, cell type, and context. In human cells, DHX9 is normally localized to the nucleoplasm and excluded from the

nucleolus[30, 72]. However, under conditions of RNA PolII-mediated transcriptional inhibition, growth arrest, or stress induced by viral replication or low temperature treatment, DHX9 is translocated into the nucleolus[30, 72, 73]. Specifically, it localizes to the dense fibrillar components (DCFs) within the nucleoli, where ribosomal RNA biogenesis takes place[72]. Transport into the nucleolus is dependent on functional NTPase and helicase activity and is mediated by the dsRBDII and C-terminal nuclear transport domains[73]. In certain tumor cells, such as the breast cancer carcinoma line MCF-7, DHX9 is situated at the nucleolar periphery, bound to a F-actin network, and depolymerization of F-actin promotes entry into the nucleolus[74]. In murine cells, the opposite situation is observed: DHX9 is enriched in the DFCs of nucleoli but shuttles out into the nucleoplasm upon RNA polymerase I-mediated transcriptional inhibition, thermal stress, or cell cycle arrest[30]. The reasons underlying the different nuclear localizations of human and murine DHX9 are not entirely clear, but likely have to do with the fact that the latter has a much larger RGG-box at the C-terminus. It is possible that mouse cells may have higher rRNA transcriptional requirements, and the nucleolar localization of DHX9 may be an adaptation to accommodate this.

1.3.2 DHX9 expression, half-life, and role in development

DHX9 is an abundant protein and is ubiquitously expressed. In humans, expression is high in the skin, small and large intestines, stomach, pancreas, kidney, breast, skeletal muscle, bone marrow, and reproductive organs. The liver, spleen, lung, heart, smooth muscle, adipose tissues, and lymph nodes show a moderate level of expression[75-77]. DHX9 appears to be relatively stable, and its protein and mRNA half-lives have been measured in several cell lines. In murine NIH3T3 fibroblasts, its half-life was determined to be 81.1 hours at the protein level and 13.9 hours at the mRNA level[78]. In murine renal mpkCCD epithelial cells, its protein half-life is ~48 hours[79, 80]. DHX9's mRNA half-life is shorter in mouse embryonic stem cells, at 5.3 hours[81]. DHX9 participates in a variety of important biological processes and in many cell lines depletion is lethal[73, 82, 83]. DHX9 is essential during embryonic development. Homozygous DHX9 knockout mice are embryonic lethal, with marked apoptosis in embryonic ectodermal cells, suggesting a function for the helicase in the differentiation of the embryonic ectoderm[84]. The DHX9 homolog in *C. elegans*, RHA-1, is essential for germline transcriptional control and

proliferation. Deletion of RHA-1 results in loss of lysine 9 methylation on histone H3, leading to defects in germline transcriptional silencing and consequently defective chromatin organization, reduced germ cell mitosis, and abberant meiosis[23]. In *Drosophila*, Maleless (MLE) is responsible for X-chromosome dosage compensation, a process initiated in early embryogenesis which is critical to male development[21]. Homozygous mutations in MLE was found to be lethal for male zygotes[20]. In humans, DHX9 interacts with the LIM homeodomain transcription factor LMX1B, which is essential in mesodiencephalic dopaminergic neuron development[85]. DHX9 also interacts with the stem cell-specific RNA-binding protein L1TD1, which forms a complex with Lin28 to regulate translation of the stem cell factor Oct4, thus suggesting a role for DHX9 in human embryonic stem cell renewal[86]. Hence, the current evidence indicates that DHX9 is essential to development in a number of organisms.

1.4 Biological functions of DHX9

DHX9 has a large number of interacting partners, a reflection of the many biological processes it participates in. Table 1.1 summarizes the known proteins, nucleic acids, or sequence elements with which DHX9 interacts. This diversity in partners and targets is likely a consequence of DHX9's numerous functional domains and its promiscuity in terms of substrates. It participates at multiple levels of gene regulation and is a major player in many aspects of RNA biology. The following is an overview of its roles in DNA replication, transcriptional and translational regulation, RNA processing and transport, microRNA biogenesis, and maintenance of genomic stability. This discussion will focus on human DHX9, for which the largest body of research exists; however, where appropriate, other species will be discussed as well.

1.4.1 DNA replication and maintenance of genomic stability

The *in vitro* experiments illustrating DHX9's ability to unwind complex nucleic acid structures suggest a role in DNA replication and maintenance of genomic stability, since these are transient intermediates that form during replication, transcription, or recombination and need to be resolved. This is supported by several lines of evidence. First, DHX9 associates with numerous proteins involved in DNA replication and/or the DNA damage response. These include the breast

cancer specific tumor suppressor protein BRCA1, which remodels chromatin, facilitates orderly homologous recombination, and ensures DNA replication fidelity[87]. The replication proteins PCNA (proliferating cell nuclear antigen) and topoisomerase IIα also bind DHX9[88-90]. DHX9 interacts with Ku86, an essential player in NHEJ-mediated DNA repair which has also been implicated in promoting nascent DNA synthesis at origins of replication[91, 92].

Mechanistic insight into DHX9's role in DNA replication is provided by studies investigating its relationship with WRN, a RecQ ATP-dependent helicase containing both 3'to 5' helicase and 3'to 5' exonuclease activity. WRN is involved in DNA replication, recombination, and repair, and defects in this helicase are a cause of Werner's syndrome, a rare autosomal recessive genetic disorder characterized by premature aging, increased genomic instability, and increased cancer susceptibility. In terms of substrate specificities, DHX9 shares many similarities with WRN (see ***1.2.3. In vitro characterization of DHX9***). These two helicases were found to interact, with the interaction sites mapping to the dsRBDII and RGG domains of DHX9 and the N-terminal exonuclease domain of WRN[93]. DHX9 enhances the exonuclease activity of WRN and stimulates the WRN-catalyzed unwinding of Okazaki fragment-like DNA:RNA hybrids and Holliday junction-like structures. Because DHX9 itself does not catalyze unwinding of either of these substrates, it is thought that it may aid in resolving RNA secondary structures at the 5'end of the Okazaki-like fragments[36, 93]. Okazaki fragments are formed on the lagging strand during DNA replication[94]. The *in vitro* results suggest that DHX9 may be loaded onto these sites, aiding WRN to remove the primer RNA-containing Okazaki fragments and promoting lagging strand maturation. Holliday junction-like intermediates are formed during replication fork stalling[95]. By resolving these structures and converting them to functional replication forks, DHX9 and WRN may act to ensure efficient DNA replication. Because both DHX9 and WRN interact with common replication-associated proteins such as PCNA and Ku86, it is possible that they may function as part of a larger replication complex[88, 89, 91, 96, 97].

DHX9's involvement in maintenance of genomic stability has been demonstrated both *in vitro* and *ex vivo*. *In vitro,* DHX9 binds to H-DNA, a naturally occurring intra-molecular DNA triplex[98]. H-DNA is an aberrant structure which induces genomic instabilities, such as gross rearrangements, point mutations and double-stranded breaks. Suppression of DHX9 in U2OS cells overexpressing an H-DNA-forming sequence derived from the human c-MYC gene

promoter resulted in a significant increase in mutagenic events. Thus, DHX9 is purported to limit genomic instability by resolving H-DNA[98]. The ability of DHX9 to unwind G-quadruplexes is also suggestive of a role in genome maintenance. DNA G-quadruplexes are formed at G-rich telomeric sequences and may protect chromosomal ends against nucleases. However, these structures need to be resolved to permit telomere synthesis by the telomerase enzyme[99]. DHX9 may play a role in telomere maintenance by resolving telomeric G-quadruplexes, and this is supported by research showing that its interacting partner WRN plays a role in telomere processing[100]. Although DNA G-quadruplexes are most abundant at telomeres, they are also found at GC-rich regions at 90% of human DNA replication origins[101-103]. They can lead to replication fork stalling and represent an impediment to the replication process[104, 105]. The documented ability of DHX9 to cooperate with WRN in resolving stalled replication fork-like structures suggests that it may aid in promoting efficient replication by resolving G-quadruplexes.

Further evidence supporting a role in DNA repair and maintenance of genomic stability is demonstrated by evidence that DHX9 is phosphorylated by DNA-PK, a major player in NHEJ-mediated DNA repair. This is further corroborated by the observation that DHX9 interacts with Ku, the DNA binding subunit of DNA-PK[91]. DHX9 was found to interact with γH2AX via its helicase core domain, and this association is significantly increased upon actinomycin D treatment, where DHX9 accumulates in RNA-containing nuclear bodies adjacent to γH2AX foci[106]. Upon DNA damage, DHX9 also localizes to promyelocytic leukemia (PML) nuclear bodies, which are involved in the DNA damage response[107, 108]. Association of DHX9 with sites of DNA damage is consistent with its interaction with the polycomb group protein PHF1, which is recruited to double-stranded breaks upon exposure to DNA damage[109].

1.4.2 Transcriptional regulation

The *in vitro* experiments showcasing DHX9's ability to unwind RNA forks, R-loops, and RNA-based tetraplexes strongly suggested a role in transcription, since these are aberrant structures formed during stalled transcription. By resolving them, it was postulated that DHX9 may act to speed up transcriptional events. The earliest evidence of its role in transcription *in vivo* was

studies in *Drosophila* that showed that MLE associates with the X chromosome and regulates dosage compensation. In Drosophila, sex is determined by the ratio of X chromosomes to autosome haploid sets (X:A ratio). A X:A ratio of 1 (e.g. two X chromosomes in a diploid cell) results in development of a female, whereas a X:A ratio of 0.5 (e.g. 1 X chromosome) gives rise to males[110, 111]. More complex ratios can also occur (e.g. >1 or <0.5) resulting in metafemales or metamales. Contrary to its mammalian counterpart, the Y chromosome is not involved in sex determination but instead contains genes important for sperm formation in adults. Dosage compensation is required to equalize the levels of X chromosome-linked gene products between the sexes: the level of transcription of the single X chromosome in males is doubled in order to match that of the double X chromosome in females. Although expressed in both males and females, MLE is bound to hundreds of sites along the X chromosome of males but not females[21]. The male X-chromosome shows a diffuse morphology, and male MLE homozygous null mutants show reduced transcription rates along the entire X chromosome and die during the larval stage[112]. MLE is a subunit of the dosage compensation complex (DCC), also known as the male specific lethal (MSL) complex, which includes the ubiquitin ligase MSL2, structural proteins MSL1 and MSL3, and male absent on the first (MOF), a histone acetyl transferase. In addition, two long non-coding RNAs, RNA on the X1 (roX1) and RNA on the X2 (roX2), are also components of the DCC[113]. Binding of MLE to the X-chromosome requires functional MSL1, MLS2, and MSL3[114]. Activity of the DCC proteins is regulated by the sex-lethal (Sxl) gene, a feminizing master switch in the sex determination process. A X:A ratio of 1 leads to transcriptional activation of Sxl by X-chromosome-encoded proteins Sisterless-a and Sisterless-b during early embryogenesis. Sxl activates *transformer*, leading to a series of events resulting in female sexual differentiation. Sxl also represses translation of MSL2 and prevents binding of MLE to the X-chromosomes. On the other hand, when the X:A ratio is 0.5, Sxl is inactivated by high expression of autosomally encoded proteins Deadpan and Extramacrohaetae, MLS2 is translated, and the DCC is able to associate with the X-chromosome[113]. Binding of MLE to the X-chromosome is RNA dependent, as it can be disrupted by RNase treatment[115], and it has been shown to interact directly with roX2[116, 117]. The NTPase and helicase activities of MLE are essential to its role in dosage compensation[35].

In mammals, dosage compensation occurs through an entirely different mechanism. Here,

transcription of genes on one of the two X-chromosomes in females is suppressed by the non-coding RNA XIST, achieving the same level of transcription as the single male X-chromosome[118]. There has so far been no evidence that DHX9 plays a sex-specific role in mammalian development, although it is essential for normal gastrulation in mice in both sexes[84]. Nevertheless, it has been implicated in transcription activation. DHX9 was discovered to be a bridging factor between the transcriptional co-activator CREB-binding protein (CBP)/p300 and RNA PolII. During CBP/p300-mediated transcriptional activation, phosphorylation of the cAMP response element-binding protein (CREB) results in complex formation with co-activator CBP/p300 and binding to a cAMP responsive element (CRE) in the promoter of specific genes[119]. DHX9 binds directly to both CBP/p300 and RNA polymerase II, recruiting the latter to the CREB/CBP/p300 complexes at the promoter[120]. Interaction with RNA PolII is mediated through the 50 amino-acid MTAD region which contains six hydrophobic residues conserved amongst DHX9 homologs[61, 121]. Mutational analyses indicate that three tryptophan residues within the MTAD are essential for PolII binding and transcriptional activation[61, 121]. Interaction with CBP occurs in a region between amino acids 1-250 in DHX9, where the two dsRBDs lie[120]. Aside from recruitment of PolII, the NTPase/helicase activity of DHX9 is also important for CREB-dependent transcription, suggesting a dual mechanism of transcriptional regulation[61]. The function of the MTAD is conserved in *Drosophila* and *C. elegans*. DHX9 from both species are able to recruit PolII and activate transcription via the MTAD[122].

Other instances of human DHX9 serving as a bridging factor between PolII and transcriptional co-factors have been uncovered. DHX9 links PolII to BRCA1, which in addition to its roles in DNA replication and DNA repair, also functions in transcriptional regulation[123]. Binding to BRCA1 occurs between a region in the N-terminus of DHX9 (residues 230-325) and the C-terminus of BRCA1, and resulted in transcriptional activation in reporter assays[124]. Although both located at the N-terminus, it is notable that the binding region for BRCA1 is distinct from that for CBP/p300 (residues 1-250). Nuclear β-actin is another component of the transcription pre-initiation complex[125], and DHX9 serves as an adaptor to link it with PolII. This interaction was reported to enhance transcription from the actin-dependent CSF-1 promoter. Contrary to what was observed in the case of CBP/p300, DHX9 interacts with β-actin via its C-

terminal RGG region, and its catalytic activity is not required[126].

DHX9 participates in nuclear factor-κB (NF-κB)-mediated transcriptional activation, where members of the NF-κB family including p65, RelB and c-Rel upregulate transcription in response to exposure to a variety of inducers, such as interleukin-1 and tumor necrosis factor. DHX9 directly binds p65 and enhances NF-κB-dependent transcriptional activation, an event dependent on functional NTPase/helicase activity[127]. Since p65 is known to utilize CBP/p300 as a co-activator[128], it is possible that DHX9, p65, CBP/p300 and PolII may all be part of the same transactivation complex. Activation of CREB/CBP/p300-mediated transcription by the mineralocorticoid receptor[129], the methyl-CpG binding domain protein 2 (MBD2a)[130], and the E2-like enzyme UBC9[131] are also dependent on interaction with DHX9. Other known DHX9-binding transcription activators include the osteoblast-specific transcriptional factor osterix[132], nuclear factor 110 (NF110)[133], the Zic2 zinc finger protein[134], topoisomerase IIα[90] and LMX1B[85].

DHX9 also binds directly to promoters in a sequence specific manner. It enhances transcription of the tumor suppressor p16INK4A by binding specifically to the sequence $^{5'}$CGGACCGCGTGCGC$^{3'}$ within its promoter[135]. Another example of selective transcriptional regulation is that of the multidrug resistance gene 1 (MDR1). DHX9 is a component of the MDR1 promoter-enhancing factor (MEF1) complex and binds to the CAAT-like *cis*-acting element in the MDR1 promoter[136]. As well, DHX9 participates in EGF receptor (EGFR)-mediated transcriptional activation. Here, EGFR translocates from the cell surface to the nucleus in response to EGF signaling and activates transcription via an AT-rich sequence (ATRS) in the promoter of target genes[137]. EGFR-responsive genes include cyclin D1 and iNOS. EGFR lacks a DNA-binding domain; DHX9 mediates this interaction by simultaneously binding both EGFR and the promoter ATRS[138].

DHX9 can interact with RNA to regulate transcription. It has been found to bind both the insulin-like growth factor 2 (IGF2) mRNA and miR-483-5p, a microRNA that enhances IGF2 transcription, promoting the miR-483-5p-mediated induction of IGF2 mRNA[139]. In an example of regulation of viral nucleic acids, it interacts with the viral transactivation response element (TAR) RNA via its dsRBDII to stimulate HIV-1 transcription, a process that is

dependent on DHX9's ATPase and PolII-binding activities[140, 141].

In addition to activating transcription, it appears that in some situations DHX9 can also repress it. Association with the transcriptional activator TonE (tonicity-responsive enhancer)-binding protein (TonEBP) inhibits TonEBP activity[142]. Although the mechanism is not clear, it is possible that DHX9 may recruit other proteins that directly inhibit TonEBP. The *C. elegans* homolog, RHA-1, enables normal germline proliferation and development by silencing transcription. A temperature-sensitive mutant, RHA-1(tm329), caused loss of lysine 9 histone H3 methylation (normally associated with silenced chromatin) and resulted in transcriptional desilencing. This resulted in defects in germ cell mitosis, meiosis, and gametogenesis, leading to a sterile phenotype[23]. Again, the mechanism of how RHA-1 silences transcription is unclear, but it may be direct (e.g. by promoting formation of heterochromatin) and/or indirect (e.g. by recruiting transcriptional repressors).

1.4.3 Translational regulation

Beyond its role in transcription, DHX9 also participates in regulation of gene expression at the translational level. Many mRNAs contain highly structured 5'UTRs, a feature that represents an impediment to translational initiation, the rate-limiting step of cap-dependent translation. The eIF4A (DDX2) subunit of the eIF4F complex is responsible for unwinding structures to facilitate ribosome recruitment to the mRNA template[143-145]. However, a subset of mRNAs contains complex structural elements in their 5'UTRs that require resolution by additional specific helicases. One such element is the 5'post-transcription control element (PCE). Originally identified in the 5' long terminal repeats of avian spleen necrosis virus[146] and subsequently in the 5'UTR of other retroviral RNAs, such as those found in HIV-1 and HTLV-1 (e.g. gag RNA), the PCE forms a complex secondary structure containing two stem-loop structures[147]. A PCE is also present in the 5'UTR of the cellular transcription factor JUND. DHX9 is necessary for the efficient translation of viral and JUND mRNA containing the PCE. It associates with structural features of the PCE via conserved lysine residues in the distal α-helices of the two dsRBDs and facilitates translation of said mRNAs by stimulating polyribosome incorporation[148, 149]. The NTPase/helicase activity of DHX9 is required for this function[150]. Association with PCE is sequence-specific and occurs both in the nucleus and in the cytoplasm, indicating it to be an

early event in the post-transcriptional expression of PCE-containing mRNA, and may satisfy a RNA-surveillance checkpoint that ensures efficient translation in the cytoplasm[148]. It has been proposed that DHX9 induces RNA-protein and RNA-RNA rearrangements to enable efficient association of ribosomes and thus increase the rate of protein synthesis. It is also possible that DHX9 stimulates ribosome recycling by securing circularization of the mRNA template via interaction with the poly(A)-binding protein (PABP), although this has not been verified[148]. Since JUND regulates cell growth in response to stress, its selective and tightly controlled translational regulation by DHX9 provides a means to rapidly link these two responses.

DHX9 also facilitates translation of type I collagen, another mRNA with a unique 5'UTR structural element. Type I collagen is a heterotrimer composed of two α1(I) polypeptides and one α2(I) polypeptide. The mRNAs encoding both polypeptides contain a unique 5' stem-loop structure (5'SL) in their 5'UTR. La ribonucleoprotein domain family member 6 (LARP6) is known to bind with high affinity to the 5'SL[151]. DHX9 does not interact directly with the type I collagen 5'UTRs, but instead forms a complex with LARP6, which tethers it to the 5'SL. This enables polysome loading and efficient translation initiation. As is the case with PCE-mediated regulation, binding of DHX9/LARP6 to the 5'SL occurs in the nucleus as well as the cytoplasm, indicating that regulation begins prior to the onset of translation initiation[152]. In another example of regulation of a specific set of mRNAs by DHX9, the helicase interacts with Lin28 to enhance translation of Lin28 target mRNAs. Lin28 is a RNA-binding protein which plays a role in development, cell growth, pluripotency, and differentiation. It was first characterized as a key player in the biogenesis of let-7 family miRNAs[153]. More recently, it has been shown to regulate the translation of select mRNAs including IGF-2, the key pluripotency factor Oct4, histone H2a, cyclins A and B, and CDK4[154-157]. DHX9 interacts with Lin28 via both its N- and C- terminal regions. This interaction promotes DHX9 association with polysomes and stimulates translation of Oct4 mRNA[155, 158]. It is thought that once recruited to Lin28 target mRNAs, DHX9 may aid in resolving inhibitory secondary structures. Further support for a role in Lin28-mediated translation regulation is provided by evidence that DHX9 also interacts with L1TD1, which forms a complex with Lin28 to regulate Oct4 translation in human embryonic stem cells[86].

Recent studies indicate that DHX9 also helps regulate IRES-mediated translation.

Exposure to DNA damaging agents causes stabilization of the p53 tumor suppressor protein. However, recent evidence has shown that p53 translation is also increased upon DNA damage[159-161]. It was discovered that p53 mRNA contains an IRES in its 5'UTR[162, 163]. DHX9 was found to bind simultaneously to the p53 IRES and to translation control protein 80 (TCP80). DHX9 and TCP80 cooperatively stimulate p53 IRES-mediated translation. This stimulation is significantly enhanced upon exposure to DNA damage as a result of increased binding of TCP80 to the p53 IRES and improved interaction between DHX9 and TCP80. It is predicted that DHX9 likely helps unwind the p53 5'IRES, thereby promoting efficient translation[164, 165].

1.4.4 MicroRNA biogenesis and processing

Involvement in microRNA (miRNA) biogenesis and processing is another means by which DHX9 regulates post-transcriptional gene expression. miRNAs are first transcribed as long double-stranded RNAs, called primary miRNAs (pri-miRNAs) by RNA polymerase II. The pri-miRNAs are then cleaved into ~60 nt long stem-looped structured double-stranded precursor miRNAs (pre-miRNAs) by the ribonuclease III enzyme, Drosha, and exported into the cytoplasm. There, the pre-miRNAs are processed into mature miRNAs (18-25 bps) by another ribonuclease III enzyme, Dicer. Mature miRNAs are incorporated into the RNA-induced silencing complex (RISC), a large ribonucleoprotein complex whose core components include Dicer, transactivating response RNA-binding protein (TRBP) which contains three dsRBDs, and the RNase Argonaut-2 (Ago-2). siRNAs introduced exogenously are incorporated into RISC in the same manner as the endogenous miRNAs. The conventional model is that Dicer and TRBP loads the miRNA/siRNA onto Ago-2, whereby the passenger strand is degraded and the guide strand directs the RISC to complementary target mRNAs which are subsequently cleaved by Ago-2[166-169]. Aside from the core catalytic components of the RISC, many other factors are involved in the miRNA processing process. DHX9 has been implicated at multiple stages of miRNA biogenesis. It associates with pri-miRNA, and along with its binding partner, BRCA1, forms part of the Drosha microprocessor complex, which also contains DGCR8, DDX5, and DDX17. The concerted action of DHX9 and BRCA1 enhances processing of the pri-miRNA into their mature forms[170]. Further downstream in the miRNA processing cascade, DHX9 was also

identified as a component of the active RISC. It binds directly to Dicer, TRBP, Ago-2, and siRNA duplexes, and association with all these components is mediated by key residues in dsRBDI and dsRBDII[171]. Isothermal titration calorimetric assays revealed that dsRBDI has a higher binding affinity than dsRBDII for the siRNA, but both dsRBDI and dsRBDII act cooperatively to bind the duplex[32]. The DHX9 ATPase/helicase activity is important but not absolutely essential for its association with Dicer, TRBP, and Ago-2, as an ATPase mutant only partially impaired these interactions. DHX9 depletion inhibits siRNA- and shRNA-mediated gene silencing *in vivo* and reduces siRNA association with the RISC, thus demonstrating that DHX9 is an essential component of the RISC and defining a role for it as a siRNA/miRNA loading factor[171].

1.4.5 RNA processing and transport

As described above, human DHX9, while normally excluded from the nucleolus, can shuttle into said compartment under conditions of transcriptional inhibition or cellular stress[30, 72, 73]. DHX9 has also been identified in human prespliceosomes[172], binds to both mRNA and pre-mRNA[64], and interacts with the splice regulator muscleblind 1 (MBNL1)[173] as well as the survival motor neuron (SMN) protein, a component of small nuclear ribonucleoproteins (snRNPs) involved in pre-mRNA splicing[174-176]. This suggests a role in mRNA splicing and is supported by evidence that DHX9, in concert with ADAR2 (an adenosine deanimase that acts on RNA) coordinates the editing and splicing of glutamate receptor subunit B pre-mRNA. mRNA editing and splicing are competing events – ADAR2 editing requires a stable stem-loop, which may sequester the 5' splice site. It is thought that DHX9 helps overcome this splicing inhibition by resolving the stem-loop[177]. An example of coordinated editing and splicing can also be found in *Drosophila*. In a process distinct from its role in dosage compensation, MLE links editing and splicing of the para sodium channel pre-mRNA. A mutation near the NTP-binding site of MLE results in aberrant splicing and exon skipping, again suggesting that the *Drosophila* DHX9 homolog may act to resolve secondary structures concealing splice sites[178, 179].

A role in RNA transport is suggested by the observation that DHX9 binds directly to both filamentous actin (F-actin) and hnRNP C1 in the nucleus, mediating their association[180]. F-

actin is a major component of the nucleoskeleton, a network of interacting structural proteins that provides a scaffold for transcription, chromatin remodeling, and RNA processing and transport[181]. By facilitating the association of hnRNP C1, which plays a role in pre-mRNA processing, to F-actin, DHX9 enables efficient processing and transport of mRNAs. DHX9 also plays a role in the transport and splicing of viral RNAs. Nuclear export of simian type D retroviruses is dependent on host cellular proteins and mediated by a *cis*-acting constitutive transport element (CTE) on the viral RNA. DHX9 binds specifically to the CTE and interacts with two other shuttle proteins, Tip-associated protein (Tap) and HAP95, to allow export of CTE-containing viral RNAs[182-185]. DHX9 also facilitates transport of more complex viral RNAs such as HIV-1. Here, it cooperates with the viral protein Rev and cellular protein Sam68 to mediate nuclear export of viral RNAs containing the Rev response element (RRE)[186-189]. In addition, DHX9 modulates HIV-1 RNA splicing, a function that is mediated by its OB-fold[28].

Table 1.1 Protein and nucleic acid interacting partners of DHX9

Interacting partner	Biological process	DHX9 homolog(s) characterized	DHX9 domains/amino acid residues involved (if known)	Reference(s)
Protein partners				
Importin-α	Nuclear import of DHX9	Human	NLS (1155-1173)	[29]
PRMT1	Nuclear import of DHX9	Human	NLS (1155-1173)	[67]
WRN	Replication	Human	dsRBDII and RGG-box	[93]
PCNA	Replication	Human		[88, 89]
Topoisomerase IIα	Replication/ transcription	Human		[90]
Ku86	Replication/ DNA repair	Human		[91]
Myxoma virus protein M029	Viral replication	Human		[190]
Influenza A virus protein NS1	Viral replication/ transcription	Human		[191]
γH2AX	DNA damage response	Human	Helicase core domain (313–952)	[106]
PML	DNA damage response	Human		[107, 108]
PHF1	DNA damage response	Human		[109]
RNA polymerase II	Transcription	Human, *Drosophila*, *C. elegans*	MTAD (331-380)	[61, 120-122]
CBP/p300	Transcription	Human	dsRBDI+dsRBDII (1-250)	[61, 120, 121]
BRCA1	Transcription/ miRNA biogenesis	Human	dsRBDII (230-325)	[124, 170]
EGFR	Transcription	Human	623-1270	[138]
p65	Transcription	Human	1-649	[127]
β-actin	Transcription	Human	RGG-box (1150–1270)	[126]

osterix	Transcription	Human		[132]
MEF1	Transcription	Human		[136]
Mineralocorticoid receptor	Transcription	Human	1-331	[129]
MBD2a	Transcription	Human		[130]
TonEBP	Transcription	Human	N-terminus (1-250) and C-terminus (1062–1270)	[139]
Zic2	Transcription	Human		[134]
NF110	Transcription	Human		[133]
LMX1B	Transcription	Human		[85]
UBC9	Transcription	Human	1-137	[131]
EWS-FLI1	Transcription	Human	630-1020	[192]
DDX5 (p68)	Transcription/ miRNA biogenesis	Human		[170, 193]
DDX17 (p72)	Transcription/ miRNA biogenesis	Human		[170, 193]
LARP6	Translation	Human		[152]
Lin28	Translation	Human	N-terminus (1-300) and RGG-box (1161–1270)	[158]
L1TD1	Translation	Human		[86]
TCP80	Translation	Human		[164, 165]
Dicer	miRNA biogenesis	Human	dsRBDI+dsRBDII	[32, 171]
TRBP	miRNA biogenesis	Human	dsRBDI+dsRBDII	[32, 171]
Ago-2	miRNA biogenesis	Human	dsRBDI+dsRBDII	[32, 171]
MBNL1	RNA processing	Human		[173]
SMN	RNA processing	Human	RGG-box	[174]
hnRNP C	RNA processing	Human		[180]
F-actin	RNA transport	Human	C-terminus	[180]
HAP95	Viral RNA transport	Human	C-terminus	[182-185]
Tip-associated protein (Tap)	Viral RNA transport	Human		[182-185]

Sam68	Viral RNA transport	Human		[189]
Rev viral protein	Viral RNA transport	Human		[186, 189]
KIF1Bβ	Apoptosis	Human		[68]
IPS-1	Host antiviral response	Human	Helicase core domain and C-terminus	[194]
Nucleic acid partners/sequence elements				
pINK4A promoter (CGGACCGCGTGCGCTG)	Transcription	Human	dsRBDI+dsRBDII (1-250)	[135]
MDR1 promoter (CAAT-like sequence)	Transcription	Human		[136]
miR-483-5p	Transcription	Human		[139]
Viral TAR RNA	Viral transcription	Human	dsRBDII (235–249)	[188]
roX2 RNA	Transcription	*Drosophila*		[116]
5'UTR PCE of mRNAs	Translation	Human	N-terminus (1-300)	[148-150]
Collagen 5'UTR stem-loop	Translation	Human		[152]
p53 5'UTR IRES	Translation	Human		[164, 165]
Viral CTE	Viral RNA transport	Human		[182-185]

1.5 Implications of DHX9 in human diseases

The role played by DHX9 in a multitude of cellular processes, including multiple levels of gene regulation, and its association with a large number of key regulatory binding partners, makes it an important protein in maintaining normal cellular homeostasis. However, this also means that defects in DHX9 may have serious effects on cell growth or viability, and usurpation of its functions may lead to a variety of human diseases.

1.5.1 Implication of DHX9 in cancer

The human DHX9 gene maps to the major susceptibility locus for prostate cancer at chromosome band 1q25[25], and DHX9 expression is under control of the transcription factor SOX4, which is overexpressed in prostate cancer[195]. Interaction of SOX4 with inhibitory protein plakoglobin inhibits binding of SOX4 to the DHX9 promoter and results in reduced DHX9 expression[196]. SOX4 also regulates transcription of RISC components Dicer and Ago-1, both of which interact with DHX9[171, 195], and in fact, Dicer itself is overexpressed in prostate cancer[197]. These studies suggest that DHX9 may play a role in prostate cancer development, although further work is needed to validate a direct mechanistic link. DHX9 is overexpressed in several cancer types. Two separate studies analyzing DHX9 levels in panels of lung cancer samples showed that DHX9 is overexpressed in tumor samples compared to normal lung tissues[198, 199], and that DHX9 overexpression was correlated with poorer patient survival[199].

As discussed previously, DHX9 interacts with EGFR to activate transcription of EGFR-responsive genes. EGFR is an oncogene overexpressed in several human cancers and drugs targeting EGFR are in clinical use (e.g. gefitinib, erlotinib, and cetuximab)[200-203]. An analysis of a panel of human breast tumor samples showed a strong positive correlation between the nuclear expression of DHX9, EGFR, and the EGFR target cyclin D1[138]. Mutations in BRCA1, a DHX9-interacting tumor suppressor, increases risk of breast and ovarian cancers. Expression of a truncated form of DHX9 spanning the BRCA1 binding site (residues 89-344) but lacking other functional domains in normal mammary epithelial cells inhibited recruitment of BRCA1 to sites of DNA repair and resulted in pleomorphic nuclei, tetraploidy, and aberrant

mitoses with extra chromosomes – a phenotype similar to that observed in BRCA1-deficient cells[204]. Furthermore, sequence analysis of DHX9 in a cohort of 96 breast cancer individuals from high-risk French Canadian families who do not harbor BRCA1/BRCA2 mutations identified two missense mutations (P89A and S625C) that lie in the dsRBDI (within the CBP/p300 binding site) and the helicase core domain, respectively[205]. The importance of these variations awaits further assessment.

DHX9 is also implicated in osteosarcoma and Wilms' tumor. Gene expression profiling of osteosarcoma cell lines showed overexpression of DHX9 in cells with high metastatic ability compared to those with low metastatic ability. Several other genes in the NF-κB pathway were upregulated as well; since DHX9 is a NF-kB binding partner, this supports a role for NF-κB signaling in osteosarcoma metastasis[206]. DHX9 cooperates with the miRNA miR-483-5p to induce IGF2 expression. Both miR-483-5p and IGF are overexpressed in Wilms' tumors and sarcomas, and ectopic expression of miR-483-5p in sarcoma cells and mouse xenographs enhances tumorigenesis[139].

Although much research implicates DHX9 as a promoter of tumorigenesis, there are also indications that it has tumor-suppressive properties. Its ability to unwind aberrant polynucleotide structures and to aid WRN in ensuring the fidelity and efficiency of DNA replication shows that it plays a role in maintaining genomic stability. It also activates transcription of p16INK4A, a tumor suppressor[135]. Its cooperation with the tumor suppressor BRCA1 in activating its target genes is also suggestive of an anti-tumor function[124]. It is a downstream mediator of KIF1Bβ tumor-suppressor function in neuroblastoma. KIF1Bβ-mediated activation of the pro-apoptotic XIAP-associated factor 1 (XAF1) and subsequent induction of apoptosis requires nuclear localization of DHX9[68]. Perhaps the most compelling evidence is the IRES-mediated upregulation of p53 translation by DHX9 and TCP80 (see ***1.4.3 Translational regulation***). It was found that cellular levels of DHX9 and TCP80 positively correlated with the efficiency of p53 IRES-mediated translation and effective induction of p53 signaling in response to DNA damage. Specifically, the breast cancer cell lines, ZR75-1 and MDA-MB-175, which express wild-type p53 but do not exhibit p53 induction following DNA damage, contain extremely low levels of both DHX9 and TCP80 compared to MCF-7 cells (which show a normal p53 response), and exhibit low p53-IRES activity when exposed to DNA damaging agents. IRES-mediated p53

translation was rescued by overexpression of DHX9 and TCP80[165]. This shows that DHX9 levels can have a direct effect on the ability of p53 to suppress tumorigenesis. It appears that the relationship between DHX9 and oncogenesis is a complex one that may be dependent on cellular context and/or levels or activity of its interacting partners.

1.5.2 Role of DHX9 in viral infection

Viruses can hijack various aspects of the host cell machinery for their own purposes. This includes using host proteins to facilitate the replication, transcription, translation, or transport of their own nucleic acids or proteins. DHX9 interacts with the viral TAR RNA to stimulate HIV-1 transcription[140, 141]. As indicated above, it facilitates translation of viral RNAs containing a PCE in the 5'UTR[148, 149] and mediates nuclear export of both CTE-containing (e.g. simian type D retrovirus) and RRE-containing (e.g. HIV-1) RNA[182-189]. DHX9's involvement in aiding many aspects of viral function serves to enhance infection efficiency, and indeed it has been implicated in promoting infectivity of a whole range of viruses including HIV-1[28, 140, 141, 150, 186, 188, 207, 208], HCV[209], cytomegalovirus[210], adenovirus[211], and Hepatitis E[212], influenza A[191], myxoma[190], classical swine fever[213], and foot and mouth disease viruses[214].

Surprisingly, DHX9 has also been implicated in antiviral immune responses. For example, it is recruited to PML bodies in response to IFN-α stimulation and is phosphorylated by the dsRNA-binding kinase PKR[108, 140]. It also interacts with IFN-β promoter stimulator (IPS)-1 and acts as a sensor for double-stranded RNA to promote IFN and inflammatory responses[194]. The importance of DHX9 in innate immunity is highlighted by the observation that the DHX9 homolog is missing from chickens and ducks, thus rendering these species more susceptible to many viruses than mammals (e.g. the avian influenza H5N1)[215]. Avian influenza is particularly pathogenic in chickens because they are also deficient in another viral sensor, RIG-1 (DDX58), which is present in ducks and can partially compensate for the loss of DHX9[215, 216]. The opposing roles of DHX9 in both pro-viral and anti-viral response suggests that there may be a tug-of-war between the host cell's attempts to combat viral infection and the viruses' attempts to hijack cellular machinery – a battle in which DHX9 appears to play a crucial part.

1.5.3 Role of DHX9 in autoimmune disease

Systemic lupus erythematosus (SLE) is an autoimmune disease in which the body launches an immune response against healthy tissues. It is characterized by the generation of antibodies against the body's own proteins, termed autoantigens, most of which are nuclear proteins. This leads to inflammation and complications such as skin rashes, photosensitivity, and atherosclerosis[217]. DHX9 was detected as an autoantigen in the sera of SLE patients[218]. Autoantibodies against DHX9 were found in ~6% of patients with SLE and this percentage was increased to 23% in SLE patients of Mexican descent, consistent with population differences in the manifestation of SLE. It is also more common in the early stages of disease[219, 220]. DHX9 is a substrate of caspase-3 cleavage during apoptosis and it is thought that the cleaved fragments produced may trigger an autoimmune response[218]. Hence, DHX9 may be clinically useful as a marker in aiding the diagnosis of SLE. Further work is needed to determine why DHX9 autoantibodies are generated in some SLE patients but not others, and whether there are additional subsets of SLE patients with particularly high instances of DHX9 as an autoantigen.

1.6 p53-dependent pathways regulating apoptosis and cell cycle progression

As discussed above, DHX9 has been implicated in tumorigenesis. As a prelude to discussing recent advances in targeting DHX9 as a chemotherapeutic approach, I will give a brief overview of p53 and the pathways regulating apoptosis and cell cycle progression, as well as a discussion of the role of p53 in chemotherapy.

1.6.1 The p53 tumor suppressor protein

p53 is a tumor suppressor which lies at the nexus of a network of signaling pathways regulating cell cycle progression, apoptosis, and DNA repair. Named the "guardian of the genome"[221], it is the most frequently mutated gene in tumors, with over 50% of cancers harboring a defect in p53[222, 223]. It is a transcription factor which activates a broad range of genes in response to cellular stresses such as DNA damage, oncogene activation, and replication stress. These target genes allow the cell to arrest or undergo apoptosis, thereby preventing aberrant replication and

genomic instability[221]. The p53 gene is located on chromosome 17 in humans and is encoded by 11 exons[224]. Highly conserved amongst vertebrates, it consists of five domains, each with distinct functions: the N-terminal region containing two transactivation domains, a proline rich region, a central DNA-binding domain, a tetramerization domain which also harbors a nuclear export signal (NES), and a lysine-rich basic C-terminal region containing three nuclear localization signals (NLS) and a non-specific DNA-binding region that binds to damaged DNA (Figure 1.5)[225-227]. Over 95% of p53 mutations occur in the central DNA-binding domain, highlighting its main role as a sequence-specific DNA-binding protein[226].

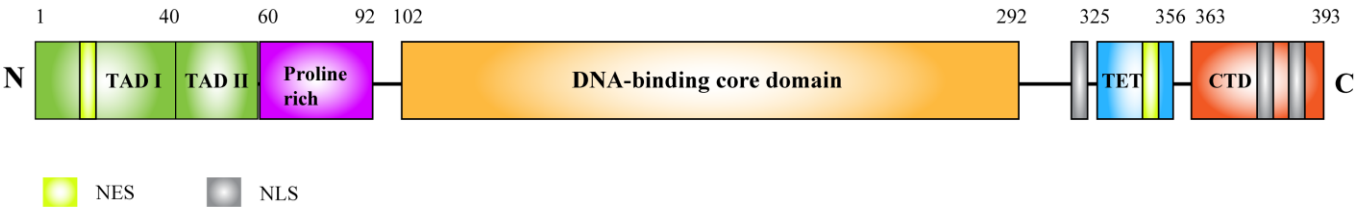

Figure 1.5 Domain structure of p53.

Schematic representation of p53 functional domains. Numbers indicate amino acid positions in human p53. TAD, transcriptional activation domain; TET, tetramerization domain; CTD, C-terminal domain; NES, nuclear export signal; NLS, nuclear localization signal.

1.6.2 Regulation and activation of p53

p53 protein levels and activity are tightly regulated. Under normal cellular conditions, p53 is maintained at low levels by virtue of negative regulators. The most well characterized negative regulator is MDM2, an E3 ubiquitin ligase which binds to p53, suppresses its transcriptional activity, and marks it for proteosomal degradation via ubiquitination as well as mediating its nuclear export[228-231]. Because MDM2 is a transcriptional target of p53, they form part of an autoregulatory loop also involving ARF, which inhibits MDM2 and is negatively regulated by p53 (Figure 1.6)[232-234]. Thus, MDM2 levels are upregulated and ARF is inhibited upon p53

activation, and this allows p53 levels to be brought back down after cessation of activating stress signals.

p53 is activated in response to a variety of stresses, both extrinsic and intrinsic to the cell. These include DNA damage (e.g. from ionizing or UV radiation or chemical agents), spindle damage, oncogene activation, hypoxia, oxidative stress, replication stress, loss of cell-cell or cell-matrix contacts, ribosomal stress (e.g. rNTP depletion), and heat or cold shock (Figure 1.6) [222, 235]. The stress signals are detected by upstream mediators and communicated to p53 primarily through post-translational modifications which stabilize p53 and/or modulate its transcriptional activity (Figure 1.6). The precise mediators and post-translational modifications involved largely depend on the nature of the stress signal. For example, p53 is phosphorylated by the kinases ATM and CHK2 following double-stranded DNA breaks resulting from ionizing radiation or DNA damaging agents such etoposide or doxorubicin[236-238]. UV-induced DNA lesions and replication stress activate ATR and the downstream kinase CHK1, which phosphorylates p53[236, 239]. Members of the MAP kinase (MAPK) family phosphorylate p53 in response to oxidative stress and heat shock[240, 241]. Phosphorylation disrupts the interaction between p53 and MDM2, leading to p53 stabilization[242, 243]. It also enhances the interaction between p53 and transcriptional co-activators[244, 245]. Acetylation by CBP and p300 on lysine residues in p53's C-terminal region is another modification that occurs in response to a variety of stresses, including UV radiation, oxidative stress, hypoxia, and actinomycin D[246]. Acetylation stabilizes p53, possibly by protecting lysine residues from being ubiquitylated, as well as increasing its DNA-binding activity[246, 247]. Hypoxia activates p53 through a mechanism involving ATR, von Hippel-Lindau (VHL), and the hypoxia inducible factor (HIF) 1α, which binds to p53 to promote its stabilization[248, 249]. ARF is upregulated by certain oncogenes (e.g. E1A and c-MYC) and activates p53 by inhibiting MDM2 activity[250-252]. p53 may also be modified by methylation, SUMOylation, or NEDDylation[253-263]. The diversity of mediators and post-translational modifications allow for a myriad of pathways and mechanisms of p53 activation in response to different types of stress.

1.6.3 p53-mediated transcriptional regulation

p53 activates its downstream signaling pathways primarily through transcriptional upregulation

of target genes. Once activated, p53 forms a tetramer via its tetramerization domain and binds to specific DNA sequences called p53 response elements (RE) located in the promoter and introns of target genes[264, 265]. The p53-RE is defined as two repeats of the sequence RRRCWWGYYY (where R is a purine, Y is a pyrimidine and W is A or T) linked by a variable spacer[266, 267]. p53 interacts with transcriptional co-activators via its N-terminal transactivation domain to facilitate efficient transcription of target genes[268]. To date, over 100 p53 target genes have been identified; these have a broad range of functions and participate in a multitude of cellular pathways. As a result, p53 activation can lead to a number of possible biological outcomes, including cell cycle arrest, senescence, apoptosis, differentiation, angiogenesis inhibition, autophagy, metabolism control, and DNA repair (Figure 1.6)[227]. The specific cell fate is determined by the nature and strength of the stress signal, the cellular microenvironment, and the levels of various p53 target genes, regulators, and interacting proteins in the cell[269].

In addition to its role as a transcriptional activator, p53 can also repress transcription of certain genes. This may be accomplished by competitively binding promoters regulated by other transcription factors, or by interacting with other DNA-binding transcriptional activators or components of the basal transcriptional machinery, thereby inhibiting their ability to activate their target genes. p53 may also recruit co-repressors and histone deacetylases, the latter which modify chromatin structure and reduce promoter accessibility[270]. The transcriptional repressor SIN3A has been found to interact with p53 and elicit repression of several genes[271]. Examples of genes negatively regulated by p53 include ARF[234], survivin - an inhibitor of apoptosis[272], the microtubule-associated protein MAP4[273], and the transcription factor NANOG[274].

1.6.4 p53-dependent cell cycle arrest and senescence

The cell cycle is an ordered sequence of events which allow DNA replication and cell division to take place. It is comprised of four distinct phases: G0/G1, S, G2, and M[275, 276]. During the G1 phase, the cell undergoes growth and engages in the biosynthesis of proteins and organelles.

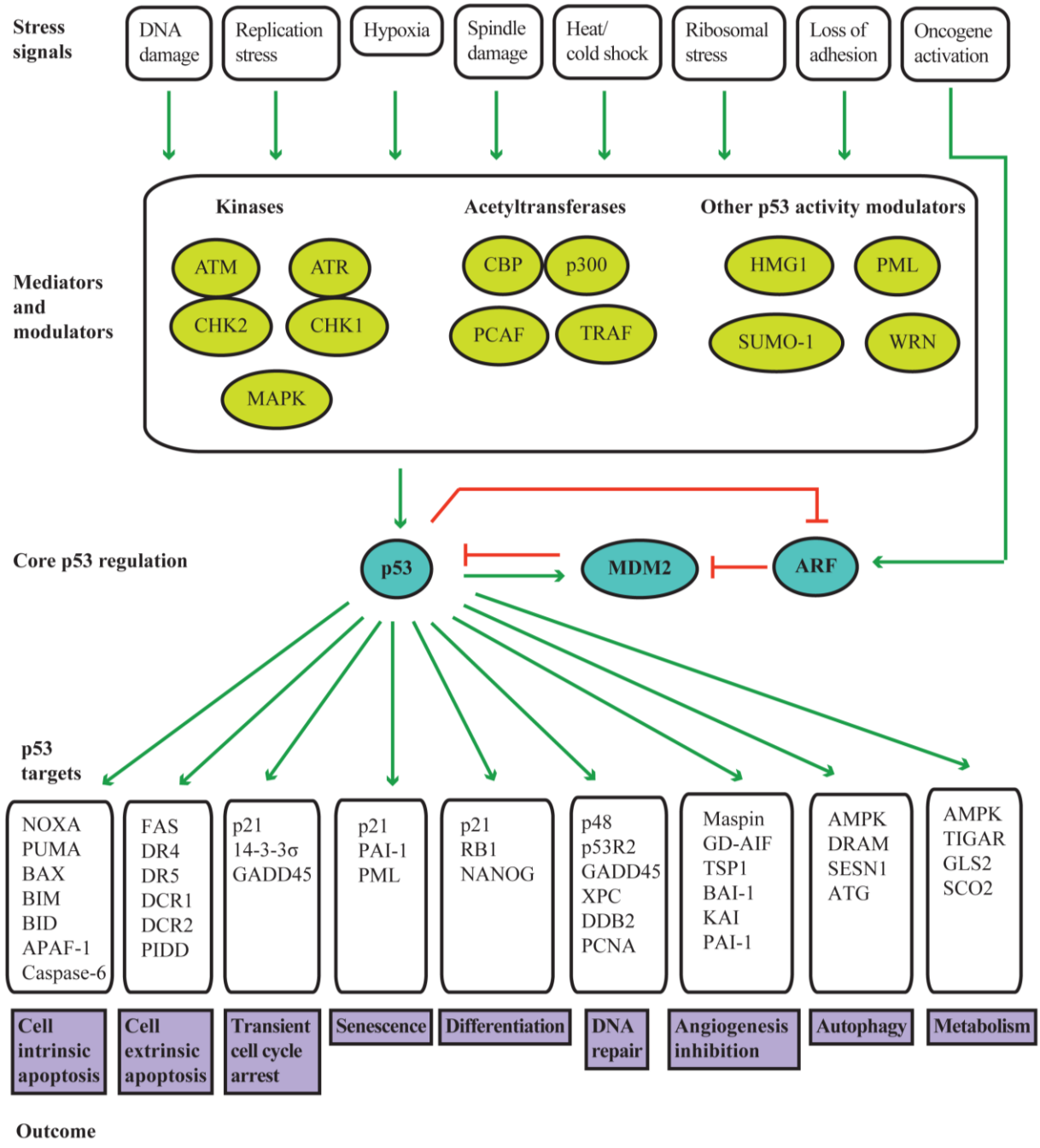

Figure 1.6 The p53 signaling pathway.

p53 signaling is initiated by a variety of stress signals. These signals activate upstream mediators and modulators, which activate p53 via post-translational modifications. p53 then transcriptionally activates a variety of targets, leading to numerous cellular outcomes. Regulation of p53 occurs in the form of a negative feedback loop involving MDM2 and ARF.

DNA replication takes place during the S phase, followed by the G2 phase where further cell growth and biosynthesis occurs. The mitotic (M) phase consists of nuclear division followed by cytokinesis[275, 276]. Non-dividing cells (e.g. differentiated cells) are maintained in the quiescent (G0) phase, which is an extended G1 phase. Cell cycle progression is controlled by a series of checkpoints and involves regulatory proteins known as cyclins and cyclin-dependent kinases (CDKs). CDKs contain a serine/threonine-specific catalytic core and act as a complex with cyclins to phosphorylate substrates required for a particular cell cycle phase. During the G1 phase, CDK2/cyclin E and CDK4/cyclin D complexes phosphorylate the retinoblastoma protein RB1, which disrupts its binding to the E2F family of transcription factors and enables the latter to activate E2F responsive genes. This includes proteins required for the G1/S transition (e.g. cyclin E, cyclin A, and CDK1), nucleotide biosynthesis enzymes, and DNA replication factors[277-279]. During the S and G2 phases, CDK2/cyclin A and CDK1/cyclin B phosphorylate FoxM1 which results in the upregulation of proteins involved in chromosome segregation and mitosis[280-282]. The activity of CDKs is inhibited by CDK inhibitors (CKIs), which comprise two families: the Cip/Kip (CDK interacting protein/Kinase inhibitory protein) family and the INK4A (Inhibitor of Kinase 4) family[283]. The Cip/Kip family, which is comprised of p21 (Cip1), p27 (Cip2) and p57 (Kip2), binds to G1-phase CDK/cyclin complexes and to a lesser extent CDK1/cyclin B[284]. The INK4 family includes p15 (INK4B), p16 (INK4A), p18 (INK4C), p19 (INK4D), and specifically inactivate G1 CDKs (CDK4 and CDK6) and prevent association with cyclins[285].

One of the most well characterized p53 targets is the CKI p21 (also known as Cip1 or CDKN1A). p21 primarily inhibits the kinase activity of CDK2/cyclin E, arresting the cell cycle in the G1 phase, but also to a lesser extent inhibits CDK2/cyclin A, which is required for progression through S phase, and CDK1/cyclin A and CDK1/cyclin B, which mediate transition through the G2 and M phases[286, 287]. CDK2/cyclin E inhibition prevents RB1 phosphorylation, which result in the E2F transcription factors remaining bound to RB1 and unable to transcribe genes required for G1-S progression (Figure 1.7). p21 may also inhibit proliferation independently of CDK2 or RB1. For example, it has been shown to associate directly with E2F1 to suppress its transcriptional activity[288]. It also binds to and inhibits the replication factor PCNA, thereby impeding DNA replication[289, 290]. p21 has been shown to

inhibit apoptosis[291]; hence high levels of p21 tend to favor a cell cycle arrest response rather than an apoptotic one following p53 activation. Another p53 target, 14-3-3σ, is responsible for mediating G2 arrest. 14-3-3σ inhibits the phosphatase CDC25, which dephosphorylates cyclin B-bound CDK1 and is essential for the G2/M progression. 14-3-3σ inhibits CDC25's activity by sequestering it in the cytoplasm, thereby causing the cell to arrest in the G2 phase[292]. Similarly, GADD45 also regulates the subcellular localization of CDK1/cyclin B, contributing to G2 arrest (Figure 1.7)[293].

Cell cycle arrest resulting from p53 activation may be transient, allowing the cell the opportunity to undergo DNA repair, or it may be permanent, resulting in senescence or differentiation. Senescence, essentially defined as an irreversible growth arrest, may be caused by the attrition of telomeres (termed "replicative senescence"), which occurs in primary cells after a limited number of cell divisions, or may be induced by various stimuli long before the cell reaches the end of its replicative lifespan - this is known as "premature senescence". Premature senescence may be caused by DNA damaging agents[294, 295], oxidative stress[296], replication stress[297], overexpression of oncogenes[298-301] and inactivation of tumor suppressors[302, 303]. Although many proteins and pathways are common to both transient cell cycle arrest and senescence - for instance, p21 is essential in both, the latter features some additional factors, pathways, and markers. Of note, senescence often involves activation of the p16-RB1 pathway in addition to p53 signaling[304]. p16 is an INK4 family CKI which specifically inhibits CDK4 and CDK6, preventing phosphorylation of RB1 and blocking E2F-dependent transcription as described above. The p53 transcriptional targets plasminogen activator inhibitor-1 (PAI-1) and PML play roles in mediating the senescence response[305-308]. PAI-1, an extra-cellular matrix (ECM)-associated protein, inhibits the activity of the secreted protease uPA which participates in the G1-S transition[308]. PML mediates p53 acetylation in response to oncogenic signals[305-307]. Senescent cells exhibit distinct phenotypical changes, adopting a flattened, enlarged, and irregular morphology[301, 309, 310], and acquire distinct and widespread alterations in gene expression, with massive downregulation of genes required for cell cycle progression and DNA replication, and upregulation of cell cycle inhibitors and proteins that remodel the extracellular matrix or mediate local inflammation[311-316]. They express various biomarkers, the most distinctive one being elevated senescence-associated β-

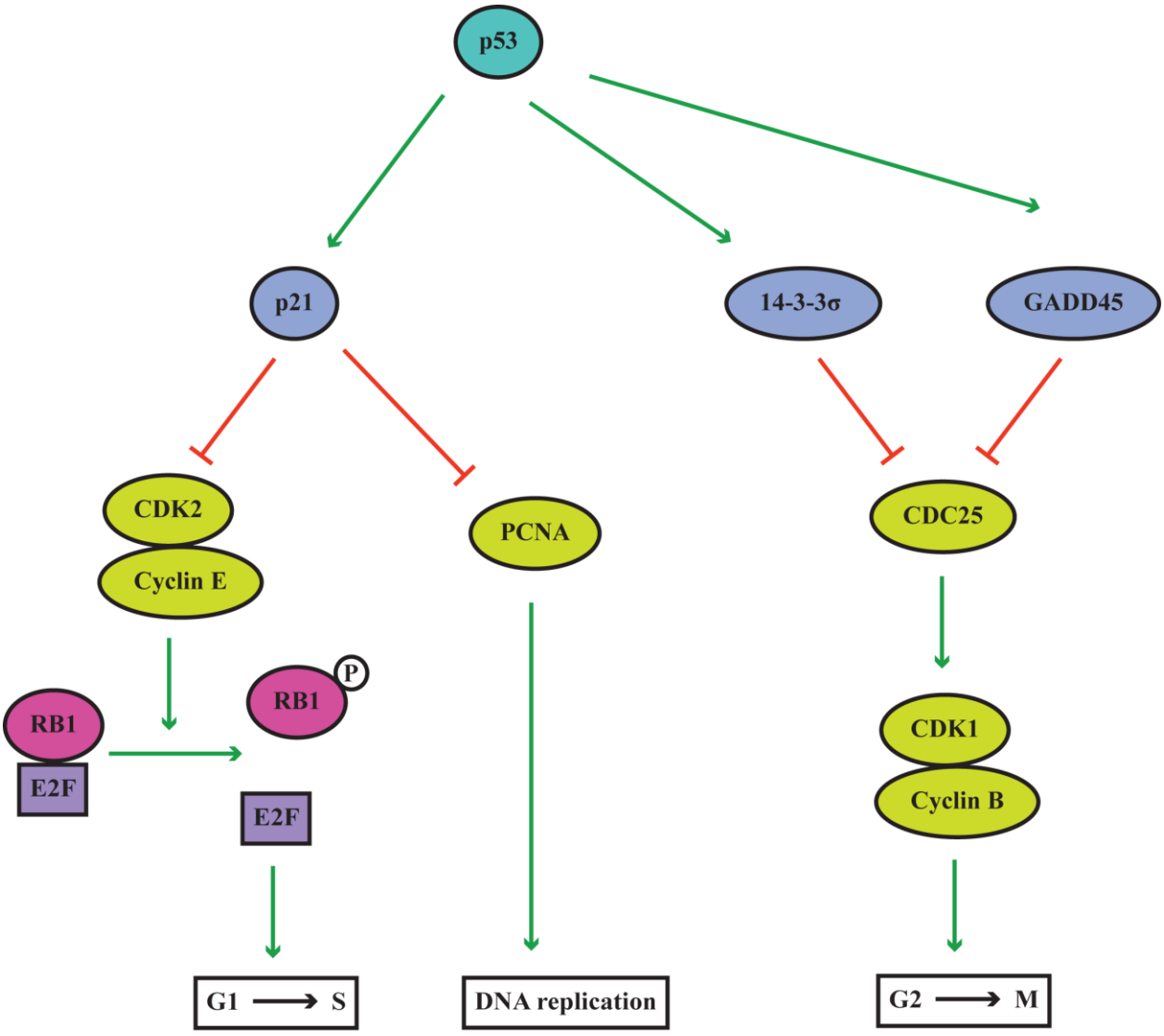

Figure 1.7 The role of p53 in cell cycle control.

Under normal cellular conditions, CDK2/cyclin E phosphorylates RB1, causing the release of E2F, which then transcribes genes required for G1-S progression. Activation of CDK1/cyclin B by CDC25 is required for the G2-M transition. Upon transcriptional upregulation by p53, p21 inhibits the CDK2/cyclin E complex, leading to accumulation of hypophosphorylated RB1 which remains bound to E2F, arresting the cell in the G1 phase. p21 also inhibits PCNA, which is required for DNA replication. The p53 targets 14-3-3σ and GADD45 inhibit CDC25 activity, leading to cell cycle arrest in the G2 phase.

galactosidase (SA-β-gal) activity[317]. SA-β-gal reflects the increased lysosomal biogenesis which accompanies cellular senescence, and is exclusive to senescent cells and not observed in arrested or terminally differentiated cells[318]. Senescent cells may also harbor senescence-associated DNA damage foci (SDFs) and senescence-associated heterochromatin foci (SAHFs)[319, 320] but these are neither universal nor exclusive to the senescent state.

Differentiation is another outcome associated with cell cycle arrest, and requires activation of RB1 in addition to p21, as well as p53-mediated repression of NANOG[274, 321]. Arrested cells may re-enter the cell cycle after DNA repair, a process which requires p53-mediated activation of several genes including GADD45, p53R2, p48, PCNA, DDB2, and XPC[322-326].

1.6.5 p53-dependent apoptosis

The other major cell fate following p53 activation is apoptosis. In metazoan cells, apoptosis proceeds through one of two signaling cascades, termed the cell-extrinsic (ligand-dependent) and the cell-intrinsic (mitochondrial-dependent) pathways, both converging on caspase activation. Most of the stimuli which activate p53 signaling (e.g. DNA damage, cell stress) lead to cell intrinsic apoptosis. This pathway is largely mediated by the BCL-2 family of proteins which regulate mitochondrial outer membrane permeabilization (MOMP), leading to caspase activation and cell death. BCL-2 family members contain one to four α-helical BCL-2 homology (BH) domains (named BH1, BH2, BH3 and BH4) through which they can interact, and are categorized into three subfamilies - one anti-apoptotic (or pro-survival) and two pro-apoptotic[327, 328]. The anti-apoptotic group, also known as “BCL-2 like”, includes BCL-2, BCL-XL, MCL-1, A1 and BCL-W. These proteins maintain the outer-mitochondrial membrane integrity by binding to and inhibiting members of the “BAX-like” pro-apoptotic family, which is comprised of BAX and BAK (Figure 1.8). Oligomerization of BAX and BAK enables formation of pore structures which penetrate the outer mitochondrial membrane and effect MOMP[329, 330]. This releases cytochrome C and other mitochondrial intermembrane space proteins into the cytoplasm. Cytochrome C binds the apoptotic peptidase activating factor 1 (APAF-1), leading to the assembly of a heptameric protein ring called the apoptosome, which recruits procaspase-9. Procaspase-9 is the inactive precursor to the caspase-9, an initiator caspase. Once bound to the

apoptosome, it becomes activated through dimerization. Caspase-9 then activates downstream effector caspases through proteolytic cleavage (e.g. caspase-3 and caspase-7), which then carry out degradation of cellular components (Figure 1.8)[329, 330]. The other pro-apoptotic BCL-2 subfamily is called the "BH3-only" family, so named because the members contain only one BH domain (BH3), and includes NOXA, PUMA, BIM, BAD, BID, BMF and HRK. BH3-only proteins initiate MOMP either by direct activation of BAX/BAK oligomerization, or indirectly by binding to and sequestering the BCL-2-like pro-survival proteins (Figure 1.8)[329, 330].

Many of the BCL-2 family proteins, in particular BAX, NOXA, PUMA, BIM, and BID, are transcriptional targets of p53, and hence their upregulation upon stress-induced p53 activation initiates apoptosis[331-336]. NOXA, PUMA, and BIM all promote apoptosis by inhibiting BCL-2-like pro-survival factors, but differ in their specificity: PUMA and BIM bind strongly to all BCL-2-like members, whereas NOXA can only bind MCL-1 and A1 efficiently[337]. BID and BIM can bind to and activate BAX directly by inducing its oligomerization with BAK and its insertion into the mitochondrial outer membrane[338-341]. In addition, p53 transcriptionally activates components of the apoptotic effector machinery, namely APAF-1 and caspase-6[342-345]. p53-mediated transcriptional repression also contributes to the apoptotic pathway. Survivin is a member of the inhibitor of apoptosis (IAP) family which binds to caspase-3 and caspase-7 and prevents processing of these caspases into their active forms[346]. p53 represses survivin expression by recruiting histone deacetylases to its promoter region[347]. Although p53 regulates its target genes primarily at the transcriptional level, it has been shown to elicit apoptosis via transcription-independent mechanisms as well. A study by Chipuk and colleagues demonstrated that cytosol-localized p53 was able to directly activate BAX, inducing its oligomerization with BAK and enabling MOMP. p53 also released BAX and BAK from binding to BCL-XL, demonstrating that it functioned as a BH3-only type protein[348]. This illustrates the multifaceted nature of p53 and the complexity of its role in the intrinsic apoptotic pathway.

p53 also regulates the extrinsic apoptotic pathway. Here, cell surface transmembrane

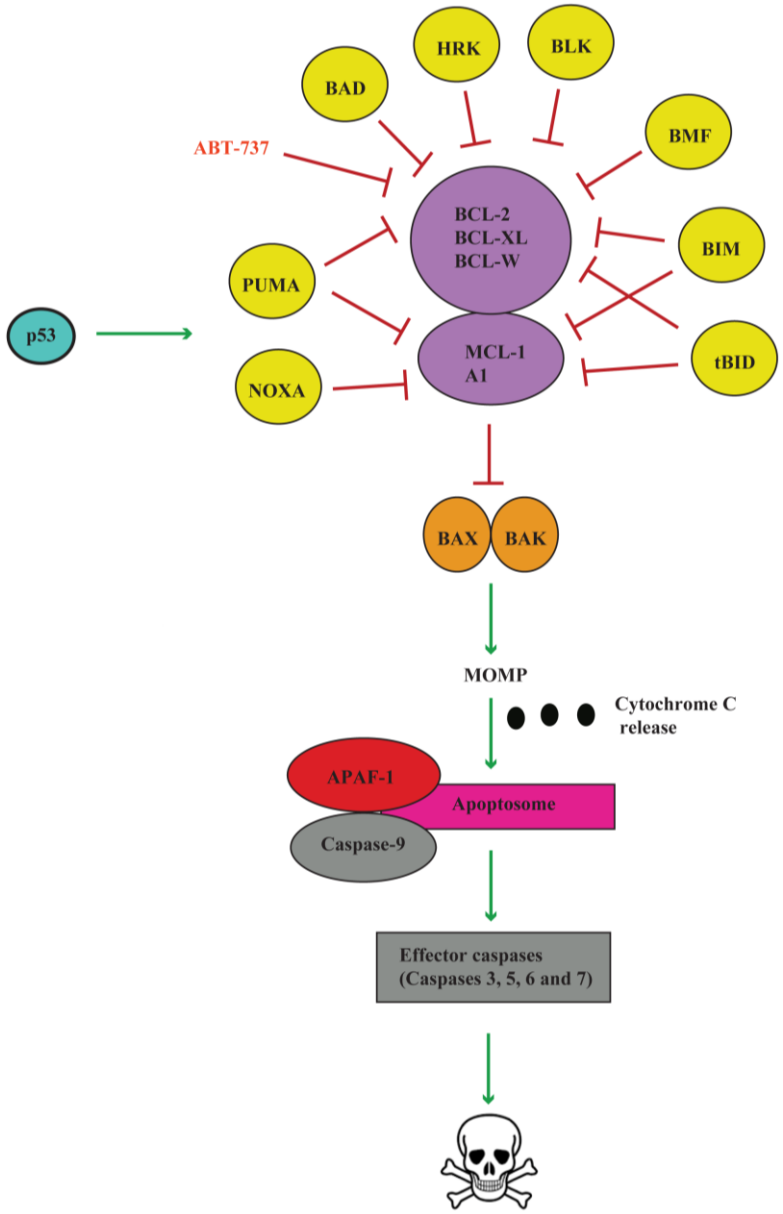

Figure 1.8 Schematic representation of the intrinsic apoptotic pathway regulated by BCL-2 family members.

The intrinsic apoptotic pathway is regulated by the BCL-2 family of proteins which comprise three subfamilies: the anti-apoptotic BCL-2-like proteins (BCL-2, BCL-XL, BCL-W, MCL-1 and A1), the pro-apoptotic BAX and BAK subgroup, and the pro-apoptotic BH3-only proteins (shown in yellow). BAX/BAK oligomerization induces mitochondrial outer membrane permeabilization (MOMP), which initiates the caspase cascade. Many BCL-2 family members are transactivated by p53. ABT-737, a BH3 mimetic, has a similar binding profile as BAD.

receptors called “death receptors” are activated by extracellular ligands. This typically occurs as part of immune responses. Three well characterized death receptors are Fas, TNF-R1, and DR5, which bind the FasL, TNF, and TRAIL ligands respectively. Ligand binding induces a conformational change in the receptor, leading to recruitment of adaptor molecules and binding of an initiator caspase, caspase-8[349-352]. This leads to the dimerization and activation of caspase-8 through self-cleavage, which then cleaves and activates the effector caspases (caspase-3 and caspase-7), leading to apoptosis[353]. Crosstalk between the extrinsic and intrinsic pathways occurs through caspase-8-mediated cleavage and activation of BID, which allows it to translocate into the mitochondria and effect cell intrinsic apoptosis[354]. The death receptors FAS, DR5, DR4, DCR1, and DCR2, the FAS ligand, and the adaptor protein PIDD are all direct p53 targets[355-362].

1.6.6 p53 and chemotherapy

The fact that various stimuli are able to activate p53 signaling and induce cell cycle arrest/senescence or apoptosis has been exploited in anti-cancer drug development. Traditional chemotherapy makes use chemical agents that create DNA lesions via a variety of different mechanisms. Some agents, such as bleomycin, induce DNA double-stranded breaks directly, which are then detected by p53’s upstream mediators[363]. Other chemicals create DNA breaks via more indirect mechanisms. Alkylating agents are the oldest class of antineoplastic drugs and act by covalently transferring alkyl groups to DNA, resulting in either intrastrand or interstrand DNA crosslinks. Attempts to replicate crosslinked DNA leads to breakage[364, 365]. This class of drugs include nitrogen mustards (e.g. cyclophosphamide, bendamustine, and melphalan)[366-368], nitrosoureas (e.g. carmustine and lomustine)[369, 370], and platinum-containing agents (cisplatin, carboplatin, and oxaliplatin)[371]. Another class of chemotherapeutics is topoisomerase inhibitors, which inhibit either topoisomerase I or topoisomerase II. Topoisomerases are responsible for releasing the torsional strain of DNA during DNA double-helix unwinding (e.g. during DNA replication or transcription) and do so by creating transient single-stranded (in the case of topoisomerase I) or double-stranded (in the case of topoisomerase II) breaks which are then religated[372, 373]. Topoisomerase inhibitors trap the DNA-enzyme intermediate as a complex, preventing religation of the break which is then detected by upstream

mediators of p53 signaling[374]. Camptothecin is an inhibitor of topoisomerase I whereas etoposide and doxorubicin are examples of topoisomerase II inhibitors[375-379]. Doxorubicin also belongs to a class of compounds called anthracyclines, which in addition to topoisomerase inhibition, have other mechanisms of action including basepair intercalation and generation of free oxygen radicals[380, 381]. Chemotherapeutics may also induce p53 activation through replication stress. Anti-metabolites mimic the structure of normal cellular molecules and interfere with DNA or RNA synthesis. Examples include pyrimidine analogs such as 5-fluorouracil (5-FU) and cytosine arabinoside which mimic thymidine and cytosine respectively[382, 383], and purine analogs including 6-mercaptopurine and thioguanine which mimic adenine and guanine respectively[384, 385]. The analogs may be incorporated into DNA, but addition of subsequent nucleosides is blocked, preventing chain elongation and leading to stalled replication. DNA replication may also be impeded by compounds which interfere with the synthesis of nucleosides; these include methotrexate and pemetrexed which inhibit dihydrofolate reductase[386-388] and hydroxyurea which inhibits ribonucleotide reductase[389-391]. Microtubule poisons (e.g. paclitaxel) which prevent microtubule polymerization or depolymerisation represent yet another class of chemotherapeutics[392].

Traditional strategies act by killing rapidly dividing cells and take advantage of the fact that cancer cells typically have higher rates of proliferation compared to normal cells. However, these chemotherapeutics often have significant toxic side effects, owing to the fact that they also damage normal cells, especially in highly proliferative tissues. More recently, targeted molecular therapeutics, which are a class of drugs that inhibit specific gene products involved in tumor maintenance, offer greater selectivity in eliminating cancer cells. Many of these drugs inhibit the activity of growth factors and oncogenes, while others inhibit normal proteins on which tumor cells have a higher dependency. Targeted therapeutics include tyrosine kinase inhibitors such as imatinib (which inhibits Abl, c-kit and PDGF-R and is used to treat chronic myelogenous leukemia harboring the Bcr-Abl translocation)[393]; the EGFR inhibitors gefitinib, erlotinib and cetuximab[200-203, 394]; and crizotinib, bevacizumab, and trastuzumab which target the ALK, VEGF, and ERBB2 receptors respectively[395-397]. Another means of curtailing tumorigenesis involves targeting components of the RAF/MEK/ERK and PI3K/AKT/mTOR pathways involved in cell proliferation and the downstream translational machinery, which are often

deregulated in cancers. These include the MEK inhibitor trametinib, the BRAF inhibitor dabrafenib[398], and mTOR inhibitors rapamycin, temsirolimus and everolimus[399, 400], which are currently used in the clinic, as well as small molecule inhibitors currently in clinical trials or which show promise as chemotherapeutic agents in cell culture or preclinical models. Several compounds which target components of the eIF4F complex show promising anti-tumor activity. These include cap analogs (e.g. 4Ei-1)[401], eIF4A inhibitors (e.g. hippuristanol, pateamine A, silvestrol and other rocaglamides)[402-404], and compounds targeting the eIF4E/eIF4G interaction (e.g. 4EGI-1, 4E1RCat, 4E2RCat)[405-407].

1.6.7 Targeting the apoptotic machinery in chemotherapy

The clinical efficacy of most of the chemotherapeutic drugs described above is dependent upon their ability to induce apoptosis in tumor cells. Hence, resistance may arise due to defects in p53 itself or in components of the downstream apoptotic pathway, which uncouples apoptosis from the upstream stress signals. Overexpression of anti-apoptotic proteins or defects in BH3-only proteins often results in poor clinical outcomes[408-410]. In particular, MCL-1 and BCL-2 are frequently overexpressed in many cancers, and lead to resistance to conventional chemotherapy[411]. There has therefore been much interest in the development of drugs which act directly on the apoptotic machinery. One class of drugs which target apoptotic factors are the BH3 mimetics - small molecules that mimic the interactions between native BH3-only proteins and the anti-apoptotic BCL-2-like proteins[412]. BH3 mimetics bind to the α-helical groove in the BH3 domains of the anti-apoptotic proteins, interfering with their inhibitory binding to BAX and BAK and thereby allowing MOMP to proceed[412]. ABT-737 (and its orally available analog ABT-263 (Navitoclax)) is the best characterized amongst these. A mimic of BAD, it binds to BCL-2, BCL-XL, and BCL-W with high affinity but can only bind weakly to MCL-1 and A1[413, 414]. It has been shown to be effective in treating tumors harboring high BCL-2 levels and low MCL-1 levels, including many B lymphoid tumors and chronic lymphocytic leukemia (CLL) cells, as well as small cell lung cancer carcinomas[413]. However, many cancers acquire resistance through upregulation of MCL-1[414-416].

The field of chemotherapeutic development is a fast-growing one and faces many challenges. Both traditional chemotherapy and targeted therapeutics can have deleterious effects

on normal cells, and finding a good therapeutic index is often difficult. The problem of chemotherapeutic resistance, whether to targets within the apoptotic pathway or upstream of it, is a recurrent one. Attempts to overcome these limitations include the use of combination therapy, the simultaneous administration of two or more drugs. Another problem is that many targets are not directly druggable, due to their structure or the mechanism by which their function is regulated. For example, the oncogene Ras is mutated in approximately 30% of all cancers, but no effective Ras inhibitors have yet been developed, although there have been promising recent studies[417, 418]. MYC is another oncogene which is frequently mutated in cancers, but finding potent and selective inhibitors has been difficult due to lack of well-defined druggable sites[419, 420]. One solution to this is to find other proteins in the same pathway that may be more easily targeted. Indeed, much effort is currently being made to identify novel chemotherapeutic targets for use either as a single agent or in combination with existing therapeutics.

1.7 DHX9 as a potential chemotherapeutic target

Recent research has supported the notion of targeting DHX9 as a chemotherapeutic approach. Ewing's sarcoma family tumors (ESFTs) is a pediatric cancer driven by a t(11;22) chromosomal translocation which fuses the 5' transactivation domain of EWS with the 3' ETS domain of the transcription factor FLI1. The resulting fusion protein, EWS-FLI1, is oncogenic and acts as a potent aberrant transcription factor[421]. DHX9 interacts with EWS-FLI1 and is required as a transcription co-activator of EWS-FLI1-responsive genes[192]. A small molecule (YK-4-279) blocking the interaction between DHX9 and EWS-FLI1 was found to induce apoptosis in ESFT cells and inhibit tumor growth in xenograph models[82]. YK-4-279 activity has been optimized through pharmacokinetic studies and an orally available formulation has been developed, thus making it a promising candidate for clinical development[422, 423].

The Pelletier lab had previously uncovered DHX9 as a hit in an shRNA screen for sensitizers to ABT-737. ABT-737 has been shown to be an effective chemotherapeutic in many tumor settings[413, 424-427]; however, many cancers are resistant to ABT-737 treatment alone[428-430]. One of the factors mediating sensitivity to ABT-737 is the relative levels of various apoptotic proteins in the cell. Given that ABT-737 potently inhibits BCL-2, BCL-XL,

and BCL-W but not MCL-1 and A1[414, 431], many cancers acquire resistance through upregulation of MCL-1 and inhibition of MCL-1 dramatically improves the effectiveness of ABT-737 intervention[414-416]. To widen the therapeutic window of ABT-737, an shRNA screen was conducted to search for other genes which were not lethal themselves, but when knocked down, would increase sensitivity to ABT-737 in resistant cells. Using a focused shRNA library which included RNA helicase family members, the screen was performed in *Arf*$^{-/-}$ Eμ–*Myc*/Bcl-2 mouse lymphoma cells, which overexpress MYC and exogenous BCL-2 and are resistant to ABT-737. From this screen, it was found that several shRNAs targeting DHX9 synergized with ABT-737 in killing the lymphoma cells[432]. Further investigation demonstrated that this synergy was p53-dependent, with p53 and many of its downstream transcriptional targets being activated upon DHX9 knockdown. The p53 target NOXA was required for the DHX9-ABT-737 synergy. The synergy was also MYC-dependent, and loss of DHX9 activated a replicative stress pathway characterized by increased levels of phospho-ATR (S428), phosph-CHK1 (S345), and defective S-phase progression. Taken together, a model was constructed whereby DHX9 suppression induces replicative stress, which, together with MYC overexpression, leads to p53 activation and upregulation of NOXA. NOXA in turn inhibits MCL-1, resulting in ABT-737 sensitization and ultimately apoptosis[432]. Structure-function analysis using DHX9 mutants determined that the DHX9-ABT-737 synthetic lethal relationship was dependent on functional NTPase/helicase activity, as well as intact dsRBDI, dsRBDII, and C-terminal regions[432]. The *Arf*$^{-/-}$Eμ-*Myc*/Bcl-2 model recapitulates several clinically relevant features of non-Hodgkin's lymphomas; DHX9 may therefore show promise as a candidate target to suppress in combination with ABT-737 or its derivatives.

1.8 Overview and rationale for thesis

DHX9's interaction with an extensive and varied array of nuclear and cytoplasmic protein and nucleic acid partners, in the context of many different biological processes, indicates that it is an important regulator of gene expression. Although much has been uncovered about DHX9 in the past three decades, there is still a lot of information to be gained with respect to its structure,

substrates, binding partners, and functions. There remain many unanswered questions concerning the mechanistic properties of DHX9 – for example, the processivity of its helicase activity, why it prefers certain substrates to others, and how it is able to recognize and bind to specific sequences or structures on DNA or RNA. In addition, the precise role of DHX9 in many of the biological processes in which it participates is currently unclear. While recent studies have implicated DHX9 in a variety of human diseases, research on the potential of using DHX9 as an anti-neoplastic or anti-viral target is still very much in its infancy.

As discussed above, our lab had identified DHX9 as a potential chemotherapeutic target for use in combination therapy with ABT-737, using *Arf*$^{-/-}$Eμ-*Myc*/Bcl-2 mouse lymphomas. In this thesis, I followed up on previous studies in our research group by further characterizing the relationship between DHX9 and p53. In Chapter 2, we established a role for DHX9 in DNA replication and cell cycle progression and showed that suppression of DHX9 in primary human diploid fibroblasts activates a p53-dependent senescence response. In Chapter 3, we explored in greater depth the therapeutic potential of targeting DHX9 by first examining the consequences of DHX9 suppression in various tumor models, and next assessing the effect of systemic DHX9 suppression at the organismal level using a doxycycline-inducible shDHX9 transgenic mouse model. We observed that loss of DHX9 is deleterious in most tumor settings but is well tolerated in adult mice, which supports the targeting of DHX9 as a chemotherapeutic approach. Finally, in Chapter 4, we demonstrated that although DHX9-mediated apoptosis or senescence is p53-dependent in certain settings, there is also a p53-independent aspect. We investigated the outcome of suppressing DHX9 in p53-deficient cells and examined the mechanisms underlying this p53-independent effect.

CHAPTER 2: SUPPRESSION OF THE DHX9 HELICASE INDUCES PREMATURE SENESCENCE IN HUMAN DIPLOID FIBROBLASTS IN A P53-DEPENDENT MANNER

Published in:

Lee T, Di Paola D, Malina A, Mills JR, Kreps A, Grosse F, Tang H, Zannis-Hadjopoulos M, Larsson O, and Pelletier J. (2014). Suppression of the DHX9 Helicase Induces Premature Senescence in Human Diploid Fibroblasts in a p53-Dependent Manner. *J Biol Chem* **289(33):**22798-22814.

2.1 Preface to Chapter 2

Our lab had initially uncovered DHX9 as a hit in an shRNA screen for sensitizers to the BH3-mimetic ABT-737. ABT-737 is effective against many, but not all cancers, and upregulation of the anti-apoptotic protein MCL-1 is a major cause of resistance. DHX9 suppression sensitized *Arf*$^{-/-}$Eμ-*Myc*/Bcl-2 mouse lymphomas to ABT-737. This was accomplished via aggravation of replicative stress, which acted in concert with MYC elevation to activate a pro-apoptotic p53 signaling pathway. The p53 target NOXA was essential for this process, and the results led to a model whereby aggravation of replicative stress resulting from loss of DHX9 activated p53, which transcriptionally upregulated NOXA. NOXA can then inhibit MCL-1, enabling the cells to undergo apoptosis[432]. While this study established a relationship between p53 and the DHX9-ABT-737 synergy, the mechanism of how loss of DHX9 activated p53 was not entirely clear. During the course of this study, it was noted that suppression of DHX9 in NIH3T3 cells resulted in a dramatic reduction in growth rates. We wished to determine whether this phenomenon extended to non-transformed cells, and whether suppressing DHX9 in primary cells could provide us with greater insight on the DHX9-p53 relationship. In this chapter, we assessed the consequences of suppressing DHX9 in primary human diploid fibroblasts which harbored functional p53 signaling. We observed a premature senescence phenotype upon DHX9 suppression in the fibroblasts, and we investigated the role of p53 signaling in triggering the senescence response. In addition, we analyzed changes in gene expression following DHX9 suppression, as well as the effect on DNA replication.

2.2 Abstract

DHX9 is an NTP-dependent DExH-box helicase with a multitude of cellular functions. Its ability to unwind both DNA and RNA, as well as aberrant, non-canonical polynucleotide structures, has implicated it in transcriptional and translational regulation, DNA replication and repair, and maintenance of genome stability. We report that loss of DHX9 in primary human fibroblasts results in premature senescence, a state of irreversible growth arrest. This is accompanied by morphological defects, elevation of senescence-associated β-galactosidase levels, and changes in gene expression closely resembling those encountered during replicative (telomere-dependent) senescence. Activation of the p53 signaling pathway was found to be essential to this process.

ChIP analysis and investigation of nascent DNA levels revealed that DHX9 is associated with origins of replication and that its suppression leads to a reduction of DNA replication. Our results demonstrate an essential role of DHX9 in DNA replication and normal cell cycle progression.

2.3 Introduction

One of the earliest observations made with respect to the culturing of normal somatic cells derived from human tissue is the fact that they do not propagate indefinitely, but invariably enter a state of irreversible growth arrest after a limited number of cell divisions[433]. Hayflick and Moorhead reported that primary human fibroblasts undergo a period of relatively rapid proliferation following establishment in culture, but that cell division slowed with increasing time and eventually ceased altogether after an average of ~50 cumulative population doublings [433]. This phenomenon, termed "cellular senescence", was subsequently attributed to the attrition of telomeres. With each round of DNA replication and cell division, the telomeres capping the ends of chromosomes become shortened due to the inability of DNA polymerase to fully synthesize the 3' ends of DNA[434, 435]. When the telomeres reach a critical length, a DNA damage response is triggered, leading to cell cycle arrest and inhibition of further replication[436].

In addition to telomere-dependent senescence, termed "replicative senescence", various stimuli have been shown to cause primary cells to senesce long before they reach the end of their replicative lifespan. This "premature senescence" can be induced by DNA damaging agents [294, 295], oxidative stress[296], persistent replication stress[297], overexpression of oncogenes [298-301] and inactivation of certain tumor suppressors[302, 303]. Loss or mutation of genes involved in the maintenance of genomic stability, such as the WRN and BLM helicases, can also lead to early senescence[437-440]. Premature senescence is of particular interest both in studies of the aging process and aging-related disorders, and in cancer research as a potential chemotherapeutic strategy. Indeed, induction of senescence has been shown to be an important mechanism in eliciting an anti-tumor response[311, 441-443].

Senescent cells exhibit several characteristics which can be used as identifiers of this biological phenomenon. The most prominent is a permanent, irreversible cell cycle arrest in the

G1 phase[444]. Senescent cells adopt a flattened, expanded, and irregular morphology, are often multinucleated, and may contain increased vacuolar structures[301, 309, 310]. A distinctive biomarker, one which can be used to distinguish senescent cells from quiescent or terminally differentiated cells, is the expression of senescence-associated β-galactosidase (SA-β-gal) activity[317]. In addition, senescence is accompanied by changes in the gene expression profile [316]; in particular, activation of the p53 and p16-RB1 signaling pathways and changes in expression of cell cycle proteins have been observed[301, 445].

DHX9 (also known as Nuclear DNA Helicase II (NDH II) and RNA helicase A (RHA)) is a DExH-box helicase that exhibits both RNA and DNA helicase activity[1], as well as triple helical DNA unwinding activity[2]. It was originally isolated from bovine tissue[16] and consists of two RNA-binding domains at the N-terminus, a core helicase region consisting of seven conserved helicase motifs, and a DNA-binding domain and nuclear localization signal at the C-terminus[26]. DHX9 is a multifunctional protein that has been implicated in several biological processes, including regulation of transcription[120, 124, 138], translation[148, 152], RNA transport[182], miRNA processing[171], and genome maintenance processes[2, 38, 98]. Its interacting partners include the transcriptional coactivator CREB-binding protein, EGFR, the tumor suppressor BRCA1, and RNA polymerase II[120, 124, 138]. It has also been found to be associated with the Ku protein complex, a component of DNA-PK which plays a role in non-homologous end-joining-mediated DNA repair[91].

We previously conducted an shRNA screen in search of modifiers of sensitivity to ABT-737 (an inhibitor of BCL-2 family pro-survival factors) in *Arf*$^{-/-}$*Eμ-Myc*/Bcl-2 lymphoma cells, and found that DHX9 suppression was synthetic lethal with ABT-737[432]. Subsequent experiments showed that ABT-737 sensitization caused by DHX9 suppression was due to the activation of a p53-dependent apoptotic program[432]. To further characterize DHX9, we investigated its role in primary human diploid fibroblast cell lines and find that its suppression leads to pronounced p53-dependent growth arrest and premature senescence. Chromatin Immunoprecipitation (ChIP) assays and analysis of nascent DNA production revealed that DHX9 is located at origins of replication and that DNA replication is inhibited upon DHX9 knockdown. Our results are consistent with a role of DHX9 in DNA replication and suggest that its suppression leads to senescence in primary human diploid fibroblast cells brought on by an

inhibition of replication.

2.4 Results

2.4.1 Loss of DHX9 results in morphological changes, senescence-associated β-galactosidase activity, and growth arrest in primary human cells

We have previously shown that suppression of DHX9 acts in concert with elevated MYC expression to enhance ABT-737 sensitivity[432]. During the course of these experiments, we noted that suppression of DHX9 in NIH3T3 cells resulted in a dramatic reduction in growth rates (Figure 5A in Ref. [432]). In order to assess if this phenomenon extended to non-transformed cells, we sought to investigate the consequences of DHX9 suppression in MRC-5 cells, a primary human diploid lung fibroblast line. Reduction in DHX9 levels via lentiviral transduction using two independent shRNAs resulted in striking morphological changes in MRC-5 cells (Figure 2.1A, day 14 P.I.). Whereas control cells are small, spindle-shaped, and refractile, suppression of DHX9 leads to cells that are more flattened, enlarged, and irregularly shaped. Morphologically, they resemble cells overexpressing the mutant hRAS V12 oncogene (resulting in oncogene-induced senescence) and late passage MRC-5 cells which had been in culture for over 5 months. In addition, DHX9-suppressed cells stained positive for SA-β-gal, a distinguishing marker of senescent cells (Figure 2.1B, day 14 P.I.). DHX9 shRNA-expressing cells show a significantly higher percentage of SA-β-gal-positive cells compared to MRC-5 controls (50-57% for DHX9 knockdown cells compared to 3% for shFLuc.1309-expressing cells) (Figure 2.1D, day 14 P.I.). The morphological changes and SA-β-gal expression required time to manifest, as the differences were only apparent at day 14 post-infection but not at day 6 post-infection (Figure 2.1A, B, and D). These results were not restricted to MRC-5 cells and extended to IMR-90, another primary human diploid fibroblast cell line (Figure 2.1E). Measurements of the growth rates of DHX9-depleted MRC-5 cells indicated these to be at least two-fold lower than control cells, and similar to hRAS V12-expressing cells (Figure 2.2A). Cell cycle analyses showed an increase in the percentage of cells in the G0/G1 phase and a decrease in the percentage of cells in

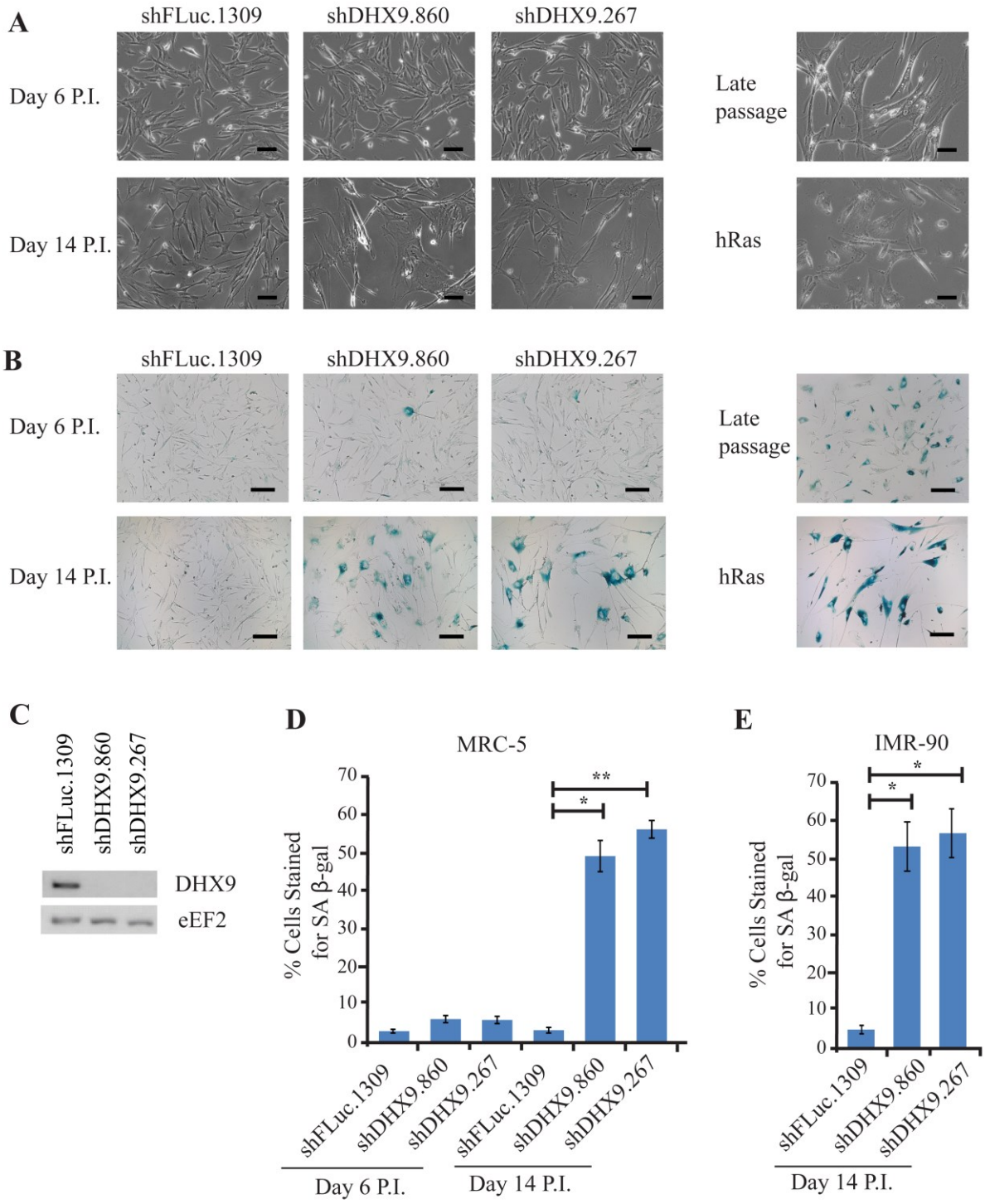

Figure 2.1 DHX9 knockdown results in morphological changes and increased senescence-associated β-galactosidase staining in primary human cells. Figure legend on following page.

Figure 2.1 DHX9 knockdown results in morphological changes and increased senescence-associated β-galactosidase staining in primary human cells.

(A) Phase and **(B)** β-galactosidase staining of MRC-5 cells transduced with lentivirus expressing the indicated shRNAs or hRAS V12 cDNA, harvested 6 and 14 days post-infection (P.I). Late passage MRC-5 cells and senescent cells induced by hRAS V12 transduction are shown for comparison. Bars represent 100 μm for the phase images and 200 μm for the β-galactosidase-stained images. **(C)** Western blot showing knockdown efficiencies of DHX9 shRNAs in MRC-5 cells following transduction with lentiviral vectors. Extracts were prepared from cells 8 days following infection, fractionated by SDS-PAGE, transferred to PVDF membrane and probed with antibodies to the indicated proteins. **(D)** Quantitation of β-galactosidase staining from (B). Cells from at least 5 independent fields/experiment were quantitated. Error bars represent SEM, N=3. *$p<0.01$, **$p<0.001$. **(E)** Quantitation of β-galactosidase staining from IMR-90 cells transduced with the indicated shRNAs. Cells from at least 5 independent fields/experiment were quantitated. Error bars represent SEM, N=3. *$p<0.01$.

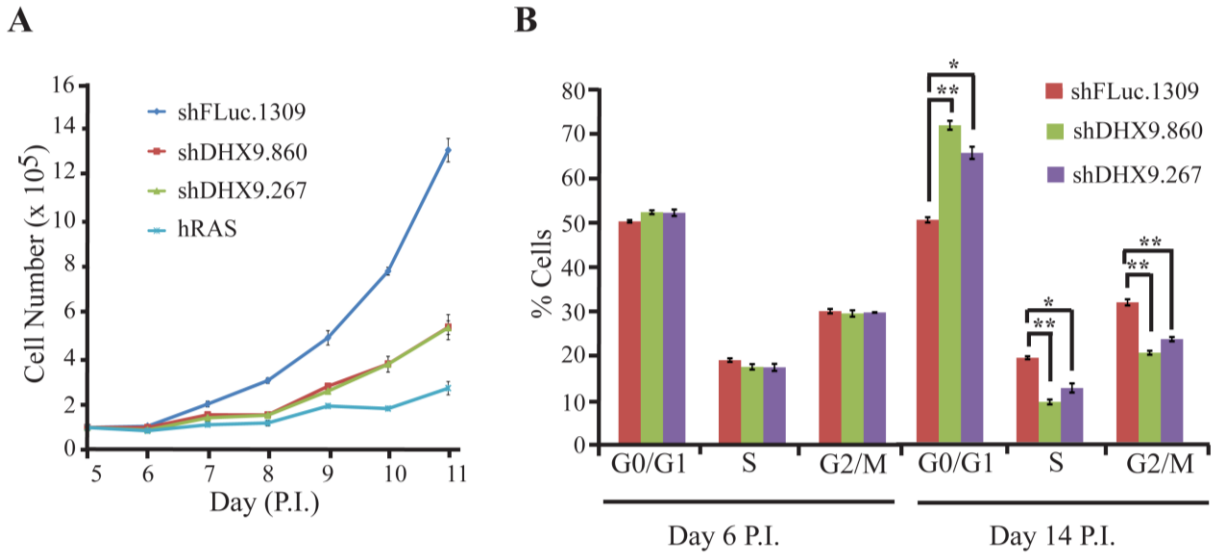

Figure 2.2 DHX9 knockdown results in a pronounced growth arrest in MRC-5 cells.

(A) Growth curves for MRC-5 cells transduced with hRAS V12 cDNA, shFLuc.1309 or DHX9 shRNAs. Cells were counted between days 5 and 11 post-infection (P.I.). Error bars represent SEM, N=3. **(B)** Cell cycle analysis of MRC-5 cells transduced with control or DHX9 shRNAs, at 6 and 14 days post-infection (P.I.). Error bars represent SEM, N=3. *p<0.01, **p<0.001.

the S and G2 phases 14 days after infection of DHX9 shRNAs (Figure 2.2B). Taken together these results demonstrate that suppression of DHX9 causes premature senescence in MRC-5 cells.

2.4.2 DHX9 suppression leads to changes in some cell cycle regulatory and DNA damage response proteins

To gain insight into the possible mechanisms through which loss of DHX9 induces premature senescence, we examined the expression of various cell cycle and DNA damage response proteins (Figure 2.3). Hyperphosphorylated RB1 levels were markedly decreased, indicating RB1 activation (Figure 2.3A, C). Hypophosphorylated RB1 levels were slightly increased, although the increase did not appear to compensate for the levels of the decreased hyperphosphorylated form; this may be due to increased RB1 degradation or due to the fact that the RB1 antibody may not bind to phosphorylated and non-phosphorylated RB1 with equal efficiency. Elevated levels of p53 and p21 is a common feature of cellular senescence, and we observed a moderate increase in p53 levels and a substantial increase in p21 in shDHX9-transduced cells compared to control cells, both at 4 and 8 days post-infection (Figure 2.3B, C). Activation of p53, p21, and RB1 is consistent with previous data showing that these proteins are upregulated during senescence induced by Ras expression or etoposide treatment[301, 446]. However, contrary to what is observed with etoposide and Ras-induced senescence, p16 levels are not elevated upon DHX9 knockdown[301, 447]. In addition, we examined markers of DNA damage and replicative stress, phospho-H2AX (S139), 53BP1, and phospho-CHK1 (S345) respectively. Whereas these markers show an increase in the case of etoposide-induced senescence, no change was detected in their levels upon loss of DHX9 (Figure 2.3 and data not shown). ATR, another marker of DNA damage and replicative stress, is activated in many forms of senescence[448], but no activation was observed under our tested conditions. Our results indicate that the p53 and RB1 pathways are involved in DHX9-induced senescence; however, the precise mechanism of action differs from that of etoposide and Ras-induced senescence, and appears not to involve an increase in DNA damage.

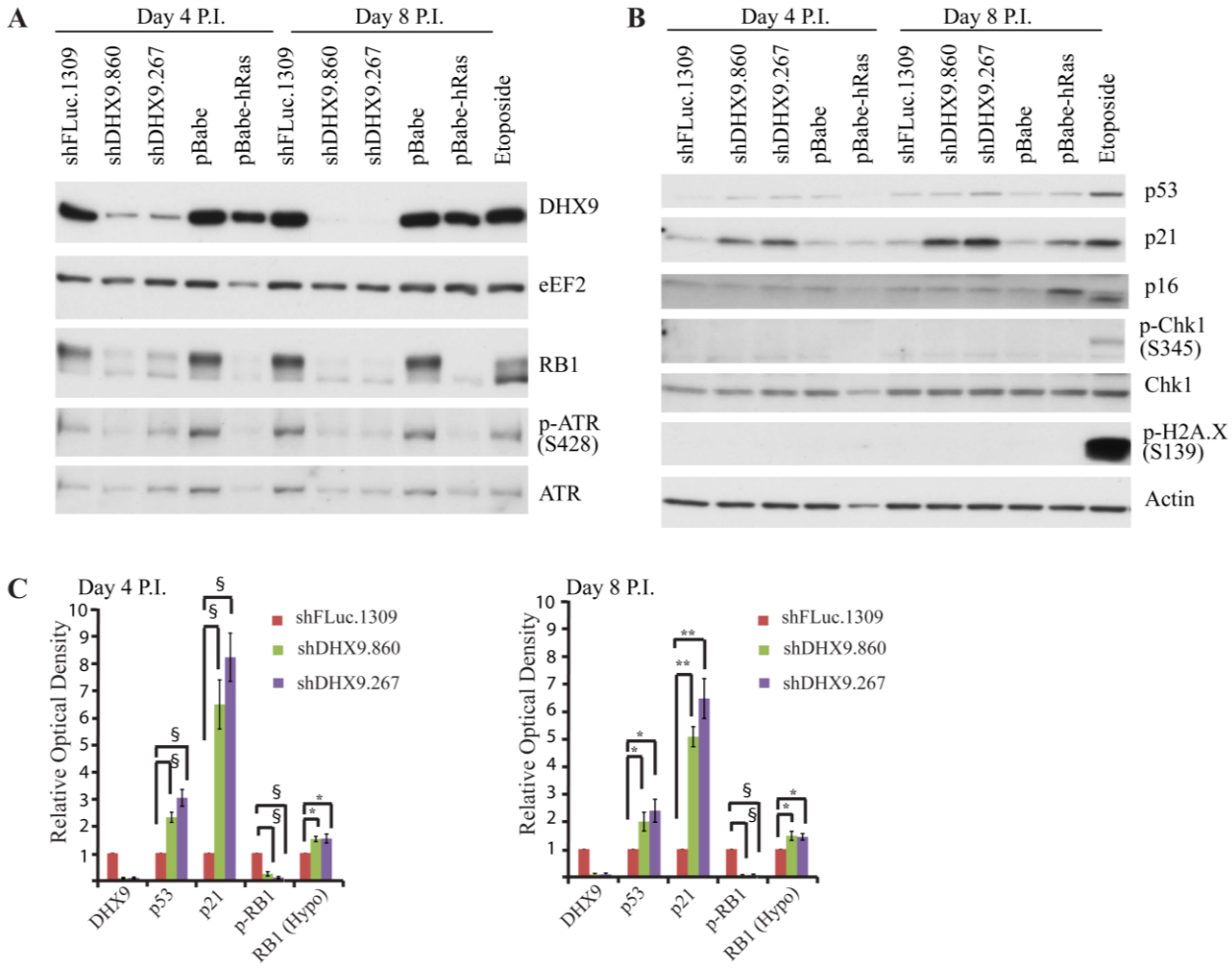

Figure 2.3 Effect of DHX9 suppression on cell cycle regulatory and DNA damage response proteins.

Western blot analysis of extracts from MRC-5 cells transduced with control (shFLuc.1309) or DHX9 shRNAs, 4 and 8 days post-infection (PI). pBabe-hRAS-infected and etoposide-treated cells were used as controls. Extracts were fractionated on 6% **(A)** or 15% **(B)** polyacrylamide gels. Blots were probed with antibodies to the proteins indicated to the right. eEF2 and actin are used as loading controls. **(C)** Quantitation of the relative optical densities of Western blot bands from extracts prepared 4 and 8 days post-infection. Shown are extracts from MRC-5 cells transduced with shRNA against FLuc.1309, DHX9.860, or DHX9.267, probed with various antibodies. Error bars represent SEM, N=3-6. The optical densities of the shDHX9.860 and shDHX9.267 bands are normalized to that of the shFLuc.1309 bands. *, $p<0.05$; **, $p<0.01$; ***, $p<0.005$; and §, $p<0.001$.

2.4.3 p53 is essential for DHX9-induced senescence

Based on our observation that the p53 and RB1 pathways are activated upon DHX9-induced senescence, we sought to determine whether induction of p53 and/or RB1 was essential to this process. To accomplish this, we first transduced MRC-5 cells with shRNAs targeting p53 or RB1 and then examined the effect of DHX9 suppression in these cells. Loss of RB1 had no effect on the increase in SA-β-gal staining or growth inhibition exhibited upon DHX9 suppression, compared to the vector control (Figure 2.4A, B). In contrast, loss of p53 completely abolished the SA-β-gal staining and rescued the growth defect in DHX9 knockdown cells (Figure 2.4A, B). In addition, loss of p53 eradicates the p21 and RB1 responses in the DHX9 knockdown cells, compared to the vector control (Figure 2.4C). This demonstrates that p53 is essential for DHX9-induced senescence, and that RB1, while not essential for the senescence, acts downstream of the p53 signaling pathway, along with p21.

2.4.4 DHX9 suppression is associated with a senescence signature

To further characterize the cellular response to reduced DHX9 expression, we quantified genome-wide steady state mRNA levels. To this end, DHX9 was suppressed using shDHX9.860 and shDHX9.267 and triplicate samples were analyzed for global gene expression changes. A comparison of the data between cells transduced with virus expressing either of the DHX9 shRNAs identified 1535 genes as differentially expressed (compared to shFLuc.1309 control cells) under at least one condition (fold-change>1.5 and false discovery rate [FDR]<0.05; Table A.1). The two DHX9 shRNAs affected expression of an overlapping set of genes (Figure 2.5A) and only one differentially expressed gene showed dis-concordant regulation (as judged by fold-change) between shDHX9.860 and shDHX9.267 transduced cells (LOC100996637 [mucin-19-like]) (Figure 2.5B). This is consistent with the vast majority of observed changes in gene expression being related to DHX9 suppression and not off-target effects (Figure 2.5A). To examine if reduced DHX9 expression resulted in activation of a p53 transcriptional program at a genome-wide level, we collected a set of p53 target genes and studied their expression following reduced DHX9 expression. Consistent with activation of a p53 transcriptional program, p53 targets were induced as compared to all genes in the cell (Figure 2.5C). This response was broad

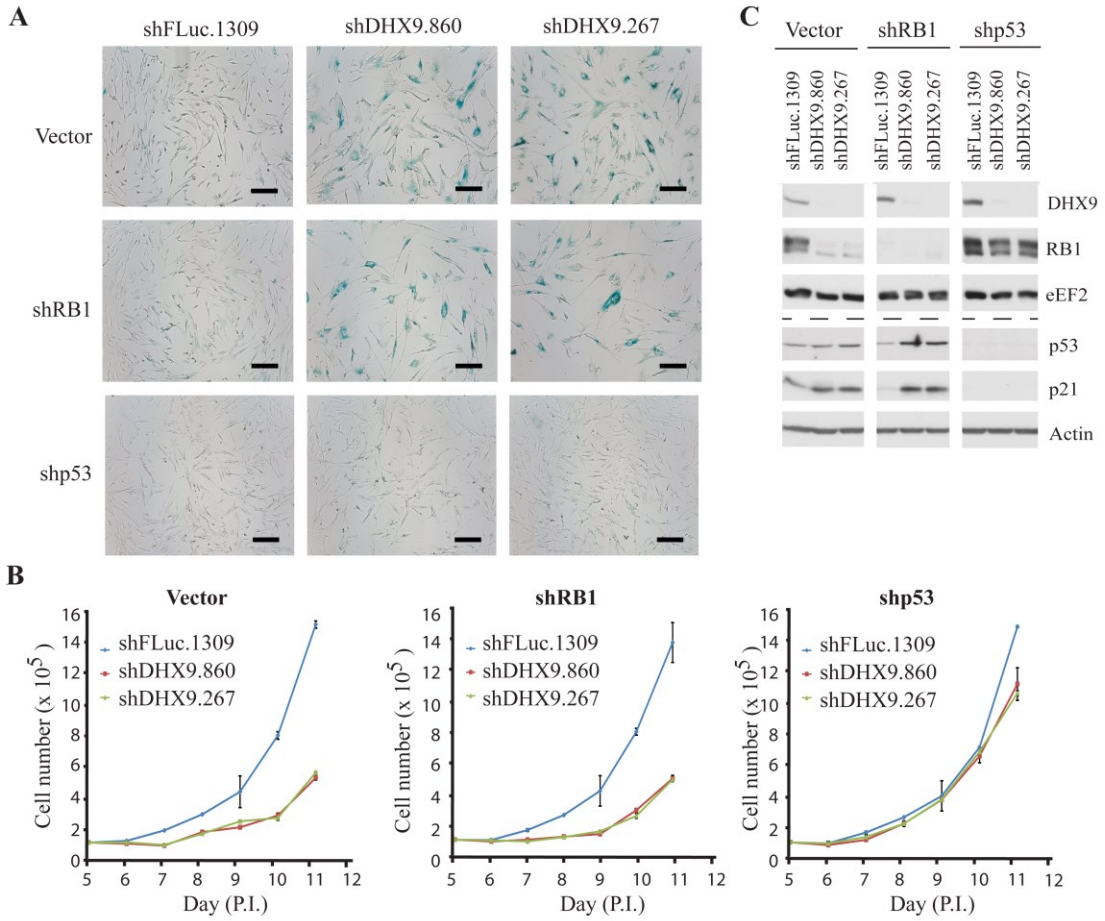

Figure 2.4 DHX9-induced senescence is p53 dependent.

(A) β-galactosidase staining of MRC-5 cells transduced with virus expressing the indicated shRNAs, 14 days post-transduction. Bars represent 200 μm. **(B)** Growth curves of MRC-5 cells transduced with virus expressing the indicated shRNAs. Cells were counted between days 5 and 11 post-transduction. **(C)** Western blot analysis of p53, p21, RB1, and DHX9 from MRC-5 cells transduced with virus expressing the indicated shRNAs.

and included most selected genes with the exception of PLK1 whose expression was reduced (Figure 2.5D). To further characterize the genes that are affected by DHX9 expression we searched for enrichment of genes annotated to shared biological processes among genes that were up- or down-regulated following transduction with DHX9 shRNAs. The analysis identified 46 non-redundant biological processes (FDR<0.001), the majority enriched among genes that were down-regulated (Figure 2.5E). Such processes included several related to DNA replication and cell cycle progression (Table A.1) consistent with the observed senescent phenotype.

To directly test whether the observed expression pattern overlaps with that of senescent cells we compared the DHX9 expression signature to those obtained previously from fibroblasts undergoing replicative senescence[316]. Indeed there was a strong overlap between the signatures as judged by the number of genes showing concordant regulation across the comparisons compared to what would be expected by chance (Figure 2.5F; all Fisher-test p-values<e-20). Thus expression profiling supports the notion that reduced DHX9 expression induces a premature cellular senescence program which closely resembles replicative senescence.

In contrast to the observed activation of a p53 gene expression program (Figure 2.5C and D), the microarray data indicated that p53 transcript levels were not elevated, despite the fact that we observed a moderate increase in p53 protein levels in DHX9 knockdown cells (Figure 2.3A, C and Figure 2.6A). Indeed, qRT-PCR analysis indicated no significant difference in p53 levels while p21 levels were induced 3-5 fold upon DHX9 suppression (Figure 2.6B). These results suggest that the increase in p53 protein observed upon DHX9 suppression in MRC cells is a post-transcriptional response which in turn activates the senescence program (see Discussion).

2.4.5 Structure/function analysis of DHX9 in the senescence response

As DHX9 is a multi-domain, multifunctional protein, we wished to elucidate which function of DHX9 might be involved in its role in senescence. To this end, we used a series of DHX9 mutants in which various activities were targeted. Three of these, K417N, D511A/E512A, and S543L, are point mutants in the core helicase region targeting domains I, II and III respectively (Figure 2.7A). We also used mutants with deletions in the RNA-binding domain I

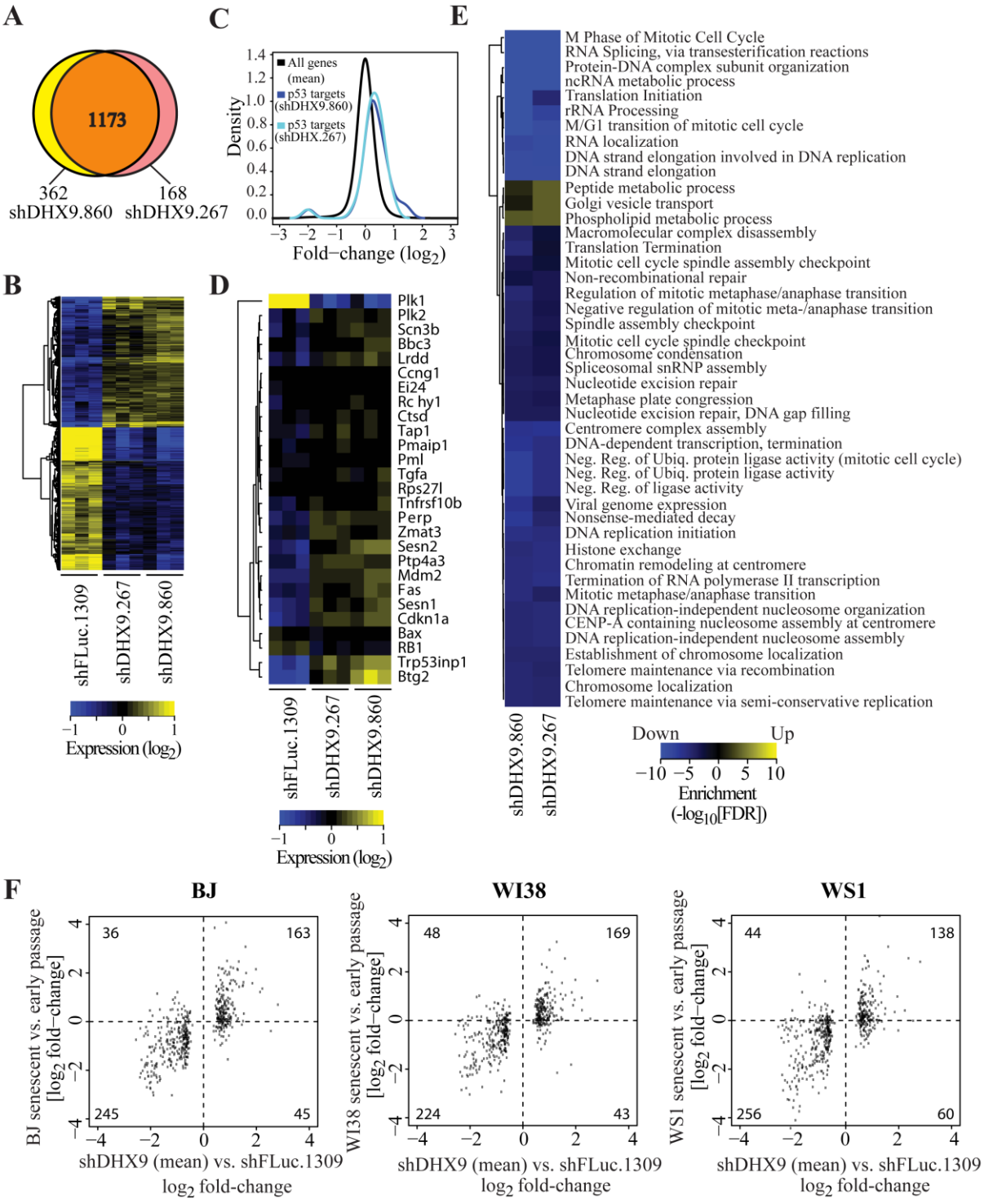

Figure 2.5 The gene expression signature induced by DHX9 suppression resembles that of replicative senescence. Figure legend on following page.

Figure 2.5 The gene expression signature induced by DHX9 suppression resembles that of replicative senescence.

(A-B) Gene expression signatures in cells transduced with shDHX9.267 or shDHX9.860 overlap. Shown is a Venn diagram highlighting the number of common and distinct differentially expressed genes from cells transduced with either of the two DHX9 shRNAs (**A**) and a heatmap showing a reproducible and concordant expression pattern (B). **(C)** Reduced expression of DHX9 induces a p53 gene expression program. Densities of fold-changes (DHX9 shRNAs vs FLuc shRNA) for all genes and a subset of p53 target genes are shown. **(D)** Heatmap of the p53 target genes identified in (C). **(E)** Highly significant enrichment of biological processes among genes that are differentially expressed upon reduced DHX9 expression. A heatmap indicating the significances of enrichments (FDRs for cells transduced with each DHX9 shRNA separately) for non-redundant biological processes defined by the Gene Ontology Consortium is presented. **(F)** A comparison between genes differentially expressed by reduced expression of DHX9 compared to previously described signatures of replicative senescence in fibroblasts. Shown is a scatter plot of fold-changes for specific genes. The number of genes in each quadrant is indicated. The p-values for the comparison between the number of genes showing concordant regulation (i.e. elevated or repressed in both comparisons) to what is expected by chance (i.e. equal distribution of the genes in all quadrants) are: BJ, p-value = 2.46e-29; WI38, p-value = 8.14e-25; WS1, p-value = 5.24e-22.

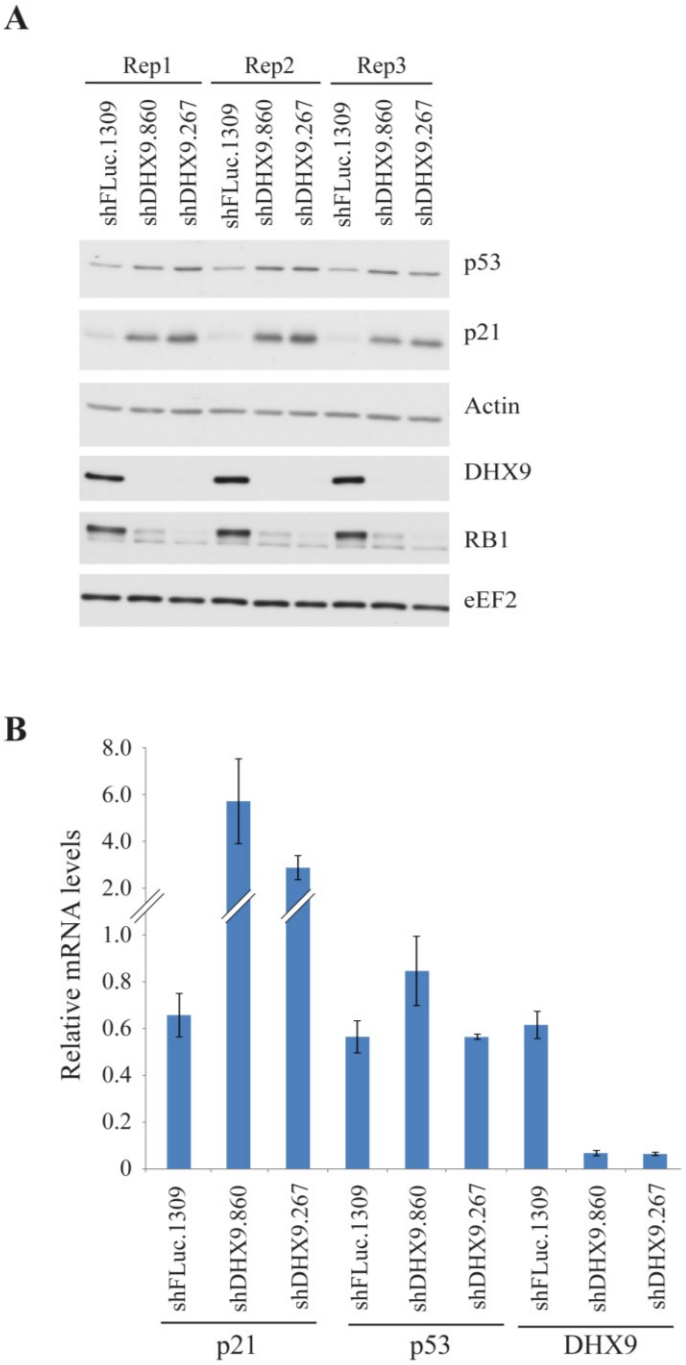

Figure 2.6 Western blot and quantitative RT-PCR analysis of microarray samples.

(A) Western blot analysis of MRC-5 cells transduced with a control (shFLuc.1309) or DHX9 shRNAs, corresponding to the samples used for microarray analysis presented in Figure 2.5. **(B)** Quantitative RT-PCR analysis of selected genes regulated by DHX9 suppression. Error bars indicate SEM, N=3.

(ΔRBDI) or in both RBD domains (ΔRBDI+II) (Figure 2.7A). To ensure that the cDNA constructs were not targeted by the DHX9 shRNAs, the wobble amino acid positions in the region targeted by the DHX9.267 shRNA were altered (see Materials and Methods). The DHX9 cDNAs were expressed in MRC-5 cells to similar levels, with the exception of the ΔRBDI mutant, which consistently showed significantly high expression levels (Figure 2.7B). Whereas 63% of cells transduced with the empty vector control, MSCV, in combination with the DHX9.267 shRNA exhibited β-galactosidase staining, cells transduced with the WT DHX9 cDNA effectively rescued the senescent phenotype, reducing the staining to 20% (Figure 2.7C, D). On the other hand, none of the mutants were able to rescue the senescent phenotype, suggesting that helicase and the two RNA-binding domains are essential to DHX9's role in premature senescence (Figure 2.7C, D).

2.4.6 Loss of DHX9 induces senescence through inhibition of DNA replication

Our expression profile analysis uncovered that many genes involved in DNA replication are downregulated upon loss of DHX9. We wished to further investigate whether DHX9 might play a role in DNA replication. We examined whether DHX9 suppression affected the synthesis of new ("nascent") DNA at specific origins of replication. Nascent DNA abundance was quantitated at three known origins in MRC-5 cells: LB2P (located at the Lamin B2 locus), MYC11 (c-MYC locus) and hORS8P (hORS8 locus). Within the vicinity of these loci, there are also negative control regions which do not contain an origin (e.g. LB2C1, MYC1, and hORS8C) [92]. Since we were interested in newly synthesized DNA levels, we first verified that total genomic DNA levels were unchanged upon DHX9 knockdown at the origins of replication (Figure 2.8A). Loss of DHX9 resulted in a 3 – 6 fold decrease in the abundance of nascent DNA at all three origins, compared to the shFLuc.1309 controls (Figure 2.8B). The regions containing no origins (LB2C1, MYC1, and hORS8C) showed background levels of nascent DNA. To determine whether DHX9 was present at the aforementioned origins of replication, chromatin IP (ChIP) was performed in MRC-5 cells using a DHX9 antibody and the associated DNA

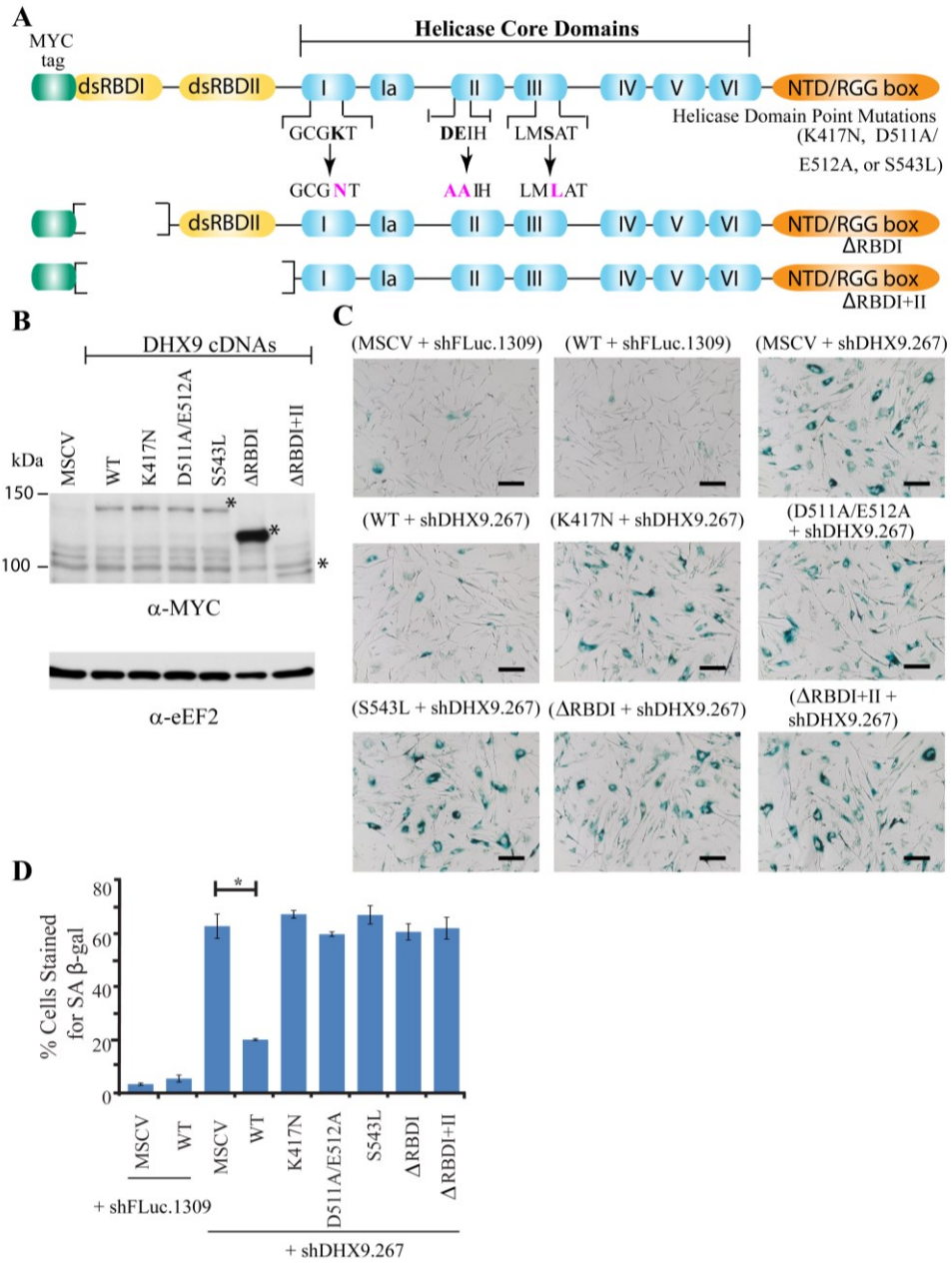

Figure 2.7 Functional analysis of DHX9 using various mutant cDNA constructs.

(A) Schematic diagram of DHX9 cDNA and mutants used in this study. **(B)** Western blot analysis of WT DHX9 and mutants expressed in MRC-5 cells. The empty vector, MSCV, is used as a control. *, denotes position of migration of recombinant protein. **(C)** β-galactosidase staining of MRC-5 cells transduced with lentivirus expressing the indicated shRNAs in combination with various DHX9 cDNAs. **(D)** Quantitation of β-galactosidase staining from (C). Cells from at least 5 independent fields/experiment were quantitated. Error bars represent SEM, N=3. *$p<0.01$.

abundance determined by quantitative PCR using primers directed against each origin region. As controls, the ChIP was performed using antibodies against ORC2 and Ku86 (known to associate with origins)[92], and NFκB (previously shown to not associate with origins)[449] (Figure 2.8C-D). Our results show that the positive controls, ORC2 and Ku86, pulled down significant levels of LB2P, MYC11, and hORS8P DNA, whereas the same regions were not significantly enriched from NGS treated samples. DNA from non-origin-containing sites (LB2C1, MYC1, and hORS8C) was also not enriched in DHX9 IPs. The DHX9 ChIP showed a DNA abundance that was intermediate between that of the positive and negative controls for all three origins of replication (Figure 2.8D), indicating that DHX9 is associated with the origins of replication, but possibly that the association may not be as stable as it is for ORC2 or Ku86. Taken together, our results illustrate that loss of DHX9 is accompanied by a pronounced reduction in DNA replication, suggesting that DHX9 plays a role in this process.

Although the above results implicate a role for DHX9 in DNA replication, it is important to note that senescent cells may exhibit reduced levels of nascent DNA synthesis irrespective of the agent causing the senescence. In order to establish that DHX9 plays a direct role in DNA replication, we chose to assess levels of nascent DNA synthesis in MRC-5 cells transduced with a p53 shRNA in combination with a control (FLuc.1309) or DHX9 shRNAs. In these cells, the senescent phenotype is completely rescued by knockdown of p53 (Figure 2.4); therefore, any effect on DNA replication would be independent of the senescence phenotype. We observed that loss of DHX9 results in a 2-4 fold decrease in the abundance of nascent DNA at the LB2P, MYC11, and hORS8P origins (Figure 2.9B). This demonstrates that the inhibition of DNA replication occurs even in the absence of senescence, and must therefore occur before the growth arrest and senescence phenotype.

Given that the helicase and RNA-binding domains of DHX9 appeared to be essential for its role in inducing senescence, we examined whether these mutations had any effect on the ability of DHX9 to bind to origins. ChIP was performed in MRC-5 cells expressing the WT DHX9 cDNA or the K417N, D511A/E512A, and ΔRBDI+II mutants. PCR analysis of the abundance of LB2P, MYC11, and hORS8P DNA showed that none of the mutants affected the binding of DHX9 to any of these origins (Figure 2.10 B-D), suggesting that these domains are not involved in binding to origins of replication.

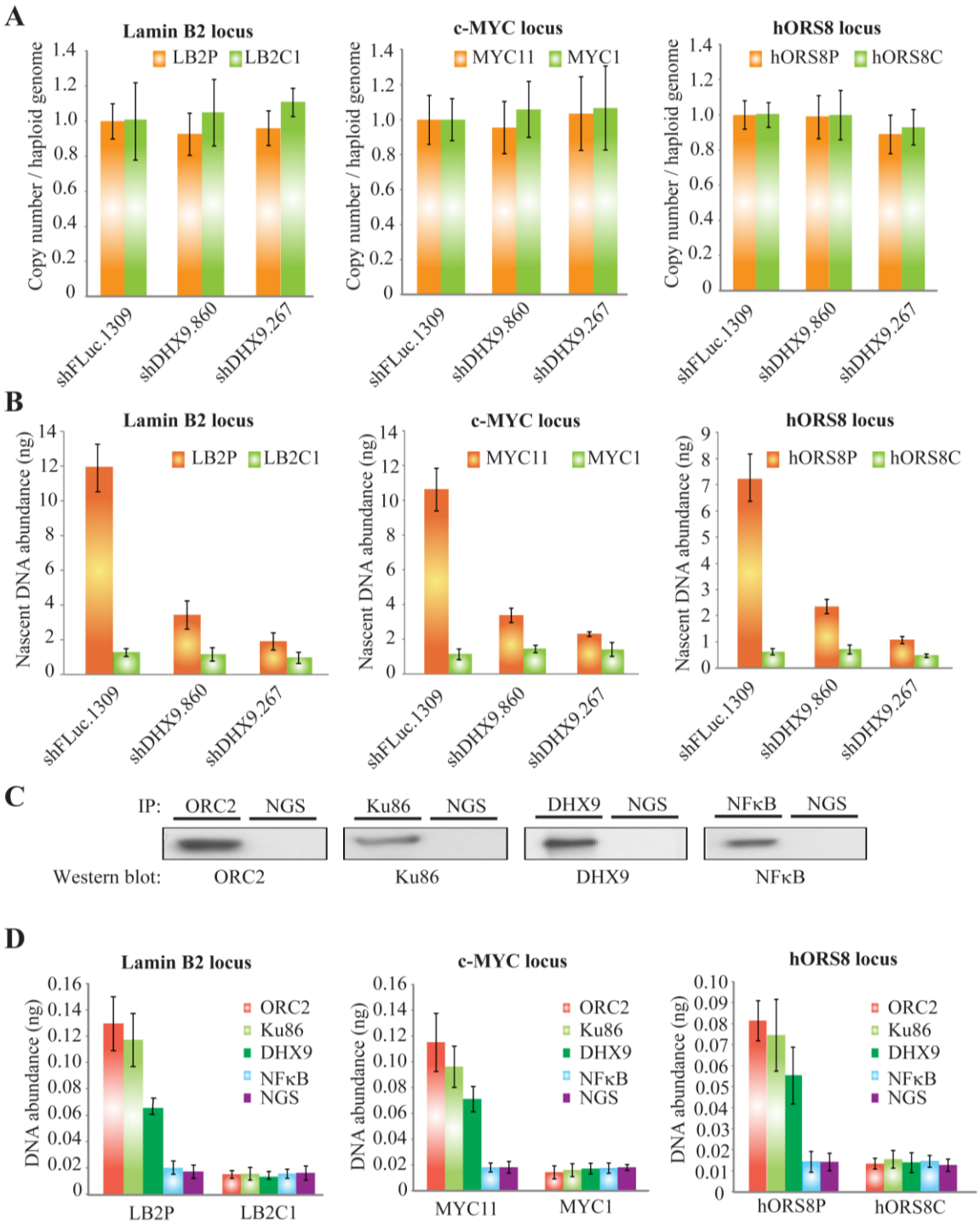

Figure 2.8 Loss of DHX9 inhibits DNA replication. Figure legend on following page.

Figure 2.8 Loss of DHX9 inhibits DNA replication.

(A) Copy number per haploid genome at the indicated chromosomal loci in MRC-5 cells transduced with a control (shFLuc.1309) or DHX9 shRNAs and harvested 6 days post-infection. Results are normalized to the shFLuc.1309 sample. Error bars represent SD; N=3. **(B)** Quantification by qPCR of nascent DNA abundance (ng) at the indicated loci in MRC-5 cells transduced with a control (shFLuc.1309) or DHX9 shRNAs, 6 days post-transduction. The location and sequence information of the primers used for the amplification of the origin-containing regions (LB2P, MYC11, and hORS8P; orange bars) and the non-origin-containing control regions (LB2C1, MYC1, and hORS8C; green bars) are as described in Table 2.1. Error bars represent SD; N=3. **(C)** Western blot analysis of the ChIP performed with the indicated proteins. Following ChIP, an aliquot of the IP was fractionated by SDS-PAGE, transferred to Immobilon-P and probed with antibodies to the indicated proteins. **(D)** Quantification by qPCR of immunoprecipitated DNA abundance (ng) at the indicated chromosomal loci in MRC-5 cells transduced with a control (shFLuc.1309) or DHX9 shRNAs. Chromatin IP was performed with antibodies directed against ORC2 (red bars), Ku86 (light green bars), DHX9 (dark green bars) and NFκB (blue bars); normal goat serum (NGS) (purple bars) was used as a negative control. Error bars represent SD; N=3.

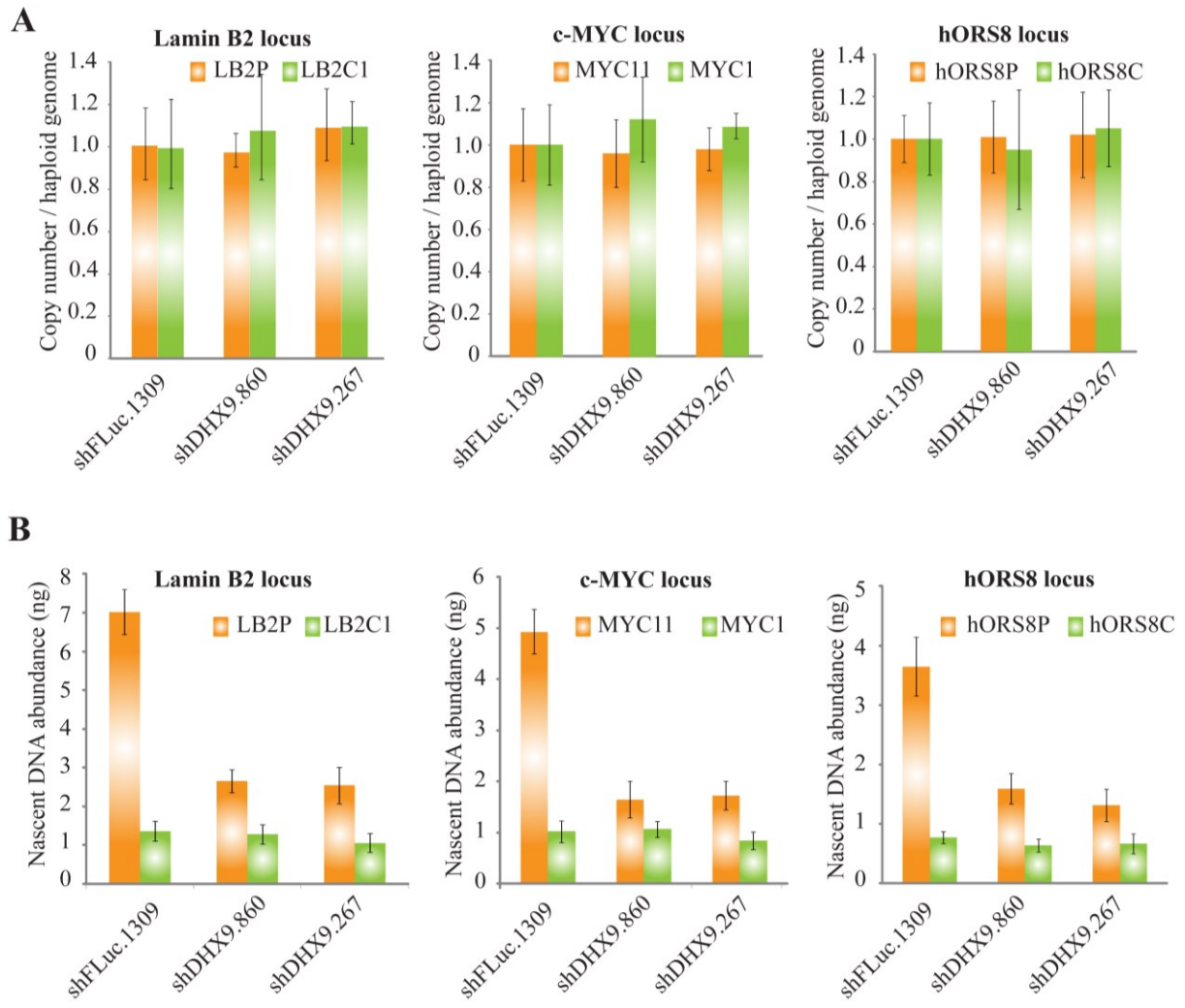

Figure 2.9 Inhibition of DNA replication occurs before DHX9-induced senescence.

(A) Copy number per haploid genome at the indicated chromosomal loci in MRC-5 cells transduced with a p53 shRNA in combination with a control (shFLuc.1309) or DHX9 shRNAs. Results are normalized to the shFLuc.1309 sample. Error bars represent SD; N=3. (**B**) Quantification by qPCR of nascent DNA abundance (ng) at the indicated loci in MRC-5 cells transduced with a p53 shRNA and either a control (FLuc.1309) or DHX9 shRNAs, 6 days post-transduction. The location and sequence information of the primers used for the amplification of the origin-containing regions (LB2P, MYC11, and hORS8P; orange bars) and the non-origin-containing control regions (LB2C1, MYC1, and hORS8C; green bars) are as described in Table 2.1. Error bars represent SD; N=3.

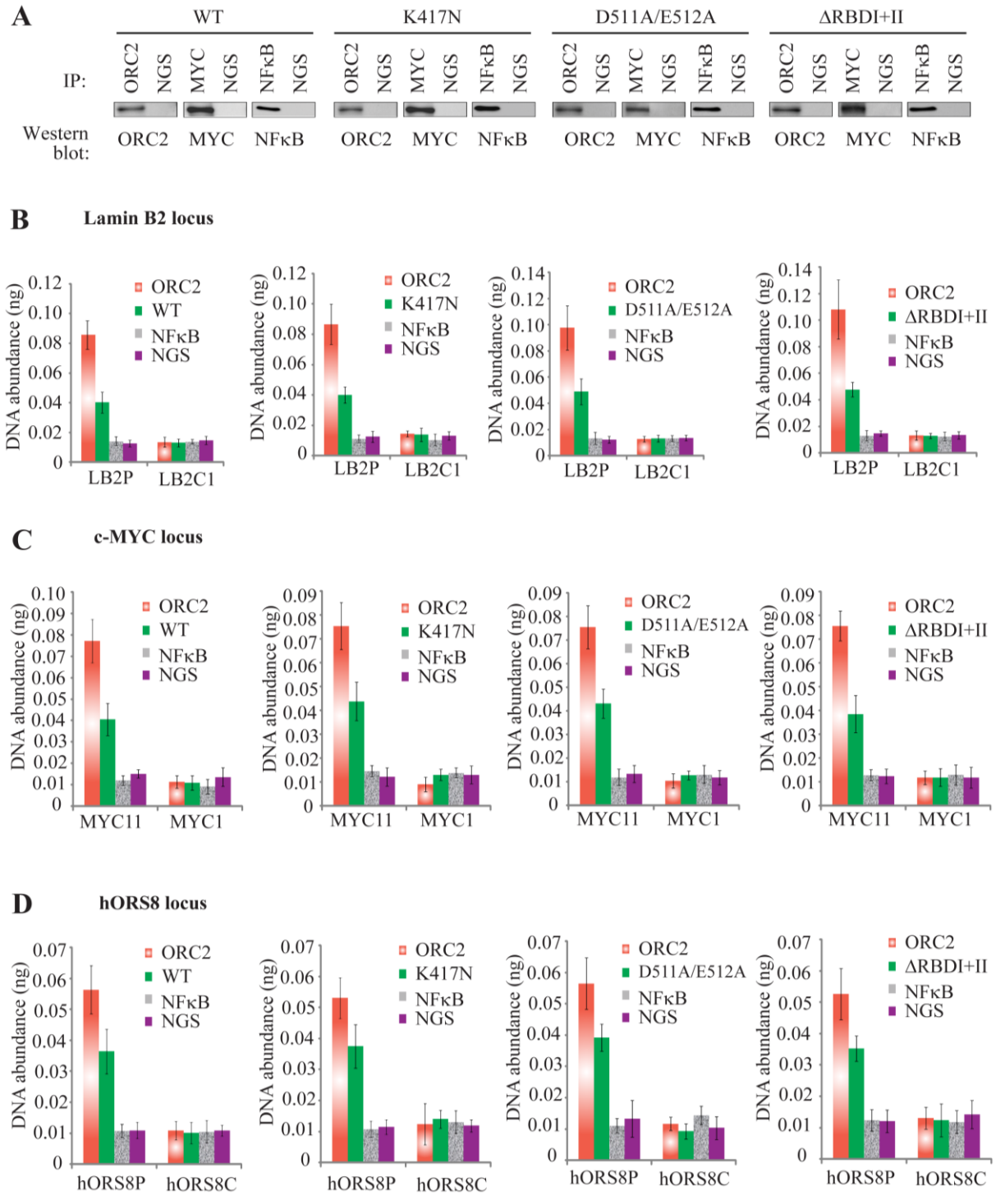

Figure 2.10 Binding of DHX9 to origins is not dependent on its helicase or RBD domains.
Figure legend on following page.

Figure 2.10 Binding of DHX9 to origins is not dependent on its helicase or RBD domains.

(A) Western blot analysis of the ChIP performed with the indicated proteins. MRC-5 cells were transduced with a MYC-tagged construct expressing either the WT DHX9 cDNA or the K417N, D511A/E512A, or ΔRBDI+II mutants. Following ChIP, an aliquot of the IP was fractionated by SDS-PAGE, transferred to Immobilon-P and probed with antibodies to the indicated proteins. **(B-D)** Quantification by qPCR of immunoprecipitated DNA abundance (ng) at the Lamin B2 **(B)**, c-MYC **(C)** or hORS8 **(D)** chromosomal loci in MRC-5 cells expressing either the WT DHX9 cDNA or the K417N, D511A/E512A, or ΔRBDI+II mutants. Chromatin IP was performed with antibodies directed against ORC2 (red bars), MYC (green bars) and NFκB (grey bars). Normal goat serum (NGS) (purple bars) was used as a negative control. Error bars represent SD; N=3.

2.5 Discussion

In this study, we show that loss of DHX9 results in premature senescence in primary human fibroblasts. This is characterized by distinctive morphological changes, elevated levels of SA-β-gal, and a pronounced growth arrest, and supported by a gene expression signature comparable to that of replicative senescence. Increased p53, p21, and RB1 activity was noted with p53 being essential for DHX9-induced senescence. We found DHX9 to be associated with origins of replication and demonstrated that levels of newly replicated DNA were significantly lower at various replication origins in DHX9-suppressed cells.

The stimuli for premature senescence are many and varied; however, a common feature is activation of either the p53 and/or p16-RB1 signaling pathways. Both p53 and RB1 are tumor suppressors which respond to various cellular signals such as DNA damage or oncogenic stimuli [450]. Activation of p53 or RB1 leads to inhibition of downstream proliferative genes. Here we showed that p53 and p21 protein levels increased upon DHX9 knockdown, and that RB1 was activated. However, no increase in p16 levels was detected. Knocking down p53 rescued the senescent phenotype caused by DHX9 suppression, whereas suppression of RB1 had no effect, indicating that p53, but not RB1 is essential for this process. In the p16-RB1 pathway, p16 inhibits cyclin-dependent kinases (CDKs) such as cyclin D1, CDK4, and CDK6, which in turn maintains RB1 in its phosphorylated (inactive) form. Hence, an increase in p16 levels would result in a shift from the hyper- to the hypo-phosphorylated (active) form of RB1. Due to crosstalk between the p53 and RB1 pathways, RB1 can also be activated by increased levels of p21, which also inhibit CDKs independently of p16 (reviewed in Ref. [451]). Our data suggests that the latter situation is occurring in DHX9-induced senescence: activated p53 transcriptionally activates p21, which inhibits CDKs, leading to activation of RB1. This is supported by the fact that knocking down p53 abolishes RB1 activation. Loss of RB1 does not prevent senescence since p21 alone is sufficient to lead to cell arrest independently of RB1.

Our microarray analysis identified many genes involved in mitosis, cell cycle progression, and DNA replication which were downregulated upon loss of DHX9, as well as activation of a p53 transcriptional program. This is consistent with our data showing growth arrest and p53/p21 activation (Figures 2.1-2.3). Previously, our lab had performed expression profiling in *Arf*$^{-/-}$*Eμ-Myc*/Bcl-2 lymphoma cells, where activation of p53 transcriptional targets

upon DHX9 suppression was likewise observed[432]. However, it should be noted that there is otherwise very little overlap between the expression profiles obtained upon suppression of DHX9 in MRC-5 cells compared to the *Arf*$^{-/-}$*Eμ-Myc*/Bcl-2 lymphomas. For instance, downregulation of genes involved in replication, mitosis, and cell cycle progression were not observed in the lymphoma setting. This is not surprising, given that loss of DHX9 elicits an apoptotic response in *Arf*$^{-/-}$*Eμ-Myc*/Bcl-2 lymphomas, which could be attributed to elevated levels of MYC (a strong promoter of both apoptosis and DNA replication) in these cells[432]. Indeed, overexpression of MYC in NIH3T3 fibroblasts can overcome the growth arrest which suppressing DHX9 would otherwise cause[432]. This indicates that induction of senescence is highly dependent on the particular biological wiring of the cell type in question, a notion supported by previous studies[452].

Based on our observation that many factors involved in DNA replication were found to be downregulated in the microarray expression data, we explored this avenue as a potential mechanism through which loss of DHX9 may be inducing senescence. We found DHX9 to be present at origins of replication and that production of nascent DNA is inhibited at various well characterized replication origins upon DHX9 knockdown (Figure 2.8). The ChIP results demonstrate that DHX9 is not as strongly associated with the origins of replication as Ku86 or Orc2, suggesting that DHX9 may not be directly associated with the origins or may be bound to the origins only a fraction of the time. This is perhaps consistent with its function as a helicase where DHX9 might be transiently present at a given location. Indeed, the structure-function analysis of DHX9 shows that both its helicase activity and RNA-binding functions are essential in this process (Figure 2.7).

While the above data suggests a role for DHX9 in DNA replication, the question remained as to whether the observed replication inhibition is a direct or indirect consequence of DHX9 suppression, since growth-arrested and senescent cells in general will exhibit reduced rates of DNA replication. We believed that DHX9 suppression was directly responsible for the inhibition of replication based on the fact that both the microarray and nascent DNA quantification experiments were performed at a timepoint where the shDHX9-transduced cells were pre-senescent (5-6 days post-transduction). Here, the DHX9 knockdown cells did not exhibit significant differences in morphology and SA-β-gal staining compared to the control

cells (Figure 2.1A, B, and D, day 6 P.I.). Furthermore, the cell cycle distribution of DHX9-suppressed cells at this timepoint is similar to that of the shFLuc.1309 control, indicating that the cells are not yet growth-arrested (Figure 2.2B, day 6 P.I.). To confirm that DHX9 knockdown directly affects DNA replication, we examined nascent DNA synthesis at various well characterized origins in a cell line that is resistant to DHX9-induced senescence. MRC-5 cells expressing the p53 shRNA showed a significant decrease in nascent DNA production upon DHX9 knockdown, despite exhibiting no significant growth defects or markers of senescence (Figure 2.9 and 2.4). This implies that the blockage in replication occurs upstream of the p53 pathway and is likely a cause of the growth arrest and senescent phenotype when p53 is present. We have also previously observed inhibition of DNA replication in the absence of senescence in NIH3T3 cells overexpressing MYC (Figure 5A and 6F in Ref. [432]). In both the p53-knockdown and MYC-overexpression scenarios, cell cycle progression is allowed to occur in the presence of replication stress either due to the absence of a checkpoint control (p53) or the presence of a strong promoter of proliferation (MYC). Taken together, our results indicate that the observed downregulation in genes associated with DNA replication and cell cycle progression, and the reduction in nascent DNA synthesis, is an effect of DHX9 suppression rather than an indirect consequence of the senescence itself.

To gain additional mechanistic insight into the role of DHX9 in DNA replication, we assessed the ability of some DHX9 mutants to bind to origins of replication. Despite being essential to the role of DHX9 in senescence, the helicase and RNA-binding mutants had no effect on the binding of DHX9 to the three origins tested. This suggests that these domains are not involved in the binding of DHX9 to the DNA, but may have other functions at the origins. Further experiments would need to be performed to determine the specific role of DHX9 in DNA replication. It may be required to aid in the opening of the origins, to resolve tertiary structures at the origins, or to clear transcripts from the origins (since the ones studied herein occur near promoter regions).

Since p53 signaling is activated by a myriad of signals, we also investigated other possible mechanisms through which DHX9 may be inducing senescence. One possibility would be through infliction of DNA damage. We examined markers of DNA damage, phospho-H2A.X (S139) and 53BP1, and failed to detect an increase in levels of these proteins upon DHX9

suppression (Figure 2.3B and data not shown). In addition, no increase was detected in markers of replicative stress, such as ATR and phospho-Chk1 (S345) (Figure 2.3). Thus, it is likely that DHX9-mediated senescence is caused by a blockage in replication rather than DNA damage.

The link between replication inhibition, p53 activation, and cell cycle arrest has been previously documented. In a study by Taylor and colleagues, inhibition of DNA synthesis using hydroxyurea or aphidicolin led to increased levels of p53 and p21, and resulted in inhibition of entry into mitosis[453]. Machida et al.[454] demonstrated that low levels of replication initiator proteins caused cells to arrest in the G1 phase. Furthermore, p21 has been found to associate with PCNA, a DNA replication factor[455]. Based on our data, we propose the following model: under normal cellular conditions, DHX9, in concert with other origin-interacting proteins such as ORCs and replication factors, facilitates proper assembly of the pre-replicative complex at origins of replication, leading to DNA replication (Figure 2.11). In the absence of DHX9, DNA replication is inhibited, possibly due to the inability of the pre-replicative complex to form. This activates a p53-dependent stress response, leading to transcriptional activation of p21, which inhibits CDKs (Figure 2.11). Since CDKs normally inactivate RB1, the result is a shift from the inactive to active form of RB1, which suppresses the E2F family of transcription factors and prevents transcription of genes involved in cell proliferation. In addition, p21 may also lead to cell cycle arrest and senescence independently of RB1. This may involve direct suppression of DNA replication factors or inhibition of E2F-independent cell cycle progression or mitotic proteins.

Inhibition of cell cycle progression upon low levels of replication is an important mechanism in protecting cells from aberrant DNA replication and genomic instability. Our findings support previous data implicating DHX9 in DNA replication and maintenance of genomic stability. DHX9 has been found to be associated with components of the DNA replication machinery (e.g. BRCA1, PCNA, and topoisomerase IIα)[88-90, 204]. It stimulates the unwinding of Okazaki fragment-like DNA:RNA hybrids *in vitro* by WRN, a RecQ helicase which when mutated, results in genomic instability[36] and may be implicated in a role involving lagging strand synthesis. DHX9 is able to unwind non-canonical DNA structures such as triple helices - aberrant structures which induce double-stranded breaks and promote genomic rearrangements[2, 98]. By resolving these structures, DHX9 aids in maintaining genomic

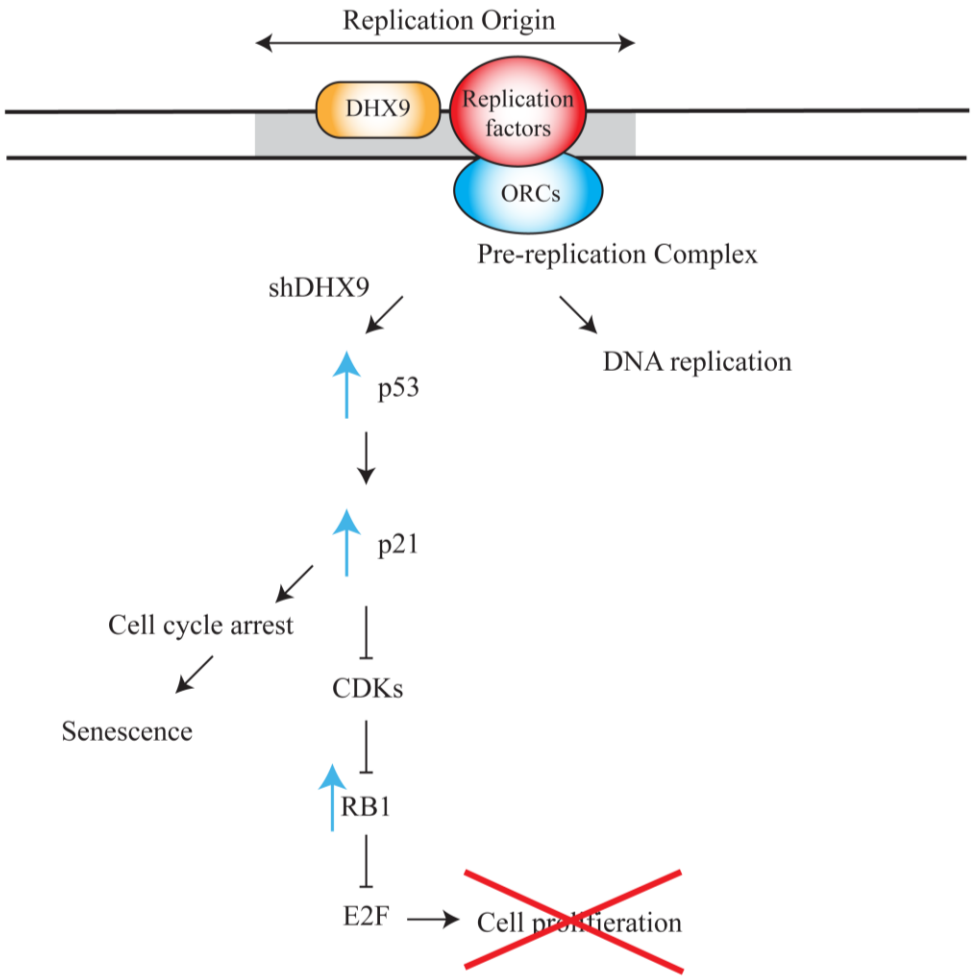

Figure 2.11 Model highlighting mechanism by which DHX9 suppression leads to senescence.

Under normal cellular conditions, DHX9 facilitates DNA replication at origins of replication. Loss of DHX9 leads to inhibition of DNA replication at origins of replication. This results in a defect in downstream recruitment of factors onto chromatin which activates a p53 stress response leading to transcriptional activation of p21. Activation of p21 inhibits downstream CDKs and prevents RB1 phosphorylation, which inhibits E2F and blocks transcription of genes required for proliferation. Additionally, p21 may effect cell cycle arrest independent of RB1. Genes involved in DNA replication, cell cycle progression, and mitosis are downregulated upon DHX9 knockdown, contributing to the growth arrest (see Discussion for details).

stability. DHX9 has been shown to interact with Ku86, an essential protein in NHEJ-mediated DNA repair which has more recently been implicated in promoting nascent DNA synthesis at origins of replication[92]. It is quite possible that DHX9 and Ku86 may act in concert at the origins of replication. In addition, since DHX9 is a multi-functional protein, some of its other functions may contribute to the senescence phenotype. In particular, transcription-related activities of DHX9 could play a role in upregulating genes involved in cell cycle arrest, or downregulating genes involved in growth and cell cycle progression. DHX9's involvement in miRNA and translational regulation may also contribute. For example, DHX9 has been found to associate with both the insulin-like growth factor 2 (IGF2) mRNA and miR-483-5p, a miRNA which enhances transcription of IGF2; DHX9 promotes the miR-483-5p-mediated induction of IGF2 mRNA[139]. IGF2, which plays an essential role in growth and development, has been shown to be involved in senescence, along with other proteins in the IGF signaling pathway [456, 457].

Our results present DHX9 as a somewhat unique agent whose suppression leads to premature senescence. In most cases where the p53 pathway is activated, senescence is accompanied by the presence of DNA damage and involves activation of the DNA damage response[458]. This is obviously the case for premature senescence caused by DNA damaging agents such as etoposide or IR. It has also been shown that oncogene-induced senescence is a consequence of a DNA damage response (DDR) triggered by DNA hyper-replication. Di Micco and colleagues[459] demonstrated that Ras-induced senescence resulted in accumulation of DNA breaks and activation of an ATR-dependent DDR. Replicative senescence occurs when erosion of telomeres activates the DDR[320, 436, 448]. DHX9-induced senescence, however, appears to occur in the absence of DNA damage. Instead, this particular type of premature senescence is brought on by a defect in replication, which triggers a stress-response program. It has previously been demonstrated that inhibition of replication upon suppression of the DHX9 interaction partner Ku86 results in growth arrest in the absence of markers of DNA damage[92]. Hence, it is conceivable that inhibition of DNA replication in general may represent a DNA damage-independent mechanism of causing growth arrest and premature senescence. In conclusion, our data has uncovered a novel role for DHX9 in replication and senescence, and contributes to an

increased understanding of the biological function of this multi-faceted helicase.

2.6 Materials and Methods

2.6.1 Cell lines, cell culture and plasmids

All cell lines used in this study were maintained in DMEM supplemented with 10% fetal bovine serum (Multicell). HEK293T/17 cells were obtained from ATCC. MRC-5 fibroblast cells were kindly provided by Dr. Nahum Sonenberg (McGill University, Canada). The MRC-5 cells were used between 10 and 30 population doubling levels (PDLs) and routinely subcultured 1:4 every 3 days; each passage was considered 2 PDLs.

Two shRNAs targeting human DHX9 (DHX9.860 and DHX9.267) and a control shRNA targeting firefly luciferase (FLuc.1309) were transduced into cells using pPrime-PGK-Puro (Addgene), a 2nd generation lentiviral vector. An shRNA targeting human p53, pLVUH-shp53, was obtained from Addgene and has been previously described[460]. The shRNA to human retinoblastoma (RB1), MLP-shRB1, was obtained from Dr. Scott Lowe (Memorial Sloan-Kettering Cancer Center, NY)[461], and subcloned into pPrime-GFP. The retroviral vector pBabepuro-hRas V12, used to express a constitutively active form of hRas, was obtained from Addgene. Lentiviral transduction was performed following published procedures[462]. Briefly, 15 μg of pPrime-PGK-Puro-shRNA, 7.5 μg of packaging plasmid pSPAX2, and 3.75 μg of envelope-encoding vector, CMV-VSVG, were mixed and transfected into HEK293T/17 cells in a 10 cm dish by calcium phosphate-mediated delivery. The media was changed 12 hours later and 48 hours post-transfection, lentiviral supernatant was collected every 8 hours up to 72 hours and added to target cells. Forty-eight hours after the final transduction, stable integrants were selected using 2 μg/ml puromycin for at least 3 days. For transduction of retroviral vectors (e.g. pBabepuro-hRas V12) into human cells, the same procedure as lentiviral transduction was followed, except that the packaging plasmid pUMVC was used instead of pSPAX2.

2.6.2 shRNA sequences

The FLuc.1309, DHX9.860 and DHX9.267 shRNAs were cloned into the miR30 backbone of pPrime-PGK-Puro via unique XhoI and EcoRI restriction sites[463]. The guide strand sequences

of the shRNAs used in this study are: FLuc.1309, $^{5'}$TTAATCAGAGACTTCAGGCGGT$^{3'}$; DHX9.267, $^{5'}$CCAGGCAGAAATTCATGTGTG$^{3'}$; DHX9.860 $^{5'}$ACACGAGAACATGGATCAAAT$^{3'}$, RB1.698, $^{5'}$CGCAGTTCGATATCTACTGAA$^{3'}$; and hp53.908, $^{5'}$AGTAGATTACCACTGGAGTCTT$^{3'}$

2.6.3 Growth curves

Five days following lentiviral transduction of shRNAs, cells were plated into 18 T25 flasks at an initial concentration of 100,000 cells per flask. Each subsequent day, cells from 3 individual T25 were trypsinized, resuspended in Isoton, and counted using a Coulter Counter (Beckman). This procedure was performed for 6 consecutive days at which point cells began to approach confluency.

2.6.4 Cell cycle analysis

Cell cycle analysis was performed using ethanol fixation, acid denaturation, and propidium iodide (PI) staining[464] at days 6 and 14 after transduction with the shRNAs. Cells were seeded onto 6 cm plates and harvested at 75% confluency. The cells were trypsinized and washed twice with PBS containing 1% BSA and 5 mM EDTA, resuspended in 300 μl PBS on ice, fixed with 1 ml 70% ethanol, and stored at -20^{o}C until further processing. The fixed cells were then treated with 0.5% Triton X-100/2N HCl for 30 minutes with end-over-end incubation at room temperature to denature genomic DNA. Cells were neutralized with 0.1M sodium borate [pH 8.5], washed with PBS containing 1% BSA and 0.5% Triton X-100, and resuspended in 500 μL of PBS containing 5 μg/mL PI (Sigma). The cell cycle profile of the cells was then assessed using a GUAVA EasyCyte HT flow cytometer (Millipore).

2.6.5 Senescence-associated β-galactosidase assay

Senescence-associated β-galactosidase (SA-β-gal) activity was detected as previously described [317], with slight modifications. Following lentiviral transduction, cells were plated onto 6-well plates and the assay was performed 6 and 14 days post-transduction. Cells were fixed with 0.5% glutaraldehyde in PBS for 15 minutes at room temperature, washed with PBS, and then washed

twice with PBS supplemented with 1 mM $MgCl_2$. The cells were stained with X-Gal solution (1 mg/ml X-gal, 5 mM $K_3Fe(CN)_6$, 5 mM $K_4Fe(CN)_6 \bullet 3H_2O$ in PBS) for 8 hours at 37°C, washed 3x in PBS, and fixed with 100% methanol for 5 minutes at room temperature. Brightfield color images were taken with a Zeiss Axio Imager Z2 microscope and an AxiocamMRc camera. Experiments were performed three times, counting 1000 cells from at least 5 independent fields. Phase images were taken with a Zeiss Observer A1 microscope and an AxiocamMRm camera.

2.6.6 Immunoblot analysis

Protein extracts were prepared in RIPA lysis buffer (20 mM Tris-HCl [pH 7.5], 150 mM NaCl, 0.1% SDS, 1% NP40, 0.5% sodium deoxycholate, 1 mM β-glycerophosphate, 1 mM PMSF, 1 μg/ml leupeptin, 10 μg/ml aprotinin, and 2.5 μM pepstatin A) at 4 and 8 days post-transduction. PVDF membranes were probed with the indicated primary antibodies and HRP-conjugated secondary antibodies (rabbit (711-035-152) or mouse (115-035-146) (Jackson ImmunoResearch)), and visualized using enhanced chemiluminescence (ECL) (Perkin Elmer). The following primary antibodies were used in this study: DHX9 (M99; SC Biotech), eEF2 (#2332; Cell Signaling), RB1 (554136; BD Pharmingen), human p53 (DO-1; SC Biotech), p21 (556430; BD Pharmingen), p16 (DCS-50; SC Biotech), α-actin (clone AC-15; Sigma), phospho-ATR p-S428 (#2853; Cell Signaling), ATR (N-19; Santa Cruz), phospho-CHK1 pS345 (#2341; Cell Signaling), CHK1 (DCS-310; SC Biotech), p53 pS15 (#9284; Cell Signaling), MYC-tag (9E10, McGill Hybridoma Core Facility), γH2AX (clone JWB301; Millipore), ORC2 (3G6, SC Biotech), Ku86 (H-300, SC Biotech), and NFκB (c-20, SC Biotech). Quantification of Western blot band intensities was carried out using the NIH ImageJ software.

2.6.7 DHX9 cDNA rescue

MSCV-based expression of the wild-type and mutant human DHX9 cDNAs[73] was performed by subcloning the DHX9 cDNA preceded by an N-terminal MYC-tag into the BglII/EcoRI sites of MSCV/Puro^R, generating MSCV-MYC-hDHX9-Puro^R [432]. To allow expression in human cells without being targeted by the human DHX9 shRNAs, the wobble positions of 7 amino acid codons within the shDHX.267 target site were mutated

[5'AACAGGCAGAAATTCATGTGTGAG3' changed to 5'AATAGACAAAAGTTTATGTGCGAA3']. To enable efficient transduction of the retroviral constructs in human cells, MRC-5 cells were first infected with a lentiviral plasmid expressing the ecotropic retroviral receptor, HAGE-EcoR (kindly provided by Dr. Scott Lowe (Memorial Sloan-Kettering Cancer Center, NY), using the lentiviral transduction procedure described above and selected using puromycin. The EcoR-expressing MRC-5 cells were then transduced with the DHX9-expressing constructs using the Phoenix Ecotropic packaging cell line via calcium phosphate mediated delivery and expression was determined by Western blot. To assay for the ability of the DHX9 cDNAs to rescue the senescent phenotype caused by DHX9 knockdown, the DHX9.267 shRNA was first subcloned into a neomycin-expressing variant of the pPrime vector (pPrime-CMV-Neo, Addgene), infected into cDNA-expressing MRC-5 cells, and selected using G418 (Bioshop, Ontario, CA). Cells were assayed for SA-β-gal expression 14 days after infection of the DHX9.267 (or the control FLuc.1309) shRNAs, as described above.

2.6.8 Microarray analysis and validation

Total RNA from MRC-5 cells was extracted using TRIzol as per the manufacturer's instructions (Life Technologies) five days after infection with shRNAs targeting DHX9 (DHX9.860 and DHX9.267) or FLuc.1309. Extracts from three biological replicates were submitted to the McGill University and Génome Québec Innovation Center's microarray facility. RNA quality was assessed using an Agilent 2100 Bioanalyzer (Agilent Technologies) and the cDNA was generated and hybridized onto the Affymetrix Human Gene 2.0 ST Array. Custom CDF definitions were used for data extraction[465] because of their superior performance compared to standard CDFs[466] and data were normalized using robust multichip averaging (RMA) in R (www.r-project.org) using the "rma" function from the "affy" package with default settings (in R<3.0). Identifiers which showed no variance were removed. We identified differentially expressed genes using a two-tailed t-test that incorporates variance shrinkage[467] and adjusted the resulting p-values using the Benjamini-Hochberg false discovery rate method[468]. Genes were designated differentially expressed if they showed an FDR<0.05 and an absolute fold-change>1.5. For heatmaps (generated by the heatmap.2 function in the "gplots" bioconductor

package) of genes a per-gene normalization was performed. A set of p53 target genes were collected as described previously[432] and their fold-changes (for each shRNA separately) were compared to those of all genes (after excluding the p53 set) using the "density" function in R with a fixed common "bw" parameter. Enrichment of biological processes (as defined by the Gene Ontology Consortium) at the extreme ends of gene lists ordered by signed (up [+] or down [-]) $-\log_{10}$(p-values) derived from the comparison of each DHX9 shRNA to control separately was performed using GAGE[469]. The esset.grp function was used to remove redundant biological processes (e.g. those that are enriched by a common set of genes) and those with a FDR<0.001 were considered significant. For the comparison to data sets of replicative senescence[316], normalized data were downloaded from the Stanford Microarray Database. Only non-flagged genes were considered. For each cell-type (BJ, WI38 or WS1) the mean $\log_2$ fold-change (senescent vs early passage) was calculated. Mean fold-changes for genes that were differentially expressed by either of the DHX9 shRNAs and were represented in the data for each of the cell lines (separately) were collected and plotted. Fisher's exact test (in R) was used to assess if there were more genes showing concordant regulation than expected by chance.

The following qRT-PCR primers (all against human targets) were used for validation: p53 FWD, $^{5'}$CAGCACATGACGGAGGTTGT$^{3'}$; p53 REV, $^{5'}$TCATCCAAATACTCCACACGC$^{3'}$; p21 FWD, $^{5'}$CGATGGAACTTCGACTTTGTCA$^{3'}$; p21 REV, $^{5'}$GCACAAGGGTACAAGACAGTG$^{3'}$; DHX9 FWD, $^{5'}$CAGGAGAGAGAGTTACTGCCT$^{3'}$; DHX9 REV, $^{5'}$CTCTGCTGCTCGGTCATTCTG$^{3'}$; GAPDH FWD, $^{5'}$GAAGGTGAAGGTCGGAGTC$^{3'}$; and GAPDH REV, $^{5'}$GAAGATGGTGATGGGATTC$^{3'}$.

2.6.9 Genomic and nascent DNA isolation and quantitation

Genomic DNA was isolated using the GenElute Mammalian Genomic DNA Miniprep Kit (Sigma), as per the manufacturer's instructions. Nascent DNA was prepared 6 days after transduction with the FLuc.1309 or DHX9 shRNAs, using the λ-exonuclease method, as previously described[470], with the following modifications. The λ-exonuclease-digested samples were heated at 100°C for 3 minutes, then immediately subjected to electrophoresis on a 2% agarose gel. DNA was visualized by staining with 0.02% (w/v) methylene blue (Sigma) and

the origin-containing nascent DNA, ranging between 350bp to 1000bp in size was excised from the gel, purified using the Sephaglas BandPrep Kit (GE Healthcare), as per the manufacturer's instructions, and resuspended in TE. Real-time PCR quantification analysis was performed using the BioRad CFX96 instrument, as previously described[432]. The sequences and amplification conditions for all primer sets are shown in Table 2.1. Genomic DNA from MRC-5 cells was used to generate the standard curves needed for quantification of all the PCR products. A negative control without template DNA was included with each set of reactions. PCR products were also resolved on 2% agarose gels, visualized with ethidium bromide, and photographed with an Eagle Eye apparatus (Speed Light/BT Sciencetech-LT1000).

2.6.10 Chromatin immunoprecipitation (ChIP) assays

Cells cultured in complete media were washed with pre-warmed PBS and treated with 1% formaldehyde for 10 minutes to crosslink proteins and DNA *in vivo*[471]. They were then washed and scraped into ice-cold PBS and resuspended in lysis buffer (50mM HEPES-KOH [pH 7.5], 140mM NaCl, 1% Triton X-100, 2mM EDTA) supplemented with a complete protease inhibitor tablet (Roche Molecular Biochemicals). Following passage through a 21G needle three times, the nuclei were harvested, resuspended in one packed nuclear volume of lysis buffer, and sonicated until DNA fragments of less than 1 kb were obtained. Chromatin size was monitored by electrophoresis. For cell counting, one untreated plate was scraped into PBS and resuspended. The cells were then counted with a hemocytometer, and this number was used to determine the total number of treated cells. The protein concentration of the extracts was determined using the Bradford protein assay (BioRad). IPs were carried out as previously described[471], with the following modifications: sheared chromatin lysates (500 µg) were pre-cleared by incubation with 50 µl of Protein G-Agarose (Roche Molecular Biochemicals) followed by incubation for 6 hours with either 20 µg of antibody against ORC2 (3G6, SC Biotech), Ku86 (H-300, SC Biotech), DHX9 (B-5, SC Biotech), NFκB (C-20, SC Biotech), or normal goat serum (NGS) at 4°C with constant rotation. Protein G-Agarose (50µl) was added and incubated overnight at 4°C. The pelleted beads were washed successively twice with 1 ml of lysis buffer for 15 minutes each at 4°C, followed by 1 ml of WB1 (50 mM Tris-HCl [pH 7.5], 500 mM NaCl, 0.1% NP40, 0.05% sodium deoxycholate, complete protease inhibitor tablet), 1 ml of WB2 (50 mM Tris-HCl [pH

7.5], 0.1% NP40, 0.05% sodium deoxycholate, complete protease inhibitor tablet) and 1 ml of sterile TE. The beads were resuspended in 200 µl TE/1% SDS, incubated at room temperature for 15 minutes and centrifuged at 3000 rpm for 1 minute at room temperature. Half of the supernatant was then incubated overnight at 65°C to reverse the crosslinks, followed by digestion with 100 µg of Proteinase K at 55°C for 2 hours. The DNA was purified using the QIAquick PCR purification kit (Qiagen) and eluted in 100µl TE. The remaining half of the supernatant was boiled for 10 minutes in SDS-PAGE loading buffer and subjected to SDS-PAGE for Western blot analysis. For ChIP analysis of MYC-tagged DHX9 mutants, MRC-5 HAGE-EcoR cells were first tranduced with a MSCVpuro-MYC construct expressing either the WT DHX9 cDNA or the K417N, D511A/E512A, or ΔRBDI+II mutants, and the same procedure as above was followed except that the MYC antibody (9E10, SC-Biotech) was used in place of the DHX9 antibody.

2.7 Acknowledgements

Brightfield images were taken at the McGill Advanced BioImaging Facility (ABIF). This work is supported by a grants from the Canadian Institutes of Health Research [MOP-115126] and National Institutes of Health [CA163291] to J.P, grants from the Swedish Research Council and the Swedish Cancer Society to O.L., and fellowships from the Strategic Training Initiative in Chemical Biology and the Systems Biology Training Program (both sponsored by the Canadian Institutes of Health Research) to T.L.

Table 2.1 Sequences and amplification conditions of primers used for real-time qPCR

Primer Name [a]	Sequence (5'→3')	Size of Amplicon (bp)	qPCR Annealing Temp (^{o}C)
LB2P-F	GGCTGGCATGGACTTTCATTTCAG	232	66
LB2P-R	GTGGAGGGATCTTTCTTAGACATC		
LB2C-F	GTTAACAGTCAGGCGCATGGGCC	240	66
LB2C-R	CCATCAGGGTCACCTCTGGTTCC		
MYC11-F	TATCTACACTAACATCCCACGCTCTG	221	66
MYC11-R	CATCCTTGTCCTGTGAGTATAAATCATCG		
MYC1-F	TTCTCAACCTCAGCACTGGTGACA	249	66
MYC1-R	GACTTTGCTGTTTGCTGTCAGGCT		
hORS8P-F	TTGCACTTCACAGAGCAGTCAT	320	66
hORS8P-R	GACCCACAAAGGCAAAAGTACC		
hORS8C-F	CCCTGAGGCAGGAGTGTTTGCC	520	66
hORS8C-R	GTATGCTCAATCTGCCCAACGG		

[a] F: forward primers; R: reverse primers;
LB2P (peak region) and LB2C1 (control region ~4kb away) at the region of the *lamin B2* locus; MYC11 (peak region) and MYC1 (control region ~6kb away) at the region of the *c-MYC* locus; hORS8P (peak region) and hORS8C (control region ~2kb away) at the region of the human ORS8 locus

CHAPTER 3: Tumor Cell Survival Dependence on the DHX9 DExH-Box Helicase

Published in:

Lee T, Paquet M, Larsson O, and Pelletier J. (2016). Tumor Cell Survival Dependence on the DHX9 DExH-Box Helicase. *Oncogene* **35(39)**:5093-5105.

3.1 Preface to Chapter 3

The Pelletier lab had previously characterized DHX9 as a modifier of ABT-737 sensitivity in *Arf*$^{-/-}$Eμ-*Myc*/Bcl-2 mouse lymphomas which overexpressed both MYC and BCL-2. DHX9 suppression synergized with both ABT-737 and MYC to trigger an apoptotic response in these cells[432]. Whereas DHX9 suppression was synthetic lethal with ABT-737 in the *Arf*$^{-/-}$Eμ-*Myc*/Bcl-2 cells, interestingly, we also noted that loss of DHX9 on its own was lethal in tumors where BCL-2 was not supra-elevated. In this chapter, we extended these results by assessing the consequences of DHX9 suppression on its own in a variety of human and mouse tumor cells. We showed that reduction of cellular fitness following DHX9 suppression is a general phenomenon that is applicable to many different types of cancers. We further explored the therapeutic potential of targeting DHX9 by assessing whether DHX9 suppression would be tolerated at the organismal level. Our lab had previously utilized a novel inducible RNAi platform to examine the consequences of knocking down eIF4E *in vivo*. Using the same technology, we generated a doxycycline-inducible shDHX9 transgenic mouse model and examined the effect of systemic DHX9 suppression on the health, physiology, and biochemistry of the mice, as well as the pathology of various tissues. Our results allowed us to predict whether a suitable therapeutic index for targeting DHX9 can be attained.

3.2 Abstract

The ATP-dependent DExH/D-box helicase DHX9 is a key participant in a number of gene regulatory steps, including transcriptional, translational, microRNA-mediated control, DNA replication, and maintenance of genomic stability. DHX9 has also been implicated in tumor cell maintenance and drug response. Here, we report that inhibition of DHX9 expression is lethal to human cancer cell lines and murine Eμ–*Myc* lymphomas. Using a novel conditional shDHX9 mouse model, we demonstrate that sustained and prolonged (6 months) suppression of DHX9 does not result in any deleterious effects at the organismal level. Body weight, blood biochemistry, and histology of various tissues were comparable to control mice. Global gene expression profiling revealed that although reduction of DHX9 expression resulted in multiple transcriptome changes, these were relatively benign and did not lead to any discernible

phenotype. Our results demonstrate a robust tolerance for systemic DHX9 suppression *in vivo* and support the targeting of DHX9 as an effective and specific chemotherapeutic approach**.**

3.3 Introduction

DHX9 (also known as Nuclear DNA Helicase II (NDH II) and RNA helicase A (RHA)) is an ATP-dependent DExH/D-box helicase capable of unwinding both RNA and DNA[1], as well as aberrant polynucleotide structures[2]. Initially purified from bovine thymus[16], homologs have been subsequently identified in human, mouse, Drosophila, and *C. elegans*[17, 18, 472]. DHX9 is comprised of two RNA-binding domains at the N-terminus, a core helicase region consisting of seven conserved motifs, and a DNA-binding domain and nuclear localization signal at the C-terminus[26]. The presence of numerous functional domains likely contributes to the multifunctional nature of DHX9, which has been implicated in a variety of biological processes. It participates at multiple levels of gene regulation, including transcriptional regulation via interaction with a number of transcription factors and complexes (e.g. CREB-binding protein, EGFR, BRCA1, NF-κB, and RNA polymerase II)[120, 124, 127, 138], translational regulation of specific mRNAs[148, 152], miRNA processing[171], and RNA transport[182]. DHX9 is also an important factor in DNA repair[91] and maintenance of genome stability[2, 38, 98].
We previously uncovered DHX9 as a synthetic lethal hit from an shRNA screen for modifiers of sensitivity to ABT-737 (an inhibitor of BCL-2 family pro-survival factors)[432]. Suppression of DHX9 acted in concert with MYC to sensitize lymphoma cells overexpressing BCL-2 to ABT-737. Subsequent examination of the effects of DHX9 suppression in primary human diploid, non-transformed fibroblasts revealed a pronounced growth arrest and premature senescence phenotype, but not cell death[473]. This was attributed to inhibition of DNA replication which activated a p53-dependent stress response to protect cells from aberrant DNA replication and genomic instability[473]. Hence, DHX9 appears to play an important role in DNA replication and normal cell cycle progression.

Although we initially discovered that inhibiting DHX9 had therapeutic properties in combination with ABT-737 in lymphomas overexpressing BCL-2, we also noted that long-term suppression of DHX9 in tumors with reduced BCL-2 overexpression was lethal on its own (see Suppl. Figs. 10 and 13 in Ref. [432]). In this study, we explore the possibility of DHX9 as a

potential single-agent anti-neoplastic target and assess whether its suppression at the organismal level would be tolerated through the use of an inducible RNAi platform enabling DHX9 suppression *in vivo* in the mouse[474, 475]. Despite having detrimental effects on cellular fitness of tumor cells *ex vivo* and *in vivo*, we observed no adverse consequences resulting from reduced DHX9 expression at the organismal level. Our results support the notion of inhibiting DHX9 as a potential chemotherapeutic target with tolerable side effects.

3.4 Results

3.4.1 DHX9 suppression reduces human cancer cell fitness

Whereas short-term suppression of DHX9 is synthetic lethal in combination with ABT-737 in *Arf*$^{-/-}$Eμ-*Myc/Bcl-2* lymphomas, we previously noted that DHX9 suppression is not well tolerated if BCL-2 is not supra-elevated[432]. To further document this latter effect on transformed cells, we suppressed DHX9 in different human tumor cell lines as well as in the non-immortalized MRC-5 line (Figure 3.1A). Initially, a representative panel of cell lines derived from different types of cancer was tested, including multiple myeloma (KMS-11, JJN-3, and IM-9), osteosarcoma (U2OS), breast (MCF-7 and MDA-MB231), lung (A549), and cervical (Hela) cancers. Infected cells (GFP^+) were co-cultured with non-infected cells (GFP^-) and the $\%GFP^+$ cells determined at t=0 and 10 days (Figure 3.1B). Suppression of DHX9 in all cell lines except MCF-7 led to a decrease in the GFP^+ population over time (Figure 3.1B). To understand the molecular basis of this depletion, we quantified the extent of cell death that ensued following DHX9 suppression and found elevated apoptosis in all tumor lines (Figure 3.1C; 1.4 to 3.7-fold increase), except MCF-7 and U2OS. As previously reported[473], MRC-5 cells did not show evidence of cell death but rather senesced (Figure 3.1C and D). We carried out cell cycle analysis on the tumor cell lines at day 10 after transduction with control or DHX9 shRNAs (Figure 3.2). Upon DHX9 suppression, U2OS cells exhibited a pronounced (~15%) increase in the cells in the G0/G1 phase, and a 7-9% decrease in the number of cells in both the S and G2/M phases (Figure 3.2). This demonstrates that U2OS cells were arresting in the G0/G1 phase, and that this correlated with depletion of shDHX9-expressing cells shown in Figure 3.1B. The IM-9 cells also showed a small G0/G1 arrest (~5% increase in G0/G1 cells). The remaining cell lines (KMS-11, JJN-3, MDA-MB231, A549, and Hela) did not show any significant changes in cell cycle

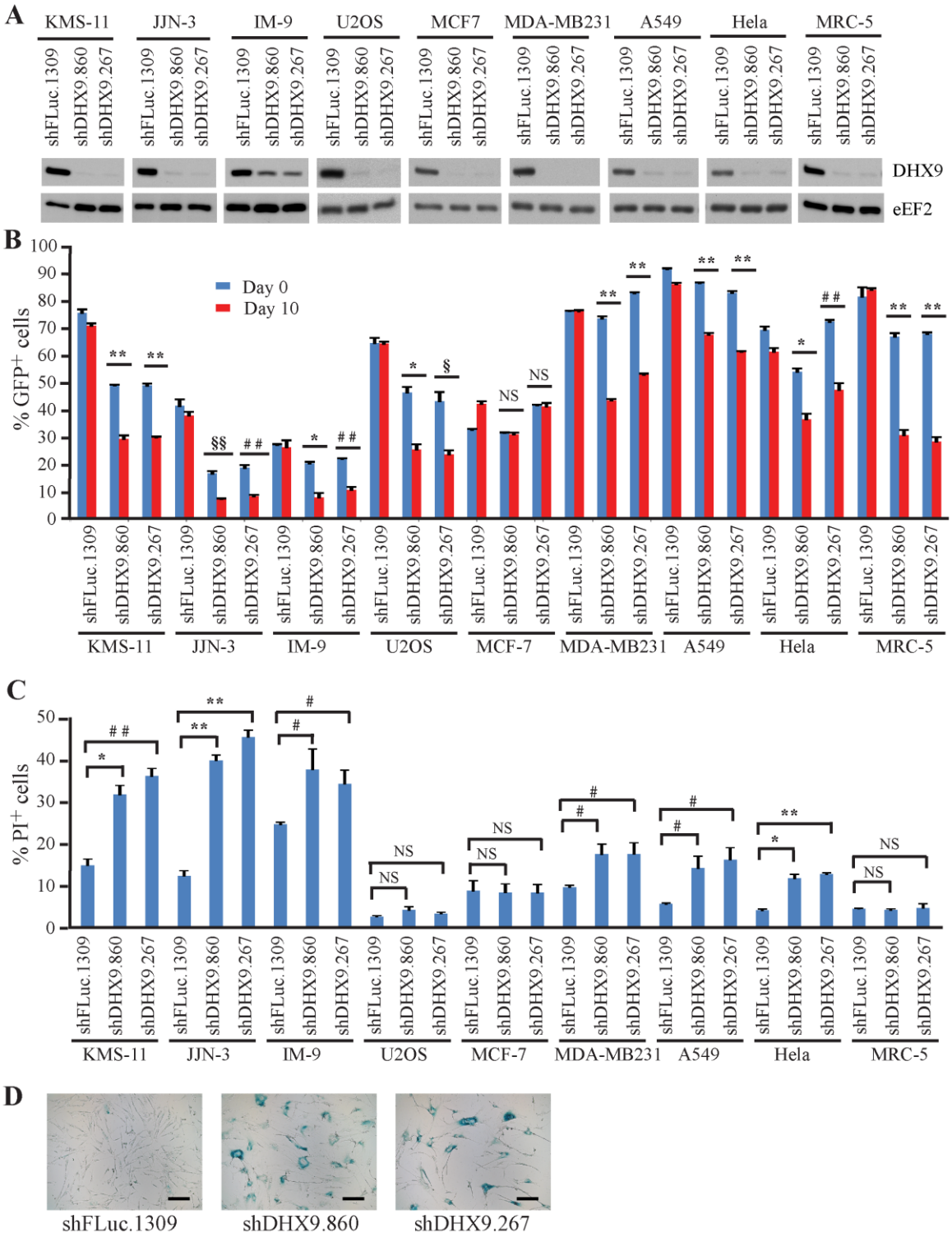

Figure 3.1 DHX9 suppression leads to reduced fitness in human cancer cell lines. Figure legend on following page.

Figure 3.1 DHX9 suppression leads to reduced fitness in human cancer cell lines

(A) Western blot probing for DHX9 levels in the indicated cell lines infected with lentivirus expressing shRNAs targeting DHX9 or a neutral control, FLuc. **(B)** Competition assays showing the percentage of GFP^+ cells over time, following infection of cell lines with the indicated shRNAs. T=Day 0 represents 48h following the final infection. N=3 biological replicates, each with 2 technical replicates, ±SEM. **(C)** Propidium Iodide (PI) staining of the indicated cell lines expressing the indicated shRNAs 7 days post-transduction. N=3 biological replicates, each with 2 technical replicates, ±SEM. **(D)** Senescence-associated β-galactosidase staining of MRC-5 cells transduced with lentivirus expressing the indicated shRNAs, 14 days post-infection. Bars represent 200 μm. # $p \leq 0.05$, § $p \leq 0.01$, * $p \leq 0.005$, ## $p \leq 0.001$, §§ $p \leq 0.0005$, ** $p \leq 0.0001$, NS – not significant.

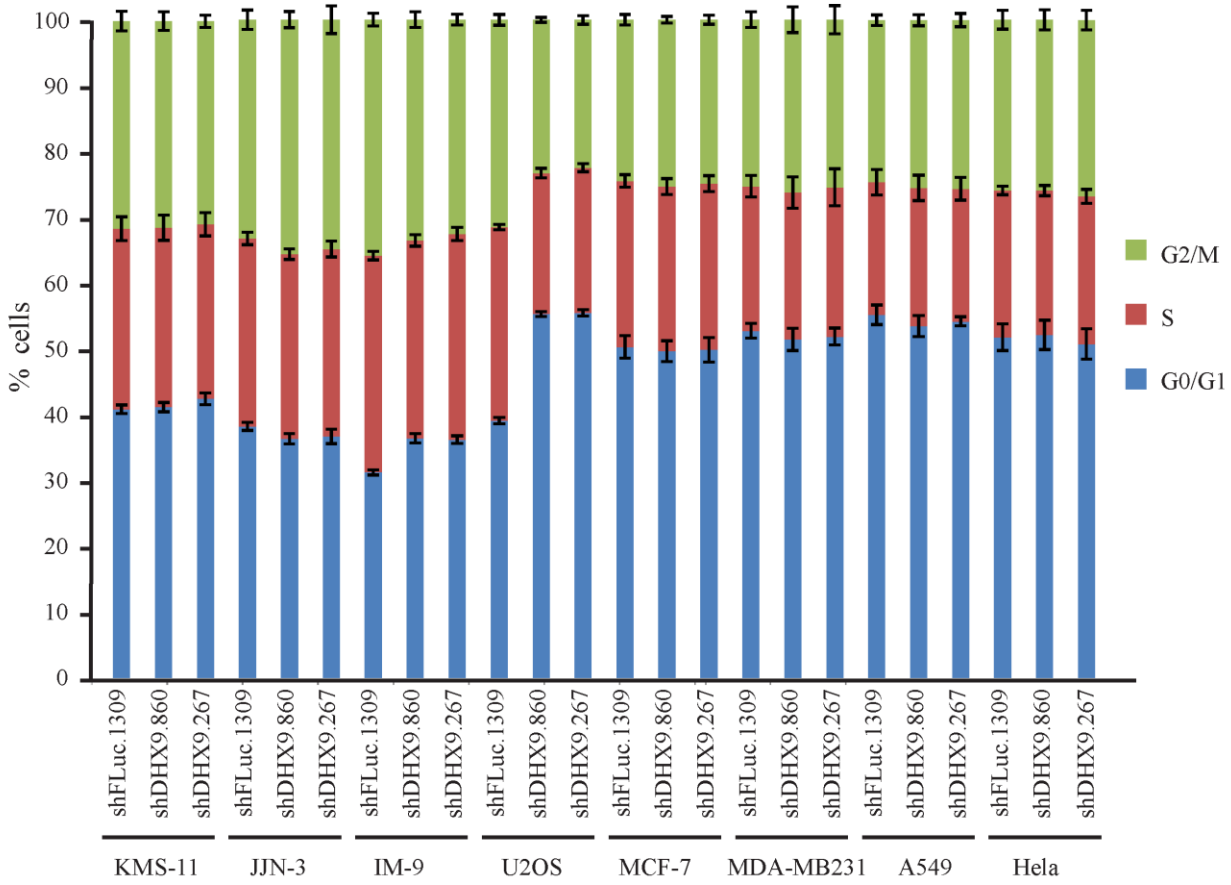

Figure 3.2 Effect of DHX9 suppression on cell cycle distribution in human cancer cell lines.

Cell cycle analysis was performed on the indicated cell lines transduced with shFLuc.1309 or DHX9 shRNAs 10 days post-infection. N=3 biological replicates, each with 2 technical replicates, ±SEM.

distribution upon DHX9 knockdown, suggesting that apoptosis was the main mechanism of the depletion of shDHX9-expressing cells in these lines. The striking difference in phenotype obtained upon DHX9 suppression in the majority of transformed cells versus non-transformed cells prompted us to investigate DHX9 suppression as a potential anti-neoplastic approach.

To gain insight into the possible mechanisms contributing to the differences in response to DHX9 suppression among tumor cells, we compared the expression level of various cell cycle and apoptotic proteins (Figure 3.3). Of all the cell lines tested, only U2OS and MRC-5 demonstrated a significant increase in p21 levels, which may explain why DHX9 suppression elicited a growth arrest response rather than an apoptotic one. We observed a robust increase in p53 expression in JJN-3 and KMS-11 and a moderate increase in U2OS and MRC-5 cells. MDA-MB231 exhibited high basal levels of p53 but no upregulation upon DHX9 suppression, whereas Hela cells had almost non-existent p53 levels – these results are consistent with the former harboring mutated p53 (Ref. [476, 477]) and the latter overexpressing the E6 protein from human papillomavirus type 16, which induces the degradation of p53 (Ref. [478]). While p53 activation may have contributed to the deleterious effect of DHX9 suppression in some of the cancer lines, it is not the only determinant, since both MDA-MB231 and Hela cells were susceptible to DHX9 inhibition. c-MYC expression was relatively high in A549 and Hela cells. Expression of the anti-apoptotic proteins MCL-1 and BCL-2 was highest in KMS-11, JJN-3 and MCF-7 cells. All cell lines expressed similar levels of the pro-apoptotic protein BAX, except for MCF-7, which expressed lower levels. Expression of BIM, another pro-apoptotic protein, was elevated in the three multiple myeloma lines compared to the other cancer lines. High levels of MCL-1 and BCL-2, combined with low levels of BAX and BIM, may have contributed to the resistance of MCF-7 cells to DHX9 suppression. These results indicate that the response of this set of cell lines to DHX9 suppression is not easily attributed to a single cell cycle or apoptotic modulator.

Given that all three multiple myeloma-derived lines showed robust depletion of GFP^+ cells upon loss of DHX9 in the competition assay (Figure 3.1B), we were interested in extending these results. To this end, we assessed the effect of DHX9 suppression in 5 additional multiple myeloma lines: RPMI8226, U266B1, H929, OPM1.1, and OPM2. Of these, RPMI8226, H929, and OPM1.1 showed GFP depletion upon DHX9 knockdown in a competition assay (Figure 3.4B). In total, 6 out of 8 multiple myeloma cell lines exhibited sensitivity to DHX9 suppression

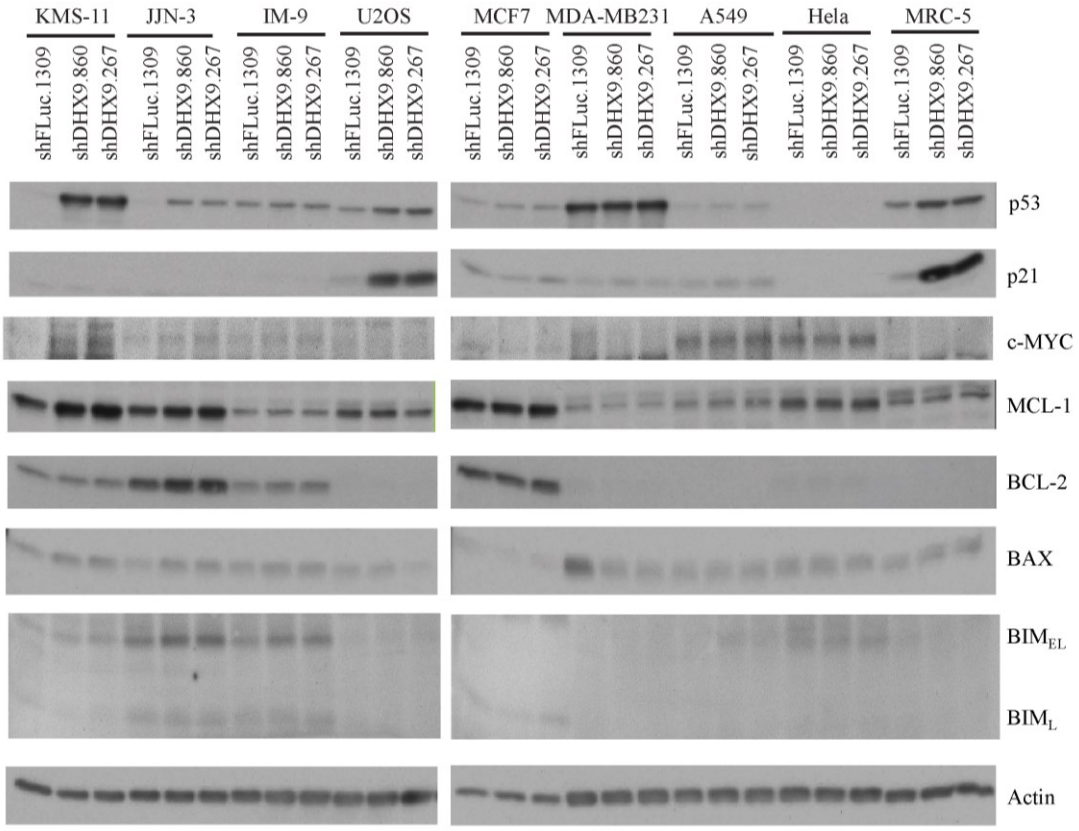

Figure 3.3 Analysis of cell cycle regulatory and apoptotic proteins in various human cancer cell lines.

Western blot analysis of human cell lines transduced with lentivirus expressing FLuc or DHX9 shRNAs. Extracts were probed with antibodies to the proteins indicated to the right of the blots.

(Figure 3.1B and Figure 3.4B). We also examined whether DHX9 would synergize with dexamethasone, a glucocorticoid (GC) used to treat multiple myeloma. Here we tested KMS-11 cells which are responsive to GC (IC_{50} = 50 nM following a 48 h exposure)[479], JJN-3 cells which are resistant to GC with the defect occurring downstream of the GC receptor (IC_{50} >> 3 μM following a 48 h exposure)[479], and IM-9 cells – a GC-resistant lymphoblastoid cell line. Loss of DHX9 was found to sensitize KMS-11 cells to dexamethasone by ~ 1.4-1.5 fold and JJN-3 cells by ~1.7 fold, but had little effect on IM-9 cells (Figure 3.4C). These results indicate that DHX9 suppression is not well tolerated by a number of tumor cells, with multiple myeloma being a particularly susceptible cancer type.

3.4.2 Modeling DHX9 suppression in Eμ-Myc lymphomas

Given the above results, we sought to model the consequences of DHX9 knockdown in a more tractable murine model. First, we recapitulated the results described above using *Tsc2*$^{+/-}$Eμ-*Myc* lymphomas, a MYC-driven tumor model[480]. Suppression of DHX9 in these cells was not well tolerated, with significant depletion of GFP^+ cells occurring within 2 days post-infection using two independent DHX9 shRNAs (Figure 3.5A). This was comparable to what was observed with cells expressing shrpL15.498, which suppresses expression of the essential ribosomal protein, rpL15 (Ref. [481]) (Figure 3.5A). *Tsc2*$^{+/-}$Eμ-*Myc* lymphomas infected with MLS/shRLuc.713, a neutral shRNA targeting *Renilla* luciferase, were unaffected. A significant increase in apoptotic events was observed in DHX9 shRNA-expressing cells, compared to shRLuc.713-expressing cells, and was associated with elevated p53 and p21 levels (Figures 3.5B and C).

To determine whether the lethal effect of DHX9 could be recapitulated *in vivo*, shRNA-expressing *Tsc2*$^{+/-}$Eμ-*Myc* lymphomas were introduced into C57BL/6 mice via tail-vein injection. Injected mice showed an increase in the percentage of splenic B-cells (~75-85%) compared to non-injected controls (45%), consistent with onset of lymphomagenesis (Figure 3.5D). Ten days later, spleens were harvested from the mice and the %GFP^+ *Tsc2*$^{+/-}$Eμ-*Myc* tumor cells determined (Figure 3.5E). *Tsc2*$^{+/-}$Eμ-*Myc* tumor cells expressing the neutral shRLuc.713 control comprised the majority of the splenic cell population and showed a similar GFP^+/GFP^- ratio as the initial injected cell population (Figure 3.5E). In contrast, mice that had

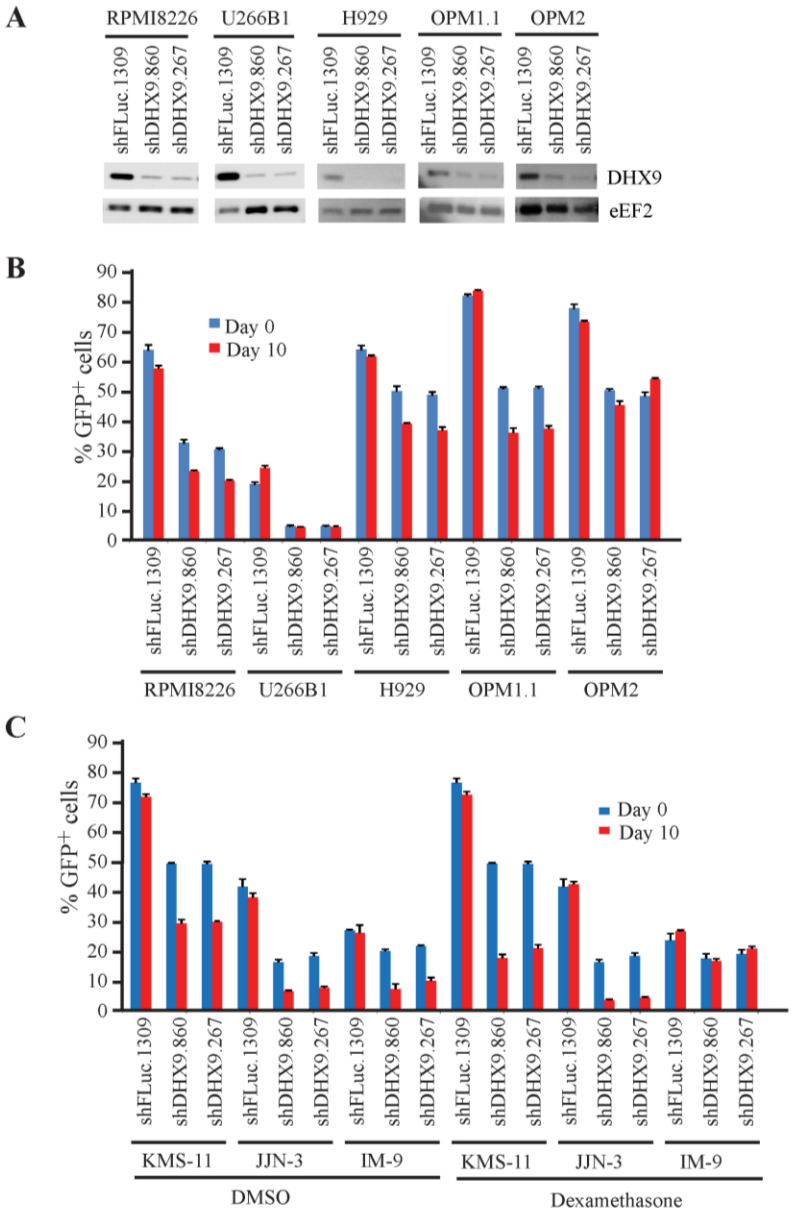

Figure 3.4 Extended panel of multiple myeloma cell lines and sensitivity to DHX9 suppression.

(A) Western blot probing for DHX9 levels in the indicated cell lines infected with lentivirus expressing shRNAs targeting DHX9 or a neutral control, FLuc. **(B)** Competition assays showing the percentage of GFP^+ cells over time, following infection of cell lines with the indicated shRNAs. T=Day 0 represents 48h following the final infection. N=3 biological replicates ±SEM. **(C)** Competition assay demonstrating the effect of DHX9 suppression in combination with dexamethasone treatment. Cells were infected with indicated shRNA and treated with dexamethasone (10 nM for KMS-11 and 100 nM for JJN-3 and IM-9) or a DMSO control. N=3 biological replicates ±SEM.

received *Tsc2*$^{+/-}$Eμ-*Myc* tumor cells expressing shDHX9.1241, shDHX9.1271, or shL15.498 showed a profound (12-18 fold) depletion of GFP^{+} tumor cells 10 days following injection, with the majority of tumor cells exhibiting a GFP^{-} phenotype, likely representing an outgrowth of non-infected tumor cells (~40-50%) arising from the initial population (Figure 3.5E). Taken together, these results demonstrate that DHX9 suppression is lethal in *Tsc2*$^{+/-}$Eμ-*Myc* lymphomas *ex vivo* and *in vivo*.

To determine whether DHX9 suppression had an effect on survival of mice harboring *Tsc2*$^{+/-}$Eμ-*Myc* lymphomas, we took advantage of an shRNA doxycycline-inducible expression system utilizing the TRMPV vector[482] (Figure 3.6A). Here, constitutive expression of Venus facilitates monitoring of infection efficiency whereas dsRed and miR30 expression are dependent on doxycycline and co-expression of rtTA. *Tsc2*$^{+/-}$Eμ-*Myc* lymphomas expressing rtTA were generated by crossing *Tsc2*$^{+/-}$Eμ-*Myc* mice with Rosa26-M2rtTA mice and harvesting the resulting tumors from triple-transgenic progeny[475]. *Tsc2*$^{+/-}$Eμ-*Myc*/R26-M2rtTA tumors were transduced with TRMPV retroviruses expressing RLuc, DHX9 or L15 shRNAs. *Ex vivo*, addition of DOX resulted in robust induction of shRNA expression, as assessed by the percentage of Venus and dsRed double positive cells (Figure 3.6B and C). Conditional suppression of DHX9 resulted in a >6-fold increase in cell death (8 days post-induction) relative to shRLuc.713-infected controls (Figure 3.6D). *Tsc2*$^{+/-}$Eμ-*Myc*/R26-M2rtTA lymphomas infected with TRMPV-shRNAs were then introduced into C57BL/6 mice via tail-vein injection with 50% of each cohort receiving doxycycline (DOX) 6 days post-injection. Spleens harvested at terminal disease stage were enlarged, showed an increased percentage of B-cells compared to non-injected controls (Figure 3.6F), and the majority of splenic B-cells were both Venus and dsRed positive in the DOX-treated mice (Figure 3.6G), demonstrating successful transplantation of the tumor cells and induction by DOX. Untreated and DOX-treated mice harboring tumors expressing shRLuc.713 reached terminal disease 9-10 days following tumor cell transplantation (Figure 3.6H). In contrast, DOX-treated mice harboring tumors expressing shDHX9.1241 and shDHX9.1271 reached terminal disease stage 12-14 days post-injection. Survival was extended to 13-20 days for the shL15.498 +DOX mice (Figure 3.6H). These results are consistent with suppression of DHX9 *in vivo* delaying lymphomagenesis and conferring a survival advantage.

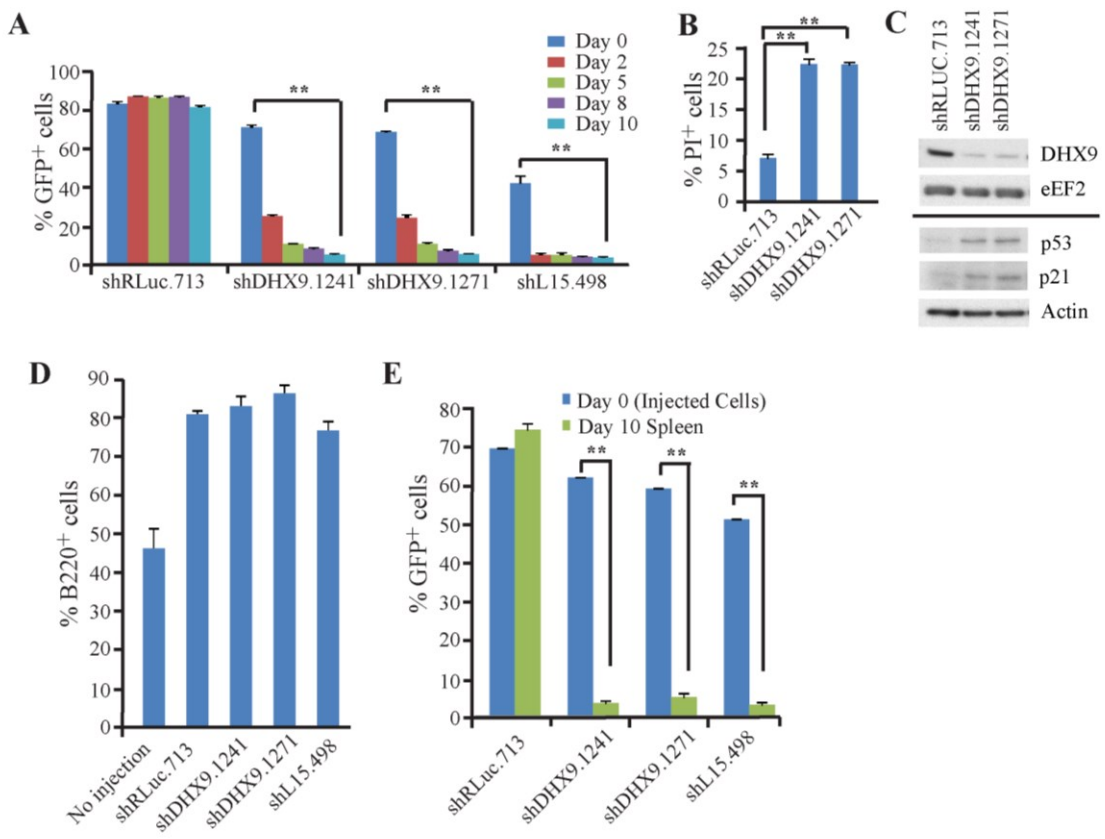

Figure 3.5 DHX9 suppression is lethal in *Tsc2*$^{+/-}$Eμ-*Myc* lymphoma cells.

(A) *Ex vivo* competition assay documenting %GFP^{+} cells over time following infection of *Tsc2*$^{+/-}$ Eμ-*Myc* cells with shRNAs targeting DHX9, RLuc (neutral control), or rpL15 (lethal positive control). The experiment was started 48 hours after the final infection (t=Day 0). N=5 biological replicates ±SEM. **(B)** PI staining of *Tsc2*$^{+/-}$Eμ-*Myc* cells expressing the indicated shRNAs 7 days post-infection. N=5 biological replicates ±SEM. **(C)** Western blot analysis of extracts from *Tsc2*$^{+/-}$Eμ-*Myc* cells expressing the indicated shRNAs. **(D)** Quantitation of the %B220^{+} cells in spleens harvested from mice which had been injected with *Tsc2*$^{+/-}$Eμ-*Myc* cells expressing the indicated shRNAs. Spleens were harvested 10 days after injection. N=5 biological replicates ±SEM. (**E**) *In vivo* competition assay with *Tsc2*$^{+/-}$Eμ-*Myc* cells. *Tsc2*$^{+/-}$Eμ-*Myc* cells expressing the indicated shRNAs were introduced into mice via tail-vein injection 24h after the final infection (t=Day 0). Spleens were harvested 10 days post-injection and the %GFP^{+} tumor cells assessed. N=5 biological replicates ±SEM. ** p≤0.0001.

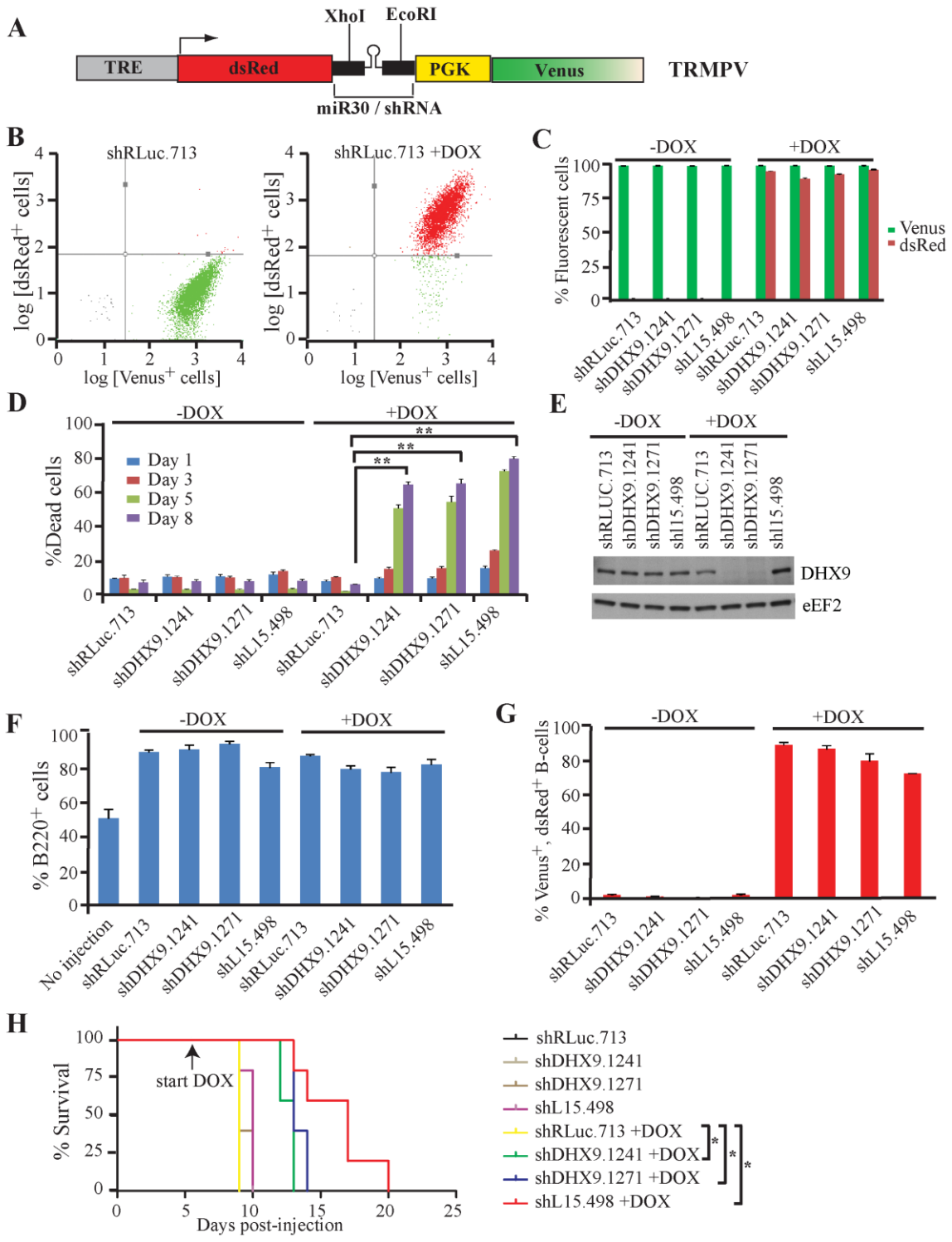

Figure 3.6 DHX9 suppression enhances the survival of mice harboring *Tsc2*$^{+/-}$Eμ-Myc lymphomas. Figure legend on following page.

Figure 3.6 DHX9 suppression enhances the survival of mice harboring *Tsc2*$^{+/-}$Eμ-*Myc* lymphomas.

(A) Schematic diagram of the doxycycline-inducible vector, TRMPV. **(B)** Representative flow cytometry plots of *Tsc2*$^{+/-}$Eμ-*Myc*/R26-M2rtTA cells transduced with TRMPV-shRLUC.713. Following infection, cells were sorted for a pure Venus-expressing population and then exposed to 1 μg/ml DOX. The %Venus^{+} and %dsRed^{+} cells were assessed 24h after DOX induction. **(C)** Quantification of Venus^{+} and dsRed^{+} *Tsc2*$^{+/-}$Eμ-*Myc*/R26-M2rtTA cells transduced with DOX-responsive retroviruses expressing the indicated shRNAs. Cells were sorted and treated with DOX as in (b), and the %Venus^{+} and %dsRed^{+} cells were assessed 24h after DOX induction. N=6 biological replicates ±SEM. **(D)** Assessment of cell death in *Tsc2*$^{+/-}$Eμ-*Myc*/R26-M2rtTA cells transduced with DOX-responsive retroviruses expressing the indicated shRNAs. Dead cells were stained with the blue-fluorescent viability dye eFluor450 and the %dead cells was determined at the indicated time points post-DOX induction. N=5 biological replicates ±SEM, ** $p \leq 0.0001$. **(E)** Western blot analysis of extracts from *Tsc2*$^{+/-}$Eμ-*Myc*/R26-M2rtTA cells expressing the indicated shRNAs. **(F)** Quantification of the %B220^{+} cells from spleens harvested from C57BL/6 mice injected with *Tsc2*$^{+/-}$Eμ-*Myc*/R26-M2rtTA cells expressing the indicated shRNAs (treated with vehicle or 1 mg/ml DOX) at terminal disease stage. N=5 mice ±SEM. **(G)** Quantification of the %Venus^{+} dsRed^{+} B220^{+} spleen cells harvested from C57BL/6 mice injected with *Tsc2*$^{+/-}$Eμ-*Myc*/R26-M2rtTA cells expressing the indicated shRNAs (treated with vehicle or 1 mg/ml DOX) at terminal disease stage. N=5 mice ±SEM. (**H**) Kaplan-Meier survival curve of C57BL/6 mice injected with *Tsc2*$^{+/-}$Eμ-*Myc*/R26-M2rtTA cells expressing the indicated shRNAs. Mice were treated with vehicle or 1 mg/ml DOX at day 6 following injection of the tumor cells. * $p<0.005$ for comparisons between shRLuc.713+DOX and each of the shDHX9.1241+DOX, shDHX9.1271+DOX and shL15.498 cohorts. N=5 mice per condition.

3.4.3 Modeling conditional DHX9 suppression in the mouse

Whereas intriguing, the aforementioned results do not address whether DHX9 suppression would be tolerated at the organismal level. To this end, we took advantage of a previously described FLP/FRT-mediated site-specific recombination approach to introduce DHX9 shRNAs into the mouse germline[475] (Figure 3.7A). As a prelude to these studies, we tested several DHX9 shRNAs for suppression potency (Table 3.1 and Figure 3.7B). Several shRNAs (DHX9.1241, DHX9.1271 and DHX9.837) showed potent DHX9 suppression and two of these (DHX9.1271 and DHX9.837) were chosen for generating transgenic mice. Two mouse strains were generated, *DHX9.837/rtTA* and *DHX9.1271/rtTA,* containing DHX9 shRNA expression under TRE regulation at the Col1A1 locus and rtTA expression driven from the Rosa26 locus. Transgenic mice expressing a neutral shRNA targeting Firefly luciferase (*FLuc.1309/rtTA*) were used as controls[475].

Examination of DHX9 expression in various tissues from *FLuc.1309/rtTA*, *DHX9.837/rtTA*, and *DHX9.1271/rtTA* mice treated with either vehicle or 1 mg/ml DOX for 14 days revealed suppression in all tissues examined, although the extent varied (Figure 3.8). The small intestine, large intestine, and thymus exhibited potent knockdown of DHX9 in both *shDHX9* strains. In the skin, liver and heart, knockdown was moderate and the spleen exhibited weaker, mosaic suppression (Figure 3.8). Expression of DHX9 was predominantly nuclear (Figure 3.9), consistent with previous studies[66]. TurboGFP, as expected, was DOX-inducible (Figure 3.10). These results were confirmed by Western blot analysis of DHX9 knockdown and turboGFP expression in the aforementioned tissues (Figure 3.11).

Previous studies have shown that DHX9 knockdown increases p53 protein levels and activity in human fibroblasts, *Arf*$^{-/-}$Eμ-*Myc*/*Bcl-2* lymphomas, and U2OS cells[432, 473]. To determine whether these changes were recapitulated in our murine models, we examined RB1, p53, and p21 status following DHX9 suppression (Figure 3.11). We observed no consistent, robust induction of p53 in tissues from the two shDHX9 mouse strains either by Western blotting (Figure 3.11) or immunohistochemistry (Figure 3.12). There was also no consistent activation of the p53 target, P21. RB1 was expressed at very low levels in the skin and liver, and was unchanged upon DHX9 knockdown in all tissues analyzed (Figure 3.11). These results indicate

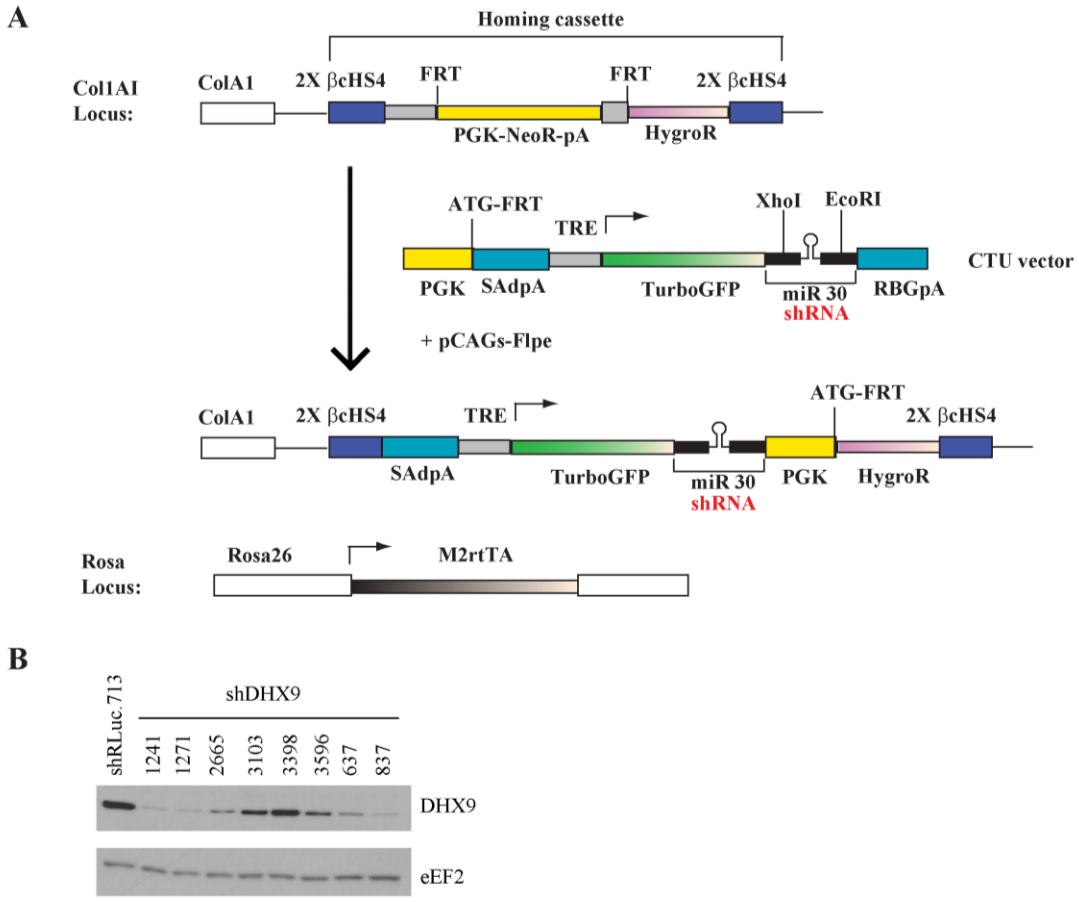

Figure 3.7 Generation of sh*DHX9/rtTA* transgenic mice.

(A) Design of the Col1A1-targeting vector. The shRNA, embedded in the miR30 backbone, was targeted to the Col1A1 locus on chromosome 11 using FLP-mediated recombination, as previously described[474, 483]. The M2rtTA transgene is present at the Rosa26 locus on chromosome 6 in KH2 ES cells[475]. Note that whereas the DHX9.837 and DHX9.1271 shRNAs are linked to turboGFP, in shFLuc.1309 mice it is linked to GFP. TRE, tetracycline response element; FRT, flippase recombinase target; SAdpA, splice acceptor-double polyA; βcHS4, chicken β-globin control region hypersensitive site 4; RGBpA, rabbit β-globin polyA. **(B)** Knockdown efficiency of DHX9 shRNAs. NIH3T3 cells were infected with MLP vectors expressing either shRLuc.713 or shRNAs targeting DHX9 and stable integrants were selected using puromycin. Extracts prepared from infected cells were analyzed by Western blotting.

Table 3.1 Sequences of shRNAs used in this study

List of 22-bp guide strand sequences for shRNAs used, as well as the source of sequence design.

	22mer guide (5'to 3')	Source
RLuc.713	TAGATAAGCATTATAATTCCTA	BIOPREDsi prediction
FLuc.1309	TTAATCAGAGACTTCAGGCGGT	BIOPREDsi prediction
DHX9.1241	TAATTCATTCTTAAGGTCCATG	BIOPREDsi prediction
DHX9.1271	TAAATTATGATCTTGTTCCATC	BIOPREDsi prediction
DHX9.837	TTTAGATCCATGTTCACGTGCG	Sensor assay
DHX9.637	TATCCACTTCTTCTGACTCTAG	Sensor assay
DHX9.3271	TAAAAACAAAGAAAGGAGATGG	Sensor assay
DHX9.2021	TCATTCAACTGAGACATGCTCA	Sensor assay
DHX9.3398	TTCCAGTCATCTATAAACACAA	Sensor assay
DHX9.3596	TTTACACTTCCAATCATAAGGT	Sensor assay
DHX9.267	TCACACATGAATTTCTGCCTGT	BIOPREDsi prediction
DHX9.860	TATTTGATCCATGTTCTCGTGC	BIOPREDsi prediction

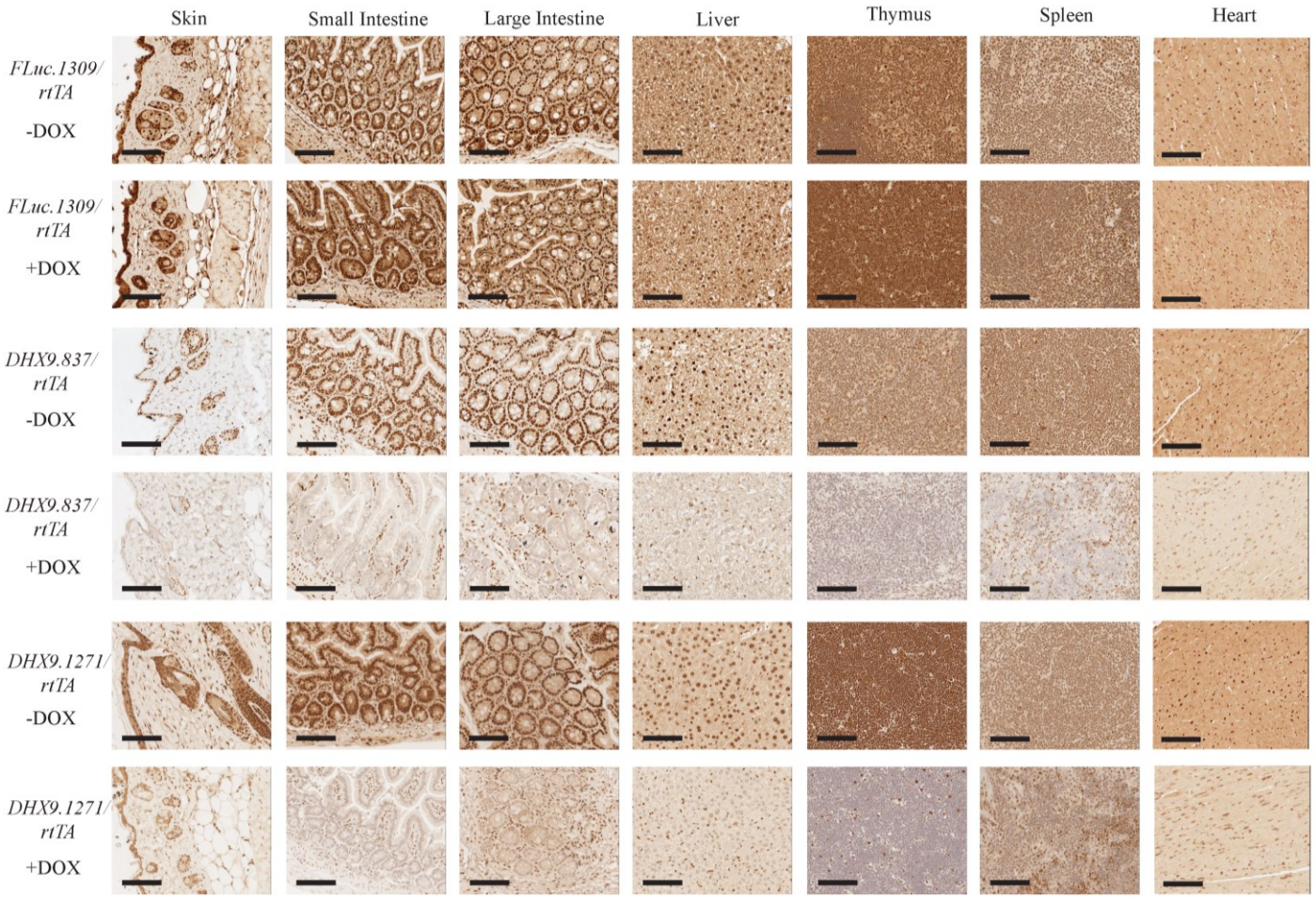

Figure 3.8 DOX-mediated DHX9 suppression in *DHX9/rtTA* mice.

Immunohistochemical analysis of representative tissues from *FLuc.1309/rtTA*, *DHX9.837/rtTA*, and *DHX9.1271/rtTA* mice treated with vehicle or 1 mg/ml DOX for 14 days. Sections were probed with anti-DHX9 antibody and counterstained with hematoxylin. Bars represent 100 μm.

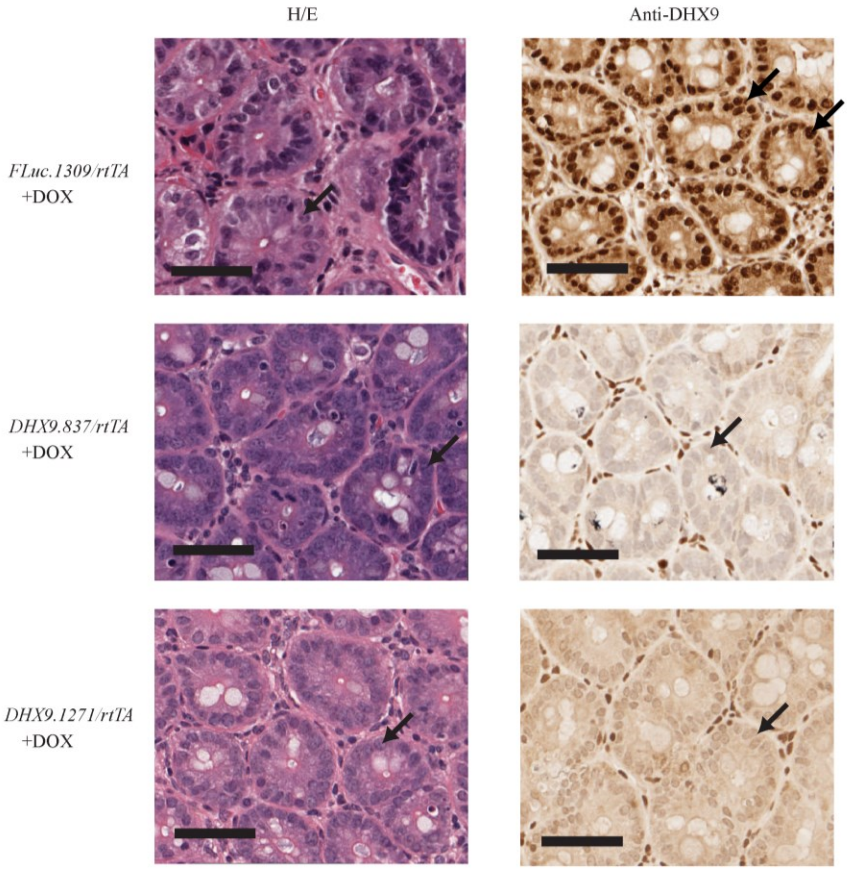

Figure 3.9 Expression of DHX9 is predominantly nuclear in transgenic mice.

Immunohistochemical analysis of large intestine from DOX-treated (14 days) *FLuc.1309/rtTA*, *DHX9.837/rtTA*, and *DHX9.1271/rtTA* mice, stained with H/E or DHX9 antibody. Bars represent 50 μm. Arrows indicate nuclei.

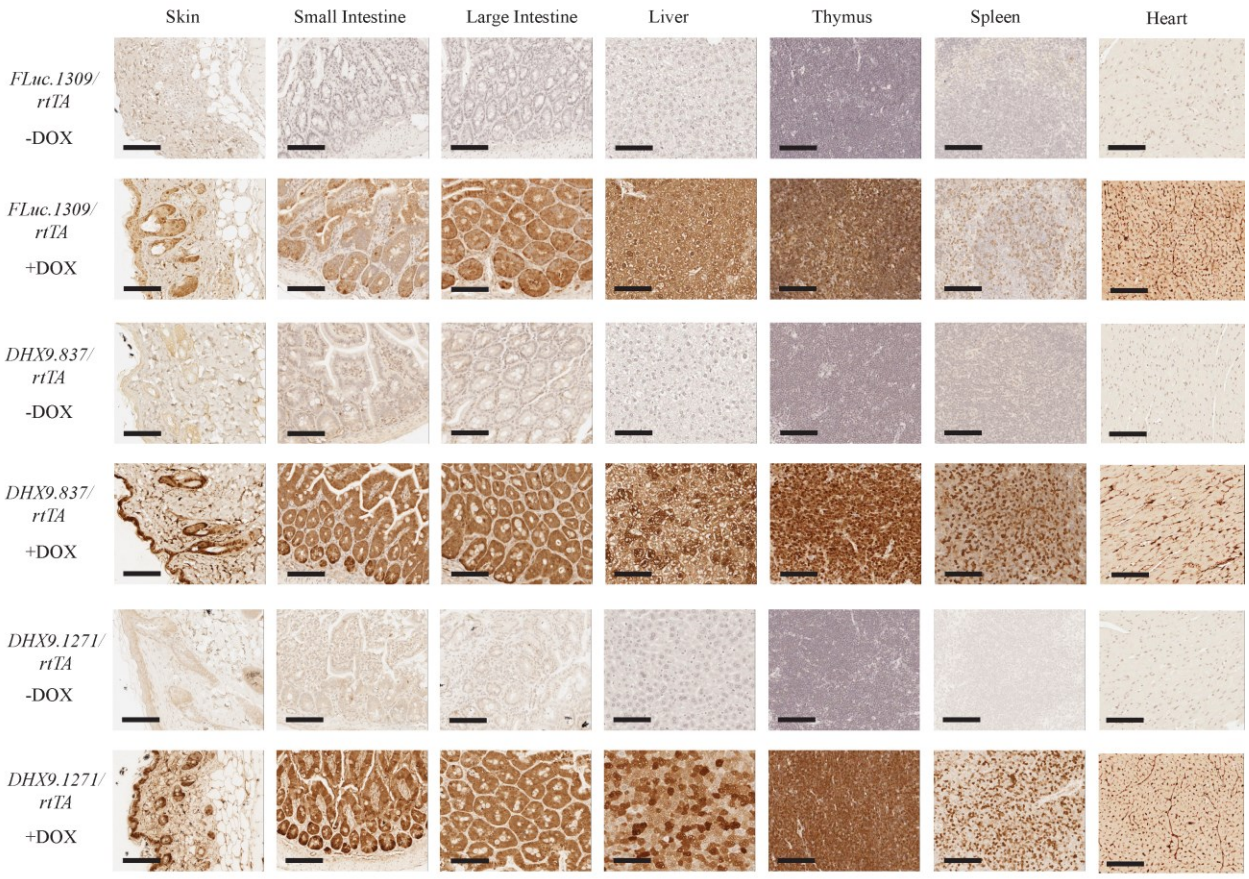

Figure 3.10 Inducible expression of turboGFP in sh*DHX9/rtTA* mice.

Immunohistochemical analysis of representative tissues from untreated and DOX-treated (14 days) *FLuc.1309/rtTA*, *DHX9.837/rtTA*, and *DHX9.1271/rtTA* mice. Sections were probed with anti-GFP (for *FLuc.1309/rtTA*) or anti-turboGFP (for *DHX9.837/rtTA* and *DHX9.1271/rtTA*) antibodies and counterstained with hematoxylin. Bars represent 100 μm.

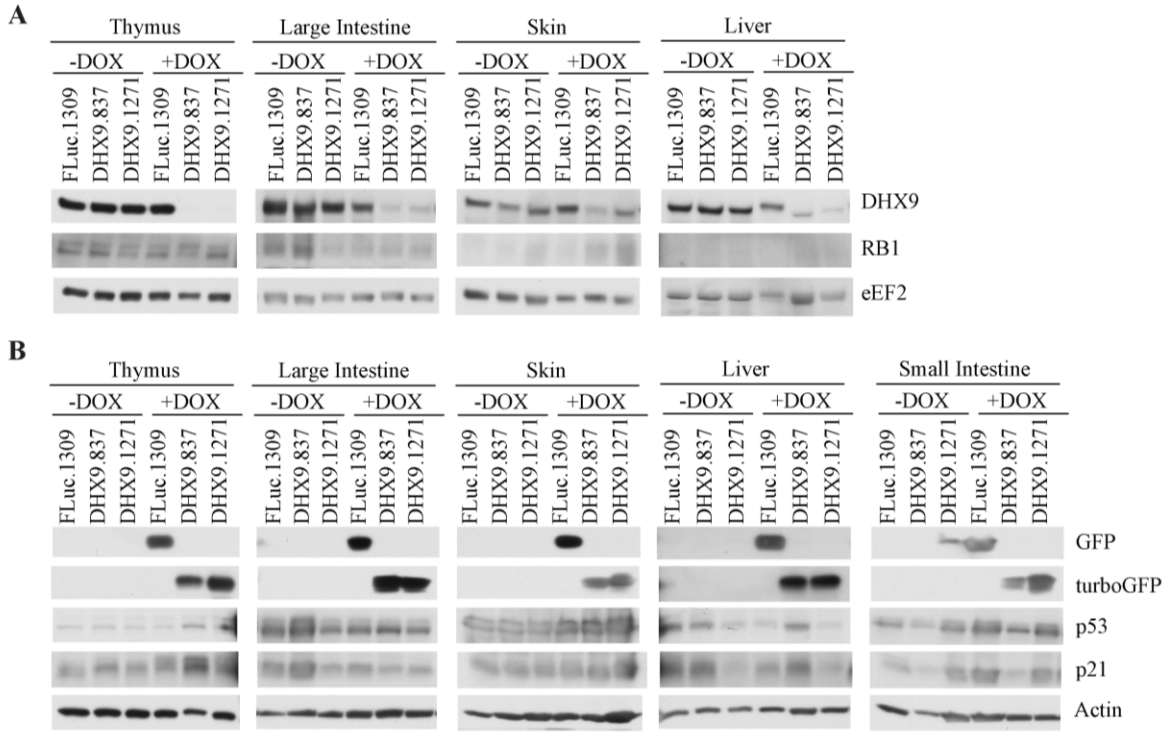

Figure 3.11 Cell cycle regulatory and DNA damage response pathways are not activated upon DHX9 suppression in mouse tissues.

Western blot analysis of indicated tissues from *FLuc.1309/rtTA*, *DHX9.837/rtTA*, and *DHX9.1271/rtTA* mice treated with vehicle or DOX for 14 days. Extracts were fractionated on 6% **(A)** or 15% **(B)** polyacrylamide gels, processed for Western blotting, and probed with antibodies to the proteins indicated to the right of the blots.

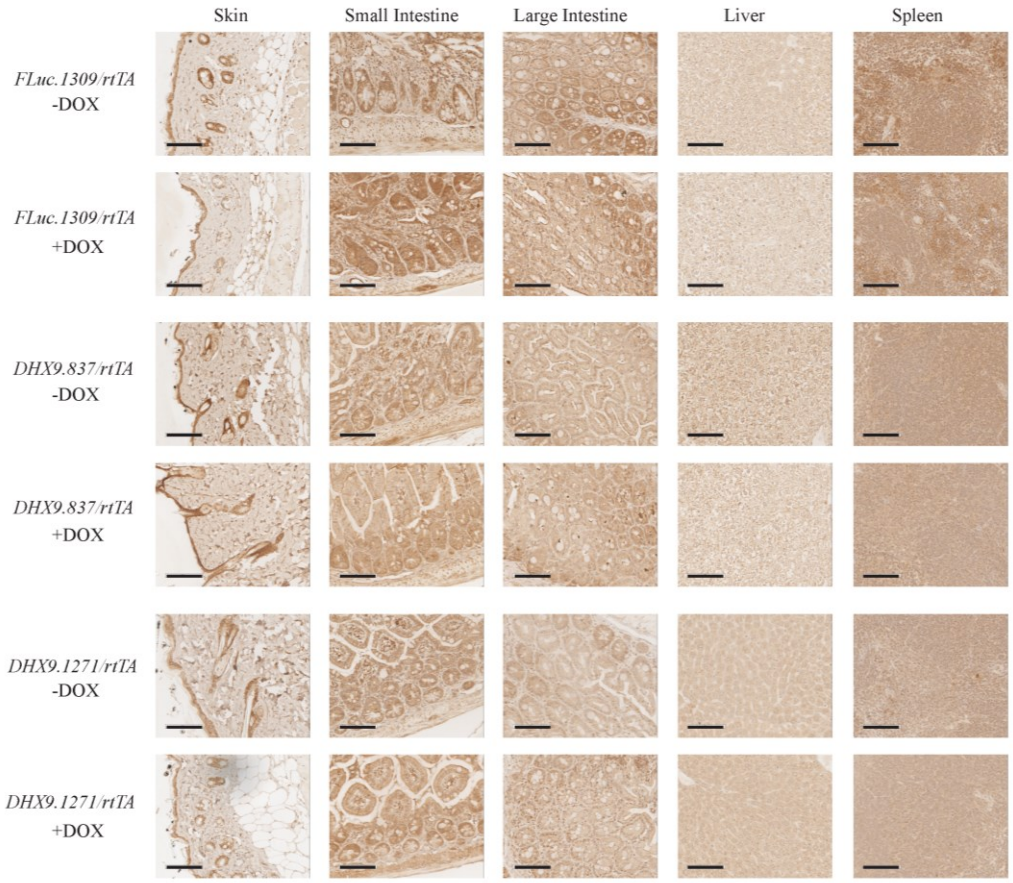

Figure 3.12 DHX9 suppression does not alter p53 levels in *shDHX9/rtTA* mice.

Immunohistochemical analysis of p53 levels in representative tissues from untreated and doxycycline (DOX)-treated (14 days) *FLuc.1309/rtTA, DHX9.837/rtTA*, and *DHX9.1271/rtTA* mice. Tissues were probed with a p53 antibody and counterstained with hematoxylin. Bars represent 100 μm.

that under the conditions analyzed, we find no evidence for robust activation of p53, P21, or RB1 upon DHX9 suppression at the organismal level.

3.4.4 DHX9 knockdown in adult mice is well tolerated

We next examined the consequences of DHX9 suppression to the general health and physiology of adult mice. Mice (4 week old) were treated with DOX for 6 months. Efficient long-term knockdown of DHX9 and induction of GFP was verified in various tissues (Figure 3.13). In this chronic DHX9-suppressed cohort, the weight, appearance, and behavior of *DHX9.837/rtTA* and *DHX9.1271/rtTA* mice on DOX were similar to those of *FLuc.1309/rtTA* (+DOX) and untreated mice (Figure 3.14A and B). We observed no evidence of weight loss, lowered activity levels, lack of grooming, hunched appearance, dehydration, or infections. Blood biochemical and hematological analyses of the treated cohorts revealed no significant differences from *FLuc.1309/rtTA* (+DOX) or untreated controls (Tables 3.2 – 3.4), implying normal physiology and bone marrow function. Histopathological analysis of tissues from mice treated with DOX for 6 months did not reveal any pathological changes in the skin, small and large intestines, spleen, thymus, and heart specific to the *DHX9/rtTA* cohort (Table 3.5 and Figure 3.14C) nor in the % of splenic B and T cells (Figure 3.14D). In addition, Ki-67 and TUNEL staining was performed on the more proliferative tissues - namely skin, spleen, and small and large intestines. DHX9 suppression had no deleterious effects on proliferation in the skin and spleen, as determined by Ki-67 staining (Figure 3.15). A slight decrease in Ki-67-positive cells was observed in the small and large intestines upon treatment with DOX, however this appeared to be due to the DOX itself, as it was seen in the *FLuc.1309/rtTA* +DOX mice as well. There appeared to be no significant difference between the *FLuc.1309/rtTA* and *DHX9/rtTA* DOX-treated samples in these tissues (Figure 3.15). TUNEL staining revealed no increase in apoptotic cells upon DHX9 suppression in any of the tissues tested (Figure 3.16).

3.4.5 Assessing DHX9 suppression on global gene expression

Having observed no apparent negative physiological effects of DHX9 suppression in mice, we asked whether reduced DHX9 levels induced any changes in global gene expression *in vivo*. To

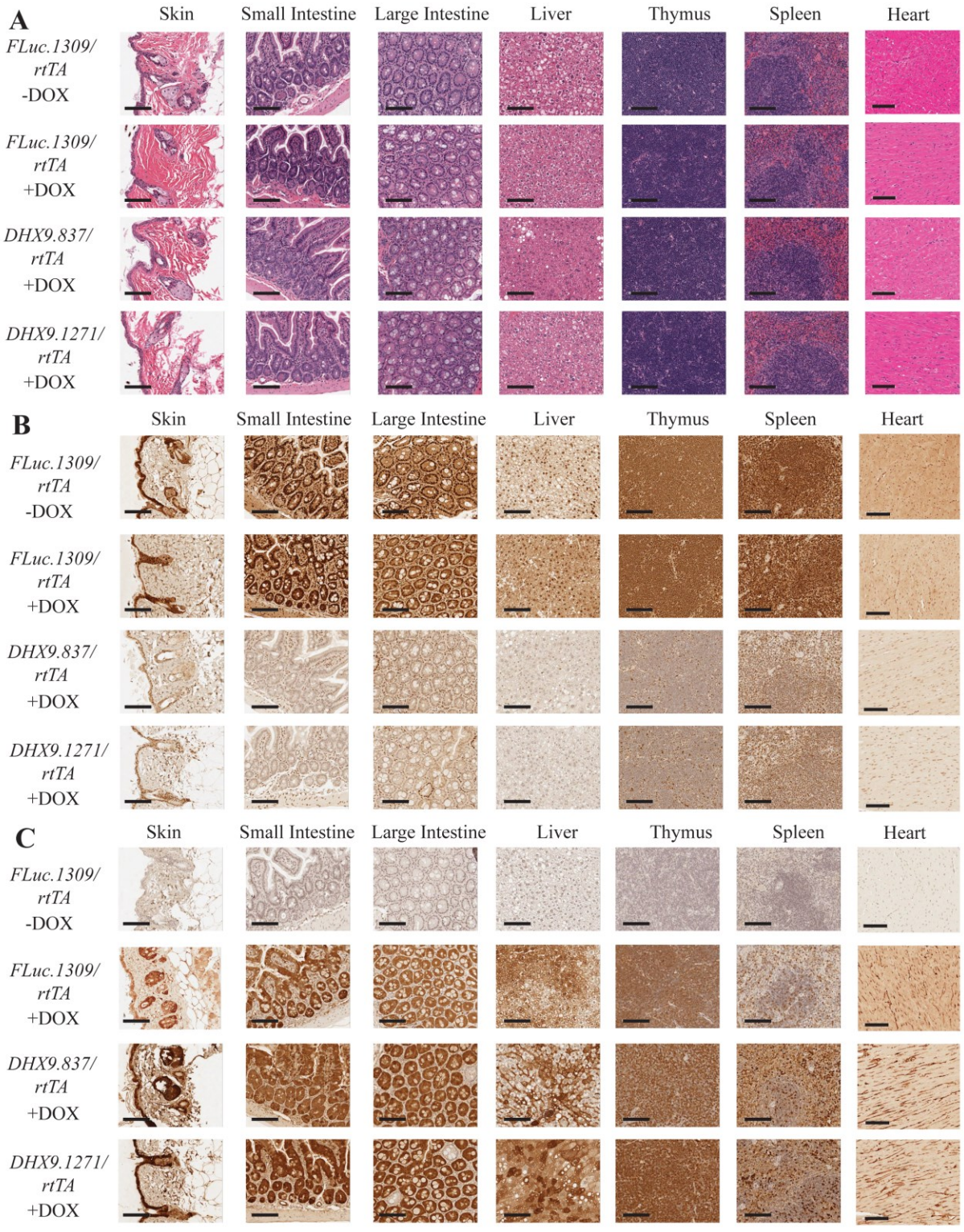

Figure 3.13 Characterization of long-term DHX9 suppression. Figure legend on following page.

Figure 3.13 Characterization of long-term DHX9 suppression.

(A) H/E staining of representative tissues from vehicle and DOX-treated (6 months) *FLuc.1309/rtTA*, *DHX9.837/rtTA*, and *DHX9.1271/rtTA* mice. Bars represent 100 μm. **(B)** Immunohistochemical analysis of representative tissues from untreated and DOX-treated (6 months) *FLuc.1309/rtTA*, *DHX9.837/rtTA*, and *DHX9.1271/rtTA* mice. Sections were probed with anti-DHX9 antibody and counterstained with hematoxylin. Bars represent 100 μm. **(C)** Immunohistochemical analysis of representative tissues from untreated and DOX-treated (6 months) *FLuc.1309/rtTA*, *DHX9.837/rtTA*, and *DHX9.1271/rtTA* mice. Sections were probed with anti-GFP (for *FLuc.1309/rtTA*) or anti-turboGFP (for *DHX9.837/rtTA* and *DHX9.1271/rtTA*) antibodies and counterstained with hematoxylin. Bars represent 100 μm.

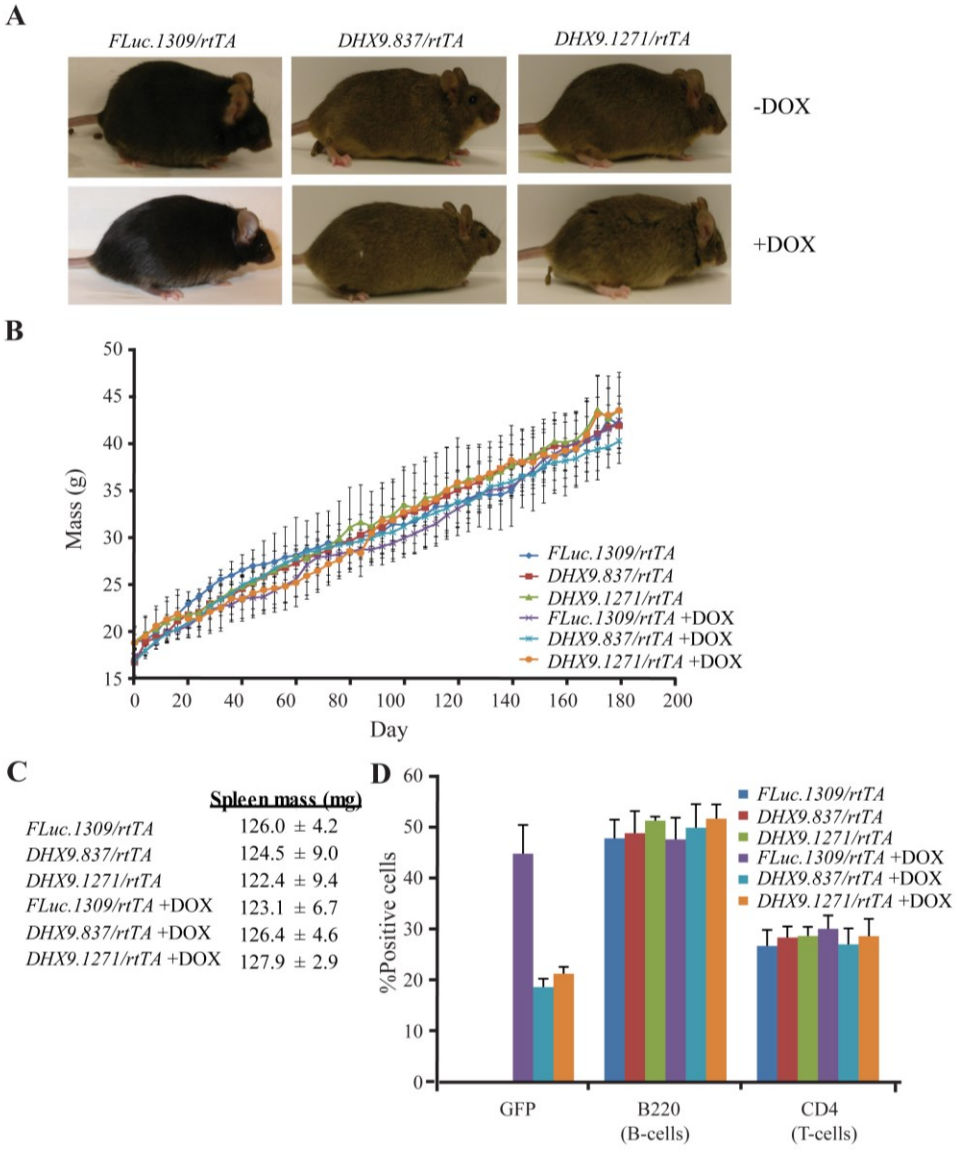

Figure 3.14 Long-term suppression of DHX9 is well-tolerated in mice.
(A) Photographs of *FLuc.1309/rtTA*, *DHX9.837/rtTA*, and *DHX9.1271/rtTA* mice after treatment with vehicle or 1 mg/ml DOX for 6 months. **(B)** Weight of *FLuc.1309/rtTA*, *DHX9.837/rtTA*, and *DHX9.1271/rtTA* mice treated with vehicle or DOX over a 6 month period. Mice were weighed every 4 days starting at 4 weeks of age (t=Day 0). N=3 mice ±SEM. **(C)** Weight of spleens extracted from *FLuc.1309/rtTA*, *DHX9.837/rtTA*, and *DHX9.1271/rtTA* mice treated with vehicle or DOX for 6 months. Spleen weights were normalized to mouse weights. N=3 mice ±SEM. **(D)** Flow cytometry analysis of splenocytes extracted from *FLuc.1309/rtTA*, *DHX9.837/rtTA*, and *DHX9.1271/rtTA* mice after treatment with vehicle or DOX for 6 months. Single-cell suspensions were prepared from mouse spleen and stained with PE-conjugated antibodies against B220 and CD4, and the percentage of stained cells determined by FACS analysis. N=3 mice ±SEM.

Table 3.2 Effect of short-term DHX9 suppression on blood biochemistry

Biochemical analysis was performed on blood extracted from *FLuc.1309/rtTA*, *DHX9.837/rtTA*, and *DHX9.1271/rtTA* mice treated with vehicle or 1 mg/ml DOX for 14 days. N=3 biological replicates, ±SEM.

			FLuc.1309/ rtTA	***DHX9.837/ rtTA***	***DHX9.1271/ rtTA***	***FLuc.1309/ rtTA***	***DHX9.837/ rtTA***	***DHX9.1271/ rtTA***
		DOX:	-	-	-	+	+	+
	Units	**REF values**						
Total protein	**g/L**	**36-66**	47.00 ± 9.00	45.67 ± 4.06	44.50 ± 2.50	39.33 ± 4.91	43.00 ± 2.39	48.00 ± 1.00
Albumin	**g/L**	**25-48**	25.00 ± 4.00	22.67 ± 2.73	21.50 ± 0.50	20.00 ± 2.31	22.75 ± 1.73	25.00 ± 1.00
Albumin/ Globulin ratio			1.15 ± 0.05	0.93 ± 0.09	0.95 ± 0.05	1.10 ± 0.10	1.15 ± 0.09	1.10 ± 0.00
BUN urea	**mmol/L**	**6.4-10.4**	5.25 ± 0.75	5.50 ± 1.13	6.10 ± 2.50	15.83 ± 10.26	5.75 ± 0.46	5.10 ± 0.50
Creatinine	**mmol/L**	**18-71**	8.50 ± 3.50	5.00 ± 0.58	10.50 ± 0.50	33.33 ± 25.44	6.50 ± 1.29	9.00 ± 2.00
Total bilirubin	**mmol/L**	**2 -15**	22.00 ± 19.00	15.33 ± 7.42	21.00 ± 1.00	16.33 ± 5.46	16.00 ± 4.05	20.50 ± 6.50
ALT	**U/L**	**28-132**	100.50 ± 53.50	142.00 ± 56.32	89.50 ± 16.50	64.33 ± 13.86	197.75 ± 102.13	116.00 ± 46.00
Alkaline Phosphatase	**U/L**	**62-209**	196.00 ± 7.00	163.33 ± 19.85	93.00 ± 12.00	218.67 ± 25.76	150.75 ± 15.57	102.50 ± 16.50
Cholesterol	**mmol/L**	**0.93-2.48**	2.12 ± 0.07	2.49 ± 0.10	2.32 ± 0.27	2.25 ± 0.29	2.04 ± 0.25	2.21 ± 0.17
Sodium	**mmol/L**	**124-174**	142.00 ± 2.00	146.67 ± 3.18	145.00 ± 3.00	144.00 ± 2.00	145.00 ± 2.25	148.00 ± 3.00
Potassium	**mmol/L**	**4.6-8**	6.90 ± 2.60	5.63 ± 1.36	6.50 ± 0.30	7.23 ± 1.02	5.70 ± 0.72	7.15 ± 0.55
Chloride	**mmol/L**	**92-120**	111.50 ± 0.50	113.67 ± 2.33	115.50 ± 4.50	112.67 ± 2.85	112.75 ± 1.57	112.50 ± 1.50
Calcium	**mmol/L**	**1.47-2.35**	2.25 ± 0.06	2.14 ± 0.05	2.16 ± 0.03	2.16 ± 0.07	2.16 ± 0.03	2.21 ± 0.01
Phosphorus	**mmol/L**	**1.97-3.26**	3.13 ± 0.47	2.71 ± 0.22	3.12 ± 0.48	4.28 ± 1.35	3.53 ± 0.30	3.03 ± 0.02
Magnesium	**mmol/L**	**0.33-1.6**	1.25 ± 0.11	1.12 ± 0.09	1.10 ± 0.14	1.84 ± 0.70	1.12 ± 0.02	1.00 ± 0.04

Table 3.3 Effect of long-term DHX9 suppression on blood biochemistry

Biochemical analysis was performed on blood extracted from *FLuc.1309/rtTA*, *DHX9.837/rtTA*, and *DHX9.1271/rtTA* mice treated with vehicle or 1 mg/ml DOX for 6 months. N=3 biological replicates, ±SEM.

			FLuc.1309/ rtTA	***DHX9.837/ rtTA***	***DHX9.1271/ rtTA***	***FLuc.1309/ rtTA***	***DHX9.837/ rtTA***	***DHX9.1271/ rtTA***
		DOX:	-	-	-	+	+	+
	Units	**REF values**						
Total protein	**g/L**	**36-66**	48.00 ± 3.51	50.00 ± 1.15	50.33 ± 0.67	50.00 ± 0.58	51.33 ± 1.76	50.67 ± 2.19
Albumin	**g/L**	**25-48**	22.33 ± 3.18	24.00 ± 0.58	26.33 ± 0.67	23.67 ± 0.33	25.00 ± 0.58	25.33 ± 1.20
Albumin/ Globulin ratio			0.90 ± 0.10	0.90 ± 0.06	1.07 ± 0.03	0.93 ± 0.03	0.97 ± 0.03	1.00 ± 0.06
BUN urea	**mmol/L**	**6.4-10.4**	6.67 ± 0.58	4.57 ± 0.69	6.70 ± 0.12	9.80 ± 1.78	4.53 ± 0.32	6.20 ± 0.53
Creatinine	**mmol/L**	**18-71**	9.00 ± 1.73	5.33 ± 0.88	5.67 ± 0.88	13.00 ± 6.03	6.67 ± 1.76	4.33 ± 0.33
Total bilirubin	**mmol/L**	**2 to 15**	6.67 ± 2.67	10.67 ± 3.84	7.67 ± 4.67	11.00 ± 1.15	8.90 ± 6.56	10.67 ± 8.17
ALT	**U/L**	**28-132**	100.67 ± 60.17	40.00 ± 7.55	61.33 ± 7.06	65.67 ± 20.08	46.33 ± 3.48	78.67 ± 15.68
Alkaline Phosphatase	**U/L**	**62-209**	64.67 ± 26.91	56.00 ± 2.31	91.67 ± 11.67	67.67 ± 5.46	120.67 ± 41.79	85.33 ± 19.85
Cholesterol	**mmol/L**	**0.93-2.48**	3.61 ± 0.52	2.77 ± 0.32	3.26 ± 0.24	3.04 ± 0.13	1.58 ± 0.24	2.96 ± 0.52
Sodium	**mmol/L**	**124-174**	143.67 ± 0.88	143.00 ± 0.58	144.67 ± 1.86	143.33 ± 0.88	147.67 ± 2.60	144.00 ± 1.53
Potassium	**mmol/L**	**4.6-8**	5.20 ± 0.25	4.83 ± 0.24	5.07 ± 0.19	5.77 ± 1.12	5.13 ± 0.19	5.20 ± 0.44
Chloride	**mmol/L**	**92-120**	110.33 ± 0.67	108.33 ± 1.20	110.33 ± 0.88	108.00 ± 0.58	110.67 ± 0.67	110.67 ± 0.33
Calcium	**mmol/L**	**1.47-2.35**	2.25 ± 0.00	2.23 ± 0.05	2.29 ± 0.03	2.25 ± 0.05	2.29 ± 0.05	2.33 ± 0.06
Phosphorus	**mmol/L**	**1.97-3.26**	2.53 ± 0.24	2.33 ± 0.26	2.64 ± 0.22	2.82 ± 0.52	2.61 ± 0.01	2.82 ± 0.12
Magnesium	**mmol/L**	**0.33-1.6**	1.15 ± 0.05	1.14 ± 0.04	1.17 ± 0.01	1.19 ± 0.13	1.07 ± 0.01	1.06 ± 0.06

Table 3.4 Effect of DHX9 suppression on mouse hematology

Hematological analysis was performed on blood extracted from *FLuc.1309/rtTA*, *DHX9.837/rtTA*, and *DHX9.1271/rtTA* mice treated with vehicle or 1 mg/ml DOX for 14 days. N=5 biological replicates, ±SEM. RBCs = red blood cells; WBCs = white blood cells; MCV = mean corpuscular volume; MCH = mean corpuscular hemoglobin; MCHC = mean corpuscular hemoglobin concentration.

			FLuc.1309/ rtTA	***FLuc.1309/ rtTA***	***DHX9.837/ rtTA***	***DHX9.1271/ rtTA***
		DOX:	-	+	+	+
	Units					
Hematocrit	**L/L**		0.38 ± 0.01	0.37 ± 0.00	0.35 ± 0.02	0.35 ± 0.01
Hemoglobin	**g/L**		136.00 ± 2.47	131.80 ± 1.24	124.20 ± 6.84	129.00 ± 4.94
RBCs	**x 10^{12}/L**		8.35 ± 0.16	8.07 ± 0.09	7.66 ± 0.40	7.83 ± 0.34
MCV	**fL**		46.00 ± 0.00	46.00 ± 0.00	45.60 ± 0.24	46.00 ± 0.00
MCH	**pg**		16.32 ± 0.08	16.34 ± 0.09	16.18 ± 0.13	16.48 ± 0.19
MCHC	**g/L**		354.00 ± 1.67	354.40 ± 2.14	354.60 ± 2.29	359.20 ± 4.04
WBCs	**x 10^{9}/L**		2.94 ± 0.19	3.26 ± 0.31	2.70 ± 0.39	2.48 ± 0.28
Neutrophils	**%**		33.20 ± 10.68	29.60 ± 9.36	29.60 ± 10.19	26.80 ± 8.59
Lymphocytes	**%**		64.60 ± 10.98	68.80 ± 9.52	62.80 ± 7.74	70.00 ± 8.64
Monocytes	**%**		0.60 ± 0.40	0.20 ± 0.20	0.20 ± 0.20	1.40 ± 0.24
Eosinophils	**%**		1.60 ± 0.40	1.40 ± 0.24	1.40 ± 0.60	1.40 ± 0.75
Neutrophils	**x 10^{9}/L**		1.02 ± 0.37	1.06 ± 0.36	0.93 ± 0.35	0.73 ± 0.26
Lymphocytes	**x 10^{9}/L**		1.85 ± 0.28	2.16 ± 0.23	1.72 ± 0.15	1.67 ± 0.19
Monocytes	**x 10^{9}/L**		0.02 ± 0.01	0.01 ± 0.01	0.01 ± 0.01	0.03 ± 0.01
Eosinophils	**x 10^{9}/L**		0.05 ± 0.01	0.04 ± 0.01	0.14 ± 0.09	0.04 ± 0.02
Platelets	**x 10^{9}/L**		723.80 ± 88.61	783.00 ± 127.22	838.00 ± 136.96	774.00 ± 101.35

Table 3.5 Histopathological analysis following long-term DHX9 suppression in *DHX9/rtTA* mice

		FLuc.1309/ rtTA	***FLuc.1309/ rtTA***	***DHX9.837/ rtTA***	***DHX9.1271/ rtTA***
	DOX:	**-**	+	+	+
Skin		N	N	N	N
Small Intestine		N	N	N	N
Large Intestine		N	N	N	N
Liver		A	A	A	A
Microgranuloma, multifocal, random		1	1	1	1
Hepatic lipidosis, microvacuolar, centrolubular, diffuse				3	
Thymus		N	N	N	N
Spleen		N	N	N	N
Heart		N	N	N	N

Histopathological analysis was performed on representative tissues extracted from *FLuc.1309/rtTA*, *DHX9.837/rtTA*, and *DHX9.1271/rtTA* mice treated with 1 mg/ml DOX for 6 months. Multifocal, random microgranulomas (Grade 1) were present in the liver of all mice analyzed and are likely a consequence of non-specific bacterial or viral infection. One *DHX9.837/rtTA* (+DOX) liver sample displayed moderate hepatic lipidosis which was not observed in the *DHX9.1271/rtTA* liver sample. Key: N = no significant lesion, A = lesion observed, 0 = no tissue; Grade 1 = modest, rare, Grade 2 = mild, infrequent, Grade 3 = moderate, frequent, Grade 4 = severe, diffuse.

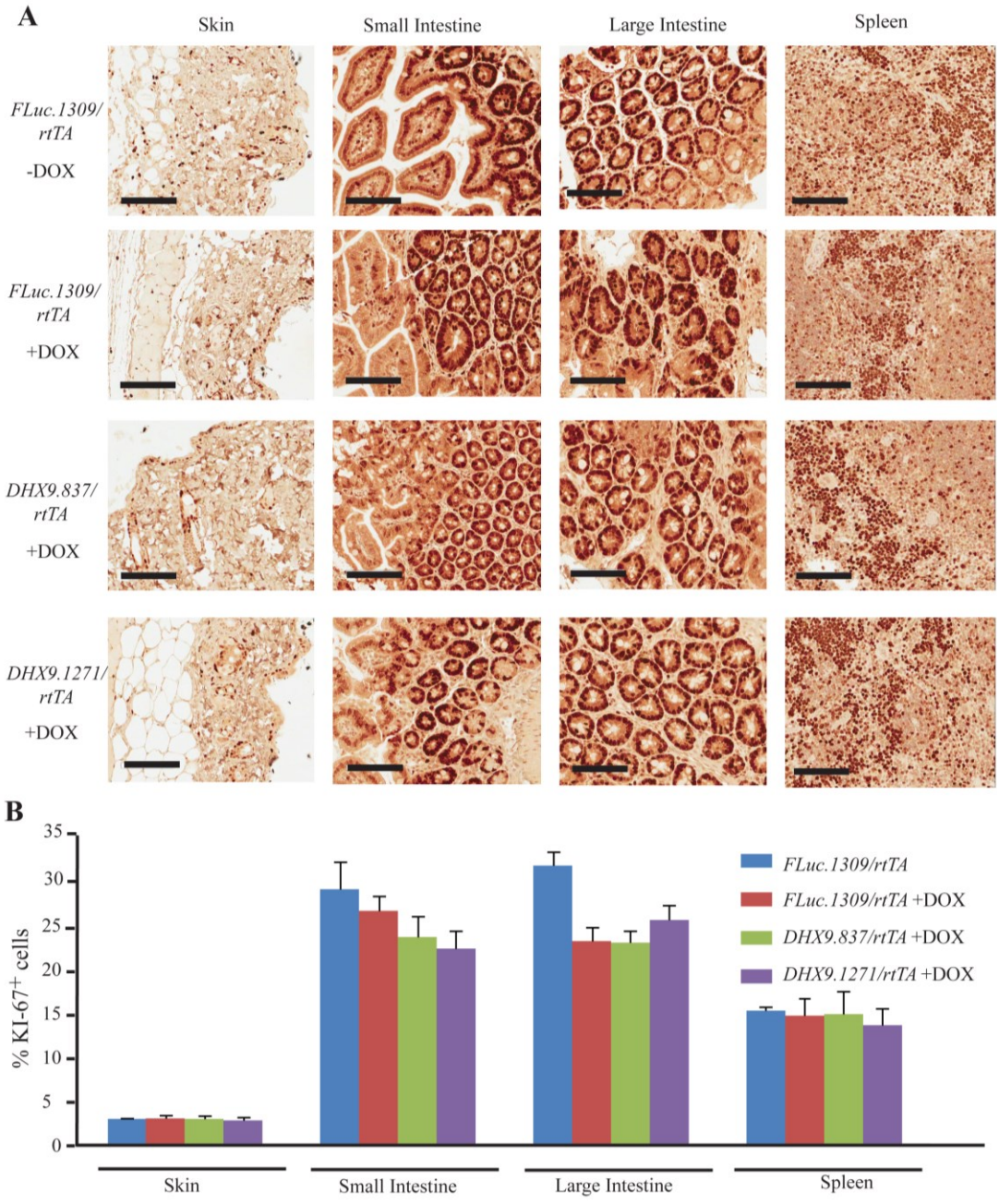

Figure 3.15 Effect of systemic DHX9 suppression on proliferation in tissues.

(A) Immunohistochemical analysis of proliferation in skin, spleen, and small and large intestines in tissues from *FLuc.1309/rtTA*, *DHX9.837/rtTA*, and *DHX9.1271/rtTA* mice treated with vehicle or DOX for 14 days. Sections were probed with a Ki-67 antibody and counterstained with hematoxylin. Bars represent 100 μm. **(B)** Quantification of Ki-67-stained cells in (A). Values represent the average of 5 random fields of view, and error bars represent SEM.

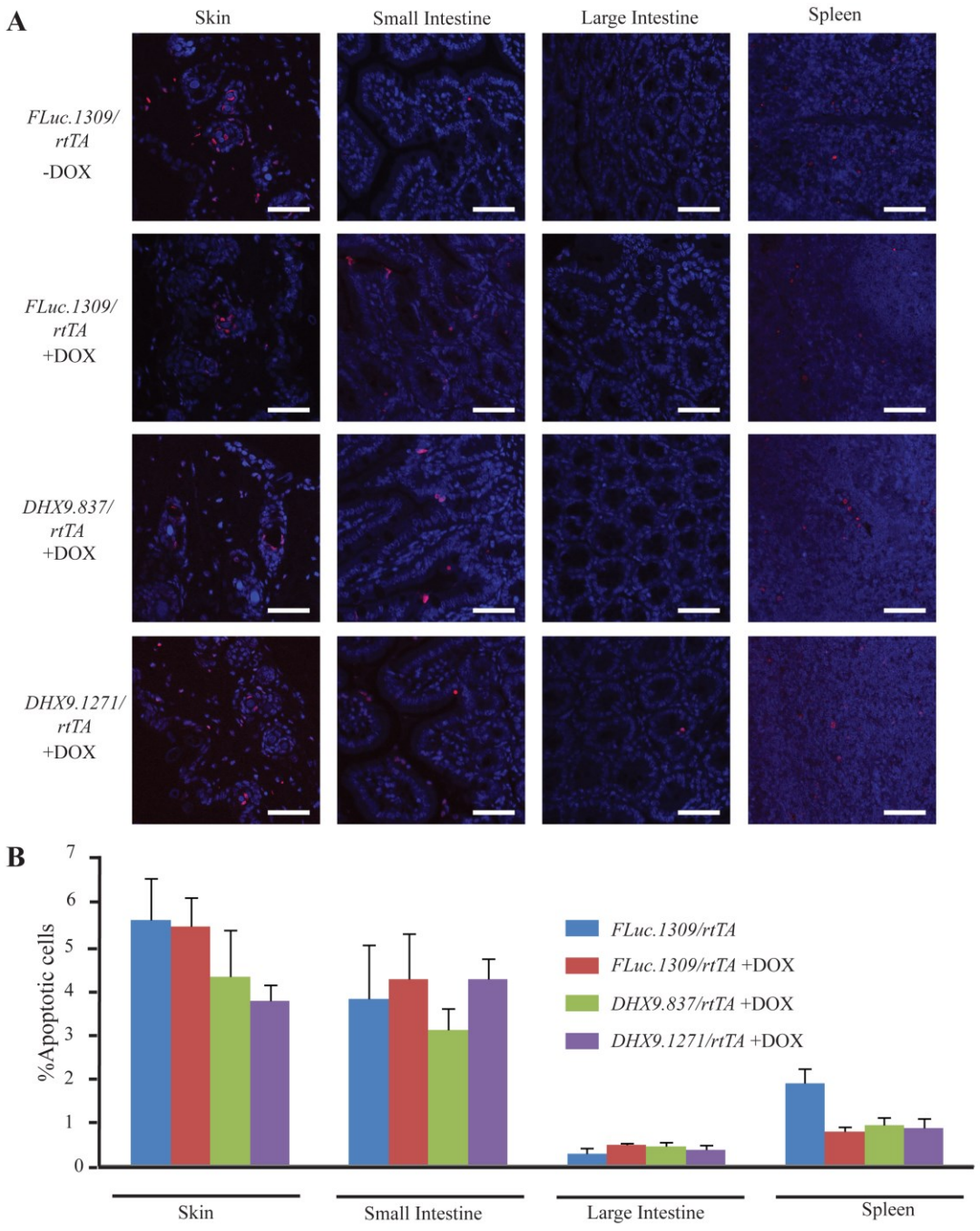

Figure 3.16 Effect of systemic DHX9 suppression on apoptosis in tissues.

(A) TUNEL assay on skin, spleen, and small and large intestines in tissues from *FLuc.1309/rtTA*, *DHX9.837/rtTA*, and *DHX9.1271/rtTA* mice treated with vehicle or DOX for 14 days. Sections were counterstained with DapI. Apoptotic cells are shown in red. Bars represent 50 μm. **(B)** Quantification of apoptotic cells in (A). Values represent the average of 6 random fields of view, and error bars represent SEM.

address this, we conducted gene expression analysis on the large intestine isolated from *FLuc.1309/rtTA*, *DHX9.837/rtTA* and *DHX9.1271/rtTA* mice treated with DOX for 14 days. The large intestine was chosen because it was one of the tissues showing potent suppression of DHX9, which was validated in samples isolated for global gene expression studies (Figure 3.17A). A comparison of the expression patterns between *DHX9/rtTA* and *FLuc.1309/rtTA* samples identified 451 transcripts as differentially expressed in at least one of the DHX9/*rtTA* mice (fold-change>1.5 and false discovery rate (FDR)<0.05; Figure 3.17B and Table A.2). Although only 77 transcripts were significantly altered in both shDHX9 transgenic samples, the fold-changes observed for the combined set of genes were largely consistent for both DHX9 shRNAs (Figure 3.17C). Our previous transcriptome-wide analysis of DHX9 suppression in cell lines showed activation of the p53 signaling pathway in *ex vivo* contexts[432, 473]. This phenomenon was not observed in the large intestine of DOX-treated *DHX9.837/rtTA* and *DHX9.1271/rtTA* mice (Figure 3.17D). Moreover, there were only minor changes in levels of p53 mRNA itself (1.2 or 1.4 fold for *DHX9.837/rtTA and DHX9.1271/rtTA,* respectively) without concomitant changes in p21, consistent with Western blot results (Figure 3.11). Gene set enrichment analysis was applied to identify functions that were enriched among genes showing differential expression. The identified biological processes found to be most affected by DHX9 suppression were DNA replication, translation, RNA splicing, non-coding RNA processes, and nuclear division (Figure 3.17E and Tables A.3 and A.4). Taken together, these results indicate significant transcriptome changes as a consequence of DHX9 suppression in the large intestine, but these do not lead to any overt pathological perturbations.

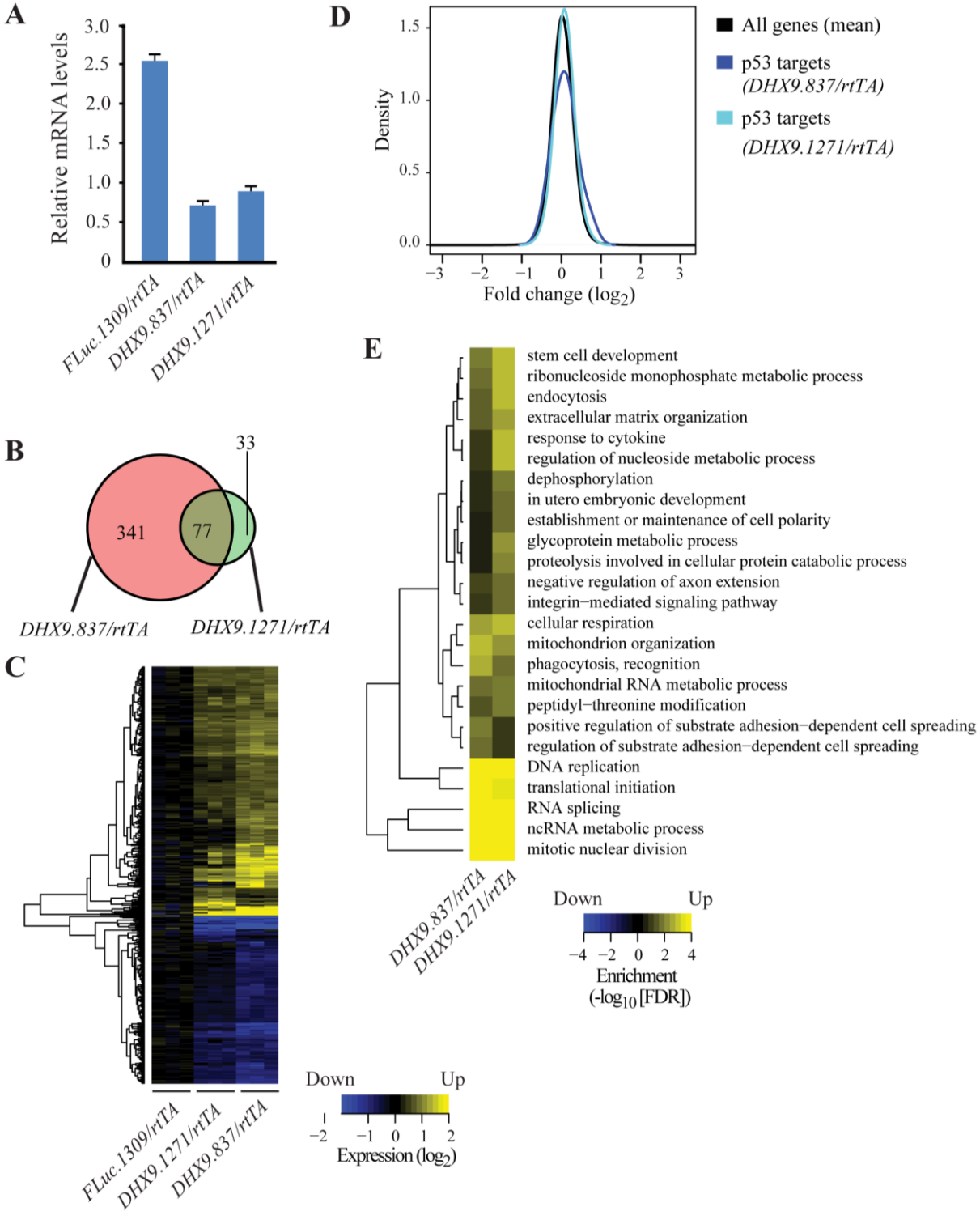

Figure 3.17 Gene expression analysis on large intestine of DHX9/rtTA mice. Figure legend on following page.

Figure 3.17 Gene expression analysis on large intestine of *DHX9/rtTA* mice.

(A) Quantitative RT-PCR analysis showing DHX9 knockdown in large intestines of *DHX9.837/rtTA* and *DHX9.1271/rtTA* mice treated with DOX for 14 days. mRNA levels were normalized to GAPDH. N=3 biological replicates ±SEM. (**B**) Venn diagram highlighting the number of common and distinct differentially expressed genes from *DHX9.837/rtTA* and *DHX9.1271/rtTA* mice. (**C**) Heatmap showing genes from *FLuc.1309/rtTA*, *DHX9.837/rtTA*, and *DHX9.1271/rtTA* mice up-or down-regulated at least 1.5 fold, FDR<0.05. (**D**) Densities of fold-changes (*DHX9/rtTA* vs *FLuc.1309/rtTA*) for all genes and a subset of p53 target genes. (**E**) Heatmap showing highly significant enrichment of biological processes among genes differentially expressed upon reduced DHX9 expression, FDR<0.01. Non-redundant biological processes were defined by the Gene Ontology Consortium.

3.5 Discussion

One of the major challenges in chemotherapy is finding a therapeutic window in which drugs can efficiently eliminate tumor cells with minimal damage to normal tissues. Traditional strategies rely on the administration of cytotoxic agents (e.g. paclitaxel, etoposide, doxorubicin, etc.), which act by killing rapidly dividing cells, a property shared by both cancer cells and highly proliferative normal cells. With the advent of targeted molecular therapeutics, the development of drugs that inhibit specific gene products involved in tumor maintenance offer greater selectivity in eliminating cancer cells. However, the challenge of finding targets with suitable therapeutic indices remains, as targeting these same gene products in normal tissues can have deleterious effects. Hence, the search for novel molecular targets for chemotherapeutic use is a critical ongoing endeavor.

In the present study, we examined the outcome of DHX9 suppression in several human cancer cell lines, mouse engineered lymphomas, and at the organismal level in the mouse. DHX9 suppression resulted in a reduction in proliferative fitness in most (10 out of 13) human cancer cell lines representing five different types of cancers. This demonstrates that targeting DHX9 can be potentially effective against many, but not all, cancers. What makes a cancer a good candidate may be dependent on the relative expression levels of genes involved in proliferation, cell cycle progression, or apoptotic pathways. What makes MCF-7 breast cancer cells resistant to DHX9 suppression (Figure 3.1B) awaits further investigation but may be due to the fact that these express high levels of the anti-apoptotic proteins BCL-2 and MCL-1, and low levels of pro-apoptotic proteins c-MYC, BIM, and BAX (Figure 3.3 and Ref. [484]). Although the multiple myeloma lines JJN-3 and KMS-11 express BCL-2, the fact that they also express the pro-apoptotic proteins BIM, BAX, and BAK at relatively high levels (Figure 3.3 and Ref. [485]) may contribute to their inability to tolerate DHX9 suppression. All cell lines tested herein (Figure 3.1) have been reported to contain wildtype p53, with the exception of MDA-MB231 (Ref. [476, 477]). Hela cells contain wildtype p53 but overexpress the E6 protein from human papillomavirus type 16, which induces the degradation of p53 (Ref. [478]). KMS-11 and JJN-3 exhibited the highest fold-increase in p53 levels, which may be a contributing factor to the robust depletion of DHX9 shRNA-expressing cells observed in the competition assay for these cell lines. However, the level of p53 activation was not the only determinant of susceptibility to

DHX9. Both MDA-MB231 and Hela cells were sensitive to DHX9 suppression, despite harboring mutated p53 or low p53 levels, while MCF-7 cells, which contain wild-type p53, were resistant. Thus, it is likely that susceptibility of a cancer cell line to DHX9 inhibition is not dependent on a single factor, a topic that will require further investigation. Of the cancer cell lines which showed GFP depletion upon DHX9 suppression in the competition assay (Figure 3.1B), increased cell death was documented in all cell lines except the U2OS osteosarcoma line, which underwent a G0/G1 arrest instead (Figure 3.2). We note that only the U2OS and MRC-5 cells demonstrated a significant increase in p21 levels, an inhibitor of proliferation. Activation of p21 has been shown to lead to cell cycle arrest and senescence rather than apoptosis[451, 486]. In fact, studies have shown that in some cases it may actually inhibit apoptosis[291] and may explain why loss of DHX9 does not result in increased cell death in U2OS and MRC-5 cells but causes growth arrest and/or senescence[432, 473, 487]. In all the other cell lines, which did not show p21 induction, it appeared that apoptosis rather than cell cycle arrest was primarily responsible for the decrease in proliferative fitness observed upon DHX9 knockdown (Figure 3.1C and Figure 3.2). These results illustrate that the precise effects of DHX9 suppression may depend on biological context. The lethal effect observed in several human cancer lines with DHX9 suppression was recapitulated in murine Eμ-*Myc* lymphomas *ex vivo* and *in vivo*.

Having demonstrated that DHX9 suppression is not tolerated by most tumor cells, we investigated the consequences on normal tissues *in vivo*. To this end, we generated inducible RNAi-based transgenic mice to study the consequences of DHX9 loss at the organismal level. This inducible model allowed us to achieve conditional and reversible suppression of DHX9, which would not have been possible using a straight knockout model. Indeed, Lee and colleagues previously generated a DHX9 knockout mouse and observed that homozygous loss leads to embryonic lethality[84]. Their results suggest that DHX9 is essential for the differentiation of the embryonic ectoderm[84]. Consistent with this, the *C. elegans* homolog, rha-1, is necessary for germline transcriptional control and proliferation[23]. In this report, we find that partial suppression of DHX9 is well tolerated at the organismal level in adult mice, a situation that reflects the scenario one would expect with a small molecule inhibitor of DHX9. Indeed, chronic suppression of DHX9 in the mouse for 6 months had no noticeable effect, indicating that the organism appears well buffered to tolerate profound changes in DHX9 levels.

Although the mice appeared to suffer no ill effects resulting from DHX9 suppression, analysis of global gene expression in the large intestine identified numerous genes whose expression was affected upon DHX9 loss (Figure 3.17). Our enrichment analysis revealed that genes involved in metabolism, DNA replication, translational initiation, mitotic nuclear division, RNA splicing, amongst others, were upregulated. It should be noted this analysis included genes which negatively regulate the aforementioned processes. An example is the increased expression of eIF4EBP1, a translational inhibitor. However, eIF4G1, eIF2A, and DHX29, all known to stimulate translation[488, 489], were also upregulated (Tables A.3 and A.4); thus the net result on translation is difficult to predict. Similarly, genes involved in mitotic nuclear division found to be upregulated included promoters of this process (e.g. SMC2, CDK1, CDC20, CDC25C, and PLK1) as well as checkpoint proteins (e.g. Mad2/1, CHEK1, CDC27) (Tables A.3 and A.4). Hence, there may be little net effect on cell cycle progression. Interestingly, there appeared to be no activation of a p53 transcriptional program upon DHX9 suppression, in contrast to previous genome-wide expression studies in *Arf*$^{-/-}$*Eμ-Myc/Bcl-2* lymphomas and MRC-5 human fibroblasts, where p53 pathway activation elicited an apoptotic or senescence response respectively[432, 473]. On a more general level, comparison of our present data with previous data generated in *Arf*$^{-/-}$Eμ-*Myc/Bcl-2* and MRC-5 cells revealed no significant overlap with the previous studies (data not shown). In MRC-5 cells, DHX9 suppression resulted in downregulation of many genes involved in promoting DNA replication, mitosis, and cell cycle progression[473]. This was not recapitulated *in vivo*. The fact that we did not observe activation of the p53 pathway or global downregulation of proliferative and replication genes at the organismal level is consistent with the lack of detectable phenotype resulting from reduced DHX9 expression in mice. Conversely, the upregulation of many biological processes may represent a compensatory response to the cellular perturbations caused by DHX9 suppression – a mechanism that may occur *in vivo* but not *ex vivo*. In any event, the changes in global gene expression were small compared to those sustained *ex vivo*, and appear to be relatively benign, as they resulted in no drastic consequences in the mice.

While the two DHX9 shRNAs exhibited similar levels of knockdown *ex vivo* and in most tissues *in vivo* (Figures 3.7B, 3.8, 3.10, 3.11, 3.13 and 3.17A), histopathological analysis revealed that the *DHX9.837/rtTA* +DOX mice exhibited moderate hepatic lipidosis, which was

not found in the *DHX9.1271/rtTA* +DOX mice (Table 3.5). Although we have not investigated the potential reasons for this additional phenotype, we do not feel it can be explained by differences in knockdown potency (which appear quite similar). We cannot rule out that it may represent a possible off-target effect of shDHX9.837 at this time.

Why loss of DHX9 has such detrimental effects on tumor cells but no negative impact on normal adult tissues is not entirely clear, but this finding has been documented in a number of previous settings with key regulatory proteins. DDX5 is a DEAD-box RNA helicase with many similarities to DHX9. It is multifunctional, with important roles in transcriptional regulation, microRNA processing, RNA splicing, and ribosome biogenesis[490-493]. Furthermore, loss of DDX5 is embryonic lethal[492]. In a study by Mazurek et al.[494], DDX5 knockdown induced apoptosis in acute myeloid leukemia (AML) cells but was well tolerated in adult mice. Mice expressing DDX5 shRNAs were healthy, gained weight normally, suffered no physiological defects, and had no deleterious effects on organ morphology[494]. Similarly, Soucek and colleagues modeled the therapeutic impact of systemic MYC inhibition in a KRas-induced lung cancer mouse model using a dominant-negative MYC allele[495]. Conditional expression of the mutant (termed Omomyc) allele impeded initiation and maintenance of KRas-induced lung adenomas by eliciting apoptosis in the tumors. On the other hand, adult mice expressing Omomyc exhibited no significant differences compared to control mice in terms of body weight, blood chemistry, and general health and activity[495]. Organs with low proliferative indices were unaffected by MYC inhibition; however, highly proliferative tissues such as skin and intestines did suffer from increased apoptosis, degeneration, and decreased proliferation, effects that were reversible upon restoration of MYC function. Another example illustrating the differential effects of suppressing a protein in tumor cells versus normal tissues involves suppression of the translation initiation factor eIF4E, which catalyzes the ribosome recruitment step of translation initiation. Suppression of eIF4E in the *Eμ-Myc* lymphoma model significantly delayed MYC-dependent tumor initiation by augmenting apoptosis and impairing cell division in premalignant B-cells[474]. eIF4E suppression in adult mice resulted in a reduction in body weight and increased apoptosis and loss of differentiation in the intestines, but these effects were reversible upon DOX withdrawal[474]. These mouse models, like the shDHX9 mice described herein, demonstrate that although a gene product may be essential, its partial suppression (as

would be expected from a small molecule inhibitor) may be well tolerated at the organismal level.

Although our study does not identify a single major pathway affected by DHX9 suppression in tumor cells, its role in a multitude of cellular processes (see Introduction) may indicate a higher dependency of tumor cells for this gene product. In the mouse, since the majority of cells are not actively proliferating, but are instead quiescent[496], these cells may have a lower requirement for DHX9. Interestingly, DHX9 knockdown had no deleterious consequences in tissues with high proliferative indices, such as the intestines and skin. This may be due to the fact that although suppression is significant in these tissues, levels of remaining DHX9 are sufficient to maintain normal cell function and prevent activation of a p53 response. It should be noted that *ex vivo*, both tumor cells and normal diploid fibroblasts were susceptible to DHX9 knockdown, although the specific effect elicited was different (apoptosis versus senescence). The differential effects of DHX9 suppression observed *in vivo* versus *ex vivo* in terms of cellular fitness and p53 pathway activation may be partly attributed to cell culture stress. In a physiological environment, reduction in DHX9 levels may be well tolerated. However, the added stress of being cultured *ex vivo*, at higher oxygen levels and separated from their native extracellular matrix, may sensitize cells sufficiently to activate a p53 stress response. The knockdown of DHX9 *in vivo* may not be as potent as what can be achieved *ex vivo*, and may not reach a high enough threshold to activate p53. Another possible explanation is that there may be some form of compensation for the loss of DHX9 *in vivo* – for example, upregulation of other replication factors. In sum, our study demonstrates that DHX9 suppression is tolerated in the adult mouse and warrants exploration of DHX9 as an anti-neoplastic target. What makes DHX9 particularly attractive is that unlike other potential therapeutic targets that have been explored using conditional shRNA mice[474, 481, 495], its suppression does not have negative effects on tissues harboring highly proliferative cells.

3.6 Materials and methods

3.6.1 Cell lines

NIH3T3, Hela, and HEK293T/17 cells (ATCC, Manassas, VA, USA), and MRC-5 cells (a kind gift from Dr. Nahum Sonenberg, McGill University, Canada) were maintained in DMEM

(Multicell, St-Bruno, QC, Canada). U2OS cells (ATCC) were maintained in McCoy 5A (Multicell). MCF-7 (ATCC), MDA-MB231 (ATCC), and JJN-3, KMS-11, IM-9, RPMI8226, U266B1, H929, OPM1.1, and OPM2 cells (kindly provided by Dr. Michael Sebag, McGill University, Canada) were maintained in RPMI-1640 media (Multicell). A549 cells (ATCC) were maintained in F12K (Multicell). All media was supplemented with 10% fetal bovine serum (Multicell). ATCC authenticates all their cell lines using Short Tandem Repeat profiling. Cells were not tested for mycoplasma contamination. *Tsc2*$^{+/-}$Eμ–*Myc* lymphoma cells were derived from tumors in *Tsc2*$^{+/-}$ mice crossed with Eμ–*Myc* mice and inbred on the C57BL/6 (Charles River Laboratories) background for over ten generations. *Tsc2*$^{+/-}$Eμ-*Myc*/R26-M2rtTA lymphomas were generated by crossing *Tsc2*$^{+/-}$Eμ–*Myc* mice with mice expressing the M2rtTA transgene at the Rosa26 locus and harvesting tumors from the resultant triple transgenic progeny. Lymphomas were cultured in B-cell media (45% DMEM, 45% Iscove's media, 55 mM β-mercaptoethanol, 10% fetal bovine serum) on irradiated Ink4A$^{-/-}$ MEF feeder layers.

3.6.2 Virus generation and transductions

For suppression of DHX9 in murine cell lines (NIH3T3 and Eμ-*Myc* lymphomas), shRNAs targeting mouse DHX9 (DHX9.1241 and DHX9.1271) and a control shRNA targeting renilla luciferase (RLuc.713) were transduced into cells using the MSCV/LTR/miR30/PuroR-IRES-GFP (MLP) or MSCV/LTR/miR30/SV40-GFP (MLS) retroviral vectors (Table 3.1). Retroviral infections were performed using ecotropic Phoenix packaging cells following established protocols (http://www.stanford.edu/group/nolan/retroviral_systems/retsys.html). Briefly, 20 μg of plasmid were transfected into Phoenix ecotropic cells in a 10 cm dish by calcium phosphate-mediated delivery. The media was changed 12 hours later and 48 hours post-transfection, retroviral supernatant was collected every 8 hours up to 72 hours and added to target cells. For infections using MLP, forty-eight hours after the last transduction, stable integrants were selected using 2 μg/ml puromycin for at least 3 days. For suppression of DHX9 in human cell lines, two shRNAs targeting human DHX9 (DHX9.860 and DHX9.267) and a control shRNA targeting firefly luciferase (FLuc.1309) were transduced into cells using pPrime-PGK-Puro (Addgene, Cambridge, MA, USA) (Table 3.1). Lentiviral transduction was performed following published

procedures[462]. Briefly, 15 μg of pPrime-PGK-Puro-shRNA, 7.5 μg of packaging plasmid pSPAX2, and 3.75 μg of envelope-encoding vector, CMV-VSVG, were mixed and transfected into HEK293T/17 cells in a 10 cm dish by calcium phosphate-mediated delivery.

3.6.3 Generation, genotyping, and induction of transgenic mice

Transgenic mice harboring a Rosa26 (R26)-m2rtTA allele and DHX9.837 or DHX9.1271 shRNAs under the control of a tetracycline-inducible promoter (TRE) were generated through FLP/FRT-mediated site specific recombination at the Col1A1 locus on chromosome 11 by Mirimus (Cold Spring Harbor, NY, USA). PCR was used for genotyping using shRNA-specific forward primers [FLuc.1309: $^{5'}$AAGCCACAGATGTATTAATCAGAGA$^{3'}$, DHX9.837: $^{5'}$AAGCCACAGATGTATTTAGATCCAT$^{3'}$, and DHX9.1271: $^{5'}$AAGCCACAGATGTATAAATTATGAT$^{3'}$], combined with a common reverse primer, Col1A1 Rev43 [$^{5'}$GAAAGAACAATCAAGGGTCC$^{3'}$]. Genotyping for the R26-m2rtTA allele was performed using Mutant For: $^{5'}$AAAGTCGCTCTGAGTTGTTAT$^{3'}$, Rev: $^{5'}$GCGAAGAGTTTGTCCTCAACC$^{3'}$, and WT For: $^{5'}$GGAGCGGGAGAAATGGATATG$^{3'}$ primers.

All mice strains were maintained on a C57BL/6 background. Induction of shRNA expression was performed in 4-week-old shRNA/rtTA mice by supplying doxycycline (DOX) at 1 mg/ml in the drinking water (plus 5% sucrose) for 14 days (for short-term experiments) or 6 months (for long-term experiments). The DOX-supplemented water was changed every 4 days. All animal studies were approved by the McGill University Faculty of Medicine Animal Care Committee.

3.6.4 Immunohistochemical analysis and TUNEL staining of mouse tissues

Tissues from shRNA/rtTA mice were harvested, fixed in 10% formalin for 48h, and embedded in paraffin. Sections (4 μm) were deparaffinized in xylene, and rehydrated through a series of decreasing ethanol washes (100%, 95%, and 75%), followed by washing in water for 2 x 5 minutes. Antigen retrieval was performed by boiling the slides in 10 mM citric acid buffer [pH 6.0] for 15 minutes. Immunohistochemistry was performed using the HRP/DAB Detection Kit

(ab64261; Abcam, Cambridge, MA, USA) according to the manufacturer's instructions and as previously described[474]. The following primary antibodies and dilutions were used: DHX9 (ab26271; Abcam, Cambridge, MA, USA) (1:100 dilution), GFP (#2555; Cell Signaling, Danvers, MA, USA) (1:800 dilution), turboGFP (AB514; Evrogen, Moscow, Russia) (1:5000 dilution) and Ki-67 (Sp6; Neomarkers, Fremont, Ca, USA). After visualizing the signal using DAB chromogen and substrate, sections were counterstained with hematoxylin, destained with 0.5% HCl in 70% ethanol, incubated with 0.2% lithium carbonate, and rinsed with tap water. The sections were then dehydrated through an ethanol gradient (75%, 95%, and 100% ethanol), followed by xylene washes (2 x 5 minutes), and mounted using Permount (Fisher, Ottawa, ON, Canada). Sections were scanned using an Aperio ScanScope XT (Aperio Technologies, Vista, CA, USA). TUNEL staining was performed using the In situ Cell Death Detection Kit, TMR-Red (#12156792910; Roche, Mannheim, Germany) according to the manufacturer's instructions. Images were taken with a LSM 510 Meta Confocor2 Confocal Microscope (Zeiss) at 40X magnification and the percentage of apoptotic cells quantitated using ImageJ (National Institutes of Health, Bethesda, Maryland, USA).

3.6.5 Ex vivo competition assays

Ex vivo competition assays were performed by transducing cells with MLS-based (for mouse cells) or pPrime-PGK-puro-based (for human cells) shRNAs. The percentage of GFP-positive cells was measured 48h after the final infection (t=0) using a GUAVA EasyCyte HT flow cytometer (Millipore, Billerica, MA, USA). Cell death was assessed by staining cells with 4 μg/ml propidium iodide (PI) and measuring the percentage of PI-positive cells. For competition assays using the DOX-inducible vector TRMPV, *Tsc2*$^{+/-}$Eμ-*Myc*/R26-M2rtTA cells were transduced with TRMPV-shRNA and FAC-sorted to obtain a pure Venus^{+} population. shRNA expression was induced by treatment with vehicle or 1 μg/ml DOX and cell death assessed by staining with Fixable Viability Dye eFluor450 (eBioscience) and measuring the percentage of stained cells using a LSRII cytometer (BD Biosciences).

3.6.6 In vivo competition assays

Tsc2$^{+/-}$*Eμ-Myc* cells were transduced with MLS-based shRNAs and two days post-infection, 10^6 cells were injected into the tail vein of C57BL/6 recipients (not randomized or blinded to the investigator). Mice were monitored until they reached terminal disease stage (characterized by the appearance of tumors, decreased activity, hunched posture, dehydration, paralysis, and weight loss), at which point the spleen was harvested and analyzed for GFP-positive B-cells using flow cytometry.

3.6.7 Survival analysis following tumor transplantation

Tsc2$^{+/-}$Eμ-*Myc*/R26-M2rtTA lymphoma cells were transduced with TRMPV retroviruses expressing shRNAs to RLuc, DHX9 or L15, FAC-sorted to obtain a pure Venus$^+$ population, and 10^6 cells were introduced into 10 C57BL/6 mice for each shRNA via tail-vein injection. 6 days post-injection, 5 mice for each shRNA was treated with 1 mg/ml DOX (in 5% sucrose) and the other 5 mice were treated with 5% sucrose. The mice were sacrificed when they reached terminal disease stage, at which point the spleen was harvested and the percentages of B220$^+$, Venus$^+$, and dsRed$^+$ cells were analyzed by flow cytometry. The survival (number of days to reach terminal stage) of each mouse was plotted on a Kaplan-Meier curve using GraphPad Prism (v. 5.03, GraphPad Software Inc., La Jolla, CA, USA) and the p-values determined using the Log-rank (Mantel-Cox) test.

3.6.8 Immunoblot analysis

Protein extracts were prepared by lysing cells in RIPA lysis buffer (20 mM Tris-HCl [pH 7.5], 150 mM NaCl, 0.1% SDS, 1% NP40, 0.5% sodium deoxycholate, 1 mM β-glycerophosphate, 1 mM PMSF, 1 μg/ml leupeptin, 10 μg/ml aprotinin, and 2.5 μM pepstatin A). PVDF membranes were probed with the indicated primary antibodies and HRP-conjugated secondary antibodies (rabbit (711-035-152) or mouse (115-035-146) (Jackson ImmunoResearch, West Grove, PA, USA) and visualized using enhanced chemiluminescence (ECL) (Perkin Elmer, Waltham, MA, USA). The primary antibodies used in this study were: DHX9 (M99; SC Biotech (Dallas, TX, USA) for human and ab26271; Abcam (Cambridge, MA, USA) for mouse), eEF2 (#2332; Cell

Signaling, Danvers, MA, USA), GFP (#2555; Cell Signaling, Danvers, MA, USA), turboGFP (AB514; Evrogen, Moscow, Russia), RB1 (554136; BD Pharmingen, Franklin Lakes, NJ, USA), human p53 (DO-1; SC Biotech, Dallas, TX, USA), mouse p53 (NL-p53-505; Novocastra, Concord, ON, Canada), p21 (556430; BD Pharmingen, Franklin Lakes, NJ, USA), α-actin (clone AC-15; Sigma, Oakville, ON, Canada), MYC-tag (9E10, McGill Hybridoma Core Facility, Montreal, QC, Canada), and BIM (#202000, Millipore, Billerica, MA, USA). Antibodies for MCL-1 (S-19), BCL-2 (C-2), and BAX (B-9) were purchased from SC Biotech (Dallas, TX, USA).

3.6.9 Flow cytometry analysis of splenocytes

Fresh spleen cell suspensions were isolated in PBS + 2% FBS and erythrocytes were removed by lysis in ACK buffer (150 mM NH_4Cl, 10 mM $KHCO_3$, 0.1 mM EDTA). Remaining cells were collected by centrifugation and resuspended in PBS + 2% FBS. Blocking was performed by incubating samples with 1.5 μg/ml purified anti-CD16/CD32 antibody (clone: 2.4G2; BD Biosciences, Franklin Lakes, NJ, USA) for 5 minutes on ice. The sample (100 μl) was stained with a PE-conjugated CD45R/B220 antibody (clone RA3-6B2; BD Pharmingen, Franklin Lakes, NJ, USA), a marker for B lymphocytes. Another 100 μl of sample was stained with PE-conjugated CD4 antibody (clone H129.19, BD Pharmingen, Franklin Lakes, NJ, USA), a T lymphocyte marker. Final antibody concentration was 0.6 μg/ml, and the staining was performed in the dark on ice for 30 minutes. Samples were then washed twice with PBS, resuspended in PBS + 2% FBS, and the percentage of PE-positive cells assessed using a GUAVA EasyCyte HT flow cytometer (Millipore, Billerica, MA, USA). For experiments using the TRMPV vector, spleens were processed as above except that a V500-conjugated CD45R/B220 antibody (clone RA3-6B2; BD Biosciences) was used in place of the PE-conjugated B220 antibody and cells were analyzed using a LSRII cytometer (BD Biosciences).

3.6.10 Microarray analysis and validation

Total RNA was isolated from the large intestine of DOX-treated (14 days) *FLuc.1309/rtTA*, *DHX9.837/rtTA*, and *DHX9.1271/rtTA* mice using TRIzol as per the manufacturer's instructions

(Life Technologies). Verification of DHX9 knockdown was performed by qRT-PCR using the following primers: DHX9 FWD: $^{5'}$CCGAGGAGCCAACCTTAAAGA$^{3'}$, DHX9 REV: $^{5'}$TGTCCAATTTCCATGAAGCCC$^{3'}$, GAPDH FWD: $^{5'}$AGGTCGGTGTGAACGGATTTG$^{3'}$, and GAPDH REV: $^{5'}$GGGGTCGTTGATGGCAACA$^{3'}$. Extracts from three biological replicates were submitted to the McGill University and Génome Québec Innovation Center's microarray facility. RNA quality was assessed using an Agilent 2100 Bioanalyzer (Agilent Technologies, Santa Clara, CA, USA) and the cDNA generated and hybridized onto the Affymetrix Mouse Gene 2.0 ST Array. The resulting data were summarized and normalized using the oligo package version 1.30.0[497] by applying robust multiarray average (rma) in R version 3.1.1 (www.r-project.org) and bioconductor version 3.0[498]. Updated probe set definitions[499] were used because these provide improved precision and accuracy for micrarrays[466]. Reproducibility was assessed via hierarchical clustering of Spearman correlations obtained for all genes in all sample to sample comparisons. Samples clustered according to shRNA identity and the major difference was observed between the *FLuc.1309/rtTA* samples and two *DHX9/rtTA* samples – indicating good reproducibility. Differential expression was identified using the random variance model (RVM)[467] and an ANOVA model with two treatment contrasts (e.g. *DHX9.837/rtTA* vs *FLuc.1309/rtTA* and *DHX9.1271/rtTA* vs *FLuc.1309/rtTA*) as described for ANOTA[500]. The resulting p-values were adjusted for multiple testing using the Benjamini-Hochberg False Discovery Rate (FDR) method[468]. Genes that showed a FDR <0.05 and a fold-change >1.5 were considered significantly differentially expressed. Generally applicable gene set enrichment for pathway analysis (GAGE[469]) version 2.16.0 in R version 3.1.1 was used for identification of biological processes controlled by genes at the extreme ends of the ranked gene lists. For GAGE analysis RVM p-values from the two treatment contrasts were used as input and default settings were applied while setting rank.test=TRUE and only searching against biological processes as defined by the Gene Ontology Consortium[501]. We used the esset.grp function with the GAGE package to identify non-redundant biological processes and those that were significantly enriched (FDR<0.01) were collected. The microarray data is available in the NCBI GEO database, accession code GSE76765.

3.6.11 Cell cycle analysis

Cell cycle analysis was performed using ethanol fixation, acid denaturation, and propidium iodide (PI) staining[464] at day 10 after transduction with shRNAs. Cells were seeded onto 6 cm plates and harvested at 75% confluency. The cells were trypsinized and washed twice with PBS containing 1% BSA and 5 mM EDTA, resuspended in 50 µl PBS on ice, fixed with 1.25 ml 70% ethanol, and stored at -20^{o}C until further processing. The fixed cells were then treated with 0.5% Triton X-100/ 2 M HCl for 30 minutes with end-over-end incubation at room temperature to denature genomic DNA. Cells were neutralized with 0.1 M Sodium Borate [pH 8.5], washed with PBS containing 1% BSA and 0.5% Triton X-100, and resuspended in 500 µL of PBS containing 5 µg/mL PI (Sigma). The cell cycle profile of the cells was then assessed using a GUAVA EasyCyte HT flow cytometer (Millipore, Billerica, MA, USA).

3.6.12 Statistical analysis

Statistical analysis was carried out using GraphPad Prism (v. 5.03, GraphPad Software Inc., La Jolla, CA, USA) and data is shown as mean ±SEM. For all analyses except the Kaplan-Meier analysis (see above), statistically significant differences were determined using the unpaired two-tailed t-test and represented as p-values.

3.7 Acknowledgements

We thank Francis Robert for performing tail-vein injections of lymphoma cells into mice. TL was supported by a Maysie MacSporran graduate studentship and fellowships from the CIHR-sponsored Chemical Biology and Systems Biology Training Programs. This work is supported by grants from the Canadian Cancer Society Research Institute [#701362] and National Institutes of Health [CA163291] to JP and grants from the Swedish Research Council and the Swedish Cancer Society to OL.

CHAPTER 4: DEPENDENCE OF P53-DEFICIENT CELLS ON THE DHX9 DEXH-BOX HELICASE

Manuscript under revision:

Lee T and Pelletier J. (2016). Dependence of p53-deficient cells on the DHX9 DExH-box helicase. *Oncotarget.* Under revision.

4.1 Preface to Chapter 4

We have previously shown that loss of DHX9 induces senescence in human diploid fibroblasts in a p53-dependent manner. The synergy between DHX9 suppression and ABT-737 treatment in triggering an apoptotic response in *Arf*$^{-/-}$Eμ-*Myc*/Bcl-2 cells is also dependent on functional p53 signaling. In Chapter 3, the consequences of suppressing DHX9 in a panel of human cancer cell lines were examined. Although the majority of these cell lines had wildtype p53 status, it was noted that two of them, MDA-MB231 and HeLa cells, harbored a mutation in p53 or contained low p53 levels. In spite of this, DHX9 suppression was able to trigger cell death in these two lines. We therefore hypothesized that there may be a p53-independent mechanism through which DHX9 suppression can mediate cell death and/or cell cycle arrest. This is of interest because many tumors have lost or mutated p53, and the ability to target DHX9 in these tumors would increase its therapeutic potential. In Chapter 4, we sought to determine whether loss of DHX9 can be detrimental to p53-deficient systems in general. To this end, we assessed the consequences of DHX9 suppression in three different p53-null cell lines. We also investigated the underlying mechanisms by examining changes in transcript levels of known p53 targets in the p53-deficient systems.

4.2 Abstract

DHX9 is a DExH-box helicase family member with key regulatory roles in a broad range of cellular processes. It participates at multiple levels of gene regulation, including DNA replication, transcription, translation, RNA transport, and microRNA processing. It has been implicated in tumorigenesis and recent evidence suggests that it may be a promising chemotherapeutic target. Previous studies have determined that DHX9 suppression elicits an apoptotic or senescence response by activating p53 signaling. Here, we show that DHX9 inhibition can also have deleterious effects in cells lacking functional p53. Loss of DHX9 led to increased cell death in p53-deficient mouse lymphomas and HCT116 human colon cancer cells, and G0/G1 cell cycle arrest in p53-deficient mouse embryonic fibroblasts. Analysis of mRNA levels for p53 transcriptional targets showed that a subset of p53 targets in the p53-null lymphomas and HCT116 cells were activated despite the absence of functional p53. This implies an alternative pathway of DHX9-mediated activation of cell death and cell cycle arrest in p53-

deficient cells and supports the feasibility of targeting DHX9 in p53-deficient tumors.

4.3 Introduction

DHX9 (also known as Nuclear DNA Helicase II (NDH II) and RNA Helicase A (RHA)) is an NTP-dependent helicase belonging to the DExH-box family of helicase proteins. DHX9 is a multi-domain protein, consisting of a core helicase domain harboring the conserved DEIH sequence, two RNA-binding domains at the N-terminus, a nuclear transport domain and a DNA-binding RGG-box at the C-terminus[26]. It is capable of unwinding a variety of substrates, including DNA, RNA, and complex polynucleotide structures[1, 2], and has been implicated in many diverse biological processes. Its functions include regulation of transcription[120, 124, 138], translation[148, 152], RNA transport[182], microRNA processing[171], and DNA replication and genome maintenance[36, 38, 93, 98]. Over 30 interacting partners for DHX9 have been identified, in the context of its various cellular roles[502]. Due to the important regulatory role played by DHX9, there is growing evidence of its implications in human diseases such as various cancers and viral infections[502].

We previously identified DHX9 as a modifier of sensitivity to ABT-737 (an inhibitor of BCL-2 family pro-survival factors) in a mouse lymphoma model. Using *Arf*$^{-/-}$Eμ-*Myc*/Bcl-2 mouse lymphoma cells, which overexpressed c-MYC and exogenous BCL-2 and were resistant to ABT-737, we found that suppression of DHX9 synergized with ABT-737 to reverse resistance. This was accomplished through aggravation of replicative stress and activation of p53 signaling, leading to apoptosis[432]. We subsequently investigated the effect of DHX9 suppression in non-transformed primary human diploid fibroblasts, where we demonstrated that loss of DHX9 resulted in a pronounced growth arrest and premature senescence. This resulted from inhibition of DNA replication which activated a p53-dependent stress response[473]. In both the *Arf*$^{-/-}$Eμ-*Myc*/Bcl-2 mouse lymphoma and primary human fibroblast models, functional p53 signaling was essential for the ABT-737 synergy or senescence response.

Further exploration of the chemotherapeutic potential of targeting DHX9 has been carried out in other mouse and human cancer models. Whereas DHX9 was targeted in combination with ABT-737 treatment in the aforementioned Arf$^{-/-}$Eμ-*Myc*/Bcl-2 lymphomas, it was found that loss of DHX9 on its own had a lethal effect on tumor cells where BCL-2 was not supra-elevated. In

MYC-driven *Tsc2*$^{+/-}$Eμ-*Myc* lymphomas, DHX9 suppression had a straight lethal effect both *ex vivo* and *in vivo*[503]. Knockdown of DHX9 in a representative panel of human cancer cell lines, including multiple myeloma, osteosarcoma, and breast, lung, and cervical cancer cells, demonstrated that DHX9 suppression was detrimental in the majority of cancer cells[503]. In assessing the levels of various apoptotic and cell cycle proteins in the different cell lines, we noted that two of them, MDA-MB231 breast cancer cells and HeLa cervical cancer cells, harbored a mutation in p53 or were p53-deficient. Despite the absence of functional p53, however, loss of DHX9 had a deleterious effect on both cell lines[503]. This suggested that p53 was not the only factor mediating the apoptotic effect of DHX9 suppression, and that there may be a p53-independent mechanism triggering cell death upon DHX9 suppression.

In this study, we investigate the phenomenon and underlying mechanisms of DHX9-mediated cell death and growth arrest in p53-deficient systems. We compare the consequences of DHX9 suppression in p53-wildtype and p53-deficient settings in three different *ex vivo* models: mouse lymphomas, mouse embryonic fibroblasts (MEFs), and human colon cancer cells. We demonstrate that in all three cases, loss of DHX9 leads to a reduction in cellular fitness in both p53-wildtype and p53-deficient cells. Analysis of the levels of p53 transcriptional targets in each system shows that in the absence of p53, some targets were nevertheless activated upon DHX9 suppression. Our results support the existence of a p53-independent aspect to DHX9-mediated cell death and cell cycle arrest, and highlight the value of targeting DHX9 in p53-defective tumors.

4.4 Results

4.4.1 DHX9 suppression reduces cellular fitness in both p53-wildtype and p53-null settings

Previous studies in both non-transformed cells and tumor models initially suggested that functional p53 signaling is essential for the cell death or senescence response resulting from DHX9 inhibition[432, 473]. Further investigation, however, demonstrated that MDA-MB231 cells, which harbor a point mutation in p53, and HeLa cells, which are p53-deficient due to overexpression of the E6 protein from human papillomavirus type 16, also showed increased cell death upon DHX9 suppression[503]. To characterize this response, we knocked down DHX9 in

p53-wildtype and p53-null settings in three different cell types. *p53*$^{-/-}$Eμ-*Myc* lymphomas were compared to *Tsc2*$^{+/-}$Eμ-*Myc* lymphomas – the latter of which were previously characterized and shown to contain functional p53 signaling as well as being highly responsive to DHX9 suppression[480, 503, 504]. A competition assay was carried out in which cells infected with shRNAs targeting DHX9 or a neutral renilla luciferase control (shRLuc.713) were co-cultured with non-infected cells (Figure 4.1A). Cells harboring DHX9 shRNAs were depleted (represented by a decrease in %GFP+ cells) in both *Tsc2*$^{+/-}$Eμ-*Myc* and *p53*$^{-/-}$Eμ-*Myc* lymphomas; however, the kinetics of the depletion was slower in the case of the *p53*$^{-/-}$Eμ-*Myc* lymphomas (Figure 4.1A). This result was recapitulated in INK4A$^{-/-}$ (p53$^{+/+}$) and p53$^{-/-}$ MEFs (Figure 4.1B). Here, shDHX9-expressing cells were depleted in both p53$^{+/+}$ and p53$^{-/-}$ MEFs, but the kinetics were slower in the latter compared to the former. We also examined the outcome of knocking down DHX9 in HCT116 p53$^{+/+}$ and HCT116 p53$^{-/-}$ cells. HCT116 p53$^{-/-}$ cells were derived from parental HCT116 p53$^{+/+}$ cells through disruption of both alleles of the p53 gene by homologous recombination and hence are isogenic cell lines[505]. As with the lymphomas and MEFs, both the HCT116 p53$^{+/+}$ and HCT116 p53$^{-/-}$ cells exhibited depletion of GFP+ cells following DHX9 suppression (Figure 4.1C). Here, the kinetics of depletion are relatively similar, with the depletion in the HCT116 p53$^{-/-}$ cells being only slightly slower than that of the HCT116 p53$^{+/+}$ cells. The variation in kinetics is unlikely due to differences in DHX9 knockdown, which were quite similar in all three pairs of cell lines examined (Figure 4.1D-F). The p53 status in all three cell types was verified by Western blot analysis, and in the p53$^{+/+}$ scenarios, DHX9 suppression led to elevation of p53 levels (Figure 4.1D-F), in agreement with prior studies[432, 473, 503]. Our results demonstrating that shDHX9-expressing cells were depleted in three independent p53-null cell lines support previous observations that DHX9 suppression can be detrimental to cells without functional p53.

4.4.2 Context-dependent effects of DHX9 suppression in p53-deficient cells

To gain insight into the underlying causes for the difference in kinetics observed between p53-wildtype and p53-deficient systems, we quantitated the levels of cell death that ensued following DHX9 knockdown. DHX9 suppression resulted in a ~1.5-fold increase in cell death in *p53*$^{-/-}$Eμ-

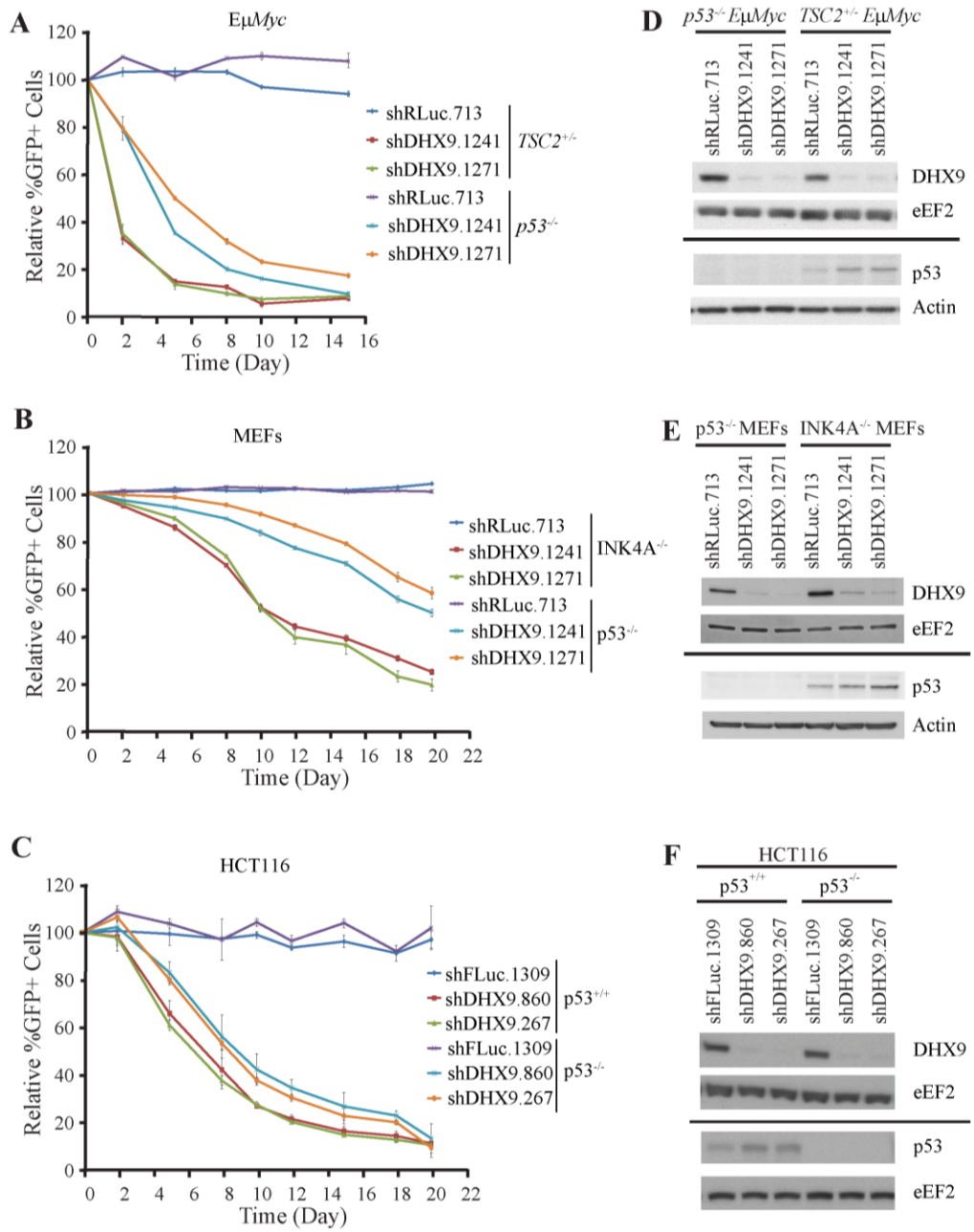

Figure 4.1 DHX9 suppression reduces cellular fitness in both p53-wildtype and p53-null systems.

Ex vivo competition assay with **(A)** *Tsc2*$^{+/-}$Eμ-*Myc* (p53$^{+/+}$) and *p53*$^{-/-}$ Eμ-*Myc* lymphomas, **(B)** INK4A$^{-/-}$ (p53$^{+/+}$) and p53$^{-/-}$ MEFs, and **(C)** HCT116 p53$^{+/+}$ and HCT116 p53$^{-/-}$ cells. Cells were infected with shRNAs targeting DHX9 or a neutral control and the relative %GFP monitored over time. The experiment was started 48 hours after the final infection (t=Day 0). N=3 ±SEM. **(D-F)** Western blot analysis of extracts from the indicated cell lines. Membranes are probed with antibodies indicated to the left. Solid bar indicates a different set of Western blots were probed.

Myc lymphomas, compared to a ~3-fold increase in *Tsc2*$^{+/-}$Eμ-*Myc* lymphomas (Figure 4.2A); this difference in the extent of cell death induced is consistent with the slower kinetics of depletion exhibited by the *p53*$^{-/-}$Eμ-*Myc* lymphomas in the competition assay (Figure 4.1A). In the MEFs, neither the INK4A$^{-/-}$ nor the p53$^{-/-}$ MEFs showed an increase in cell death (Figure 4.2B). The HCT116 p53$^{-/-}$ cells exhibited a 2.9-3.5-fold increase in cell death, compared to a 4.4-4.9 fold increase in the p53$^{+/+}$ cells (Figure 4.2C), which again, was consistent with the slight difference in kinetics observed in the competition assay. Given that the MEFs showed no induction of cell death upon DHX9 suppression, we carried out cell cycle analysis on the three different cell types following transduction with control or DHX9 shRNAs. Indeed, the INK4A$^{-/-}$ MEFs exhibited a marked increase (~24%) in the percentage of cells in G0/G1 phase, and a ~12% decrease in the number of cells in both the S and G2/M phases upon DHX9 suppression, indicating a G0/G1 growth arrest. In the case of the p53$^{-/-}$ MEFs, changes in cell cycle distribution following DHX9 knockdown were smaller, with a ~15% increase in the number of cells in G0/G1 phase, a 10% decrease in the cells in S phase, and a ~5% decrease in the number of cells in the G2/M phase (Figure 4.2E). This correlated with the slower kinetics of depletion in the competition assay for the p53$^{-/-}$ MEFs (Figure 4.1B). Neither the HCT116 p53$^{+/+}$ nor the HCT116 p53$^{-/-}$ cells displayed any significant changes in cell cycle distribution, suggesting that depletion of the shDHX9-expressing cells was likely solely due to induction of cell death rather than growth arrest (Figure 4.2F). Both *Tsc2*$^{+/-}$Eμ-*Myc* and *p53*$^{-/-}$ Eμ-*Myc* lymphomas underwent a slight S-phase arrest upon loss of DHX9, with a small (3.5-4.6%) increase in the percentage of S-phase cells and a concomitant decrease in G2/M-phase cells (Figure 4.2D); however, cell death appeared to be the primary mechanism by which DHX9 suppression reduced the proliferative fitness of the lymphomas. These results indicate that irrespective of the p53 status, DHX9 suppression may elicit a cell death or cell cycle arrest response, or a combination of both, depending on the cellular context.

4.4.3 DHX9 suppression activates p53 targets in both p53-wildtype and p53-null systems

To better understand how loss of DHX9 elicits a cell death or growth arrest response in p53-wildtype and p53-null systems, we quantified the relative mRNA levels of a set of known,

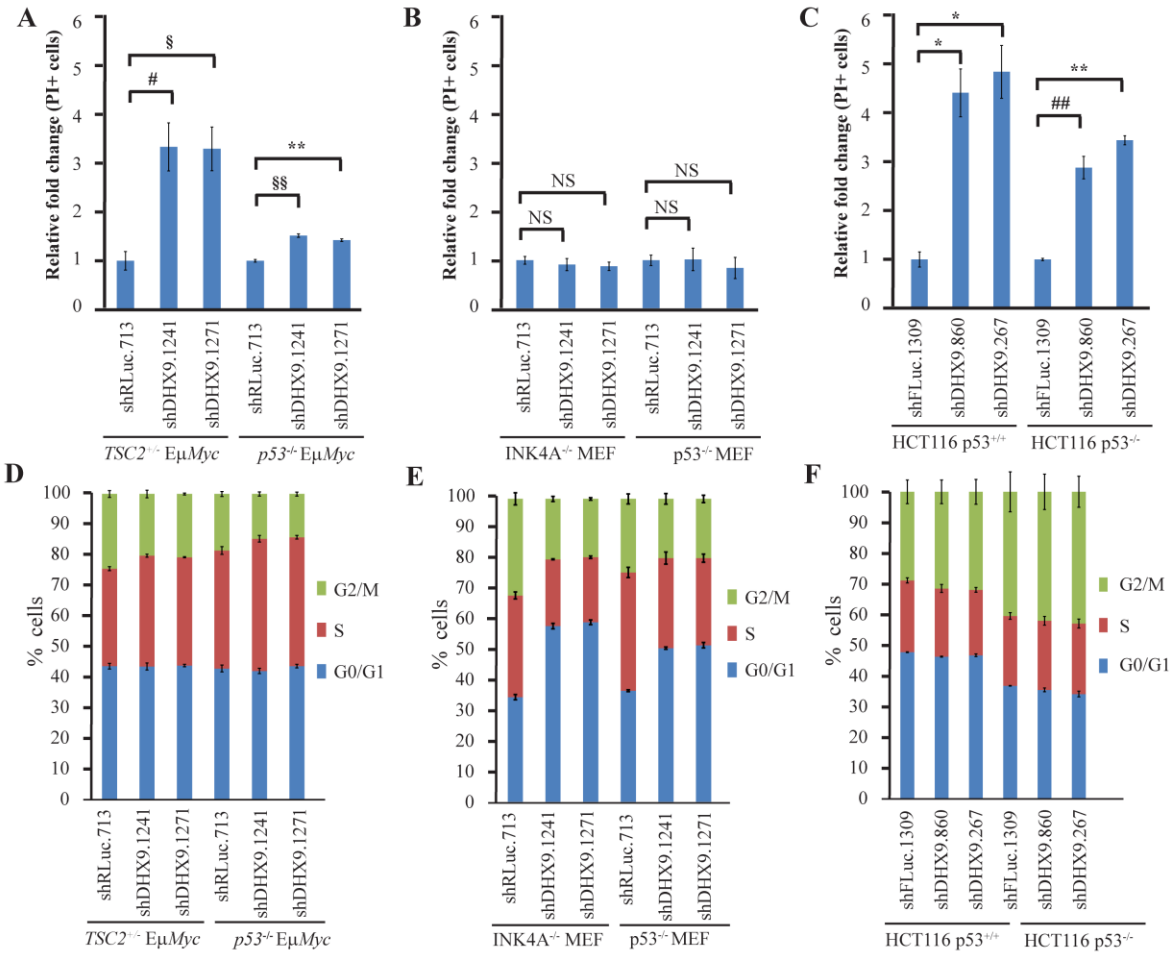

Figure 4.2 Context-dependent consequences of DHX9 suppression.

PI staining of **(A)** *Tsc2*$^{+/-}$Eμ-*Myc* (p53$^{+/+}$) and *p53*$^{-/-}$ Eμ-*Myc* lymphomas, **(B)** INK4A$^{-/-}$ (p53$^{+/+}$) and p53$^{-/-}$ MEFs, and **(C)** HCT116 p53$^{+/+}$ and HCT116 p53$^{-/-}$ cells expressing the indicated shRNAs 7 days post-infection. N=3 ±SEM. # p≤0.05, § p≤0.01, * p≤0.005, ## p≤0.001, §§ p≤0.0005, ** p≤0.0001, NS – not significant. Cell cycle analysis of **(D)** *Tsc2*$^{+/-}$Eμ-*Myc* (p53$^{+/+}$) and *p53*$^{-/-}$ Eμ-*Myc* lymphomas, **(E)** INK4A$^{-/-}$ (p53$^{+/+}$) and p53$^{-/-}$ MEFs, and **(F)** HCT116 p53$^{+/+}$ and HCT116 p53$^{-/-}$ cells expressing the indicated shRNAs 10 days post-infection. N=3 ±SEM.

previously validated p53 transcriptional target genes[432, 506] using quantitative RT-PCR analysis. Nine p53 target genes were analyzed in *Tsc2*$^{+/-}$Eμ-*Myc* and *p53*$^{-/-}$ Eμ-*Myc* lymphomas, INK4A$^{-/-}$ and p53$^{-/-}$ MEFs, and HCT116 p53$^{+/+}$ and p53$^{-/-}$ cells, six days after transduction with control or DHX9 shRNAs. Amongst these were the cyclin dependent kinase inhibitor p21, BCL-2 family proteins PUMA, BAX, NOXA, BIM, and MCL-1, the c-MYC oncogene, and other targets MDM2, PLK2, and SESN1. DHX9 knockdown and p53 levels were validated in the RNA samples for each cell type (Figures 4.3-4.5). p53 mRNA levels were not elevated in response to DHX9 knockdown, suggesting that the observed increase in p53 protein (Figure 4.1D-F) is likely due to a post-transcriptional response. DHX9 suppression in *Tsc2*$^{+/-}$Eμ-*Myc* cells resulted in elevated levels of p21, PUMA, BAX, NOXA, BIM, c-MYC, and PLK2. Of these, NOXA and PLK2 were also elevated in *p53*$^{-/-}$ Eμ-*Myc* lymphomas; however, the magnitude of induction for both genes was approximately 1.5-2-fold less than that experienced in the *Tsc2*$^{+/-}$Eμ-*Myc* lymphomas (Figure 4.3B). p21, BIM, MDM2, and SESN1 levels were significantly increased upon DHX9 knockdown in INK4A$^{-/-}$ MEFs, but none of the p53 targets tested appeared to be activated in p53$^{-/-}$ MEFs (Figure 4.4B). p21, PUMA, BAX, NOXA, BIM, MDM2, c-MYC, and PLK2 transcript levels increased following DHX9 suppression in HCT116 p53$^{+/+}$ cells, and the HCT116 p53$^{-/-}$ cells exhibited significant increases in NOXA, c-MYC, and PLK2 levels (Figure 4.5B). Similar to what was observed in the lymphomas, the magnitude of the increases in NOXA and PLK2 was approximately 1.5-2-fold less in the HCT116 p53$^{-/-}$ cells compared to HCT116 p53$^{+/+}$ cells. These results illustrate that in cells harboring functional p53, DHX9 suppression activates a transcriptional program consisting of several targets known to lead to cell death or cell cycle arrest. In the absence of p53, a small subset of classic p53 targets is also activated and this may contribute to the cell death response elicited in these cells.

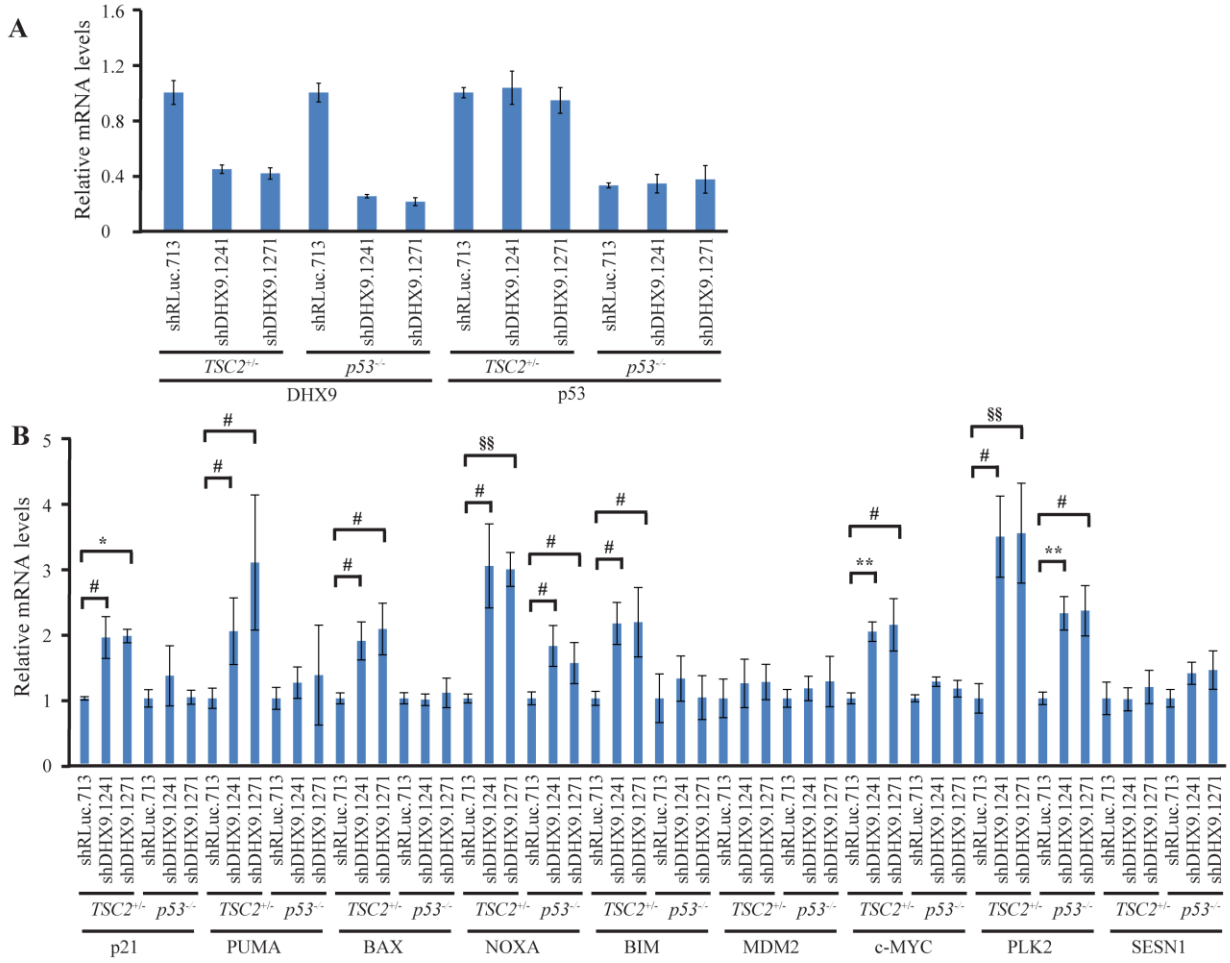

Figure 4.3 Consequences of DHX9 knockdown on p53 targets in *Tsc2*$^{+/-}$Eμ-*Myc* (p53$^{+/+}$) and *p53*$^{-/-}$ Eμ-*Myc* lymphoma cells.

(A) Quantitative RT-PCR analysis documenting DHX9 knockdown and p53 levels in *Tsc2*$^{+/-}$Eμ-*Myc* (p53$^{+/+}$) and *p53*$^{-/-}$ Eμ-*Myc* lymphomas**.** The indicated cell lines were transduced with control shRLuc.713 or DHX9 shRNAs and harvested 6 days post-infection. mRNA levels were normalized to GAPDH and the mRNA levels of the shDHX9 samples were then normalized to that of the shRLuc.713 sample for each cell line. N=3 ±SEM. (**B**) Quantitative RT-PCR analysis of p53 transcriptional targets in *Tsc2*$^{+/-}$Eμ-*Myc* (p53$^{+/+}$) and *p53*$^{-/-}$ Eμ-*Myc* lymphomas. The analysis was performed 6 days post-transduction with control shRLuc.713 or DHX9 shRNAs. mRNA levels for each cell line and target were normalized as in (A). N=3 ±SEM. Significant differences between shDHX9 and shRLuc.713 samples (where p≤0.05) are indicated as follows: # p≤0.05, § p≤0.01, * p≤0.005, ## p≤0.001, §§ p≤0.0005, ** p≤0.0001.

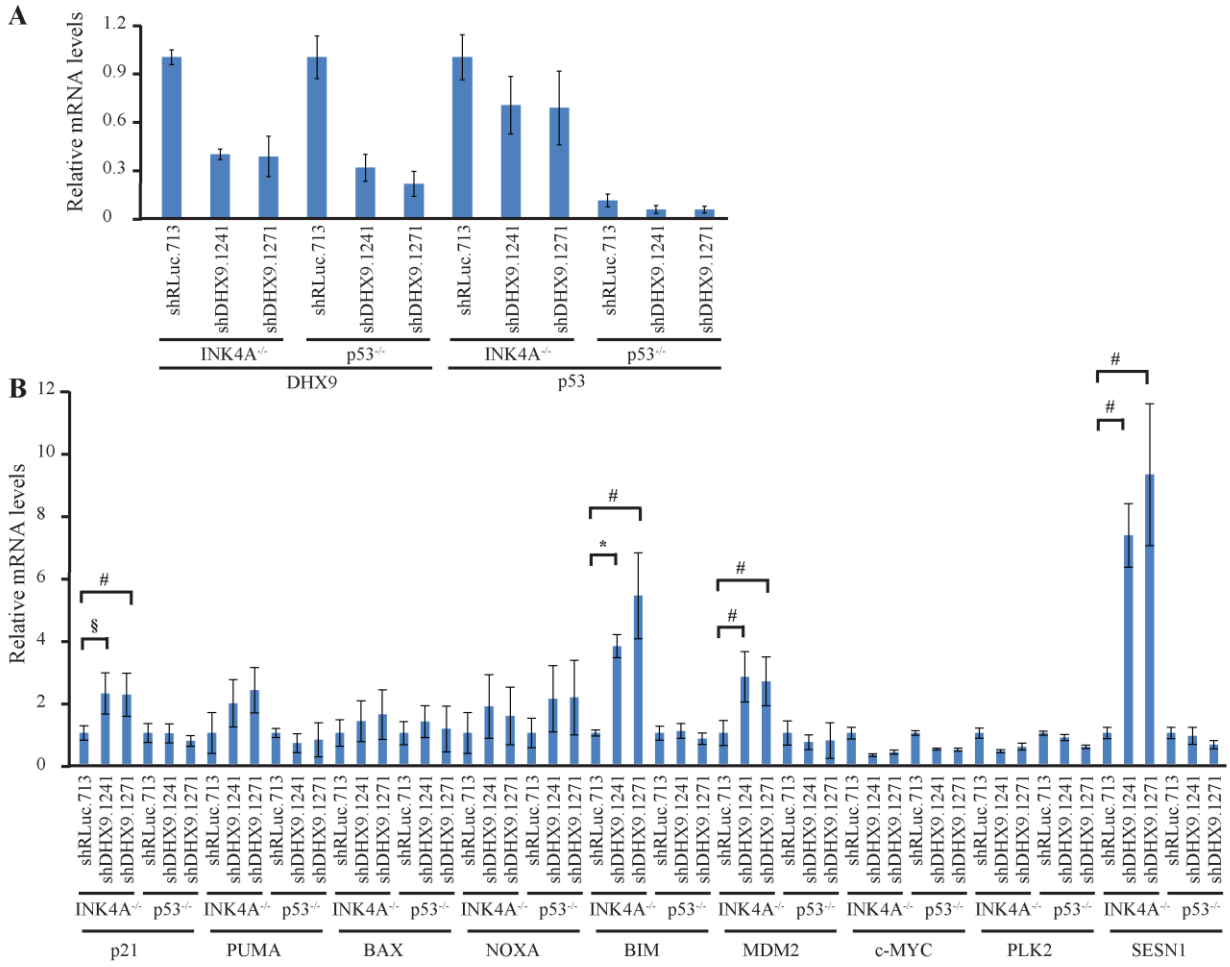

Figure 4.4 Consequences of DHX9 knockdown on p53 targets in INK4A$^{-/-}$ (p53$^{+/+}$) and p53$^{-/-}$ MEFs.

(A) Quantitative RT-PCR analysis showing DHX9 knockdown and p53 levels in INK4A$^{-/-}$ (p53$^{+/+}$) and p53$^{-/-}$ MEFs**.** The indicated cell lines were transduced with control shRLuc.713 or DHX9 shRNAs and harvested 6 days post-infection. mRNA levels were normalized to GAPDH and the mRNA levels of the shDHX9 samples were then normalized to that of the shRLuc.713 sample for each cell line. N=3 ±SEM. **(B)** Quantitative RT-PCR analysis of p53 transcriptional targets in INK4A$^{-/-}$ (p53$^{+/+}$) and p53$^{-/-}$ MEFs. The analysis was performed 6 days post-transduction with control shRLuc.713 or DHX9 shRNAs. mRNA levels for each cell line and target were normalized as in (A). N=3 ±SEM. Significant differences between shDHX9 and shRLuc.713 samples (where $p \leq 0.05$) are indicated using the same key as in Figure 4.3.

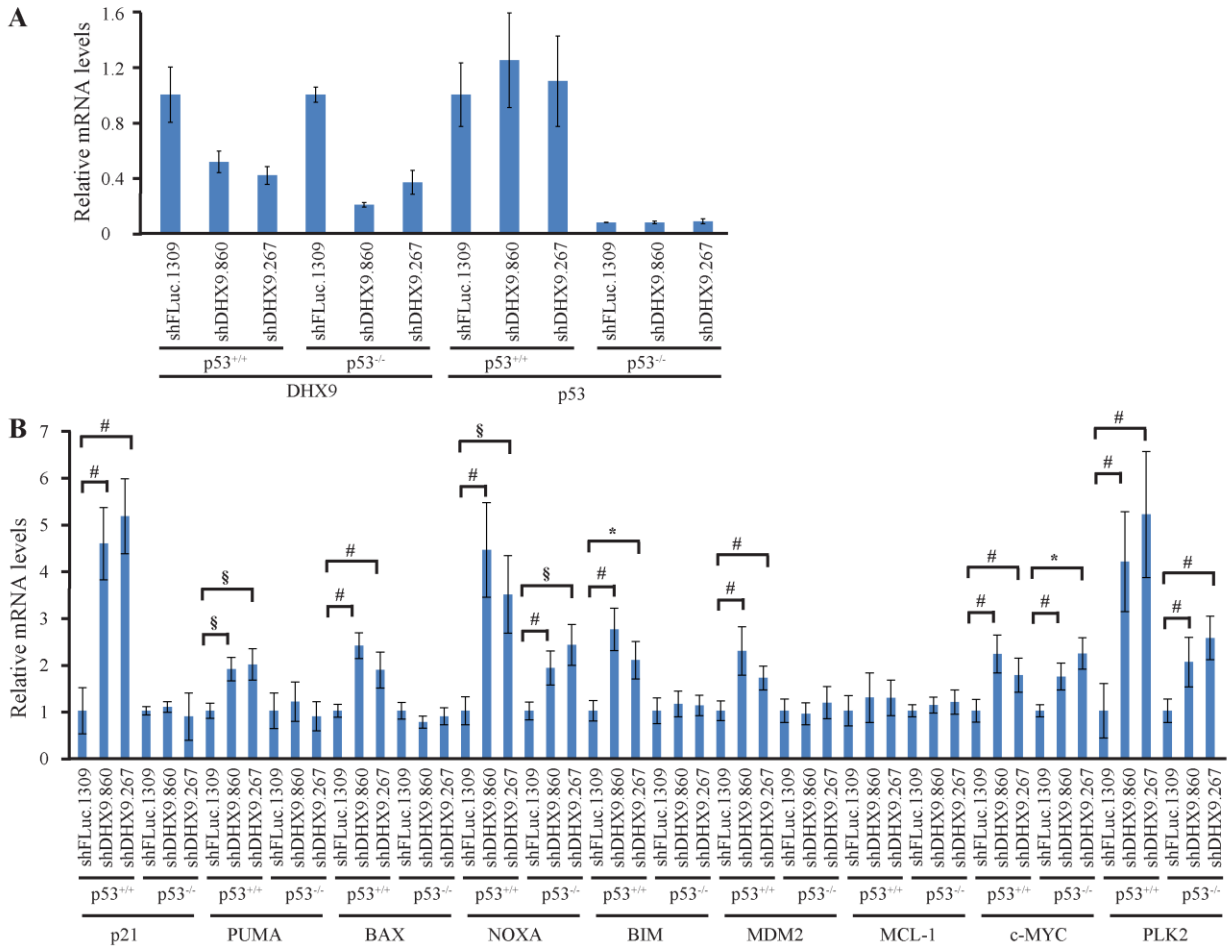

Figure 4.5 Consequences of DHX9 knockdown on p53 targets in HCT116 p53$^{+/+}$ and p53$^{-/-}$ cells.

(A) Quantitative RT-PCR analysis showing DHX9 knockdown and p53 levels in HCT116 p53$^{+/+}$ and p53$^{-/-}$ cells**.** The indicated cell lines were transduced with control shFLuc.1309 or DHX9 shRNAs and harvested 6 days post-infection. mRNA levels were normalized to GAPDH and the mRNA levels of the shDHX9 samples were then normalized to that of the shFLuc.1309 sample for each cell line. N=3 ±SEM. **(B)** Quantitative RT-PCR analysis of p53 transcriptional targets in HCT116 p53$^{+/+}$ and p53$^{-/-}$ cells. The analysis was performed 6 days post-transduction with control shFLuc.1309 or DHX9 shRNAs. mRNA levels for each cell line and target were normalized as in (A). N=3 ±SEM. Significant differences between shDHX9 and shFLuc.1309 samples (where $p \leq 0.05$) are indicated using the same key as in Figure 4.3.

4.5 Discussion

The tumor suppressor p53 plays a central regulatory role in cell cycle progression, apoptosis, and DNA repair. It transcriptionally activates genes with a wide range of functions in response to cellular stresses such as DNA damage, reactive oxygen species, and replication stress, allowing the cell to arrest or undergo apoptosis to prevent aberrant replication and genomic instability [221]. p53 transcriptional targets include the cyclin-dependent kinase inhibitor p21[507, 508], the tumor suppressor PTEN[509], members of the BCL-2 family of pro-apoptotic factors such as PUMA, NOXA, and BAX[331-334], as well as components of the apoptotic effector machinery (e.g. APAF-1 and caspase-6)[342-345]. Due to its importance, it is not surprisingly the most frequently mutated gene in human cancer, with over 50% of cancers harboring a defect in p53[222, 223]. Since many traditional genotoxic agents act through p53 to induce apoptosis or cell cycle arrest, this poses a problem for chemotherapy because it restricts the use of these agents to settings where p53 is functional. Investigating means of eliciting a cell cycle arrest or cell death response in the absence of functional p53 is therefore of great therapeutic interest.

Previous studies from our research group have supported the notion of inhibiting of DHX9 as a chemotherapeutic approach, primarily in p53-wildtype settings. In the present study, we assessed the consequences of suppressing DHX9 in p53-deficient cells and compared the outcome to that achieved in p53-wildtype scenarios. We demonstrated that p53-null mouse lymphomas, MEFs, and HCT116 cells are susceptible to DHX9 suppression. When comparing isogenic $p53^{+/+}$ and $p53^{-/-}$ HCT116 cells, the response to DHX9 suppression was quite similar, demonstrating that targeting DHX9 can be just as effective in p53-deficient settings.

We chose to examine whether common p53 targets were also being activated in p53-null cells. In *Tsc2*$^{+/-}$Eμ-*Myc* lymphomas, DHX9 suppression resulted in elevated levels of p21, PUMA, BAX, NOXA, BIM, c-MYC, and PLK2. This is consistent with activation of an apoptotic program previously observed in mouse lymphomas upon DHX9 suppression[432]. We found that NOXA and PLK2 were also elevated in *p53*$^{-/-}$ Eμ-*Myc* lymphomas. A similar situation was observed with the $p53^{+/+}$ and $p53^{-/-}$ HCT116 cells; induction of p21, PUMA, BAX, NOXA, BIM, MDM2, c-MYC, and PLK2 mRNA in the $p53^{+/+}$ cells and of NOXA, c-MYC, and PLK2 in the $p53^{-/-}$ cells. The fact that we observed increased levels of NOXA and PLK2 in both p53-null lymphomas and HCT116 cells suggests that these two proteins may be involved in common

p53-independent pathways of activating programmed cell death. The smaller magnitude of increase in NOXA and PLK2 levels in the p53-null cells, as well as the observation that fewer p53 targets were activated in the p53-null cells compared to the p53-wildtype cells, may be responsible for the slower kinetics of depletion and lower levels of cell death induced upon DHX9 loss in the p53-null cells. DHX9 suppression in INK4A$^{-/-}$ MEFs resulted in increased levels of p21, BIM, MDM2, and SESN1, all of which are known mediators of cell cycle arrest [507, 508, 510-513]. In contrast to what was observed in the p53-wildtype lymphomas and HCT116 cells, no changes in pro-apoptotic factors PUMA, BAX, and NOXA were exhibited by the INK4A$^{-/-}$ MEFs. This is consistent with the different cell fates (cell cycle arrest in the MEFs versus apoptosis in the lymphomas and HCT116 cells) resulting from DHX9 suppression (Figure 4.2).

While activation of p53 signaling is the canonical pathway by which apoptosis or cell cycle arrest is triggered, these processes have also been documented to occur in a p53-independent manner. Studies have shown that many *bona fide* p53 targets can be activated in p53-deficient settings. In some cases, p53-independent activation occurs through upregulation by other transcription factors. For example, aside from p53, p21 transcription can also be activated by E2F1, E2F3, SP1, SP3, members of the Krüppel-like transcription factor (KLF) family (e.g. KLF4 and KLF6), CDX2, BETA2, MYOD1, and a variety of nuclear receptors[514-518]. Much attention has been given to the p53 family member, p73, and its role in cell cycle control and apoptosis. p73 shares significant structural homology with p53, binds to canonical p53 promoter elements, and can transactivate many p53-dependent promoters[519-521]. Although p73 is known to function cooperatively with p53 and another p53 homolog, p63[522], it can also activate p53 targets independently of p53. Notably, p73 can transcriptionally activate NOXA, PUMA, and p21 in p53-deficient cells in response to a variety of genotoxic stimuli[523-525]. p21, NOXA, PUMA, and BIM are also transactivated by the transcription factors E2F1[526-529] and FOXO3A[530-533] in a p53-independent manner. c-MYC is another activator of NOXA [534]. Hence, cell cycle arrest or programmed cell death via the intrinsic apoptotic pathway can take place in p53-deficient settings by virtue of activation of cell cycle or apoptotic proteins by these other transcription factors. In addition, cell cycle arrest may proceed via activation of the p16-RB1 pathway independently of both p53 and p21[535], which may be a possibility for the

$p53^{-/-}$ MEFs given that none of the p53 targets examined showed any upregulation upon DHX9 suppression (Figure 4.4B). Taken together, our results suggest that DHX9-mediated cell death in the $p53^{-/-}$ lymphomas and HCT116 cells may involve p53-independent upregulation of NOXA and PLK2, which may be activated by transcription factors other than p53.

We have previously shown that DHX9 suppression resulted in senescence in primary human diploid fibroblasts and synergized with ABT-737 to induce apoptosis in *Arf*$^{-/-}$Eμ-*Myc*/Bcl-2 mouse lymphoma cells, in a p53-dependent manner[432, 473]. Here, we show that DHX9 loss can also have deleterious effects in p53-deficient cells. Taken together, these results indicate that the consequences of DHX9 suppression will be context-dependent. We have observed that DHX9 knockdown results in a cell death response in the majority of tumor cell lines but a growth arrest response in non-transformed cells. Loss of DHX9 also has a differential effect in mouse tissues *in vivo* versus cell lines *ex vivo*, as previously revealed[503]. It is therefore conceivable that p53 may be required for DHX9-mediated cell cycle arrest and senescence in non-transformed primary cells but not for a cell cycle arrest or apoptotic response in immortalized cell lines or tumor cells, which harbor significant differences in their biological wiring. Indeed, there are previously documented instances where a particular agent may cause p53-dependent apoptosis in one cellular context but p53-independent apoptosis in another. In one example, sepsis-induced apoptosis was found to be p53-dependent in thymocytes but p53-independent in splenocytes[536]. In another case, paclitaxel-mediated apoptosis was p53-dependent in EIA-transformed MEFs, but when the cells were simultaneously exposed to the cytokine tumor necrosis factor α (TNF-α), the effect became p53-independent[537]. In conclusion, our study supports the presence of a p53-independent mechanism of cell death and cell cycle arrest resulting from DHX9 inhibition. While further work is required to characterize this effect in greater depth, our results support the feasibility of targeting DHX9 as a chemotherapeutic approach in p53-deficient tumors.

4.6 Materials and methods

4.6.1 Cell lines and cell culture

HEK293T/17 cells (ATCC, Manassas, VA, USA), $INK4A^{-/-}$ $p53^{+/+}$ MEFs, and $TSC2^{+/+}$ $p53^{-/-}$ MEFs (a kind gift from Dr. David Kwiatkowski (Brigham and Women's Hospital, USA)) were

maintained in DMEM (Multicell, St-Bruno, QC, Canada). HCT116 $p53^{+/+}$ and HCT116 $p53^{-/-}$ cells were maintained in McCoy 5A (Multicell). Media was supplemented with 10% fetal bovine serum (Multicell). *Tsc2*$^{+/-}$Eμ–*Myc* lymphoma cells were derived from tumors in *Tsc2*$^{+/-}$ mice crossed with Eμ–*Myc* mice. *Tsc2*$^{+/-}$Eμ–*Myc* lymphomas retained wildtype p53, as determined by sequencing across all p53 coding exons and Western blot analysis following γ-irradiation[504]. Similarly, *p53*$^{-/-}$ Eμ-*Myc* lymphomas were derived from tumors in *p53*$^{-/-}$ mice crossed with Eμ–*Myc* mice. Lymphomas were cultured in B-cell media (45% DMEM, 45% Iscove's media, 55 mM β-mercaptoethanol, 10% fetal bovine serum) on irradiated $INK4A^{-/-}$ MEF feeder layers.

4.6.2 Plasmids, virus generation and transductions

For suppression of DHX9 in murine cell lines (MEFs and Eμ-*Myc* lymphomas), two independent shRNAs targeting mouse DHX9 (DHX9.1241 and DHX9.1271) and a control shRNA targeting renilla luciferase (shRLuc.713) were transduced into cells using the MSCV/LTR/miR30/PuroR-IRES-GFP (MLP) or MSCV/LTR/miR30/SV40-GFP (MLS-GFP) retroviral vectors. Retroviral infections were generated using ecotropic Phoenix packaging cells following established protocols (http://www.stanford.edu/group/nolan/retroviral_systems/retsys.html). For infections using MLP, stable integrants were selected using 2 μg/ml puromycin for at least 2 days after the final infection. For suppression of DHX9 in HCT116 cells, two shRNAs targeting human DHX9 (DHX9.860 and DHX9.267) and a control shRNA targeting firefly luciferase (FLuc.1309) were transduced into cells using pPrime-PGK-Puro (Addgene, Cambridge, MA, USA). Lentiviral transduction was performed following published procedures[462]. All shRNAs in this study were cloned into the miR30 backbone of their corresponding vectors via unique XhoI and EcoRI restriction sites[463]. The guide strand sequences of the shRNAs have been previously published[503].

4.6.3 Ex vivo competition assays

Ex vivo competition assays were performed by transducing cells with MLS-GFP-based (for lymphomas and MEFs) or pPrime-PGK-puro-based (for HCT116 cells) shRNAs. The percentage of GFP-positive cells was measured 48h after the final infection (t=0) using a GUAVA EasyCyte

HT flow cytometer (Millipore, Billerica, MA, USA), and assessed every 2-3 days thereafter. Cell death was assessed by staining cells with 4 μg/ml propidium iodide (PI) and measuring the percentage of PI-positive cells.

4.6.4 Cell cycle analysis

Cell cycle analysis was performed using ethanol fixation, acid denaturation, and propidium iodide (PI) staining as previously described[503]. Briefly, cells were harvested from a 6 cm plate, washed twice with PBS containing 1% BSA and 5 mM EDTA, resuspended in 50 μl PBS on ice, fixed with 1.25 ml 70% ethanol, and stored at -20^{o}C until further processing. The fixed cells were then treated with 0.5% Triton X-100/ 2 M HCl, neutralized with 0.1 M sodium borate [pH 8.5], washed with PBS containing 1% BSA and 0.5% Triton X-100, and resuspended in 500 μL of PBS containing 5 μg/mL PI (Sigma). The cell cycle profile of the cells was assessed using a GUAVA EasyCyte HT flow cytometer (Millipore, Billerica, MA, USA).

4.6.5 Immunoblot analysis

Protein extracts were prepared by lysing cells in RIPA lysis buffer (20 mM Tris-HCl [pH 7.5], 150 mM NaCl, 0.1% SDS, 1% NP40, 0.5% sodium deoxycholate, 1 mM β-glycerophosphate, 1 mM PMSF, 1 μg/ml leupeptin, 10 μg/ml aprotinin, and 2.5 μM pepstatin A). PVDF membranes were probed with the indicated primary antibodies and HRP-conjugated secondary antibodies (rabbit (711-035-152) or mouse (115-035-146) (Jackson ImmunoResearch, West Grove, PA, USA) and visualized using enhanced chemiluminescence (ECL) (Perkin Elmer, Waltham, MA, USA). The primary antibodies used in this study were: DHX9 (M99; SC Biotech (Dallas, TX, USA) for human and ab26271; Abcam (Cambridge, MA, USA) for mouse), eEF2 (#2332; Cell Signaling, Danvers, MA, USA), p53 (DO-1; SC Biotech for human and NL-p53-505; Novocastra (Concord, ON, Canada) for mouse), and α-actin (clone AC-15; Sigma, Oakville, ON, Canada).

4.6.6 Quantitative RT-PCR analysis

Total RNA was extracted from cells using TRIzol as per the manufacturer's instructions (Invitrogen, Carlsbad, CA, United States) six days after infection with shRNAs targeting DHX9

or the luciferase control. The RNA was treated with DNase I (Thermo Fisher Scientific, Waltham, MA, USA) and cDNA was generated using Superscript III Reverse Transcriptase (Invitrogen) as per the manufacturer's instructions. Quantitative RT-PCR was performed using the SsoFast EvaGreen Supermix reagent (Bio-Rad, Hercules, CA, USA) on a CFX96 Touch Real-Time PCR Detection System (Bio-Rad). The following primers were used for PCR amplification of mouse targets: DHX9 FWD-$^{5'}$CCGAGGAGCCAACCTTAAAGA$^{3'}$, REV-$^{5'}$TGTCCAATTTCCATGAAGCCC$^{3'}$; p53 FWD-$^{5'}$GCGTAAACGCTTCGAGATGTT$^{3'}$, REV-$^{5'}$TTTTTATGGCGGGAAGTAGACTG$^{3'}$; p21 FWD-$^{5'}$CCTGGTGATGTCCGACCTG$^{3'}$, REV-$^{5'}$CCATGAGCGCATCGCAATC$^{3'}$; PUMA FWD-$^{5'}$ATGCCTGCCTCACCTTCATCT$^{3'}$, REV-$^{5'}$AGCACAGGATTCACAGTCTGGA$^{3'}$; BAX FWD-$^{5'}$TGAAGACAGGGGCCTTTTTG$^{3'}$, REV-$^{5'}$AATTCGCCGGAGACACTCG$^{3'}$; NOXA FWD-$^{5'}$ACTGTGGTTCTGGCGCAGAT$^{3'}$, REV-$^{5'}$TTGAGCACACTCGTCCTTCAA$^{3'}$; BIM FWD-$^{5'}$GAGTTGTGACAAGTCAACACAAACC$^{3'}$, REV-$^{5'}$GAAGATAAAGCGTAACAGTTGTAAGATAACC$^{3'}$; MDM2 FWD-$^{5'}$TGTCTGTGTCTACCGAGGGTG$^{3'}$, REV-$^{5'}$TCCAACGGACTTTAACAACTTCA$^{3'}$; c-MYC FWD-$^{5'}$CAAATCCTGTACCTCGTCCGATTC$^{3'}$, REV-$^{5'}$CTTCTTGCTCTTCTTCAGAGTCGC$^{3'}$; PLK2 FWD-$^{5'}$GACTACTGCACCATAAGCATG$^{3'}$, REV-$^{5'}$CTTCTGGCTCTGTCAACACCT$^{3'}$; SESN1 FWD-$^{5'}$GGCCAGGACGAGGAACTTG$^{3'}$, REV-$^{5'}$AAGGAGTCTGCAAATAACGCAG$^{3'}$; and GAPDH FWD-$^{5'}$AGGTCGGTGTGAACGGATTTG$^{3'}$, REV-$^{5'}$GGGGTCGTTGATGGCAACA$^{3'}$.

The following primers were used for PCR amplification of human targets: DHX9 FWD $^{5'}$CAGGAGAGAGAGTTACTGCCT$^{3'}$, REV-$^{5'}$CTCTGCTGCTCGGTCATTCTG$^{3'}$; p53 FWD $^{5'}$CAGCACATGACGGAGGTTGT$^{3'}$, REV-$^{5'}$TCATCCAAATACTCCACACGC$^{3'}$; p21 FWD $^{5'}$CGATGGAACTTCGACTTTGTCA$^{3'}$, REV-$^{5'}$GCACAAGGGTACAAGACAGTG$^{3'}$; PUMA FWD $^{5'}$CAGACTGTGAATCCTGTGCT$^{3'}$, Rev-$^{5'}$ACAGTATCTTACAGGCTGGG$^{3'}$; BAX FWD $^{5'}$AAGAAGCTGAGCGAGTGT$^{3'}$, REV-$^{5'}$GGAGGAAGTCCAATGTC$^{3'}$; NOXA FWD $^{5'}$GCTGGAAGTCGAGTGTGCTA$^{3'}$, REV-$^{5'}$CCTGAGCAGAAGAGTTTGGA$^{3'}$; BIM FWD $^{5'}$TGGCAAAGCAACCTTCTGATG$^{3'}$, REV-$^{5'}$GCAGGCTGCAATTGTCTACCT$^{3'}$; MDM2 FWD $^{5'}$GCAGTGAATCTACAGGGACGC$^{3'}$, REV-$^{5'}$ATCCTGATCCAACCAATCACC$^{3'}$; MCL-1 FWD $^{5'}$AAGCCAATGGGCAGGTCT$^{3'}$, REV-$^{5'}$TGTCCAGTTTCCGAAGCAT$^{3'}$; c-

MYC FWD $^{5'}$AATGAAAAGGCCCCCAAGGTAGTTATCC$^{3'}$, REV-$^{5'}$GTCGTTTCCGCAACAAGTCCTCTTC$^{3'}$; PLK2 FWD-$^{5'}$TCAGCAACCCAGCAAACACAGG$^{3'}$, REV-$^{5'}$TTTCCAGACATCCCCGAAGAACC$^{3'}$; and GAPDH FWD-$^{5'}$GAAGGTGAAGGTCGGAGTC$^{3'}$, REV-$^{5'}$GAAGATGGTGATGGGATTC$^{3'}$.

4.6.7 Statistical analysis

Statistical analysis was carried out using GraphPad Prism (v. 5.03, GraphPad Software Inc., La Jolla, CA, USA) and data is shown as mean ±SEM. Statistically significant differences were determined using the unpaired two-tailed t-test and represented as p-values.

4.7 Acknowledgements

TL was supported by a Maysie MacSporran graduate studentship and fellowships from the CIHR-sponsored Chemical Biology and Systems Biology Training Programs. This work is supported by grants from the Canadian Cancer Society Research Institute [#701362] and National Institutes of Health [CA163291] to JP.

CHAPTER 5: GENERAL DISCUSSION

5.1 DHX9 and DNA replication

5.1.1 DNA replication in eukaryotes

Eukaryotic DNA replication is a conserved, multi-step process, with the participation of a large number of proteins including DNA polymerases, DNA-binding proteins, ATPases, kinases, helicases, and other enzymes[538, 539]. DNA replication is tightly coordinated with the cell cycle, and is divided into three phases: initiation, elongation, and termination. Replication is initiated during the G1 phase of the cell cycle, with the binding of the pre-replicative complex (pre-RC) to distinct genomic regions called origins of replication[540]. Assembly of the pre-RC occurs in a sequential manner. First, the origin recognition complex (ORC), which consists of ORC subunit 1 (ORC1) to ORC6 and possesses ATPase activity, is recruited to the origins[539, 541]. Because the ORC harbors no sequence-specific DNA-binding activity, it is thought that its recruitment is mediated by Ku, a heterodimer of Ku86 and Ku70[542, 543]. Ku is the DNA-binding subunit of DNA-PK, and plays a role in NHEJ[544]. More recent evidence shows that it also has functions in DNA replication and transcription[542, 543, 545, 546]. Ku has DNA end-binding as well as sequence-specific activity, and has been found to be associated with replication origins[542, 543, 547-549]. ORC assembly at the origin is followed by binding of the ATPase CDC6 and the CDC10-dependent transcript 1 (CDT1)[550]. Lastly the mini-chromosome maintenance (MCM) helicase complex, which contains the six subunits MCM2-7, is loaded as a double hexamer, completing the pre-RC[550]. Activation of origins takes place at the onset of S-phase and involves the dissolution of certain pre-RC components and recruitment of other replication factors, transforming the pre-RC to the pre-initiation complex (pre-IC)[539, 551]. CDC6 and CDT1 are released from the pre-RC. S-phase specific cyclin-dependent kinases (CDKs) and the DBF4-dependent kinase (DDK) then phosphorylate several proteins, including MCM10, CDC45, the helicase RECQL4, treslin, the GINS complex, DNA topoisomerase 2-binding protein 1 (TOPBP1), and DNA polymerase ε, resulting in their binding to the origins and forming the pre-IC. The CDKs and DDK also phosphorylate MCM2-7, leading to helicase activation and DNA unwinding)[539, 551]. The MCM double hexamers split into single complexes, and recruitment of other factors (including the replication factor C (RFC), PCNA, replication protein A (RPA), DNA polymerase α, and DNA polymerase δ) converts the pre-IC

into two functional replisomes which move away from the origin in opposite directions, creating replication forks[539, 551].

Replication elongation takes place throughout S-phase. Here, polymerase α synthesizes the RNA primer at the start of the leading strand and at the start of each Okazaki fragment (spanning 100-200 bps) on the lagging strand, and lays down the first ~20 nucleotides of new DNA[552]. DNA synthesis is then taken over by polymerases ε (for the leading strand) and δ (for the lagging strand), whose processivity is enhanced via association with PCNA which acts as a DNA clamp[553-557]. The MCM complex continuously unwinds the parental DNA ahead of synthesis, enabling the replication fork to progress. Topoisomerases I and II relieve the torsional strain caused by the unwinding by creating transient single-stranded or double-stranded DNA breaks respectively[372, 373]. Besides the aforementioned replication factors, several other proteins also contribute to the efficiency and fidelity of DNA replication. For instance, the RecQ helicase/exonuclease WRN utilizes its exonuclease activity to assist polymerase δ in removing 3'mismatches during Okazaki fragment synthesis[558]. Although DNA is unwound by the MCM helicases during replication elongation, the replication fork may encounter barriers during normal replication, such as G-quadruplexes or other unusual DNA structures, which require resolution by additional specialized helicases. Furthermore, DNA lesions or alterations in nucleotide pools may cause the replication fork to stall. WRN has been shown to unwind G-quadruplexes, bubbles, and D-loops to facilitate replication over such template sequences and prevent fork stalling[558, 559]. In the event of replication fork stalling, both WRN and another RecQ helicase, BLM, have been shown to be essential in enabling replication fork recovery and progression[560-563]. Replication termination occurs when replisomes moving in opposite directions meet, at which point the replisomes dissociate from the DNA[564].

5.1.2 DHX9's role in DNA replication

Previous studies have implicated a role for DHX9 in DNA replication. As described in the Chapter 1, DHX9 was found to associate with several proteins with known roles in DNA replication, although the significance of this association in the context of replication was not characterized in all cases. This included BRCA1 (whose association with DHX9 was actually

characterized in the context of transcription and miRNA processing)[124, 170], Ku86[91], PCNA[88, 89], topoisomerase IIα[90], and WRN[93]. In the case of WRN, DHX9 was found to stimulate WRN-catalyzed unwinding of Okazaki fragment-like DNA:RNA hybrids and Holliday junction-like structures which resemble intermediates formed during replication fork stalling[36, 93, 95]. However, these were *in vitro* experiments, performed on artificial substrates, and a role for DHX9 in DNA replication in an actual biological system had not been investigated. Our results in Chapter 2 support a role for DHX9 in replication. We provide *ex vivo* evidence that DHX9 is associated with origins of replication, and that loss of DHX9 inhibits nascent DNA production. We also show that DHX9 is essential for normal cell cycle progression in primary human fibroblasts, with DHX9-suppressed cells arresting in G1-phase.

Our study gives rise to several unanswered questions, however. Although we have established a role for DHX9 in DNA replication, its precise function, and the point in this multi-step process at which in acts, is unclear. Does DHX9 aid in the assembly of the pre-RC, or does it assist in opening the origins after the pre-RC is assembled? Does it play a role in fork progression during elongation? Does it participate in replication initiation, elongation, or both? Our results in Chapter 2 seem to suggest a role in DNA replication initiation, likely in the early stages. DHX9 binds to origins, and it interacts with Ku86 which helps recruit the ORC to the origin (Figures 2.8 and A.1A, and Ref. [91]). DHX9-suppressed primary fibroblasts arrest in G1 phase (Figure 2.2B), where the pre-RC is assembled, but not yet activated. Hence, it is possible that DHX9 aids in the assembly of the pre-RC. Perhaps it, in complex with Ku, helps recruit the other replication factors. Indeed, knockdown of Ku86 in MRC-5 fibroblasts phenocopies the senescent phenotype exhibited by DHX9-suppressed cells. Cells transfected with Ku86 siRNAs showed increased levels of SA-β-gal staining, slower growth, and elevated levels of p53 and p21 (Figure A.1). It was also previously demonstrated that Ku is important for the G1-S transition[92]. Previous studies showed that depletion of essential pre-RC components such as ORC2, CDC6, or CDT1 led to defective pre-RC assembly and resulted in cells arresting in the G1 phase[454, 565]. We observed that mutation of DHX9's helicase domain rescued the senescent phenotype. Thus, DHX9 may facilitate replication factor binding to origins by modifying the DNA environment. Because DHX9 has been demonstrated to unwind DNA G-quadruplexes *in vitro*[38], and these structures are found near the majority of origins[101-103], it

is also possible that DHX9 may facilitate DNA replication by resolving them. Another possible role is the removal of transcripts from neighboring promoters prior to replication.

On the other hand, the *in vitro* experiments with DHX9 and WRN appear to suggest a role in the elongation step of DNA replication, since the Okazaki-like fragments and Holliday junction-like intermediates are structures found during elongation. WRN itself has been demonstrated to function specifically in elongation in *ex vivo* experiments, with WRN-deficient cells exhibiting slower replication fork progression and a prolonged S-phase[563]. DHX9's interaction with WRN, PCNA, and topoisomerase IIα - all proteins involved in replication elongation – adds support for a role in elongation. With our present data, it is difficult to conclude DHX9's exact function in replication. There is a distinct possibility that it may participate at multiple steps in the replication process. Indeed, this would not be surprising, based on what we can observe of DHX9's behavior in other biological processes. For example, DHX9 takes part in both the pri-miRNA processing and RISC-loading steps of miRNA biogenesis[170, 171].

Several additional experiments could be performed to gain a better understanding of DHX9's role in DNA replication. Immunoprecipitation and colocalization experiments could be performed to determine if DHX9 associates with components of the pre-RC, the pre-IC, or the mature replisome. ChIP analysis could be executed using antibodies against various pre-RC proteins in the presence or absence of DHX9 knockdown, to determine whether loss of DHX9 affects binding of the other replication factors to the origins. This would help ascertain whether DHX9 plays a role in the assembly of the replication complexes. To gain insight into what step in the replication process DHX9 participates, cell cycle transit assays could be performed following treatment with replication inhibitors that arrest the cell at various stages of the cell cycle. Replication track assays using fluorescently labeled nucleotide analogs could be performed to monitor the progression of replication forks in cells, in the presence or absence of DHX9 knockdown – this would inform as to whether DHX9 plays a role in replication elongation. It would also be interesting to explore whether DHX9 is required for replication recovery following replication stalling or DNA damage – e.g. following exposure to hydroxyurea or methyl-methane-sulfonate.

5.1.3 Replication and p53

The link between replication stress and p53 activation has been previously documented. Replication stress could arise either through hyper-replication or through replication stalling or inhibition. Hyper-replication is most often triggered by oncogene activation. Overexpression of many oncogenes leads to activation of proteins or pathways involved in proliferation and DNA replication. The perturbation of normal replication leads to activation of a DNA damage response and cell cycle checkpoints. In a study with Ras-induced senescence, overexpression of Ras resulted in an initial proliferative burst. This was accompanied by over-firing of origins – origins were being activated more than once per cell cycle – and an increase in the number of active replicons[459]. The DNA hyper-replication led to fork instability, which eventually resulted in DNA breaks and activation of ATR/p53 signaling[301, 459]. Similarly, overexpression of cyclin E resulted in increased firing of replication origins, defective replication fork progression, and DNA damage[566]. c-MYC overexpression also resulted in increased origin firing, with the origins being highly asymmetric[567-570]. Hence, the general observation is that hyper-replication following oncogene activation leads to aberrant origin activation and abnormal replication fork dynamics, which results in fork stalling or collapse. This in turn leads to DNA double-stranded breaks, thereby activating p53[571, 572].

Conversely, replication stress can be induced by low levels of DNA replication. DNA replication may be blocked by the inability to form the pre-RC during initiation. Knockdown of either CDC6 or CDT1, which are essential components of the pre-RC, in normal human fibroblasts induces a G1 arrest in a p53-dependent manner. This was accompanied by inhibition of CDK2/cyclin E activity and hypophosphorylation of RB1[565]. Similarly, ORC2 depletion resulted in G1 arrest, with elevated levels of p21 and p27 and inhibition of CDK2/cyclin E activity[454]. Hence, G1 arrest acts as a mechanism to prevent premature S-phase entry in the absence of properly formed pre-RCs. Replication stalling during the later stages of initiation or during elongation also activates p53 signaling, and is associated with cell cycle arrest in the S-phase and/or apoptosis. Treatment of cells with hydroxyurea, which block nucleotide synthesis, and aphidicolin, which inhibits DNA polymerase activity, results in ATR activation, elevated levels of p53 and p21, and inhibition of entry into mitosis[389-391, 453, 573, 574]. Inhibition of topoisomerases I or II, which as previously described, release the torsional strain of unwinding

DNA during replication elongation, result in DNA breaks which activate p53[372-374]. Many topoisomerase inhibitors (e.g. camptothecin, etoposide, and doxorubicin) have been used as chemotherapeutics based on their ability to induce cell cycle arrest or apoptosis[375-379]. Interference with replication elongation by incorporation of nucleotide analogs (e.g. 5-FU or cytosine arabinoside) is another mechanism leading to replication stalling and p53 activation[382, 383]. It can therefore be seen that DNA replication is a tightly regulated process, and perturbations resulting in too much or too little replication may lead to p53 activation and induction of growth arrest, senescence, or apoptosis.

5.1.4 Helicases in aging and genome stability disorders

The senescence phenotype observed in primary human fibroblasts upon DHX9 suppression suggests that defects in DHX9 may lead to accelerated aging. Mutations or loss of other helicases have been documented in human progeroid syndromes. Defects in the RecQ helicases WRN, BLM, and RECQL4 give rise to the rare autosomal recessive disorders Werner, Bloom, and Rothmund-Thomson syndromes respectively[575-579]. Although the precise clinical features vary, these disorders are generally characterized by premature aging, growth retardation, increased genome instability, and increased cancer susceptibility[580-584]. Fibroblasts derived from patients with these diseases achieve significantly fewer population doublings before senescing, compared to wildtype cells[585, 586], a phenotype that was recapitulated via shRNA knockdown in primary human fibroblasts[587]. WRN, BLM and RECQL4 function at the interface of DNA replication and DNA repair, thereby maintaining genomic stability. They exhibit similar substrate specificities to DHX9, with an ability to unwind complex nucleotide structures such as D-loops and G-quadruplex DNA[57, 58, 588]. As described above, WRN assists DNA polymerase δ during DNA replication, resolves inhibitory tertiary structures during normal fork progression, and facilitates replication resumption following arrest. BLM mediates normal fork progression as well, and both WRN and BLM resolve Holliday-like junctions which form as intermediates of stalled replication forks[560-562]. Bloom syndrome cells are characterized by accumulation of abnormal replication intermediates, an increased frequency of sister chromatid exchange, and quadriradial chromosomes which result from unresolved recombination events between homologous chromosomes[589-591]. This indicates a defect in

the repair of damaged replication forks. RECQL4 is phosphorylated by CDKs during replication initiation and is a component of the pre-IC[592]. It also stimulated BLM helicase activity on DNA fork substrates *in vitro*[593]. Given the cooperativity between DHX9 and WRN observed *in vitro*, it would be interesting to see if there is any functional redundancy between DHX9 and the RecQ helicases.

5.2 The DHX9 shRNA mouse model

In order to assess the consequences of systemic DHX9 suppression *in vivo*, we generated an inducible mir30-based shRNA transgenic mouse model. DHX9 shRNAs were expressed under the control of an inducible TRE promoter, and targeted to the Col1A1 locus using FLP-mediated recombination, which was chosen because it supports high transgene expression in a variety of tissues and cell types[594]. Induction of shRNA expression is achieved via addition of doxycycline (DOX), which cooperates with the M2rtTA transactivator (expressed from the Rosa26 locus) to activate the TRE promoter. Using this system, we showed in Chapter 3 that both short-term (2 weeks) and long-term (6 months) suppression of DHX9 in the mouse was well tolerated. Our lab had previously used this model to evaluate the outcome of eIF4E suppression *in vivo*[474]. Much of the technology development for this model was done in collaboration with Dr. Scott Lowe's research group, who have used this and related systems to examine the phenotypes associated with the suppression of a variety of genes, including oncogenes, tumor suppressors, and essential genes. Examples include Oct4, the helicase DDX5, essential gene RPA3, and tumor suppressors p53, p16, and ARF, and APC[475, 481, 482, 494, 595].

The conditional shRNA mouse model offers many advantages. Unique cloning sites flanking the shRNA in the miR30 backbone of the expression cassette allow generation of transgenic mice using any miR30-based shRNA. Induction of shRNA expression is rapid and efficient, with kinetic studies showing maximum induction 5-7 days after exposure to DOX[481]. It is also easily reversible, by controlling DOX exposure. The inducible nature of this system was particularly important in evaluating the effects of DHX9 suppression in the adult mouse because DHX9 appears to be essential for development. Previous studies using a DHX9 knockout mouse demonstrated that homozygous knockout results in embryonic lethality[84]. The

importance of DHX9 in embryogenesis is supported by studies in *C. elegans* and *Drosophila*[21, 23]. Using a conditional knockdown approach allows suppression of genes at any point in the organism's life cycle and for the desired amount of time. Also of significance is that in the shRNA mouse model, partial suppression of genes is attained due to the fact that knockdown in the tissues is not complete, as in a knockout model, and as a result, there is still a certain amount of protein remaining. This becomes important when dealing with genes that have essential functions in the cell. Whereas a straight knockout model may be lethal in such instances, a conditional model allows us to ask, what happens when we partially inhibit an essential gene, for a limited amount of time? Indeed, this may be the case for DHX9. DHX9 plays important roles in many biological processes, and suppression in primary human fibroblasts in culture was not tolerated (Chapter 2), suggesting that it is an essential gene. It is possible that complete obliteration of DHX9 expression (e.g. as in a conditional knock-out model) may be detrimental to the adult organism. Yet, DHX9 knockdown in our shRNA mouse model had no deleterious effects in any of the tissues examined, opening the possibility of targeting DHX9 as a chemotherapeutic approach. The ability to effect partial and transient suppression of gene products renders this system a good approximation of the expected consequences of inhibition of the targets using small molecule inhibitors. Hence the system offers insight with respect to the level and duration of gene suppression that can be tolerated at the organismal level, and provides a means of predicting whether a gene may be a feasible chemotherapeutic target.

While the conditional RNAi platform is a highly effective one for the study of gene function in the mouse, it has several limitations, and some of the aforementioned advantages may also be disadvantageous in some instances. While partial suppression of gene expression is desirable for studying essential genes and for approximating small molecule inhibitors, there is an upper limit to the level of suppression that can be attained using this system, and the inability to completely eradicate gene expression poses problems. The shRNA mouse model may not offer a clear-cut assessment of the effects of suppressing a given gene. There are a number of possible explanations as to why we observed no phenotype upon knocking down DHX9 in the mouse (see Discussion from Chapter 3), and it is difficult to unequivocally conclude whether the shRNA knockdown levels may be insufficient to give rise to a phenotype (e.g. perhaps the low levels of remaining DHX9 are sufficient to carry out its functions), or whether it is due to another

reason such as compensatory mechanisms or DHX9 not being essential *in vivo*. A conditional knockout model may be "cleaner" in examining gene function and determining whether a gene is essential in a given tissue. Another issue is the variation in the potency of knockdown across different tissues. DHX9 knockdown was very robust in the thymus and small and large intestines, moderate in the skin, liver and heart, and mosaic and considerably weaker in the spleen (Figures 3.8 and 3.13). This is consistent with previous studies characterizing shRNA expression in various tissues using this model[475, 483, 596]. The tissues examined were amongst those previously reported to show moderate to high shRNA expression. shRNA expression was found to be much less potent in tissues such as the kidney, lung, and adipocytes, and not detectable in the brain, skeletal muscles, and testis[475, 483]. This variation is primarily attributed to limitations of the Rosa26 promoter driving the M2rtTA, whose activity can vary significantly in different tissues. In addition, expression in some tissues may be impeded by inaccessibility of DOX – for example, the inability of DOX to cross the blood-brain and blood-testis barriers[483]. Recent efforts have been made to address these shortcomings. A newer variant of the rtTA transactivator, rtTA3, was developed which has enhanced transcriptional activity and a 25-fold increase in DOX sensitivity compared to the native rtTA[597]. The rtTA3 was placed under control of the CAGs promoter, a strong synthetic promoter harboring the CMV enhancer element which offers more robust and ubiquitous expression compared to the Rosa26 promoter[598]. shRNA mouse models generated using CAGs-rtTA3 exhibited more potent knockdown in a greater ranger of tissues compared to the Rosa26-M2rtTA model[475, 596, 599]. We had attempted to take advantage of this new system by crossing the shDHX9 mice into mice expressing CAGs-rtTA3. While this double transgenic model was fine for short-term experiments, unfortunately it was not amenable to long-term DOX induction. Exposure to DOX for approximately one month resulted in deleterious effects in both control shFLuc.1309 and shDHX9 mice (data not shown). The shRNA/CAGs-rtTA3 mice became extremely sick, displaying dramatic weight loss, lack of activity, hunched posture, lack of grooming, and appearance of infections, and since this occurred in the control mice as well as the shDHX9 mice, it was attributed to the rtTA3 expression itself rather than the DHX9 suppression. It appeared that long-term rtTA activity is toxic at high levels. Because we wished to assess the long-term effects of DHX9 suppression, the Rosa26-M2rtTA system, which exhibited no short-

term or long-term toxicity, was the best option.

Our study illustrated the effect of suppressing DHX9 in a normal mouse model. In *Tsc2*$^{+/-}$ Eμ-*Myc* lymphomas injected into wildtype mice, DHX9 suppression eliminated the tumor cells and extended mouse survival, indicating that loss of DHX9 interferes with tumor maintenance. A logical next step would be to investigate the consequences of DHX9 suppression on tumor initiation in pre-clinical mouse models. The Pelletier lab has had experience with the Eμ-*Myc* mouse, a lymphoma model in which tumors develop at approximately 4 months of age[474]. The *shDHX9/rtTA* mice may be crossed to these mice and the effect on tumor-free survival monitored.

5.3 Therapeutic potential of targeting DHX9

5.3.1 Targeting DHX9 in tumor cells

Targeted molecular therapeutics exert their anti-neoplastic effects by inhibiting specific gene products involved in tumor maintenance. They generally offer higher therapeutic indices compared to traditional chemotherapy which utilize cytotoxic agents that are deleterious to all rapidly dividing cells. Targeted therapeutics have found great success in the clinic, but the problem of resistance remains, and many cancers cannot yet be effectively treated with existing drugs. Hence, there is an ongoing need to uncover novel targets for use in chemotherapy.

In Chapter 3, we showed that DHX9 suppression was lethal in the majority of mouse and human tumor cells tested. Ten out of 13 human tumor cells, derived from five different types of cancers, were susceptible to DHX9 inhibition, as were mouse lymphomas overexpressing c-MYC and harboring a deletion in TSC2. Six out of 8 human multiple myeloma cell lines were sensitive to DHX9 loss, and DHX9 synergizes with the glucocorticoid dexamethasone in the multiple myeloma cells. Loss of DHX9 extended the survival of mice harboring in *Tsc2*$^{+/-}$Eμ-*Myc* lymphomas. Previously, our lab has shown that DHX9 synergized with ABT-737 to induce apoptosis in *Arf*$^{-/-}$Eμ-*Myc*/Bcl-2 cells, which serve as a model for non-Hodgkin's lymphoma. Most of the settings examined harbored wildtype p53. However, our results in Chapter 4 revealed that p53-deficient tumor cell lines were also susceptible to DHX9 knockdown. Importantly, DHX9 suppression demonstrated no deleterious effects on normal tissues of adult

mice. Taken together, the evidence indicates DHX9 to be a promising potential chemotherapeutic target, both on its own and in combination with other therapeutics. The differential effect observed upon DHX9 suppression in the cancer cells and in the shDHX9 mice suggests that a good therapeutic index can be achieved. What is particularly attractive about DHX9 as a potential target is the fact that its suppression appears to be well tolerated in highly proliferative tissues (e.g. skin and intestines), suggesting that side effects may be minimal. Our results showing that loss of DHX9 is lethal in a wide range of settings suggest that targeting DHX9 may have broad applicability. Further studies would be required to ascertain whether there's a cancer type that's particularly suited to DHX9 targeting, although our observation that DHX9 inhibition is effective in combating the majority of multiple myeloma cells tested and that it synergizes with dexamethasone implies that multiple myeloma may be a promising cancer type on which to follow up.

5.3.2 Targeting DHX9 in p53-deficient cells

The results from Chapter 2, along with previous studies in our lab using *Arf*$^{-/-}$Eμ-*Myc*/Bcl-2 lymphomas, indicate a p53-dependence to the response following DHX9 suppression. However, our results from Chapter 4 illustrated that loss of DHX9 can also mediate cell death or cell cycle arrest independently of p53 status. p53-null mouse lymphomas, MEFs, and HCT116 cells were susceptible to DHX9 suppression. Analysis of p53 target transcript levels revealed that in both the p53-deficient lymphomas and HCT116 cells, NOXA and PLK2 levels were elevated. Although BCL-2 family-mediated apoptosis acts downstream of p53, it can also be triggered in a p53-independent manner. Transcription of NOXA and other pro-apoptotic proteins have been shown to be activated by other transcription factors such as the p53 family member p73[523-525], E2F1[526-529], FOXO3A[530-533], and c-MYC[534]. It is likely that DHX9-mediated cell death in p53-null lymphomas and HCT116 cells is induced through p53-independent activation of NOXA. The mechanism of NOXA activation remains to be determined but may involve one of the aforementioned transcription factors or perhaps a novel pathway involving a yet-unidentified transcription factor. We also observed enhanced PLK2 levels in both the *p53*$^{-/-}$ Eμ-*Myc* lymphomas and p53$^{-/-}$ HCT116 cells and increased c-MYC in p53$^{-/-}$ HCT116. PLK2 has

previously been shown to interact with both TSC1 and TSC2 and inhibit mTOR signaling, thereby providing a link between the p53 and mTOR pathways[600]. Although p53-independent mechanisms of PLK2-mediated apoptosis have not been well characterized, the mTOR inhibitor rapamycin has been found to induce apoptosis in a p53-independent manner[601, 602]. It is therefore possible that cell death resulting from DHX9 suppression in p53-deficient cells may proceed via parallel pathways involving NOXA and PLK2 which may or may not be interdependent. The transcription factors activating NOXA and PLK2 may be less efficient than p53 – for example, they may bind to the p53 response elements in the promoter, but with less efficiency compared to p53. This may partially explain why the magnitude of the increase in NOXA and PLK levels exhibited by the p53-null cells were 1.5-2-fold less than that of the corresponding p53-wildtype cells. It should also be noted that only a subset of the p53 targets found to be elevated in p53-wildtype cells were upregulated in p53-null cells. For example, PUMA, BAX, and BIM levels were unchanged in the p53-null settings. Taken together, this may have contributed to the smaller extent of cell death and slower kinetics of depletion observed in the p53-null cells compared to the p53-wildtype cells.

There have been many studies documenting the p53-independent upregulation of p21 by a variety of other transcription factors (see Discussion from Chapter 4). It was somewhat surprising that p21 levels were not elevated in the $p53^{-/-}$ MEFs, which underwent cell cycle arrest instead of apoptosis. The phenotype could not be explained by upregulation of any of the p53 targets examined. Although cell cycle arrest is most commonly mediated by p21, it can also occur independently of both p53 and p21. p16 is a cyclin kinase inhibitor whose inhibition of CDKs converges with the p21 pathway in preventing RB1 phosphorylation and E2F activation. It would be interesting to investigate whether the cell cycle arrest in the $p53^{-/-}$ MEFs may be mediated by p16. It is also possible that the mechanism may involve activation of p53 targets which were not included in the panel we examined.

The ability of DHX9 loss to provoke cell death or cell cycle arrest in p53-deficient cells widens the therapeutic potential of targeting DHX9, given that over 50% of all cancers harbor p53 defects. Future experiments should be aimed at further deciphering this p53-independent mechanism. Levels of transcriptional factors known to activate p53 targets should be assessed, and ChIP experiments can be performed to ascertain binding to NOXA and PLK2 promoters. It

would be interesting to examine whether suppression of NOXA or PLK2 in the p53-deficient cell lines could rescue the cell death phenotype – this would inform as to whether it is actually mediated through these proteins. As well, since only a subset of p53 targets were surveyed in the data presented, the analysis could be expanded to include transcript levels of many other p53 targets. Expression profiling can provide insight as to the genome-wide changes occurring in p53-deficient cells following DHX9 knockdown. Finally, the effect of DHX9 suppression in panel of p53-deficient cell lines derived from various cancer types can be assessed.

5.3.3 Context dependence of DHX9 suppression

Over the course of our investigations, we have suppressed DHX9 in a variety of settings, with different responses being elicited. DXH9 knockdown in primary human fibroblasts, U2OS cells, and MEFs resulted in growth arrest and/or senescence, whereas in the majority of cancer cells, an apoptotic response was induced. DHX9 knockdown had no effect on adult mice, or in MCF-7 breast cancer cells. *Arf*$^{-/-}$Eμ-*Myc*/Bcl-2 lymphomas were susceptible only in the presence of ABT-737. These results demonstrate that the response to DHX9 suppression is highly context-dependent, and is largely influenced by the levels of various cell cycle and apoptotic proteins in the cell. We have seen that cells that underwent growth arrest/senescence (primary human fibroblasts, U2OS, and MEFs) generally showed high induction of p21, an inhibitor of cell cycle progression. Incidentally, it was not clear whether the MEFs and U2OS cells were senescing or simply arresting, due to difficulties in staining for SA-β-gal in these cells, however, it is likely that the former scenario was occurring because the cells remained growth-arrested for many weeks following infection with DHX9 shRNAs (data not shown). Cells that underwent apoptosis upon DHX9 suppression generally expressed high levels of pro-apoptotic proteins such as BIM, BAX, BAK, or c-MYC (Figure 3.3). The anti-apoptotic factor BCL-2 appears to be a mediator of resistance to DHX9 targeting, as seen in the MCF-7 breast cancer cells and *Arf*$^{-/-}$Eμ-*Myc*/Bcl-2 lymphomas, which express high levels of this protein.

The context-dependence of DHX9 suppression is reflected in the gene expression changes in various cellular contexts. There was very little overlap between the gene expression signatures of the MRC-5 fibroblasts (Figure 2.5), *Arf*$^{-/-}$Eμ-*Myc*/Bcl-2 lymphomas[432], and

mouse large intestine tissue (Figure 3.17) following DHX9 knockdown. DHX9-suppressed MRC-5 fibroblasts, which senesced, exhibited massive downregulation of genes involved in DNA replication, proliferation, and cell cycle progression (Figure 2.5 and Table A.1). This was not observed in the *Arf*$^{-/-}$Eμ-*Myc*/Bcl-2 lymphomas, which showed strong upregulation of p53 targets involved in apoptotic signaling, such as NOXA, PUMA, and BIM[432]. The expression analysis of the large intestine from the shDHX9 mice (which exhibited no observable phenotype) was vastly different, displaying no upregulation of p53 targets, and surprisingly, upregulation of genes involved in many processes including metabolism, DNA replication, translational initiation, cell division, and RNA splicing (Figure 3.17 and Tables A.2-A.4). These differences in transcriptome changes in the different contexts no doubt contributed to the distinct cellular outcomes (senescence, apoptosis, or no effect) observed in each situation.

Our results from Chapter 4 show that p53 contributes to the strength of the DHX9 response in transformed cells, but is not always essential. Whether p53 is required or not is also context-dependent. The DHX9-mediated senescence response in human diploid fibroblasts was p53-dependent, but cell cycle arrest or cell death was able to occur independently of p53 in several transformed cell lines. A possible explanation for this may be that perhaps transformed cells express high levels of alternative transcription factors that can transactivate p53 targets. Studies of p73 levels in breast cancer showed that breast cancer tissues and cell lines overexpress p73 compared to normal tissues[603, 604]. Many other cancer types also overexpress p73[605-607]. E2F-1, another transcription factor shown to transactivate p53 targets, is also overexpressed in some cancers[608]. Hence, the inherent biological wiring of the cells may be a determinant of whether p53 is required for apoptotic or cell cycle arrest responses.

The differential response to DHX9 suppression in tumor cells versus normal tissues in the adult mouse allows for a therapeutic window to exist. The mechanism underlying this differential response has not been fully elucidated, but may be a consequence of increased requirements for DHX9 in the former. As described in Chapter 1, DHX9 is an active participant in a multitude of cellular processes, with regulatory roles in DNA replication, transcription, translation, RNA transport, miRNA processing, apoptosis, and genome maintenance. Many of these processes are dysregulated during oncogenesis. Dysregulation of transcription, translation, DNA replication, and microRNA in cancer are well-established phenomena, stemming from the heightened

biosynthetic and metabolic needs of tumor cells to sustain elevated proliferative demands[609-616]. Numerous essential processes are rewired in cancers. Thus, there is likely an increased dependency on DHX9, a key regulator in all these processes, in tumor cells, and as a consequence, reduction in DHX9 levels would have a significant impact on their ability to survive. In other words, cancer cells may become "addicted" to DHX9. Conversely, suppression of DHX9 had no effect on normal mouse tissues; this is likely due to the lower proliferative demands of normal cells, where the processes of transcription, translation, DNA replication, etc. are tightly regulated. Indeed, the majority of cells in an organism are not actively proliferating, but are instead quiescent[496]. Hence, lower levels of DHX9 activity are required, and disruption of the aforementioned cellular processes would have a much milder effect. Even in highly proliferative tissues, the low levels of DHX9 remaining after knockdown may be sufficient to allow normal function. Another distinct possibility – one that was suggested by the expression profiling of large intestine tissue from the shDHX9 mice – is that there is some form of compensatory mechanism following DHX9 suppression which occurs *in vivo*. Despite the lack of phenotype, upregulation of a large number of genes was observed. This included both positive and negative regulators of processes such as translation and mitotic nuclear division (see section 3.5). In particular, genes involved in DNA replication and cell cycle progression, such as MCM10, (1.3-1.5-fold increase) and cyclins B1, B2, and D2 (1.5-1.6-fold increase) were elevated in both shDHX9 mouse strains (Table A.2). This may have partially compensated for the reduction in DHX9 levels.

Interestingly, the ability to overexpress DHX9 is also context dependent. We were able to express DHX9 wildtype and mutant cDNAs in NIH3T3 and MRC-5 non-transformed cells relatively easily (Figure 2.7 and Ref.[432]). However, despite repeated attempts, we were never able to successfully overexpress DHX9 in *Arf*$^{-/-}$Eμ-*Myc*/Bcl-2 lymphomas (data not shown). This may indicate that DHX9 protein levels in lymphomas are tightly regulated, where either overexpression or inhibition of DHX9 may have adverse consequences.

5.3.4 Feasibility of targeting DHX9 in chemotherapy

In evaluating the feasibility of targeting DHX9 in as a neoplastic approach, two important considerations must be taken into account: (a) An achievable therapeutic index, and (b) the

availability of DHX9 inhibitors and the practicality of inhibiting DHX9. As discussed above, the differential response to DHX9 suppression observed between tumor cells and normal tissues in adult mice indicates that a good therapeutic index can be achieved. At the moment, a specific inhibitor of DHX9 activity has not been identified - the approach our lab has used for curtailing DHX9 expression utilized shRNAs. However, attempts have been made to remedy this. A primary screening assay was recently developed to uncover inhibitors of DHX9 activity, where it was found that aurintricarboxylic acid prevents DHX9-mediated ATP hydrolysis[37]. Although this compound is promiscuous and therefore not an ideal DHX9 inhibitor, this screening approach can be implemented on a large-scale basis to search for more selective inhibitors. Inhibiting helicases in general has been shown to be a viable and promising chemotherapeutic approach. The Pelletier lab has had extensive experience with small molecule inhibitors of the DEAD-box helicase eIF4A. Our lab and others have shown that eIF4A inhibition using hippuristanol, pateamine A, silvestrol and other rocaglamides demonstrated anti-neoplastic activity both in tumor cells *ex vivo* and in preclinical mouse models, both as single agents and in combination with other chemotherapeutics such as doxorubicin and ABT-737[402-404, 617-622]. A specific inhibitor of WRN, NSC 19630, induced apoptosis and sensitized cancer cells to a poly(ADP ribose) polymerase (PARP) inhibitor and to the chemotherapy drug topotecan[623]. 4-hydroxy-8-nitroquinoline-3-carboxylic acid (C5), a selective inhibitor of the nuclease/helicase DNA2, was cytotoxic to several human cancer cell lines and sensitized cancer cells to camptothecin[624]. Hence, the current evidence indicates that helicases are druggable targets.

5.4 Concluding remarks

Ever since the purification of mammalian DHX9 in 1991, immense progress has been made in understanding the biological functions of this helicase. DHX9 has been found to participate in virtually every aspect of nucleic acid metabolism, from DNA replication to miRNA processing. Part of this thesis was focused on investigating the role of DHX9 in DNA replication. Our results provide *ex vivo* evidence of DHX9's involvement in DNA replication and cell cycle progression, complementing previous *in vitro* studies. Our work also highlights the relationship between DHX9 and p53, establishing a means of triggering cell cycle arrest, senescence, and apoptosis by suppressing DHX9. The clinical relevance of DHX9 is a new but fast-growing area of research.

Our studies support the notion of targeting DHX9 as a chemotherapeutic approach in a variety of tumor settings. There remain many unanswered questions and areas for future exploration. This includes further investigation of the details and mechanisms of DHX9's role in DNA replication, the mechanisms underlying the p53-independent aspect of DHX9-mediated cell death or cell cycle arrest, and additional experiments to gain greater insight on the feasibility and therapeutic potential of targeting DHX9.

BIBLIOGRAPHY

1. Zhang S and Grosse F. (1994). Nuclear DNA helicase II unwinds both DNA and RNA. *Biochemistry* **33(13)**:3906-3912.
2. Jain A, Bacolla A, Chakraborty P, Grosse F and Vasquez KM. (2010). Human DHX9 helicase unwinds triple-helical DNA structures. *Biochemistry* **49(33)**:6992-6999.
3. Eckhard J and Fairman-Williams ME. (2010). An introduction to RNA helicases: superfamilies, families, and major themes. In: Jankowsky E, ed. *RNA Helicases*. (Cambridge, UK: Royal Society of Chemistry), pp. 1-31.
4. Cordin O, Banroques J, Tanner NK and Linder P. (2006). The DEAD-box protein family of RNA helicases. *Gene* **367**:17-37.
5. Singleton MR, Dillingham MS and Wigley DB. (2007). Structure and mechanism of helicases and nucleic acid translocases. *Annu Rev Biochem* **76**:23-50.
6. Fairman-Williams ME, Guenther UP and Jankowsky E. (2010). SF1 and SF2 helicases: family matters. *Curr Opin Struct Biol* **20(3)**:313-324.
7. Rocak S and Linder P. (2004). DEAD-box proteins: the driving forces behind RNA metabolism. *Nat Rev Mol Cell Biol* **5(3)**:232-241.
8. Linder P. (2006). Dead-box proteins: a family affair--active and passive players in RNP-remodeling. *Nucleic Acids Res* **34(15)**:4168-4180.
9. Lai JC, Ponti S, Pan D, Kohler H, Skoda RC, Matthias P and Nagamine Y. (2012). The DEAH-box helicase RHAU is an essential gene and critical for mouse hematopoiesis. *Blood* **119(18)**:4291-4300.
10. Yajima M and Wessel GM. (2011). The DEAD-box RNA helicase Vasa functions in embryonic mitotic progression in the sea urchin. *Development* **138(11)**:2217-2222.
11. Zheng HJ, Tsukahara M, Liu E, Ye L, Xiong H, Noguchi S, Suzuki K and Ji ZS. (2015). The novel helicase helG (DHX30) is expressed during gastrulation in mice and has a structure similar to a human DExH box helicase. *Stem Cells Dev* **24(3)**:372-383.
12. Uchiumi F, Seki M and Furuichi Y. (2015). Helicases and human diseases. *Front Genet* **6**:39.
13. Brosh RM, Jr. (2013). DNA helicases involved in DNA repair and their roles in cancer. *Nat Rev Cancer* **13(8)**:542-558.
14. Fuller-Pace FV. (2013). DEAD box RNA helicase functions in cancer. *RNA Biol* **10(1)**:121-132.
15. Ahmad S and Hur S. (2015). Helicases in Antiviral Immunity: Dual Properties as Sensors and Effectors. *Trends Biochem Sci* **40(10)**:576-585.
16. Zhang SS and Grosse F. (1991). Purification and characterization of two DNA helicases from calf thymus nuclei. *J Biol Chem* **266(30)**:20483-20490.
17. Lee CG and Hurwitz J. (1992). A new RNA helicase isolated from HeLa cells that catalytically translocates in the 3' to 5' direction. *J Biol Chem* **267(7)**:4398-4407.
18. Lee CG and Hurwitz J. (1993). Human RNA helicase A is homologous to the maleless protein of Drosophila. *J Biol Chem* **268(22)**:16822-16830.
19. Zhang S, Maacke H and Grosse F. (1995). Molecular cloning of the gene encoding nuclear DNA helicase II. A bovine homologue of human RNA helicase A and Drosophila Mle protein. *J Biol Chem* **270(27)**:16422-16427.
20. Fukunaga A, Tanaka A and Oishi K. (1975). Maleless, a recessive autosomal mutant of Drosophila melanogaster that specifically kills male zygotes. *Genetics* **81(1)**:135-141.

21. Kuroda MI, Kernan MJ, Kreber R, Ganetzky B and Baker BS. (1991). The maleless protein associates with the X chromosome to regulate dosage compensation in Drosophila. *Cell* **66(5)**:935-947.
22. Lee CG, Eki T, Okumura K, da Costa Soares V and Hurwitz J. (1998). Molecular analysis of the cDNA and genomic DNA encoding mouse RNA helicase A. *Genomics* **47(3)**:365-371.
23. Walstrom KM, Schmidt D, Bean CJ and Kelly WG. (2005). RNA helicase A is important for germline transcriptional control, proliferation, and meiosis in C. elegans. *Mech Dev* **122(5)**:707-720.
24. Wei W, Twell D and Lindsey K. (1997). A novel nucleic acid helicase gene identified by promoter trapping in Arabidopsis. *Plant J* **11(6)**:1307-1314.
25. Lee CG, Eki T, Okumura K, Nogami M, Soares Vda C, Murakami Y, Hanaoka F and Hurwitz J. (1999). The human RNA helicase A (DDX9) gene maps to the prostate cancer susceptibility locus at chromosome band 1q25 and its pseudogene (DDX9P) to 13q22, respectively. *Somat Cell Mol Genet* **25(1)**:33-39.
26. Zhang S and Grosse F. (1997). Domain structure of human nuclear DNA helicase II (RNA helicase A). *J Biol Chem* **272(17)**:11487-11494.
27. Xing L, Zhao X, Niu M and Kleiman L. (2014). Helicase associated 2 domain is essential for helicase activity of RNA helicase A. *Biochim Biophys Acta* **1844(10)**:1757-1764.
28. Xing L, Niu M and Kleiman L. (2014). Role of the OB-fold of RNA helicase A in the synthesis of HIV-1 RNA. *Biochim Biophys Acta* **1839(11)**:1069-1078.
29. Aratani S, Oishi T, Fujita H, Nakazawa M, Fujii R, Imamoto N, Yoneda Y, Fukamizu A and Nakajima T. (2006). The nuclear import of RNA helicase A is mediated by importin-alpha3. *Biochem Biophys Res Commun* **340(1)**:125-133.
30. Zhang S, Herrmann C and Grosse F. (1999). Nucleolar localization of murine nuclear DNA helicase II (RNA helicase A). *J Cell Sci* **112 (Pt 16)**:2693-2703.
31. Schutz P, Wahlberg E, Karlberg T, Hammarstrom M, Collins R, Flores A and Schuler H. (2010). Crystal structure of human RNA helicase A (DHX9): structural basis for unselective nucleotide base binding in a DEAD-box variant protein. *J Mol Biol* **400(4)**:768-782.
32. Fu Q and Yuan YA. (2013). Structural insights into RISC assembly facilitated by dsRNA-binding domains of human RNA helicase A (DHX9). *Nucleic Acids Res* **41(5)**:3457-3470.
33. Nagata T, Tsuda K, Kobayashi N, Shirouzu M, Kigawa T, Guntert P, Yokoyama S and Muto Y. (2012). Solution structures of the double-stranded RNA-binding domains from RNA helicase A. *Proteins* **80(6)**:1699-1706.
34. Nagata T, Tsuda K, Kobayashi N, Guntert P, Yokoyama S and Muto Y. (2013). (1)H, (13)C, and (15)N resonance assignments of the dsRBDs of mouse RNA helicase A. *Biomol NMR Assign* **7(1)**:69-72.
35. Lee CG, Chang KA, Kuroda MI and Hurwitz J. (1997). The NTPase/helicase activities of Drosophila maleless, an essential factor in dosage compensation. *EMBO J* **16(10)**:2671-2681.

36. Chakraborty P and Grosse F. (2010). WRN helicase unwinds Okazaki fragment-like hybrids in a reaction stimulated by the human DHX9 helicase. *Nucleic Acids Res* **38(14)**:4722-4730.
37. Cencic R, Senechal P and Pelletier J. (2015). Establishment of a Primary Screening Assay for the DHX9 Helicase. *Comb Chem High Throughput Screen* **18(9)**:855-861.
38. Chakraborty P and Grosse F. (2011). Human DHX9 helicase preferentially unwinds RNA-containing displacement loops (R-loops) and G-quadruplexes. *DNA Repair (Amst)* **10(6)**:654-665.
39. Kogoma T. (1996). Recombination by replication. *Cell* **85(5)**:625-627.
40. Kowalczykowski SC. (2000). Initiation of genetic recombination and recombination-dependent replication. *Trends Biochem Sci* **25(4)**:156-165.
41. Haber JE. (1999). DNA recombination: the replication connection. *Trends Biochem Sci* **24(7)**:271-275.
42. Drolet M, Broccoli S, Rallu F, Hraiky C, Fortin C, Masse E and Baaklini I. (2003). The problem of hypernegative supercoiling and R-loop formation in transcription. *Front Biosci* **8**:d210-221.
43. Gan W, Guan Z, Liu J, Gui T, Shen K, Manley JL and Li X. (2011). R-loop-mediated genomic instability is caused by impairment of replication fork progression. *Genes Dev* **25(19)**:2041-2056.
44. Gottipati P and Helleday T. (2009). Transcription-associated recombination in eukaryotes: link between transcription, replication and recombination. *Mutagenesis* **24(3)**:203-210.
45. Santos-Pereira JM and Aguilera A. (2015). R loops: new modulators of genome dynamics and function. *Nat Rev Genet* **16(10)**:583-597.
46. Mirkin SM. (2008). Discovery of alternative DNA structures: a heroic decade (1979-1989). *Front Biosci* **13**:1064-1071.
47. Zhao J, Bacolla A, Wang G and Vasquez KM. (2010). Non-B DNA structure-induced genetic instability and evolution. *Cell Mol Life Sci* **67(1)**:43-62.
48. Bacolla A and Wells RD. (2004). Non-B DNA conformations, genomic rearrangements, and human disease. *J Biol Chem* **279(46)**:47411-47414.
49. Scheffner M, Knippers R and Stahl H. (1991). Simian-virus-40 large-T-antigen-catalyzed DNA and RNA unwinding reactions. *Eur J Biochem* **195(1)**:49-54.
50. Brosh RM, Jr., Majumdar A, Desai S, Hickson ID, Bohr VA and Seidman MM. (2001). Unwinding of a DNA triple helix by the Werner and Bloom syndrome helicases. *J Biol Chem* **276(5)**:3024-3030.
51. Orren DK, Theodore S and Machwe A. (2002). The Werner syndrome helicase/exonuclease (WRN) disrupts and degrades D-loops in vitro. *Biochemistry* **41(46)**:13483-13488.
52. Bachrati CZ, Borts RH and Hickson ID. (2006). Mobile D-loops are a preferred substrate for the Bloom's syndrome helicase. *Nucleic Acids Res* **34(8)**:2269-2279.
53. Opresko PL, Sowd G and Wang H. (2009). The Werner syndrome helicase/exonuclease processes mobile D-loops through branch migration and degradation. *PLoS One* **4(3)**:e4825.

54. Popuri V, Bachrati CZ, Muzzolini L, Mosedale G, Costantini S, Giacomini E, Hickson ID and Vindigni A. (2008). The Human RecQ helicases, BLM and RECQ1, display distinct DNA substrate specificities. *J Biol Chem* **283(26)**:17766-17776.
55. Bachrati CZ and Hickson ID. (2009). Dissolution of double Holliday junctions by the concerted action of BLM and topoisomerase IIIalpha. *Methods Mol Biol* **582**:91-102.
56. Machwe A, Karale R, Xu X, Liu Y and Orren DK. (2011). The Werner and Bloom syndrome proteins help resolve replication blockage by converting (regressed) holliday junctions to functional replication forks. *Biochemistry* **50(32)**:6774-6788.
57. Sun H, Karow JK, Hickson ID and Maizels N. (1998). The Bloom's syndrome helicase unwinds G4 DNA. *J Biol Chem* **273(42)**:27587-27592.
58. Mohaghegh P, Karow JK, Brosh RM, Jr., Bohr VA and Hickson ID. (2001). The Bloom's and Werner's syndrome proteins are DNA structure-specific helicases. *Nucleic Acids Res* **29(13)**:2843-2849.
59. Booy EP, Meier M, Okun N, Novakowski SK, Xiong S, Stetefeld J and McKenna SA. (2012). The RNA helicase RHAU (DHX36) unwinds a G4-quadruplex in human telomerase RNA and promotes the formation of the P1 helix template boundary. *Nucleic Acids Res* **40(9)**:4110-4124.
60. Creacy SD, Routh ED, Iwamoto F, Nagamine Y, Akman SA and Vaughn JP. (2008). G4 resolvase 1 binds both DNA and RNA tetramolecular quadruplex with high affinity and is the major source of tetramolecular quadruplex G4-DNA and G4-RNA resolving activity in HeLa cell lysates. *J Biol Chem* **283(50)**:34626-34634.
61. Aratani S, Fujii R, Oishi T, Fujita H, Amano T, Ohshima T, Hagiwara M, Fukamizu A and Nakajima T. (2001). Dual roles of RNA helicase A in CREB-dependent transcription. *Mol Cell Biol* **21(14)**:4460-4469.
62. Lai F, Drakas R and Nishikura K. (1995). Mutagenic analysis of double-stranded RNA adenosine deaminase, a candidate enzyme for RNA editing of glutamate-gated ion channel transcripts. *J Biol Chem* **270(29)**:17098-17105.
63. Patel RC and Sen GC. (1992). Identification of the double-stranded RNA-binding domain of the human interferon-inducible protein kinase. *J Biol Chem* **267(11)**:7671-7676.
64. Zhang S, Herrmann C and Grosse F. (1999). Pre-mRNA and mRNA binding of human nuclear DNA helicase II (RNA helicase A). *J Cell Sci* **112 (Pt 7)**:1055-1064.
65. Pfaller R, Smythe C and Newport JW. (1991). Assembly/disassembly of the nuclear envelope membrane: cell cycle-dependent binding of nuclear membrane vesicles to chromatin in vitro. *Cell* **65(2)**:209-217.
66. Tang H, McDonald D, Middlesworth T, Hope TJ and Wong-Staal F. (1999). The carboxyl terminus of RNA helicase A contains a bidirectional nuclear transport domain. *Mol Cell Biol* **19(5)**:3540-3550.
67. Smith WA, Schurter BT, Wong-Staal F and David M. (2004). Arginine methylation of RNA helicase a determines its subcellular localization. *J Biol Chem* **279(22)**:22795-22798.
68. Chen ZX, Wallis K, Fell SM, Sobrado VR, Hemmer MC, Ramskold D, Hellman U, Sandberg R, Kenchappa RS, Martinson T, Johnsen JI, Kogner P and Schlisio S. (2014). RNA helicase A is a downstream mediator of KIF1Bbeta tumor-suppressor function in neuroblastoma. *Cancer Discov* **4(4)**:434-451.

69. Kudo N, Matsumori N, Taoka H, Fujiwara D, Schreiner EP, Wolff B, Yoshida M and Horinouchi S. (1999). Leptomycin B inactivates CRM1/exportin 1 by covalent modification at a cysteine residue in the central conserved region. *Proc Natl Acad Sci U S A* **96(16)**:9112-9117.
70. Wolff B, Sanglier JJ and Wang Y. (1997). Leptomycin B is an inhibitor of nuclear export: inhibition of nucleo-cytoplasmic translocation of the human immunodeficiency virus type 1 (HIV-1) Rev protein and Rev-dependent mRNA. *Chem Biol* **4(2)**:139-147.
71. Fujita H, Ohshima T, Oishi T, Aratani S, Fujii R, Fukamizu A and Nakajima T. (2005). Relevance of nuclear localization and functions of RNA helicase A. *Int J Mol Med* **15(4)**:555-560.
72. Fuchsova B and Hozak P. (2002). The localization of nuclear DNA helicase II in different nuclear compartments is linked to transcription. *Exp Cell Res* **279(2)**:260-270.
73. Liu Z, Kenworthy R, Green C and Tang H. (2007). Molecular determinants of nucleolar translocation of RNA helicase A. *Exp Cell Res* **313(17)**:3743-3754.
74. Zhang S, Kohler C, Hemmerich P and Grosse F. (2004). Nuclear DNA helicase II (RNA helicase A) binds to an F-actin containing shell that surrounds the nucleolus. *Exp Cell Res* **293(2)**:248-258.
75. Uhlen M, Fagerberg L, Hallstrom BM, Lindskog C, Oksvold P, Mardinoglu A, Sivertsson A, Kampf C, Sjostedt E, Asplund A, Olsson I, Edlund K, Lundberg E, Navani S, Szigyarto CA, Odeberg J, et al. (2015). Proteomics. Tissue-based map of the human proteome. *Science* **347(6220)**:1260419.
76. Uhlen M, Oksvold P, Fagerberg L, Lundberg E, Jonasson K, Forsberg M, Zwahlen M, Kampf C, Wester K, Hober S, Wernerus H, Bjorling L and Ponten F. (2010). Towards a knowledge-based Human Protein Atlas. *Nat Biotechnol* **28(12)**:1248-1250.
77. The human protein atlas. http://www.proteinatlas.org/ENSG00000135829-DHX9/tissue.
78. Schwanhausser B, Busse D, Li N, Dittmar G, Schuchhardt J, Wolf J, Chen W and Selbach M. (2011). Global quantification of mammalian gene expression control. *Nature* **473(7347)**:337-342.
79. Sandoval PC, Slentz DH, Pisitkun T, Saeed F, Hoffert JD and Knepper MA. (2013). Proteome-wide measurement of protein half-lives and translation rates in vasopressin-sensitive collecting duct cells. *J Am Soc Nephrol* **24(11)**:1793-1805.
80. Protein Half Lives in Renal mpkCCD Epithelial Cells (Single-Point Method). https://hpcwebapps.cit.nih.gov/ESBL/Database/ProteinHalfLives/singlepointPN.html.
81. Sharova LV, Sharov AA, Nedorezov T, Piao Y, Shaik N and Ko MS. (2009). Database for mRNA half-life of 19 977 genes obtained by DNA microarray analysis of pluripotent and differentiating mouse embryonic stem cells. *DNA Res* **16(1)**:45-58.
82. Erkizan HV, Kong Y, Merchant M, Schlottmann S, Barber-Rotenberg JS, Yuan L, Abaan OD, Chou TH, Dakshanamurthy S, Brown ML, Uren A and Toretsky JA. (2009). A small molecule blocking oncogenic protein EWS-FLI1 interaction with RNA helicase A inhibits growth of Ewing's sarcoma. *Nat Med* **15(7)**:750-756.
83. Fidaleo M, Svetoni F, Volpe E, Minana B, Caporossi D and Paronetto MP. (2015). Genotoxic stress inhibits Ewing sarcoma cell growth by modulating alternative pre-mRNA processing of the RNA helicase DHX9. *Oncotarget* **6(31)**:31740-31757.

84. Lee CG, da Costa Soares V, Newberger C, Manova K, Lacy E and Hurwitz J. (1998). RNA helicase A is essential for normal gastrulation. *Proc Natl Acad Sci U S A* **95(23)**:13709-13713.
85. Hoekstra EJ, Mesman S, de Munnik WA and Smidt MP. (2013). LMX1B is part of a transcriptional complex with PSPC1 and PSF. *PLoS One* **8(1)**:e53122.
86. Narva E, Rahkonen N, Emani MR, Lund R, Pursiheimo JP, Nasti J, Autio R, Rasool O, Denessiouk K, Lahdesmaki H, Rao A and Lahesmaa R. (2012). RNA-binding protein L1TD1 interacts with LIN28 via RNA and is required for human embryonic stem cell self-renewal and cancer cell proliferation. *Stem Cells* **30(3)**:452-460.
87. Powell SN and Kachnic LA. (2003). Roles of BRCA1 and BRCA2 in homologous recombination, DNA replication fidelity and the cellular response to ionizing radiation. *Oncogene* **22(37)**:5784-5791.
88. Ohta S, Shiomi Y, Sugimoto K, Obuse C and Tsurimoto T. (2002). A proteomics approach to identify proliferating cell nuclear antigen (PCNA)-binding proteins in human cell lysates. Identification of the human CHL12/RFCs2-5 complex as a novel PCNA-binding protein. *J Biol Chem* **277(43)**:40362-40367.
89. Loor G, Zhang SJ, Zhang P, Toomey NL and Lee MY. (1997). Identification of DNA replication and cell cycle proteins that interact with PCNA. *Nucleic Acids Res* **25(24)**:5041-5046.
90. Zhou K, Choe KT, Zaidi Z, Wang Q, Mathews MB and Lee CG. (2003). RNA helicase A interacts with dsDNA and topoisomerase IIalpha. *Nucleic Acids Res* **31(9)**:2253-2260.
91. Zhang S, Schlott B, Gorlach M and Grosse F. (2004). DNA-dependent protein kinase (DNA-PK) phosphorylates nuclear DNA helicase II/RNA helicase A and hnRNP proteins in an RNA-dependent manner. *Nucleic Acids Res* **32(1)**:1-10.
92. Rampakakis E, Di Paola D and Zannis-Hadjopoulos M. (2008). Ku is involved in cell growth, DNA replication and G1-S transition. *J Cell Sci* **121(Pt 5)**:590-600.
93. Friedemann J, Grosse F and Zhang S. (2005). Nuclear DNA helicase II (RNA helicase A) interacts with Werner syndrome helicase and stimulates its exonuclease activity. *J Biol Chem* **280(35)**:31303-31313.
94. Balakrishnan L and Bambara RA. (2013). Okazaki fragment metabolism. *Cold Spring Harb Perspect Biol* **5(2)**.
95. Petermann E and Helleday T. (2010). Pathways of mammalian replication fork restart. *Nat Rev Mol Cell Biol* **11(10)**:683-687.
96. Cooper MP, Machwe A, Orren DK, Brosh RM, Ramsden D and Bohr VA. (2000). Ku complex interacts with and stimulates the Werner protein. *Genes Dev* **14(8)**:907-912.
97. Rodriguez-Lopez AM, Jackson DA, Nehlin JO, Iborra F, Warren AV and Cox LS. (2003). Characterisation of the interaction between WRN, the helicase/exonuclease defective in progeroid Werner's syndrome, and an essential replication factor, PCNA. *Mech Ageing Dev* **124(2)**:167-174.
98. Jain A, Bacolla A, Del Mundo IM, Zhao J, Wang G and Vasquez KM. (2013). DHX9 helicase is involved in preventing genomic instability induced by alternatively structured DNA in human cells. *Nucleic Acids Res* **41(22)**:10345-10357.
99. Rhodes D and Lipps HJ. (2015). G-quadruplexes and their regulatory roles in biology. *Nucleic Acids Res* **43(18)**:8627-8637.

100. Machwe A, Xiao L and Orren DK. (2004). TRF2 recruits the Werner syndrome (WRN) exonuclease for processing of telomeric DNA. *Oncogene* **23(1)**:149-156.
101. Cayrou C, Gregoire D, Coulombe P, Danis E and Mechali M. (2012). Genome-scale identification of active DNA replication origins. *Methods* **57(2)**:158-164.
102. Cayrou C, Coulombe P, Vigneron A, Stanojcic S, Ganier O, Peiffer I, Rivals E, Puy A, Laurent-Chabalier S, Desprat R and Mechali M. (2011). Genome-scale analysis of metazoan replication origins reveals their organization in specific but flexible sites defined by conserved features. *Genome Res* **21(9)**:1438-1449.
103. Besnard E, Babled A, Lapasset L, Milhavet O, Parrinello H, Dantec C, Marin JM and Lemaitre JM. (2012). Unraveling cell type-specific and reprogrammable human replication origin signatures associated with G-quadruplex consensus motifs. *Nat Struct Mol Biol* **19(8)**:837-844.
104. Sarkies P, Reams C, Simpson LJ and Sale JE. (2010). Epigenetic instability due to defective replication of structured DNA. *Mol Cell* **40(5)**:703-713.
105. Mirkin SM. (2013). DNA replication: driving past four-stranded snags. *Nature* **497(7450)**:449-450.
106. Mischo HE, Hemmerich P, Grosse F and Zhang S. (2005). Actinomycin D induces histone gamma-H2AX foci and complex formation of gamma-H2AX with Ku70 and nuclear DNA helicase II. *J Biol Chem* **280(10)**:9586-9594.
107. Liu J, Song Y, Tian B, Qian J, Dong Y, Liu J, Liu B and Sun Z. (2010). Functional proteomic analysis of promyelocytic leukaemia nuclear bodies in irradiation-induced MCF-7 cells. *J Biochem* **148(6)**:659-667.
108. Fuchsova B, Novak P, Kafkova J and Hozak P. (2002). Nuclear DNA helicase II is recruited to IFN-alpha-activated transcription sites at PML nuclear bodies. *J Cell Biol* **158(3)**:463-473.
109. Hong Z, Jiang J, Lan L, Nakajima S, Kanno S, Koseki H and Yasui A. (2008). A polycomb group protein, PHF1, is involved in the response to DNA double-strand breaks in human cell. *Nucleic Acids Res* **36(9)**:2939-2947.
110. Steinmann-Zwicky M and Nothiger R. (1985). The hierarchical relation between X-chromosomes and autosomal sex determining genes in Drosophila. *EMBO J* **4(1)**:163-166.
111. Bridges CB. (1921). Triploid Intersexes in Drosophila Melanogaster. *Science* **54(1394)**:252-254.
112. Belote JM and Lucchesi JC. (1980). Control of X chromosome transcription by the maleless gene in Drosophila. *Nature* **285(5766)**:573-575.
113. Conrad T and Akhtar A. (2012). Dosage compensation in Drosophila melanogaster: epigenetic fine-tuning of chromosome-wide transcription. *Nat Rev Genet* **13(2)**:123-134.
114. Gorman M, Kuroda MI and Baker BS. (1993). Regulation of the sex-specific binding of the maleless dosage compensation protein to the male X chromosome in Drosophila. *Cell* **72(1)**:39-49.
115. Richter L, Bone JR and Kuroda MI. (1996). RNA-dependent association of the Drosophila maleless protein with the male X chromosome. *Genes Cells* **1(3)**:325-336.

116. Meller VH, Gordadze PR, Park Y, Chu X, Stuckenholz C, Kelley RL and Kuroda MI. (2000). Ordered assembly of roX RNAs into MSL complexes on the dosage-compensated X chromosome in Drosophila. *Curr Biol* **10(3)**:136-143.
117. Lee CG, Reichman TW, Baik T and Mathews MB. (2004). MLE functions as a transcriptional regulator of the roX2 gene. *J Biol Chem* **279(46)**:47740-47745.
118. Heard E and Disteche CM. (2006). Dosage compensation in mammals: fine-tuning the expression of the X chromosome. *Genes Dev* **20(14)**:1848-1867.
119. Gonzalez GA and Montminy MR. (1989). Cyclic AMP stimulates somatostatin gene transcription by phosphorylation of CREB at serine 133. *Cell* **59(4)**:675-680.
120. Nakajima T, Uchida C, Anderson SF, Lee CG, Hurwitz J, Parvin JD and Montminy M. (1997). RNA helicase A mediates association of CBP with RNA polymerase II. *Cell* **90(6)**:1107-1112.
121. Aratani S, Fujii R, Fujita H, Fukamizu A and Nakajima T. (2003). Aromatic residues are required for RNA helicase A mediated transactivation. *Int J Mol Med* **12(2)**:175-180.
122. Aratani S, Kageyama Y, Nakamura A, Fujita H, Fujii R, Nishioka K and Nakajima T. (2008). MLE activates transcription via the minimal transactivation domain in Drosophila. *Int J Mol Med* **21(4)**:469-476.
123. Starita LM and Parvin JD. (2003). The multiple nuclear functions of BRCA1: transcription, ubiquitination and DNA repair. *Curr Opin Cell Biol* **15(3)**:345-350.
124. Anderson SF, Schlegel BP, Nakajima T, Wolpin ES and Parvin JD. (1998). BRCA1 protein is linked to the RNA polymerase II holoenzyme complex via RNA helicase A. *Nat Genet* **19(3)**:254-256.
125. Hofmann WA, Stojiljkovic L, Fuchsova B, Vargas GM, Mavrommatis E, Philimonenko V, Kysela K, Goodrich JA, Lessard JL, Hope TJ, Hozak P and de Lanerolle P. (2004). Actin is part of pre-initiation complexes and is necessary for transcription by RNA polymerase II. *Nat Cell Biol* **6(11)**:1094-1101.
126. Tang W, You W, Shi F, Qi T, Wang L, Djouder Z, Liu W and Zeng X. (2009). RNA helicase A acts as a bridging factor linking nuclear beta-actin with RNA polymerase II. *Biochem J* **420(3)**:421-428.
127. Tetsuka T, Uranishi H, Sanda T, Asamitsu K, Yang JP, Wong-Staal F and Okamoto T. (2004). RNA helicase A interacts with nuclear factor kappaB p65 and functions as a transcriptional coactivator. *Eur J Biochem* **271(18)**:3741-3751.
128. Gerritsen ME, Williams AJ, Neish AS, Moore S, Shi Y and Collins T. (1997). CREB-binding protein/p300 are transcriptional coactivators of p65. *Proc Natl Acad Sci U S A* **94(7)**:2927-2932.
129. Kitagawa H, Yanagisawa J, Fuse H, Ogawa S, Yogiashi Y, Okuno A, Nagasawa H, Nakajima T, Matsumoto T and Kato S. (2002). Ligand-selective potentiation of rat mineralocorticoid receptor activation function 1 by a CBP-containing histone acetyltransferase complex. *Mol Cell Biol* **22(11)**:3698-3706.
130. Fujita H, Fujii R, Aratani S, Amano T, Fukamizu A and Nakajima T. (2003). Antithetic effects of MBD2a on gene regulation. *Mol Cell Biol* **23(8)**:2645-2657.
131. Argasinska J, Zhou K, Donnelly RJ, Hay RT and Lee CG. (2004). A functional interaction between RHA and Ubc9, an E2-like enzyme specific for Sumo-1. *J Mol Biol* **341(1)**:15-25.

132. Amorim BR, Okamura H, Yoshida K, Qiu L, Morimoto H and Haneji T. (2007). The transcriptional factor Osterix directly interacts with RNA helicase A. *Biochem Biophys Res Commun* **355(2)**:347-351.
133. Reichman TW, Parrott AM, Fierro-Monti I, Caron DJ, Kao PN, Lee CG, Li H and Mathews MB. (2003). Selective regulation of gene expression by nuclear factor 110, a member of the NF90 family of double-stranded RNA-binding proteins. *J Mol Biol* **332(1)**:85-98.
134. Ishiguro A, Ideta M, Mikoshiba K, Chen DJ and Aruga J. (2007). ZIC2-dependent transcriptional regulation is mediated by DNA-dependent protein kinase, poly(ADP-ribose) polymerase, and RNA helicase A. *J Biol Chem* **282(13)**:9983-9995.
135. Myohanen S and Baylin SB. (2001). Sequence-specific DNA binding activity of RNA helicase A to the p16INK4a promoter. *J Biol Chem* **276(2)**:1634-1642.
136. Zhong X and Safa AR. (2004). RNA helicase A in the MEF1 transcription factor complex up-regulates the MDR1 gene in multidrug-resistant cancer cells. *J Biol Chem* **279(17)**:17134-17141.
137. Lin SY, Makino K, Xia W, Matin A, Wen Y, Kwong KY, Bourguignon L and Hung MC. (2001). Nuclear localization of EGF receptor and its potential new role as a transcription factor. *Nat Cell Biol* **3(9)**:802-808.
138. Huo L, Wang YN, Xia W, Hsu SC, Lai CC, Li LY, Chang WC, Wang Y, Hsu MC, Yu YL, Huang TH, Ding Q, Chen CH, Tsai CH and Hung MC. (2010). RNA helicase A is a DNA-binding partner for EGFR-mediated transcriptional activation in the nucleus. *Proc Natl Acad Sci U S A* **107(37)**:16125-16130.
139. Liu M, Roth A, Yu M, Morris R, Bersani F, Rivera MN, Lu J, Shioda T, Vasudevan S, Ramaswamy S, Maheswaran S, Diederichs S and Haber DA. (2013). The IGF2 intronic miR-483 selectively enhances transcription from IGF2 fetal promoters and enhances tumorigenesis. *Genes Dev* **27(23)**:2543-2548.
140. Sadler AJ, Latchoumanin O, Hawkes D, Mak J and Williams BR. (2009). An antiviral response directed by PKR phosphorylation of the RNA helicase A. *PLoS Pathog* **5(2)**:e1000311.
141. Fujii R, Okamoto M, Aratani S, Oishi T, Ohshima T, Taira K, Baba M, Fukamizu A and Nakajima T. (2001). A Role of RNA Helicase A in cis-Acting Transactivation Response Element-mediated Transcriptional Regulation of Human Immunodeficiency Virus Type 1. *J Biol Chem* **276(8)**:5445-5451.
142. Colla E, Lee SD, Sheen MR, Woo SK and Kwon HM. (2006). TonEBP is inhibited by RNA helicase A via interaction involving the E'F loop. *Biochem J* **393(Pt 1)**:411-419.
143. Sonenberg N. (1993). Remarks on the mechanism of ribosome binding to eukaryotic mRNAs. *Gene Expr* **3(3)**:317-323.
144. Pause A, Methot N, Svitkin Y, Merrick WC and Sonenberg N. (1994). Dominant negative mutants of mammalian translation initiation factor eIF-4A define a critical role for eIF-4F in cap-dependent and cap-independent initiation of translation. *EMBO J* **13(5)**:1205-1215.
145. Rozen F, Edery I, Meerovitch K, Dever TE, Merrick WC and Sonenberg N. (1990). Bidirectional RNA helicase activity of eucaryotic translation initiation factors 4A and 4F. *Mol Cell Biol* **10(3)**:1134-1144.

146. Butsch M, Hull S, Wang Y, Roberts TM and Boris-Lawrie K. (1999). The 5' RNA terminus of spleen necrosis virus contains a novel posttranscriptional control element that facilitates human immunodeficiency virus Rev/RRE-independent Gag production. *J Virol* **73(6)**:4847-4855.
147. Roberts TM and Boris-Lawrie K. (2003). Primary sequence and secondary structure motifs in spleen necrosis virus RU5 confer translational utilization of unspliced human immunodeficiency virus type 1 reporter RNA. *J Virol* **77(22)**:11973-11984.
148. Hartman TR, Qian S, Bolinger C, Fernandez S, Schoenberg DR and Boris-Lawrie K. (2006). RNA helicase A is necessary for translation of selected messenger RNAs. *Nat Struct Mol Biol* **13(6)**:509-516.
149. Ranji A, Shkriabai N, Kvaratskhelia M, Musier-Forsyth K and Boris-Lawrie K. (2011). Features of double-stranded RNA-binding domains of RNA helicase A are necessary for selective recognition and translation of complex mRNAs. *J Biol Chem* **286(7)**:5328-5337.
150. Bolinger C, Sharma A, Singh D, Yu L and Boris-Lawrie K. (2010). RNA helicase A modulates translation of HIV-1 and infectivity of progeny virions. *Nucleic Acids Res* **38(5)**:1686-1696.
151. Cai L, Fritz D, Stefanovic L and Stefanovic B. (2010). Binding of LARP6 to the conserved 5' stem-loop regulates translation of mRNAs encoding type I collagen. *J Mol Biol* **395(2)**:309-326.
152. Manojlovic Z and Stefanovic B. (2012). A novel role of RNA helicase A in regulation of translation of type I collagen mRNAs. *RNA* **18(2)**:321-334.
153. Newman MA, Thomson JM and Hammond SM. (2008). Lin-28 interaction with the Let-7 precursor loop mediates regulated microRNA processing. *RNA* **14(8)**:1539-1549.
154. Xu B, Zhang K and Huang Y. (2009). Lin28 modulates cell growth and associates with a subset of cell cycle regulator mRNAs in mouse embryonic stem cells. *RNA* **15(3)**:357-361.
155. Qiu C, Ma Y, Wang J, Peng S and Huang Y. (2010). Lin28-mediated post-transcriptional regulation of Oct4 expression in human embryonic stem cells. *Nucleic Acids Res* **38(4)**:1240-1248.
156. Xu B and Huang Y. (2009). Histone H2a mRNA interacts with Lin28 and contains a Lin28-dependent posttranscriptional regulatory element. *Nucleic Acids Res* **37(13)**:4256-4263.
157. Polesskaya A, Cuvellier S, Naguibneva I, Duquet A, Moss EG and Harel-Bellan A. (2007). Lin-28 binds IGF-2 mRNA and participates in skeletal myogenesis by increasing translation efficiency. *Genes Dev* **21(9)**:1125-1138.
158. Jin J, Jing W, Lei XX, Feng C, Peng S, Boris-Lawrie K and Huang Y. (2011). Evidence that Lin28 stimulates translation by recruiting RNA helicase A to polysomes. *Nucleic Acids Res* **39(9)**:3724-3734.
159. Grover R, Candeias MM, Fahraeus R and Das S. (2009). p53 and little brother p53/47: linking IRES activities with protein functions. *Oncogene* **28(30)**:2766-2772.
160. Halaby MJ and Yang DQ. (2007). p53 translational control: a new facet of p53 regulation and its implication for tumorigenesis and cancer therapeutics. *Gene* **395(1-2)**:1-7.
161. Giaccia AJ and Kastan MB. (1998). The complexity of p53 modulation: emerging patterns from divergent signals. *Genes Dev* **12(19)**:2973-2983.

162. Ray PS, Grover R and Das S. (2006). Two internal ribosome entry sites mediate the translation of p53 isoforms. *EMBO Rep* **7(4)**:404-410.
163. Yang DQ, Halaby MJ and Zhang Y. (2006). The identification of an internal ribosomal entry site in the 5'-untranslated region of p53 mRNA provides a novel mechanism for the regulation of its translation following DNA damage. *Oncogene* **25(33)**:4613-4619.
164. Halaby MJ, Li Y, Harris BR, Jiang S, Miskimins WK, Cleary MP and Yang DQ. (2015). Translational Control Protein 80 Stimulates IRES-Mediated Translation of p53 mRNA in Response to DNA Damage. *Biomed Res Int* **2015**:708158.
165. Halaby MJ, Harris BR, Miskimins WK, Cleary MP and Yang DQ. (2015). Deregulation of Internal Ribosome Entry Site-Mediated p53 Translation in Cancer Cells with Defective p53 Response to DNA Damage. *Mol Cell Biol* **35(23)**:4006-4017.
166. Kim VN. (2005). MicroRNA biogenesis: coordinated cropping and dicing. *Nat Rev Mol Cell Biol* **6(5)**:376-385.
167. Cullen BR. (2004). Transcription and processing of human microRNA precursors. *Mol Cell* **16(6)**:861-865.
168. Ambros V. (2004). The functions of animal microRNAs. *Nature* **431(7006)**:350-355.
169. Pratt AJ and MacRae IJ. (2009). The RNA-induced silencing complex: a versatile gene-silencing machine. *J Biol Chem* **284(27)**:17897-17901.
170. Kawai S and Amano A. (2012). BRCA1 regulates microRNA biogenesis via the DROSHA microprocessor complex. *J Cell Biol* **197(2)**:201-208.
171. Robb GB and Rana TM. (2007). RNA helicase A interacts with RISC in human cells and functions in RISC loading. *Mol Cell* **26(4)**:523-537.
172. Hartmuth K, Urlaub H, Vornlocher HP, Will CL, Gentzel M, Wilm M and Luhrmann R. (2002). Protein composition of human prespliceosomes isolated by a tobramycin affinity-selection method. *Proc Natl Acad Sci U S A* **99(26)**:16719-16724.
173. Paul S, Dansithong W, Jog SP, Holt I, Mittal S, Brook JD, Morris GE, Comai L and Reddy S. (2011). Expanded CUG repeats Dysregulate RNA splicing by altering the stoichiometry of the muscleblind 1 complex. *J Biol Chem* **286(44)**:38427-38438.
174. Pellizzoni L, Charroux B, Rappsilber J, Mann M and Dreyfuss G. (2001). A functional interaction between the survival motor neuron complex and RNA polymerase II. *J Cell Biol* **152(1)**:75-85.
175. Terns MP and Terns RM. (2001). Macromolecular complexes: SMN--the master assembler. *Curr Biol* **11(21)**:R862-864.
176. Pellizzoni L, Baccon J, Charroux B and Dreyfuss G. (2001). The survival of motor neurons (SMN) protein interacts with the snoRNP proteins fibrillarin and GAR1. *Curr Biol* **11(14)**:1079-1088.
177. Bratt E and Ohman M. (2003). Coordination of editing and splicing of glutamate receptor pre-mRNA. *RNA* **9(3)**:309-318.
178. Reenan RA, Hanrahan CJ and Ganetzky B. (2000). The mle(napts) RNA helicase mutation in drosophila results in a splicing catastrophe of the para Na+ channel transcript in a region of RNA editing. *Neuron* **25(1)**:139-149.
179. Kernan MJ, Kuroda MI, Kreber R, Baker BS and Ganetzky B. (1991). napts, a mutation affecting sodium channel activity in Drosophila, is an allele of mle, a regulator of X chromosome transcription. *Cell* **66(5)**:949-959.

180. Zhang S, Buder K, Burkhardt C, Schlott B, Gorlach M and Grosse F. (2002). Nuclear DNA helicase II/RNA helicase A binds to filamentous actin. *J Biol Chem* **277(1)**:843-853.
181. Shumaker DK, Kuczmarski ER and Goldman RD. (2003). The nucleoskeleton: lamins and actin are major players in essential nuclear functions. *Curr Opin Cell Biol* **15(3)**:358-366.
182. Tang H, Gaietta GM, Fischer WH, Ellisman MH and Wong-Staal F. (1997). A cellular cofactor for the constitutive transport element of type D retrovirus. *Science* **276(5317)**:1412-1415.
183. Tang H and Wong-Staal F. (2000). Specific interaction between RNA helicase A and Tap, two cellular proteins that bind to the constitutive transport element of type D retrovirus. *J Biol Chem* **275(42)**:32694-32700.
184. Yang JP, Tang H, Reddy TR and Wong-Staal F. (2001). Mapping the functional domains of HAP95, a protein that binds RNA helicase A and activates the constitutive transport element of type D retroviruses. *J Biol Chem* **276(33)**:30694-30700.
185. Westberg C, Yang JP, Tang H, Reddy TR and Wong-Staal F. (2000). A novel shuttle protein binds to RNA helicase A and activates the retroviral constitutive transport element. *J Biol Chem* **275(28)**:21396-21401.
186. Xing L, Niu M and Kleiman L. (2012). In vitro and in vivo analysis of the interaction between RNA helicase A and HIV-1 RNA. *J Virol* **86(24)**:13272-13280.
187. Wodrich H, Schambach A and Krausslich HG. (2000). Multiple copies of the Mason-Pfizer monkey virus constitutive RNA transport element lead to enhanced HIV-1 Gag expression in a context-dependent manner. *Nucleic Acids Res* **28(4)**:901-910.
188. Li J, Tang H, Mullen TM, Westberg C, Reddy TR, Rose DW and Wong-Staal F. (1999). A role for RNA helicase A in post-transcriptional regulation of HIV type 1. *Proc Natl Acad Sci U S A* **96(2)**:709-714.
189. Reddy TR, Tang H, Xu W and Wong-Staal F. (2000). Sam68, RNA helicase A and Tap cooperate in the post-transcriptional regulation of human immunodeficiency virus and type D retroviral mRNA. *Oncogene* **19(32)**:3570-3575.
190. Rahman MM, Liu J, Chan WM, Rothenburg S and McFadden G. (2013). Myxoma virus protein M029 is a dual function immunomodulator that inhibits PKR and also conscripts RHA/DHX9 to promote expanded host tropism and viral replication. *PLoS Pathog* **9(7)**:e1003465.
191. Lin L, Li Y, Pyo HM, Lu X, Raman SN, Liu Q, Brown EG and Zhou Y. (2012). Identification of RNA helicase A as a cellular factor that interacts with influenza A virus NS1 protein and its role in the virus life cycle. *J Virol* **86(4)**:1942-1954.
192. Toretsky JA, Erkizan V, Levenson A, Abaan OD, Parvin JD, Cripe TP, Rice AM, Lee SB and Uren A. (2006). Oncoprotein EWS-FLI1 activity is enhanced by RNA helicase A. *Cancer Res* **66(11)**:5574-5581.
193. Wilson BJ and Giguere V. (2007). Identification of novel pathway partners of p68 and p72 RNA helicases through Oncomine meta-analysis. *BMC Genomics* **8**:419.
194. Zhang Z, Yuan B, Lu N, Facchinetti V and Liu YJ. (2011). DHX9 pairs with IPS-1 to sense double-stranded RNA in myeloid dendritic cells. *J Immunol* **187(9)**:4501-4508.

195. Scharer CD, McCabe CD, Ali-Seyed M, Berger MF, Bulyk ML and Moreno CS. (2009). Genome-wide promoter analysis of the SOX4 transcriptional network in prostate cancer cells. *Cancer Res* **69(2)**:709-717.
196. Lai YH, Cheng J, Cheng D, Feasel ME, Beste KD, Peng J, Nusrat A and Moreno CS. (2011). SOX4 interacts with plakoglobin in a Wnt3a-dependent manner in prostate cancer cells. *BMC Cell Biol* **12**:50.
197. Ambs S, Prueitt RL, Yi M, Hudson RS, Howe TM, Petrocca F, Wallace TA, Liu CG, Volinia S, Calin GA, Yfantis HG, Stephens RM and Croce CM. (2008). Genomic profiling of microRNA and messenger RNA reveals deregulated microRNA expression in prostate cancer. *Cancer Res* **68(15)**:6162-6170.
198. Wei X, Pacyna-Gengelbach M, Schluns K, An Q, Gao Y, Cheng S and Petersen I. (2004). Analysis of the RNA helicase A gene in human lung cancer. *Oncol Rep* **11(1)**:253-258.
199. Sun Z, Wang L, Eckloff BW, Deng B, Wang Y, Wampfler JA, Jang J, Wieben ED, Jen J, You M and Yang P. (2014). Conserved recurrent gene mutations correlate with pathway deregulation and clinical outcomes of lung adenocarcinoma in never-smokers. *BMC Med Genomics* **7**:32.
200. Normanno N, De Luca A, Bianco C, Strizzi L, Mancino M, Maiello MR, Carotenuto A, De Feo G, Caponigro F and Salomon DS. (2006). Epidermal growth factor receptor (EGFR) signaling in cancer. *Gene* **366(1)**:2-16.
201. Masuda H, Zhang D, Bartholomeusz C, Doihara H, Hortobagyi GN and Ueno NT. (2012). Role of epidermal growth factor receptor in breast cancer. *Breast Cancer Res Treat* **136(2)**:331-345.
202. Veale D, Ashcroft T, Marsh C, Gibson GJ and Harris AL. (1987). Epidermal growth factor receptors in non-small cell lung cancer. *Br J Cancer* **55(5)**:513-516.
203. Libermann TA, Nusbaum HR, Razon N, Kris R, Lax I, Soreq H, Whittle N, Waterfield MD, Ullrich A and Schlessinger J. (1985). Amplification and overexpression of the EGF receptor gene in primary human glioblastomas. *J Cell Sci Suppl* **3**:161-172.
204. Schlegel BP, Starita LM and Parvin JD. (2003). Overexpression of a protein fragment of RNA helicase A causes inhibition of endogenous BRCA1 function and defects in ploidy and cytokinesis in mammary epithelial cells. *Oncogene* **22(7)**:983-991.
205. Guenard F, Labrie Y, Ouellette G, Beauparlant CJ, Durocher F and BRCAs I. (2009). Genetic sequence variations of BRCA1-interacting genes AURKA, BAP1, BARD1 and DHX9 in French Canadian families with high risk of breast cancer. *J Hum Genet* **54(3)**:152-161.
206. Zucchini C, Rocchi A, Manara MC, De Sanctis P, Capanni C, Bianchini M, Carinci P, Scotlandi K and Valvassori L. (2008). Apoptotic genes as potential markers of metastatic phenotype in human osteosarcoma cell lines. *Int J Oncol* **32(1)**:17-31.
207. Roy BB, Hu J, Guo X, Russell RS, Guo F, Kleiman L and Liang C. (2006). Association of RNA helicase a with human immunodeficiency virus type 1 particles. *J Biol Chem* **281(18)**:12625-12635.
208. Xing L, Niu M, Zhao X and Kleiman L. (2013). Roles of the linker region of RNA helicase A in HIV-1 RNA metabolism. *PLoS One* **8(11)**:e78596.

209. He QS, Tang H, Zhang J, Truong K, Wong-Staal F and Zhou D. (2008). Comparisons of RNAi approaches for validation of human RNA helicase A as an essential factor in hepatitis C virus replication. *J Virol Methods* **154(1-2)**:216-219.
210. Lenarcic EM, Ziehr BJ and Moorman NJ. (2015). An unbiased proteomics approach to identify human cytomegalovirus RNA-associated proteins. *Virology* **481**:13-23.
211. Liao HJ, Kobayashi R and Mathews MB. (1998). Activities of adenovirus virus-associated RNAs: purification and characterization of RNA binding proteins. *Proc Natl Acad Sci U S A* **95(15)**:8514-8519.
212. Paingankar MS and Arankalle VA. (2015). Identification and characterization of cellular proteins interacting with Hepatitis E virus untranslated regions. *Virus Res* **208**:98-109.
213. Sheng C, Yao Y, Chen B, Wang Y, Chen J and Xiao M. (2013). RNA helicase is involved in the expression and replication of classical swine fever virus and interacts with untranslated region. *Virus Res* **171(1)**:257-261.
214. Lawrence P and Rieder E. (2009). Identification of RNA helicase A as a new host factor in the replication cycle of foot-and-mouth disease virus. *J Virol* **83(21)**:11356-11366.
215. Sato H, Oshiumi H, Takaki H, Hikono H and Seya T. (2015). Evolution of the DEAD box helicase family in chicken: chickens have no DHX9 ortholog. *Microbiol Immunol* **59(10)**:633-640.
216. Barber MR, Aldridge JR, Jr., Webster RG and Magor KE. (2010). Association of RIG-I with innate immunity of ducks to influenza. *Proc Natl Acad Sci U S A* **107(13)**:5913-5918.
217. Rahman A and Isenberg DA. (2008). Systemic lupus erythematosus. *N Engl J Med* **358(9)**:929-939.
218. Takeda Y, Caudell P, Grady G, Wang G, Suwa A, Sharp GC, Dynan WS and Hardin JA. (1999). Human RNA helicase A is a lupus autoantigen that is cleaved during apoptosis. *J Immunol* **163(11)**:6269-6274.
219. Yamasaki Y, Narain S, Yoshida H, Hernandez L, Barker T, Hahn PC, Sobel ES, Segal MS, Richards HB, Chan EK, Reeves WH and Satoh M. (2007). Autoantibodies to RNA helicase A: a new serologic marker of early lupus. *Arthritis Rheum* **56(2)**:596-604.
220. Vazquez-Del Mercado M, Palafox-Sanchez CA, Munoz-Valle JF, Orozco-Barocio G, Oregon-Romero E, Navarro-Hernandez RE, Salazar-Paramo M, Armendariz-Borunda J, Gamez-Nava JI, Gonzalez-Lopez L, Chan JY, Chan EK and Satoh M. (2010). High prevalence of autoantibodies to RNA helicase A in Mexican patients with systemic lupus erythematosus. *Arthritis Res Ther* **12(1)**:R6.
221. Lane DP. (1992). Cancer. p53, guardian of the genome. *Nature* **358(6381)**:15-16.
222. Vogelstein B, Lane D and Levine AJ. (2000). Surfing the p53 network. *Nature* **408(6810)**:307-310.
223. Hainaut P, Soussi T, Shomer B, Hollstein M, Greenblatt M, Hovig E, Harris CC and Montesano R. (1997). Database of p53 gene somatic mutations in human tumors and cell lines: updated compilation and future prospects. *Nucleic Acids Res* **25(1)**:151-157.
224. Belyi VA, Ak P, Markert E, Wang H, Hu W, Puzio-Kuter A and Levine AJ. (2010). The origins and evolution of the p53 family of genes. *Cold Spring Harb Perspect Biol* **2(6)**:a001198.

225. Laptenko O and Prives C. (2006). Transcriptional regulation by p53: one protein, many possibilities. *Cell Death Differ* **13(6)**:951-961.
226. Vousden KH and Lu X. (2002). Live or let die: the cell's response to p53. *Nat Rev Cancer* **2(8)**:594-604.
227. Vousden KH and Prives C. (2009). Blinded by the Light: The Growing Complexity of p53. *Cell* **137(3)**:413-431.
228. Fang SY, Jensen JP, Ludwig RL, Vousden KH and Weissman AM. (2000). Mdm2 is a RING finger-dependent ubiquitin protein ligase for itself and p53. *J Biol Chem* **275(12)**:8945-8951.
229. Gu J, Nie L, Wiederschain D and Yuan ZM. (2001). Identification of p53 sequence elements that are required for MDM2-mediated nuclear export. *Mol Cell Biol* **21(24)**:8533-8546.
230. Ringshausen I, O'Shea CC, Finch AJ, Swigart LB and Evan GI. (2006). Mdm2 is critically and continuously required to suppress lethal p53 activity in vivo. *Cancer cell* **10(6)**:501-514.
231. Rodriguez MS, Desterro JM, Lain S, Lane DP and Hay RT. (2000). Multiple C-terminal lysine residues target p53 for ubiquitin-proteasome-mediated degradation. *Mol Cell Biol* **20(22)**:8458-8467.
232. Barak Y, Juven T, Haffner R and Oren M. (1993). Mdm2 Expression Is Induced by Wild Type-P53 Activity. *Embo Journal* **12(2)**:461-468.
233. Eischen CM, Weber JD, Roussel MF, Sherr CJ and Cleveland JL. (1999). Disruption of the ARF-Mdm2-p53 tumor suppressor pathway in Myc-induced lymphomagenesis. *Genes Dev* **13(20)**:2658-2669.
234. Zeng Y, Kotake Y, Pei XH, Smith MD and Xiong Y. (2011). p53 binds to and is required for the repression of Arf tumor suppressor by HDAC and polycomb. *Cancer Res* **71(7)**:2781-2792.
235. Harris SL and Levine AJ. (2005). The p53 pathway: positive and negative feedback loops. *Oncogene* **24(17)**:2899-2908.
236. Appella E and Anderson CW. (2001). Post-translational modifications and activation of p53 by genotoxic stresses. *Eur J Biochem* **268(10)**:2764-2772.
237. Canman CE, Lim DS, Cimprich KA, Taya Y, Tamai K, Sakaguchi K, Appella E, Kastan MB and Siliciano JD. (1998). Activation of the ATM kinase by ionizing radiation and phosphorylation of p53. *Science* **281(5383)**:1677-1679.
238. Hirao A, Kong YY, Matsuoka S, Wakeham A, Ruland J, Yoshida H, Liu D, Elledge SJ and Mak TW. (2000). DNA damage-induced activation of p53 by the checkpoint kinase Chk2. *Science* **287(5459)**:1824-1827.
239. Tibbetts RS, Brumbaugh KM, Williams JM, Sarkaria JN, Cliby WA, Shieh SY, Taya Y, Prives C and Abraham RT. (1999). A role for ATR in the DNA damage-induced phosphorylation of p53. *Genes Dev* **13(2)**:152-157.
240. Cuadrado A, Lafarga V, Cheung PC, Dolado I, Llanos S, Cohen P and Nebreda AR. (2007). A new p38 MAP kinase-regulated transcriptional coactivator that stimulates p53-dependent apoptosis. *EMBO J* **26(8)**:2115-2126.

241. Perfettini JL, Castedo M, Nardacci R, Ciccosanti F, Boya P, Roumier T, Larochette N, Piacentini M and Kroemer G. (2005). Essential role of p53 phosphorylation by p38 MAPK in apoptosis induction by the HIV-1 envelope. *J Exp Med* **201(2)**:279-289.
242. Shieh SY, Ikeda M, Taya Y and Prives C. (1997). DNA damage-induced phosphorylation of p53 alleviates inhibition by MDM2. *Cell* **91(3)**:325-334.
243. Unger T, Juven-Gershon T, Moallem E, Berger M, Vogt Sionov R, Lozano G, Oren M and Haupt Y. (1999). Critical role for Ser20 of human p53 in the negative regulation of p53 by Mdm2. *EMBO J* **18(7)**:1805-1814.
244. Lambert PF, Kashanchi F, Radonovich MF, Shiekhattar R and Brady JN. (1998). Phosphorylation of p53 serine 15 increases interaction with CBP. *J Biol Chem* **273(49)**:33048-33053.
245. Dumaz N and Meek DW. (1999). Serine15 phosphorylation stimulates p53 transactivation but does not directly influence interaction with HDM2. *EMBO J* **18**:7002-7010.
246. Ito A, Lai CH, Zhao X, Saito S, Hamilton MH, Appella E and Yao TP. (2001). p300/CBP-mediated p53 acetylation is commonly induced by p53-activating agents and inhibited by MDM2. *EMBO J* **20(6)**:1331-1340.
247. Gu W and Roeder RG. (1997). Activation of p53 sequence-specific DNA binding by acetylation of the p53 C-terminal domain. *Cell* **90(4)**:595-606.
248. Hammond EM and Giaccia AJ. (2005). The role of p53 in hypoxia-induced apoptosis. *Biochem Biophys Res Commun* **331(3)**:718-725.
249. Roe JS, Kim H, Lee SM, Kim ST, Cho EJ and Youn HD. (2006). p53 stabilization and transactivation by a von Hippel-Lindau protein. *Mol Cell* **22(3)**:395-405.
250. de Stanchina E, McCurrach ME, Zindy F, Shieh SY, Ferbeyre G, Samuelson AV, Prives C, Roussel MF, Sherr CJ and Lowe SW. (1998). E1A signaling to p53 involves the p19(ARF) tumor suppressor. *Genes Dev* **12(15)**:2434-2442.
251. Zindy F, Eischen CM, Randle DH, Kamijo T, Cleveland JL, Sherr CJ and Roussel MF. (1998). Myc signaling via the ARF tumor suppressor regulates p53-dependent apoptosis and immortalization. *Genes Dev* **12(15)**:2424-2433.
252. Sherr CJ. (2006). Divorcing ARF and p53: an unsettled case. *Nat Rev Cancer* **6(9)**:663-673.
253. Kahyo T, Nishida T and Yasuda H. (2001). Involvement of PIAS1 in the sumoylation of tumor suppressor p53. *Mol Cell* **8(3)**:713-718.
254. Megidish T, Xu JH and Xu CW. (2002). Activation of p53 by protein inhibitor of activated Stat1 (PIAS1). *J Biol Chem* **277(10)**:8255-8259.
255. Schmidt D and Muller S. (2002). Members of the PIAS family act as SUMO ligases for c-Jun and p53 and repress p53 activity. *Proc Natl Acad Sci USA* **99**:2872-2877.
256. Watson IR and Irwin MS. (2006). Ubiquitin and ubiquitin-like modifications of the p53 family. *Neoplasia* **8(8)**:655-666.
257. Xirodimas DP, Saville MK, Bourdon JC, Hay RT and Lane DP. (2004). Mdm2-mediated NEDD8 conjugation of p53 inhibits its transcriptional activity. *Cell* **118(1)**:83-97.
258. Abida WM, Nikolaev A, Zhao W, Zhang W and Gu W. (2006). FBXO11 promotes the neddylation of p53 and inhibits its transcriptional activity.

259. Chuikov S, Kurash JK, Wilson JR, Xiao B, Justin N, Ivanov GS, McKinney K, Tempst P, Prives C, Gamblin SJ, Barlev NA and Reinberg D. (2004). Regulation of p53 activity through lysine methylation. *Nature* **432(7015)**:353-360.
260. Ivanov GS, Ivanova T, Kurash J, Ivanov A, Chuikov S, Gizatullin F, Herrera-Medina EM, Rauscher F, 3rd, Reinberg D and Barlev NA. (2007). Methylation-acetylation interplay activates p53 in response to DNA damage. *Mol Cell Biol* **27(19)**:6756-6769.
261. Jansson M, Durant ST, Cho EC, Sheahan S, Edelmann M, Kessler B and La Thangue NB. (2008). Arginine methylation regulates the p53 response. *Nat Cell Biol* **10(12)**:1431-1439.
262. Pradhan S, Chin HG, Esteve PO and Jacobsen SE. (2009). SET7/9 mediated methylation of non-histone proteins in mammalian cells. *Epigenetics* **4(6)**:383-387.
263. Shi X, Kachirskaia I, Yamaguchi H, West LE, Wen H, Wang EW, Dutta S, Appella E and Gozani O. (2007). Modulation of p53 function by SET8-mediated methylation at lysine 382. *Mol Cell* **27(4)**:636-646.
264. Kitayner M, Rozenberg H, Kessler N, Rabinovich D, Shaulov L, Haran TE and Shakked Z. (2006). Structural basis of DNA recognition by p53 tetramers. *Mol Cell* **22(6)**:741-753.
265. McLure KG and Lee PW. (1998). How p53 binds DNA as a tetramer. *EMBO J* **17(12)**:3342-3350.
266. el-Deiry WS, Kern SE, Pietenpol JA, Kinzler KW and Vogelstein B. (1992). Definition of a consensus binding site for p53. *Nat Genet* **1(1)**:45-49.
267. Funk WD, Pak DT, Karas RH, Wright WE and Shay JW. (1992). A transcriptionally active DNA-binding site for human p53 protein complexes. *Mol Cell Biol* **12(6)**:2866-2871.
268. Gevry N, Chan HM, Laflamme L, Livingston DM and Gaudreau L. (2007). p21 transcription is regulated by differential localization of histone H2A.Z. *Genes Dev* **21(15)**:1869-1881.
269. Khoo KH, Verma CS and Lane DP. (2014). Drugging the p53 pathway: understanding the route to clinical efficacy. *Nat Rev Drug Discov* **13(3)**:217-236.
270. Ho J and Benchimol S. (2003). Transcriptional repression mediated by the p53 tumour suppressor. *Cell Death Differ* **10(4)**:404-408.
271. Murphy M, Ahn J, Walker KK, Hoffman WH, Evans RM, Levine AJ and George DL. (1999). Transcriptional repression by wild-type p53 utilizes histone deacetylases, mediated by interaction with mSin3a. *Genes Dev* **13(19)**:2490-2501.
272. Hoffman WH, Biade S, Zilfou JT, Chen J and Murphy M. (2002). Transcriptional repression of the anti-apoptotic survivin gene by wild type p53. *J Biol Chem* **277(5)**:3247-3257.
273. Murphy M, Hinman A and Levine AJ. (1996). Wild-type p53 negatively regulates the expression of a microtubule-associated protein. *Genes Dev* **10(23)**:2971-2980.
274. Lin T, Chao C, Saito S, Mazur SJ, Murphy ME, Appella E and Xu Y. (2005). p53 induces differentiation of mouse embryonic stem cells by suppressing Nanog expression. *Nat Cell Biol* **7(2)**:165-171.
275. Norbury C and Nurse P. (1992). Animal-Cell Cycles and Their Control. *Annu Rev Biochem* **61**:441-470.

276. Nurse P. (1997). Regulation of the eukaryotic cell cycle. *Eur J Cancer* **33(7)**:1002-1004.
277. Harbour JW and Dean DC. (2000). The Rb/E2F pathway: expanding roles and emerging paradigms. *Genes Dev* **14(19)**:2393-2409.
278. Dyson N. (1998). The regulation of E2F by pRB-family proteins. *Genes Dev* **12(15)**:2245-2262.
279. Trimarchi JM and Lees JA. (2002). Sibling rivalry in the E2F family. *Nat Rev Mol Cell Biol* **3(1)**:11-20.
280. Chen YJ, Dominguez-Brauer C, Wang Z, Asara JM, Costa RH, Tyner AL, Lau LF and Raychaudhuri P. (2009). A conserved phosphorylation site within the forkhead domain of FoxM1B is required for its activation by cyclin-CDK1. *J Biol Chem* **284(44)**:30695-30707.
281. Laoukili J, Alvarez M, Meijer LA, Stahl M, Mohammed S, Kleij L, Heck AJ and Medema RH. (2008). Activation of FoxM1 during G2 requires cyclin A/Cdk-dependent relief of autorepression by the FoxM1 N-terminal domain. *Mol Cell Biol* **28(9)**:3076-3087.
282. Major ML, Lepe R and Costa RH. (2004). Forkhead box M1B transcriptional activity requires binding of Cdk-cyclin complexes for phosphorylation-dependent recruitment of p300/CBP coactivators. *Mol Cell Biol* **24(7)**:2649-2661.
283. Sherr CJ and Roberts JM. (1995). Inhibitors of mammalian G1 cyclin-dependent kinases. *Genes Dev* **9(10)**:1149-1163.
284. Hengst L and Reed SI. (1998). Inhibitors of the Cip/Kip Family. Current Topics in Microbiology and Immunology: Springer Science + Business Media), pp. 25-41.
285. Carnero A and Hannon GJ. (1998). The INK4 Family of CDK Inhibitors. Current Topics in Microbiology and Immunology: Springer Science + Business Media), pp. 43-55.
286. Harper JW, Elledge SJ, Keyomarsi K, Dynlacht B, Tsai LH, Zhang P, Dobrowolski S, Bai C, Connell-Crowley L, Swindell E and et al. (1995). Inhibition of cyclin-dependent kinases by p21. *Mol Biol Cell* **6(4)**:387-400.
287. Abbas T and Dutta A. (2009). p21 in cancer: intricate networks and multiple activities. *Nat Rev Cancer* **9(6)**:400-414.
288. Delavaine L and La Thangue NB. (1999). Control of E2F activity by p21Waf1/Cip1. *Oncogene* **18(39)**:5381-5392.
289. Pan ZQ, Reardon JT, Li L, Flores-Rozas H, Legerski R, Sancar A and Hurwitz J. (1995). Inhibition of nucleotide excision repair by the cyclin-dependent kinase inhibitor p21. *J Biol Chem* **270(37)**:22008-22016.
290. Waga S, Hannon GJ, Beach D and Stillman B. (1994). The p21 inhibitor of cyclin-dependent kinases controls DNA replication by interaction with PCNA. *Nature* **369(6481)**:574-578.
291. Gartel AL and Tyner AL. (2002). The role of the cyclin-dependent kinase inhibitor p21 in apoptosis. *Mol Cancer Ther* **1(8)**:639-649.
292. Hermeking H, Lengauer C, Polyak K, He T-C, Zhang L, Thiagalingam S, Kinzler KW and Vogelstein B. (1997). 14-3-3σ Is a p53-Regulated Inhibitor of G2/M Progression. *Mol Cell* **1(1)**:3-11.
293. Jin S, Tong T, Fan W, Fan F, Antinore MJ, Zhu X, Mazzacurati L, Li X, Petrik KL, Rajasekaran B, Wu M and Zhan Q. (2002). GADD45-induced cell cycle G2-M arrest

associates with altered subcellular distribution of cyclin B1 and is independent of p38 kinase activity. *Oncogene* **21(57)**:8696-8704.
294. Robles SJ, Buehler PW, Negrusz A and Adami GR. (1999). Permanent cell cycle arrest in asynchronously proliferating normal human fibroblasts treated with doxorubicin or etoposide but not camptothecin. *Biochem Pharmacol* **58(4)**:675-685.
295. Di Leonardo A, Linke SP, Clarkin K and Wahl GM. (1994). DNA damage triggers a prolonged p53-dependent G1 arrest and long-term induction of Cip1 in normal human fibroblasts. *Genes Dev* **8(21)**:2540-2551.
296. Chen QM, Prowse KR, Tu VC, Purdom S and Linskens MH. (2001). Uncoupling the senescent phenotype from telomere shortening in hydrogen peroxide-treated fibroblasts. *Exp Cell Res* **265(2)**:294-303.
297. Monasor A, Murga M, Lopez-Contreras AJ, Navas C, Gomez G, Pisano DG and Fernandez-Capetillo O. (2013). INK4a/ARF limits the expansion of cells suffering from replication stress. *Cell Cycle* **12(12)**:1948-1954.
298. Michaloglou C, Vredeveld LC, Soengas MS, Denoyelle C, Kuilman T, van der Horst CM, Majoor DM, Shay JW, Mooi WJ and Peeper DS. (2005). BRAFE600-associated senescence-like cell cycle arrest of human naevi. *Nature* **436(7051)**:720-724.
299. Lin AW, Barradas M, Stone JC, van Aelst L, Serrano M and Lowe SW. (1998). Premature senescence involving p53 and p16 is activated in response to constitutive MEK/MAPK mitogenic signaling. *Genes Dev* **12(19)**:3008-3019.
300. Zhu J, Woods D, McMahon M and Bishop JM. (1998). Senescence of human fibroblasts induced by oncogenic Raf. *Genes Dev* **12(19)**:2997-3007.
301. Serrano M, Lin AW, McCurrach ME, Beach D and Lowe SW. (1997). Oncogenic ras provokes premature cell senescence associated with accumulation of p53 and p16INK4a. *Cell* **88(5)**:593-602.
302. Courtois-Cox S, Genther Williams SM, Reczek EE, Johnson BW, McGillicuddy LT, Johannessen CM, Hollstein PE, MacCollin M and Cichowski K. (2006). A negative feedback signaling network underlies oncogene-induced senescence. *Cancer cell* **10(6)**:459-472.
303. Chen Z, Trotman LC, Shaffer D, Lin HK, Dotan ZA, Niki M, Koutcher JA, Scher HI, Ludwig T, Gerald W, Cordon-Cardo C and Pandolfi PP. (2005). Crucial role of p53-dependent cellular senescence in suppression of Pten-deficient tumorigenesis. *Nature* **436(7051)**:725-730.
304. Rayess H, Wang MB and Srivatsan ES. (2012). Cellular senescence and tumor suppressor gene p16. *Int J Cancer* **130(8)**:1715-1725.
305. de Stanchina E, Querido E, Narita M, Davuluri RV, Pandolfi PP, Ferbeyre G and Lowe SW. (2004). PML Is a Direct p53 Target that Modulates p53 Effector Functions. *Mol Cell* **13(4)**:523-535.
306. Ferbeyre G, de Stanchina E, Querido E, Baptiste N, Prives C and Lowe SW. (2000). PML is induced by oncogenic ras and promotes premature senescence. *Genes & Development* **14(16)**:2015-2027.
307. Pearson M, Carbone R, Sebastiani C, Cioce M, Fagioli M, Saito S, Higashimoto Y, Appella E, Minucci S, Pandolfi PP and Pelicci PG. (2000). PML regulates p53

acetylation and premature senescence induced by oncogenic Ras. *Nature* **406(6792)**:207-210.
308. Kortlever RM, Higgins PJ and Bernards R. (2006). Plasminogen activator inhibitor-1 is a critical downstream target of p53 in the induction of replicative senescence. *Nat Cell Biol* **8(8)**:877-884.
309. Denoyelle C, Abou-Rjaily G, Bezrookove V, Verhaegen M, Johnson TM, Fullen DR, Pointer JN, Gruber SB, Su LD, Nikiforov MA, Kaufman RJ, Bastian BC and Soengas MS. (2006). Anti-oncogenic role of the endoplasmic reticulum differentially activated by mutations in the MAPK pathway. *Nat Cell Biol* **8(10)**:1053-1063.
310. Bayreuther K, Rodemann HP, Hommel R, Dittmann K, Albiez M and Francz PI. (1988). Human skin fibroblasts in vitro differentiate along a terminal cell lineage. *Proc Natl Acad Sci U S A* **85(14)**:5112-5116.
311. Chang BD, Swift ME, Shen M, Fang J, Broude EV and Roninson IB. (2002). Molecular determinants of terminal growth arrest induced in tumor cells by a chemotherapeutic agent. *Proc Natl Acad Sci U S A* **99(1)**:389-394.
312. Mason DX, Jackson TJ and Lin AW. (2004). Molecular signature of oncogenic ras-induced senescence. *Oncogene* **23(57)**:9238-9246.
313. Shelton DN, Chang E, Whittier PS, Choi D and Funk WD. (1999). Microarray analysis of replicative senescence. *Curr Biol* **9(17)**:939-945.
314. Trougakos IP, Saridaki A, Panayotou G and Gonos ES. (2006). Identification of differentially expressed proteins in senescent human embryonic fibroblasts. *Mech Ageing Dev* **127(1)**:88-92.
315. Yoon IK, Kim HK, Kim YK, Song IH, Kim W, Kim S, Baek SH, Kim JH and Kim JR. (2004). Exploration of replicative senescence-associated genes in human dermal fibroblasts by cDNA microarray technology. *Exp Gerontol* **39(9)**:1369-1378.
316. Zhang H, Pan KH and Cohen SN. (2003). Senescence-specific gene expression fingerprints reveal cell-type-dependent physical clustering of up-regulated chromosomal loci. *Proc Natl Acad Sci U S A* **100(6)**:3251-3256.
317. Dimri GP, Lee X, Basile G, Acosta M, Scott G, Roskelley C, Medrano EE, Linskens M, Rubelj I, Pereira-Smith O and et al. (1995). A biomarker that identifies senescent human cells in culture and in aging skin in vivo. *Proc Natl Acad Sci U S A* **92(20)**:9363-9367.
318. Lee BY, Han JA, Im JS, Morrone A, Johung K, Goodwin EC, Kleijer WJ, DiMaio D and Hwang ES. (2006). Senescence-associated beta-galactosidase is lysosomal beta-galactosidase. *Aging Cell* **5(2)**:187-195.
319. Narita M, Nunez S, Heard E, Narita M, Lin AW, Hearn SA, Spector DL, Hannon GJ and Lowe SW. (2003). Rb-mediated heterochromatin formation and silencing of E2F target genes during cellular senescence. *Cell* **113(6)**:703-716.
320. Takai H, Smogorzewska A and de Lange T. (2003). DNA damage foci at dysfunctional telomeres. *Current Biology* **13(17)**:1549-1556.
321. Stiewe T. (2007). The p53 family in differentiation and tumorigenesis. *Nat Rev Cancer* **7(3)**:165-168.
322. Cheo DL, Ruven HJ, Meira LB, Hammer RE, Burns DK, Tappe NJ, van Zeeland AA, Mullenders LH and Friedberg EC. (1997). Characterization of defective nucleotide excision repair in XPC mutant mice. *Mutat Res* **374(1)**:1-9.

323. Hwang BJ, Ford JM, Hanawalt PC and Chu G. (1999). Expression of the p48 xeroderma pigmentosum gene is p53-dependent and is involved in global genomic repair. *Proc Natl Acad Sci U S A* **96(2)**:424-428.
324. Carrier F, Georgel PT, Pourquier P, Blake M, Kontny HU, Antinore MJ, Gariboldi M, Myers TG, Weinstein JN, Pommier Y and Fornace AJ, Jr. (1999). Gadd45, a p53-responsive stress protein, modifies DNA accessibility on damaged chromatin. *Mol Cell Biol* **19(3)**:1673-1685.
325. Yamaguchi T, Matsuda K, Sagiya Y, Iwadate M, Fujino MA, Nakamura Y and Arakawa H. (2001). p53R2-dependent pathway for DNA synthesis in a p53-regulated cell cycle checkpoint. *Cancer Res* **61(22)**:8256-8262.
326. Adimoolam S and Ford JM. (2003). p53 and regulation of DNA damage recognition during nucleotide excision repair. *DNA Repair (Amst)* **2(9)**:947-954.
327. Kelekar A and Thompson CB. (1998). Bcl-2-family proteins: the role of the BH3 domain in apoptosis. *Trends Cell Biol* **8(8)**:324-330.
328. Reed JC, Zha H, Aime-Sempe C, Takayama S and Wang HG. (1996). Structure-function analysis of Bcl-2 family proteins. Regulators of programmed cell death. *Adv Exp Med Biol* **406**:99-112.
329. Youle RJ and Strasser A. (2008). The BCL-2 protein family: opposing activities that mediate cell death. *Nat Rev Mol Cell Biol* **9(1)**:47-59.
330. Chipuk JE, Moldoveanu T, Llambi F, Parsons MJ and Green DR. (2010). The BCL-2 family reunion. *Mol Cell* **37(3)**:299-310.
331. Miyashita T, Krajewski S, Krajewska M, Wang HG, Lin HK, Liebermann DA, Hoffman B and Reed JC. (1994). Tumor suppressor p53 is a regulator of bcl-2 and bax gene expression in vitro and in vivo. *Oncogene* **9(6)**:1799-1805.
332. Oda E, Ohki R, Murasawa H, Nemoto J, Shibue T, Yamashita T, Tokino T, Taniguchi T and Tanaka N. (2000). Noxa, a BH3-only member of the Bcl-2 family and candidate mediator of p53-induced apoptosis. *Science* **288(5468)**:1053-1058.
333. Nakano K and Vousden KH. (2001). PUMA, a novel proapoptotic gene, is induced by p53. *Mol Cell* **7(3)**:683-694.
334. Miyashita T and Reed JC. (1995). Tumor-Suppressor P53 Is a Direct Transcriptional Activator of the Human Bax Gene. *Cell* **80(2)**:293-299.
335. Villunger A, Michalak EM, Coultas L, Mullauer F, Bock G, Ausserlechner MJ, Adams JM and Strasser A. (2003). p53- and drug-induced apoptotic responses mediated by BH3-only proteins puma and noxa. *Science* **302(5647)**:1036-1038.
336. Sax JK, Fei P, Murphy ME, Bernhard E, Korsmeyer SJ and El-Deiry WS. (2002). BID regulation by p53 contributes to chemosensitivity. *Nat Cell Biol* **4(11)**:842-849.
337. Chen L, Willis SN, Wei A, Smith BJ, Fletcher JI, Hinds MG, Colman PM, Day CL, Adams JM and Huang DC. (2005). Differential targeting of prosurvival Bcl-2 proteins by their BH3-only ligands allows complementary apoptotic function. *Mol Cell* **17(3)**:393-403.
338. Du H, Wolf J, Schafer B, Moldoveanu T, Chipuk JE and Kuwana T. (2011). BH3 domains other than Bim and Bid can directly activate Bax/Bak. *J Biol Chem* **286(1)**:491-501.

339. Eskes R, Desagher S, Antonsson B and Martinou JC. (2000). Bid induces the oligomerization and insertion of Bax into the outer mitochondrial membrane. *Mol Cell Biol* **20(3)**:929-935.
340. Walensky LD, Pitter K, Morash J, Oh KJ, Barbuto S, Fisher J, Smith E, Verdine GL and Korsmeyer SJ. (2006). A stapled BID BH3 helix directly binds and activates BAX. *Mol Cell* **24(2)**:199-210.
341. Wang K, Yin XM, Chao DT, Milliman CL and Korsmeyer SJ. (1996). BID: a novel BH3 domain-only death agonist. *Genes Dev* **10(22)**:2859-2869.
342. Yang C, Kaushal V, Haun RS, Seth R, Shah SV and Kaushal GP. (2008). Transcriptional activation of caspase-6 and -7 genes by cisplatin-induced p53 and its functional significance in cisplatin nephrotoxicity. *Cell Death Differ* **15(3)**:530-544.
343. Ehrnhoefer DE, Skotte NH, Ladha S, Nguyen YT, Qiu X, Deng Y, Huynh KT, Engemann S, Nielsen SM, Becanovic K, Leavitt BR, Hasholt L and Hayden MR. (2014). p53 increases caspase-6 expression and activation in muscle tissue expressing mutant huntingtin. *Hum Mol Genet* **23(3)**:717-729.
344. Robles AI, Bemmels NA, Foraker AB and Harris CC. (2001). APAF-1 is a transcriptional target of p53 in DNA damage-induced apoptosis. *Cancer Res* **61(18)**:6660-6664.
345. Moroni MC, Hickman ES, Lazzerini Denchi E, Caprara G, Colli E, Cecconi F, Muller H and Helin K. (2001). Apaf-1 is a transcriptional target for E2F and p53. *Nat Cell Biol* **3(6)**:552-558.
346. Tamm I, Wang Y, Sausville E, Scudiero DA, Vigna N, Oltersdorf T and Reed JC. (1998). IAP-family protein survivin inhibits caspase activity and apoptosis induced by Fas (CD95), Bax, caspases, and anticancer drugs. *Cancer Res* **58(23)**:5315-5320.
347. Mirza A, McGuirk M, Hockenberry TN, Wu Q, Ashar H, Black S, Wen SF, Wang L, Kirschmeier P, Bishop WR, Nielsen LL, Pickett CB and Liu S. (2002). Human survivin is negatively regulated by wild-type p53 and participates in p53-dependent apoptotic pathway. *Oncogene* **21(17)**:2613-2622.
348. Chipuk JE, Kuwana T, Bouchier-Hayes L, Droin NM, Newmeyer DD, Schuler M and Green DR. (2004). Direct activation of Bax by p53 mediates mitochondrial membrane permeabilization and apoptosis. *Science* **303(5660)**:1010-1014.
349. Chinnaiyan AM, O'Rourke K, Tewari M and Dixit VM. (1995). FADD, a novel death domain-containing protein, interacts with the death domain of Fas and initiates apoptosis. *Cell* **81(4)**:505-512.
350. Hsu H, Xiong J and Goeddel DV. (1995). The TNF receptor 1-associated protein TRADD signals cell death and NF-kappa B activation. *Cell* **81(4)**:495-504.
351. Sheridan JP, Marsters SA, Pitti RM, Gurney A, Skubatch M, Baldwin D, Ramakrishnan L, Gray CL, Baker K, Wood WI, Goddard AD, Godowski P and Ashkenazi A. (1997). Control of TRAIL-induced apoptosis by a family of signaling and decoy receptors. *Science* **277(5327)**:818-821.
352. Pan G, Ni J, Wei YF, Yu G, Gentz R and Dixit VM. (1997). An antagonist decoy receptor and a death domain-containing receptor for TRAIL. *Science* **277(5327)**:815-818.
353. Ozoren N and El-Deiry WS. (2003). Cell surface Death Receptor signaling in normal and cancer cells. *Seminars in cancer biology* **13(2)**:135-147.

354. Zha J, Weiler S, Oh KJ, Wei MC and Korsmeyer SJ. (2000). Posttranslational N-myristoylation of BID as a molecular switch for targeting mitochondria and apoptosis. *Science* **290(5497)**:1761-1765.
355. Lin YP, Ma WL and Benchimol S. (2000). Pidd, a new death-domain-containing protein, is induced by p53 and promotes apoptosis. *Nat Genet* **26(1)**:122-125.
356. Owen-Schaub LB, Zhang W, Cusack JC, Angelo LS, Santee SM, Fujiwara T, Roth JA, Deisseroth AB, Zhang WW, Kruzel E and et al. (1995). Wild-type human p53 and a temperature-sensitive mutant induce Fas/APO-1 expression. *Mol Cell Biol* **15(6)**:3032-3040.
357. Muller M, Wilder S, Bannasch D, Israeli D, Lehlbach K, Li-Weber M, Friedman SL, Galle PR, Stremmel W, Oren M and Krammer PH. (1998). p53 activates the CD95 (APO-1/Fas) gene in response to DNA damage by anticancer drugs. *J Exp Med* **188(11)**:2033-2045.
358. Wu GS, Burns TF, McDonald ER, 3rd, Jiang W, Meng R, Krantz ID, Kao G, Gan DD, Zhou JY, Muschel R, Hamilton SR, Spinner NB, Markowitz S, Wu G and el-Deiry WS. (1997). KILLER/DR5 is a DNA damage-inducible p53-regulated death receptor gene. *Nat Genet* **17(2)**:141-143.
359. Maecker HL, Koumenis C and Giaccia AJ. (2000). p53 promotes selection for Fas-mediated apoptotic resistance. *Cancer Res* **60(16)**:4638-4644.
360. Ruiz de Almodovar C, Ruiz-Ruiz C, Rodriguez A, Ortiz-Ferron G, Redondo JM and Lopez-Rivas A. (2004). Tumor necrosis factor-related apoptosis-inducing ligand (TRAIL) decoy receptor TRAIL-R3 is up-regulated by p53 in breast tumor cells through a mechanism involving an intronic p53-binding site. *J Biol Chem* **279(6)**:4093-4101.
361. Liu X, Yue P, Khuri FR and Sun SY. (2004). p53 upregulates death receptor 4 expression through an intronic p53 binding site. *Cancer Res* **64(15)**:5078-5083.
362. Liu X, Yue P, Khuri FR and Sun SY. (2005). Decoy receptor 2 (DcR2) is a p53 target gene and regulates chemosensitivity. *Cancer Res* **65(20)**:9169-9175.
363. Chen J, Ghorai MK, Kenney G and Stubbe J. (2008). Mechanistic studies on bleomycin-mediated DNA damage: multiple binding modes can result in double-stranded DNA cleavage. *Nucleic Acids Res* **36(11)**:3781-3790.
364. Puyo S, Montaudon D and Pourquier P. (2014). From old alkylating agents to new minor groove binders. *Crit Rev Oncol Hematol* **89(1)**:43-61.
365. Christopoulou A. (2004). Chemotherapy in metastatic colorectal cancer. *Tech Coloproctol* **8 Suppl 1(S1)**:s43-46.
366. Keating GM. (2014). Bevacizumab: a review of its use in advanced cancer. *Drugs* **74(16)**:1891-1925.
367. Shanafelt TD, Lin T, Geyer SM, Zent CS, Leung N, Kabat B, Bowen D, Grever MR, Byrd JC and Kay NE. (2007). Pentostatin, cyclophosphamide, and rituximab regimen in older patients with chronic lymphocytic leukemia. *Cancer* **109(11)**:2291-2298.
368. Facon T, Mary JY, Hulin C, Benboubker L, Attal M, Pegourie B, Renaud M, Harousseau JL, Guillerm G, Chaleteix C, Dib M, Voillat L, Maisonneuve H, Troncy J, Dorvaux V, Monconduit M, et al. (2007). Melphalan and prednisone plus thalidomide versus melphalan and prednisone alone or reduced-intensity autologous stem cell transplantation

in elderly patients with multiple myeloma (IFM 99-06): a randomised trial. *Lancet* **370(9594)**:1209-1218.
369. Ewend MG, Brem S, Gilbert M, Goodkin R, Penar PL, Varia M, Cush S and Carey LA. (2007). Treatment of single brain metastasis with resection, intracavity carmustine polymer wafers, and radiation therapy is safe and provides excellent local control. *Clin Cancer Res* **13(12)**:3637-3641.
370. Larkin JM, Hughes SA, Beirne DA, Patel PM, Gibbens IM, Bate SC, Thomas K, Eisen TG and Gore ME. (2007). A phase I/II study of lomustine and temozolomide in patients with cerebral metastases from malignant melanoma. *Br J Cancer* **96(1)**:44-48.
371. Rixe O, Ortuzar W, Alvarez M, Parker R, Reed E, Paull K and Fojo T. (1996). Oxaliplatin, tetraplatin, cisplatin, and carboplatin: spectrum of activity in drug-resistant cell lines and in the cell lines of the National Cancer Institute's Anticancer Drug Screen panel. *Biochem Pharmacol* **52(12)**:1855-1865.
372. Chen T, Sun Y, Ji P, Kopetz S and Zhang W. (2015). Topoisomerase IIalpha in chromosome instability and personalized cancer therapy. *Oncogene* **34(31)**:4019-4031.
373. Pogorelcnik B, Perdih A and Solmajer T. (2013). Recent developments of DNA poisons--human DNA topoisomerase IIalpha inhibitors--as anticancer agents. *Curr Pharm Des* **19(13)**:2474-2488.
374. Froelich-Ammon SJ and Osheroff N. (1995). Topoisomerase poisons: harnessing the dark side of enzyme mechanism. *J Biol Chem* **270(37)**:21429-21432.
375. Cutts SM, Nudelman A, Rephaeli A and Phillips DR. (2005). The power and potential of doxorubicin-DNA adducts. *IUBMB Life* **57(2)**:73-81.
376. Hertzberg RP, Caranfa MJ and Hecht SM. (1989). On the mechanism of topoisomerase I inhibition by camptothecin: evidence for binding to an enzyme-DNA complex. *Biochemistry* **28(11)**:4629-4638.
377. Chen GL, Yang L, Rowe TC, Halligan BD, Tewey KM and Liu LF. (1984). Nonintercalative antitumor drugs interfere with the breakage-reunion reaction of mammalian DNA topoisomerase II. *J Biol Chem* **259(21)**:13560-13566.
378. Burgess DJ, Doles J, Zender L, Xue W, Ma B, McCombie WR, Hannon GJ, Lowe SW and Hemann MT. (2008). Topoisomerase levels determine chemotherapy response in vitro and in vivo. *Proc Natl Acad Sci U S A* **105(26)**:9053-9058.
379. Hsiang YH, Hertzberg R, Hecht S and Liu LF. (1985). Camptothecin induces protein-linked DNA breaks via mammalian DNA topoisomerase I. *J Biol Chem* **260(27)**:14873-14878.
380. Gille L and Nohl H. (1997). Analyses of the molecular mechanism of adriamycin-induced cardiotoxicity. *Free Radic Biol Med* **23(5)**:775-782.
381. Marco A and Arcamone F. (1975). DNA complexing antibiotics: daunomycin, adriamycin and their derivatives. *Arzneimittelforschung* **25(3)**:368-374.
382. Besirli CG, Deckwerth TL, Crowder RJ, Freeman RS and Johnson EM, Jr. (2003). Cytosine arabinoside rapidly activates Bax-dependent apoptosis and a delayed Bax-independent death pathway in sympathetic neurons. *Cell Death Differ* **10(9)**:1045-1058.
383. Parker WB and Cheng YC. (1990). Metabolism and mechanism of action of 5-fluorouracil. *Pharmacol Ther* **48(3)**:381-395.

384. Zeng X and Kinsella TJ. (2010). BNIP3 is essential for mediating 6-thioguanine- and 5-fluorouracil-induced autophagy following DNA mismatch repair processing. *Cell Res* **20(6)**:665-675.
385. Kanemitsu H, Yamauchi H, Komatsu M, Yamamoto S, Okazaki S, Uchida K and Nakayama H. (2009). 6-mercaptopurine (6-MP) induces p53-mediated apoptosis of neural progenitor cells in the developing fetal rodent brain. *Neurotoxicol Teratol* **31(4)**:198-202.
386. Stone SR and Morrison JF. (1986). Mechanism of inhibition of dihydrofolate reductases from bacterial and vertebrate sources by various classes of folate analogues. *Biochim Biophys Acta* **869(3)**:275-285.
387. Manegold C. (2003). Pemetrexed (Alimta, MTA, multitargeted antifolate, LY231514) for malignant pleural mesothelioma. *Semin Oncol* **30(4 Suppl 10)**:32-36.
388. Walling J. (2006). From methotrexate to pemetrexed and beyond. A review of the pharmacodynamic and clinical properties of antifolates. *Invest New Drugs* **24(1)**:37-77.
389. Koc A, Wheeler LJ, Mathews CK and Merrill GF. (2004). Hydroxyurea arrests DNA replication by a mechanism that preserves basal dNTP pools. *J Biol Chem* **279(1)**:223-230.
390. Stearns B, Losee KA and Bernstein J. (1963). Hydroxyurea. A New Type of Potential Antitumor Agent. *J Med Chem* **6**:201.
391. El Husseini N, Schlisser AE and Hales BF. (2016). Editor's Highlight: Hydroxyurea Exposure Activates the P53 Signaling Pathway in Murine Organogenesis-Stage Embryos. *Toxicol Sci* **152(2)**:297-308.
392. Yue QX, Liu X and Guo DA. (2010). Microtubule-binding natural products for cancer therapy. *Planta Med* **76(11)**:1037-1043.
393. Hofmann WK, Komor M, Wassmann B, Jones LC, Gschaidmeier H, Hoelzer D, Koeffler HP and Ottmann OG. (2003). Presence of the BCR-ABL mutation Glu255Lys prior to STI571 (imatinib) treatment in patients with Ph+ acute lymphoblastic leukemia. *Blood* **102(2)**:659-661.
394. Ma L, Wang DD, Huang Y, Yan H, Wong MP and Lee VH. (2015). EGFR Mutant Structural Database: computationally predicted 3D structures and the corresponding binding free energies with gefitinib and erlotinib. *BMC Bioinformatics* **16(1)**:85.
395. Hudis CA. (2007). Trastuzumab--mechanism of action and use in clinical practice. *N Engl J Med* **357(1)**:39-51.
396. Los M, Roodhart JM and Voest EE. (2007). Target practice: lessons from phase III trials with bevacizumab and vatalanib in the treatment of advanced colorectal cancer. *Oncologist* **12(4)**:443-450.
397. Forde PM and Rudin CM. (2012). Crizotinib in the treatment of non-small-cell lung cancer. *Expert Opin Pharmacother* **13(8)**:1195-1201.
398. Flaherty KT, Infante JR, Daud A, Gonzalez R, Kefford RF, Sosman J, Hamid O, Schuchter L, Cebon J, Ibrahim N, Kudchadkar R, Burris HA, 3rd, Falchook G, Algazi A, Lewis K, Long GV, et al. (2012). Combined BRAF and MEK inhibition in melanoma with BRAF V600 mutations. *N Engl J Med* **367(18)**:1694-1703.
399. Sehgal SN. (2003). Sirolimus: its discovery, biological properties, and mechanism of action. *Transplant Proc* **35(3 Suppl)**:7S-14S.

400. Rubio-Viqueira B and Hidalgo M. (2006). Targeting mTOR for cancer treatment. *Curr Opin Investig Drugs* **7(6)**:501-512.
401. Ghosh B, Benyumov AO, Ghosh P, Jia Y, Avdulov S, Dahlberg PS, Peterson M, Smith K, Polunovsky VA, Bitterman PB and Wagner CR. (2009). Nontoxic chemical interdiction of the epithelial-to-mesenchymal transition by targeting cap-dependent translation. *ACS Chem Biol* **4(5)**:367-377.
402. Bordeleau ME, Matthews J, Wojnar JM, Lindqvist L, Novac O, Jankowsky E, Sonenberg N, Northcote P, Teesdale-Spittle P and Pelletier J. (2005). Stimulation of mammalian translation initiation factor eIF4A activity by a small molecule inhibitor of eukaryotic translation. *Proc Natl Acad Sci U S A* **102(30)**:10460-10465.
403. Bordeleau ME, Mori A, Oberer M, Lindqvist L, Chard LS, Higa T, Belsham GJ, Wagner G, Tanaka J and Pelletier J. (2006). Functional characterization of IRESes by an inhibitor of the RNA helicase eIF4A. *Nat Chem Biol* **2(4)**:213-220.
404. Bordeleau ME, Robert F, Gerard B, Lindqvist L, Chen SM, Wendel HG, Brem B, Greger H, Lowe SW, Porco JA, Jr. and Pelletier J. (2008). Therapeutic suppression of translation initiation modulates chemosensitivity in a mouse lymphoma model. *J Clin Invest* **118(7)**:2651-2660.
405. Moerke NJ, Aktas H, Chen H, Cantel S, Reibarkh MY, Fahmy A, Gross JD, Degterev A, Yuan J, Chorev M, Halperin JA and Wagner G. (2007). Small-molecule inhibition of the interaction between the translation initiation factors eIF4E and eIF4G. *Cell* **128(2)**:257-267.
406. Cencic R, Hall DR, Robert F, Du Y, Min J, Li L, Qui M, Lewis I, Kurtkaya S, Dingledine R, Fu H, Kozakov D, Vajda S and Pelletier J. (2011). Reversing chemoresistance by small molecule inhibition of the translation initiation complex eIF4F. *Proc Natl Acad Sci U S A* **108(3)**:1046-1051.
407. Cencic R, Desforges M, Hall DR, Kozakov D, Du Y, Min J, Dingledine R, Fu H, Vajda S, Talbot PJ and Pelletier J. (2011). Blocking eIF4E-eIF4G interaction as a strategy to impair coronavirus replication. *J Virol* **85(13)**:6381-6389.
408. Iqbal J, Neppalli VT, Wright G, Dave BJ, Horsman DE, Rosenwald A, Lynch J, Hans CP, Weisenburger DD, Greiner TC, Gascoyne RD, Campo E, Ott G, Muller-Hermelink HK, Delabie J, Jaffe ES, et al. (2006). BCL2 expression is a prognostic marker for the activated B-cell-like type of diffuse large B-cell lymphoma. *J Clin Oncol* **24(6)**:961-968.
409. Bachmann PS, Piazza RG, Janes ME, Wong NC, Davies C, Mogavero A, Bhadri VA, Szymanska B, Geninson G, Magistroni V, Cazzaniga G, Biondi A, Miranda-Saavedra D, Gottgens B, Saffery R, Craig JM, et al. (2010). Epigenetic silencing of BIM in glucocorticoid poor-responsive pediatric acute lymphoblastic leukemia, and its reversal by histone deacetylase inhibition. *Blood* **116(16)**:3013-3022.
410. Vousden KH and Lane DP. (2007). p53 in health and disease. *Nat Rev Mol Cell Biol* **8(4)**:275-283.
411. Adams JM and Cory S. (2007). The Bcl-2 apoptotic switch in cancer development and therapy. *Oncogene* **26(9)**:1324-1337.
412. Lessene G, Czabotar PE and Colman PM. (2008). BCL-2 family antagonists for cancer therapy. *Nat Rev Drug Discov* **7(12)**:989-1000.

413. Oltersdorf T, Elmore SW, Shoemaker AR, Armstrong RC, Augeri DJ, Belli BA, Bruncko M, Deckwerth TL, Dinges J, Hajduk PJ, Joseph MK, Kitada S, Korsmeyer SJ, Kunzer AR, Letai A, Li C, et al. (2005). An inhibitor of Bcl-2 family proteins induces regression of solid tumours. *Nature* **435(7042)**:677-681.
414. van Delft MF, Wei AH, Mason KD, Vandenberg CJ, Chen L, Czabotar PE, Willis SN, Scott CL, Day CL, Cory S, Adams JM, Roberts AW and Huang DC. (2006). The BH3 mimetic ABT-737 targets selective Bcl-2 proteins and efficiently induces apoptosis via Bak/Bax if Mcl-1 is neutralized. *Cancer cell* **10(5)**:389-399.
415. Letai A. (2006). Restoring cancer's death sentence. *Cancer cell* **10(5)**:343-345.
416. Vogler M, Butterworth M, Majid A, Walewska RJ, Sun XM, Dyer MJ and Cohen GM. (2009). Concurrent up-regulation of BCL-XL and BCL2A1 induces approximately 1000-fold resistance to ABT-737 in chronic lymphocytic leukemia. *Blood* **113(18)**:4403-4413.
417. Lu S, Jang H, Gu S, Zhang J and Nussinov R. (2016). Drugging Ras GTPase: a comprehensive mechanistic and signaling structural view. *Chem Soc Rev* **45(18)**:4929-4952.
418. Cox AD, Fesik SW, Kimmelman AC, Luo J and Der CJ. (2014). Drugging the undruggable RAS: Mission possible? *Nat Rev Drug Discov* **13(11)**:828-851.
419. Horiuchi D, Anderton B and Goga A. (2014). Taking on challenging targets: making MYC druggable. *Am Soc Clin Oncol Educ Book*:e497-502.
420. Soucek L and Evan GI. (2010). The ups and downs of Myc biology. *Current Opinion in Genetics & Development* **20(1)**:91-95.
421. May WA, Lessnick SL, Braun BS, Klemsz M, Lewis BC, Lunsford LB, Hromas R and Denny CT. (1993). The Ewing's sarcoma EWS/FLI-1 fusion gene encodes a more potent transcriptional activator and is a more powerful transforming gene than FLI-1. *Mol Cell Biol* **13(12)**:7393-7398.
422. Lamhamedi-Cherradi SE, Menegaz BA, Ramamoorthy V, Aiyer RA, Maywald RL, Buford AS, Doolittle DK, Culotta KS, O'Dorisio JE and Ludwig JA. (2015). An Oral Formulation of YK-4-279: Preclinical Efficacy and Acquired Resistance Patterns in Ewing Sarcoma. *Mol Cancer Ther* **14(7)**:1591-1604.
423. Hong SH, Youbi SE, Hong SP, Kallakury B, Monroe P, Erkizan HV, Barber-Rotenberg JS, Houghton P, Uren A and Toretsky JA. (2014). Pharmacokinetic modeling optimizes inhibition of the 'undruggable' EWS-FLI1 transcription factor in Ewing Sarcoma. *Oncotarget* **5(2)**:338-350.
424. Konopleva M, Contractor R, Tsao T, Samudio I, Ruvolo PP, Kitada S, Deng X, Zhai D, Shi YX, Sneed T, Verhaegen M, Soengas M, Ruvolo VR, McQueen T, Schober WD, Watt JC, et al. (2006). Mechanisms of apoptosis sensitivity and resistance to the BH3 mimetic ABT-737 in acute myeloid leukemia. *Cancer cell* **10(5)**:375-388.
425. Del Gaizo Moore V, Brown JR, Certo M, Love TM, Novina CD and Letai A. (2007). Chronic lymphocytic leukemia requires BCL2 to sequester prodeath BIM, explaining sensitivity to BCL2 antagonist ABT-737. *J Clin Invest* **117(1)**:112-121.
426. Del Gaizo Moore V, Schlis KD, Sallan SE, Armstrong SA and Letai A. (2008). BCL-2 dependence and ABT-737 sensitivity in acute lymphoblastic leukemia. *Blood* **111(4)**:2300-2309.

427. Vogler M, Dinsdale D, Sun XM, Young KW, Butterworth M, Nicotera P, Dyer MJ and Cohen GM. (2008). A novel paradigm for rapid ABT-737-induced apoptosis involving outer mitochondrial membrane rupture in primary leukemia and lymphoma cells. *Cell Death Differ* **15(5)**:820-830.
428. Witham J, Valenti MR, De-Haven-Brandon AK, Vidot S, Eccles SA, Kaye SB and Richardson A. (2007). The Bcl-2/Bcl-XL family inhibitor ABT-737 sensitizes ovarian cancer cells to carboplatin. *Clin Cancer Res* **13(23)**:7191-7198.
429. Huang S and Sinicrope FA. (2008). BH3 mimetic ABT-737 potentiates TRAIL-mediated apoptotic signaling by unsequestering Bim and Bak in human pancreatic cancer cells. *Cancer Res* **68(8)**:2944-2951.
430. Kutuk O and Letai A. (2008). Alteration of the mitochondrial apoptotic pathway is key to acquired paclitaxel resistance and can be reversed by ABT-737. *Cancer Res* **68(19)**:7985-7994.
431. Yecies D, Carlson NE, Deng J and Letai A. (2010). Acquired resistance to ABT-737 in lymphoma cells that up-regulate MCL-1 and BFL-1. *Blood* **115(16)**:3304-3313.
432. Mills JR, Malina A, Lee T, Di Paola D, Larsson O, Miething C, Grosse F, Tang H, Zannis-Hadjopoulos M, Lowe SW and Pelletier J. (2013). RNAi screening uncovers Dhx9 as a modifier of ABT-737 resistance in an Emu-myc/Bcl-2 mouse model. *Blood* **121(17)**:3402-3412.
433. Hayflick L and Moorhead PS. (1961). The serial cultivation of human diploid cell strains. *Exp Cell Res* **25**:585-621.
434. Olovnikov AM. (1971). [Principle of marginotomy in template synthesis of polynucleotides]. *Dokl Akad Nauk SSSR* **201(6)**:1496-1499.
435. Watson JD. (1972). Origin of concatemeric T7 DNA. *Nat New Biol* **239(94)**:197-201.
436. Herbig U, Jobling WA, Chen BP, Chen DJ and Sedivy JM. (2004). Telomere shortening triggers senescence of human cells through a pathway involving ATM, p53, and p21(CIP1), but not p16(INK4a). *Mol Cell* **14(4)**:501-513.
437. Gray MD, Shen JC, Kamath-Loeb AS, Blank A, Sopher BL, Martin GM, Oshima J and Loeb LA. (1997). The Werner syndrome protein is a DNA helicase. *Nat Genet* **17(1)**:100-103.
438. Pichierri P, Ammazzalorso F, Bignami M and Franchitto A. (2011). The Werner syndrome protein: linking the replication checkpoint response to genome stability. *Aging (Albany NY)* **3(3)**:311-318.
439. Cheok CF, Bachrati CZ, Chan KL, Ralf C, Wu L and Hickson ID. (2005). Roles of the Bloom's syndrome helicase in the maintenance of genome stability. *Biochem Soc Trans* **33(Pt 6)**:1456-1459.
440. Langlois RG, Bigbee WL, Jensen RH and German J. (1989). Evidence for increased in vivo mutation and somatic recombination in Bloom's syndrome. *Proc Natl Acad Sci U S A* **86(2)**:670-674.
441. Jee HJ, Kim HJ, Kim AJ, Song N, Kim M, Lee HJ and Yun J. (2013). The inhibition of Nek6 function sensitizes human cancer cells to premature senescence upon serum reduction or anticancer drug treatment. *Cancer Lett* **335(1)**:175-182.

442. Luo H, Wang L, Schulte BA, Yang A, Tang S and Wang GY. (2013). Resveratrol enhances ionizing radiation-induced premature senescence in lung cancer cells. *Int J Oncol* **43(6)**:1999-2006.
443. Braig M, Lee S, Loddenkemper C, Rudolph C, Peters AH, Schlegelberger B, Stein H, Dorken B, Jenuwein T and Schmitt CA. (2005). Oncogene-induced senescence as an initial barrier in lymphoma development. *Nature* **436(7051)**:660-665.
444. Sherwood SW, Rush D, Ellsworth JL and Schimke RT. (1988). Defining cellular senescence in IMR-90 cells: a flow cytometric analysis. *Proc Natl Acad Sci U S A* **85(23)**:9086-9090.
445. Alcorta DA, Xiong Y, Phelps D, Hannon G, Beach D and Barrett JC. (1996). Involvement of the cyclin-dependent kinase inhibitor p16 (INK4a) in replicative senescence of normal human fibroblasts. *Proc Natl Acad Sci U S A* **93(24)**:13742-13747.
446. Leontieva OV, Natarajan V, Demidenko ZN, Burdelya LG, Gudkov AV and Blagosklonny MV. (2012). Hypoxia suppresses conversion from proliferative arrest to cellular senescence. *Proc Natl Acad Sci U S A* **109(33)**:13314-13318.
447. Kosar M, Bartkova J, Hubackova S, Hodny Z, Lukas J and Bartek J. (2011). Senescence-associated heterochromatin foci are dispensable for cellular senescence, occur in a cell type- and insult-dependent manner and follow expression of p16(ink4a). *Cell Cycle* **10(3)**:457-468.
448. d'Adda di Fagagna F, Reaper PM, Clay-Farrace L, Fiegler H, Carr P, Von Zglinicki T, Saretzki G, Carter NP and Jackson SP. (2003). A DNA damage checkpoint response in telomere-initiated senescence. *Nature* **426(6963)**:194-198.
449. Meyer R, Hatada EN, Hohmann HP, Haiker M, Bartsch C, Rothlisberger U, Lahm HW, Schlaeger EJ, van Loon AP and Scheidereit C. (1991). Cloning of the DNA-binding subunit of human nuclear factor kappa B: the level of its mRNA is strongly regulated by phorbol ester or tumor necrosis factor alpha. *Proc Natl Acad Sci U S A* **88(3)**:966-970.
450. Kohn RR. (1975). Aging and cell division. *Science* **188(4185)**:203-204.
451. Campisi J and d'Adda di Fagagna F. (2007). Cellular senescence: when bad things happen to good cells. *Nat Rev Mol Cell Biol* **8(9)**:729-740.
452. Ventura A, Kirsch DG, McLaughlin ME, Tuveson DA, Grimm J, Lintault L, Newman J, Reczek EE, Weissleder R and Jacks T. (2007). Restoration of p53 function leads to tumour regression in vivo. *Nature* **445(7128)**:661-665.
453. Taylor WR, Agarwal ML, Agarwal A, Stacey DW and Stark GR. (1999). p53 inhibits entry into mitosis when DNA synthesis is blocked. *Oncogene* **18(2)**:283-295.
454. Machida YJ, Teer JK and Dutta A. (2005). Acute reduction of an origin recognition complex (ORC) subunit in human cells reveals a requirement of ORC for Cdk2 activation. *J Biol Chem* **280(30)**:27624-27630.
455. Zhang H, Xiong Y and Beach D. (1993). Proliferating cell nuclear antigen and p21 are components of multiple cell cycle kinase complexes. *Mol Biol Cell* **4(9)**:897-906.
456. Kim KS, Seu YB, Baek SH, Kim MJ, Kim KJ, Kim JH and Kim JR. (2007). Induction of cellular senescence by insulin-like growth factor binding protein-5 through a p53-dependent mechanism. *Mol Biol Cell* **18(11)**:4543-4552.

457. Fu VX, Schwarze SR, Kenowski ML, Leblanc S, Svaren J and Jarrard DF. (2004). A loss of insulin-like growth factor-2 imprinting is modulated by CCCTC-binding factor down-regulation at senescence in human epithelial cells. *J Biol Chem* **279(50)**:52218-52226.
458. d'Adda di Fagagna F. (2008). Living on a break: cellular senescence as a DNA-damage response. *Nat Rev Cancer* **8(7)**:512-522.
459. Di Micco R, Fumagalli M, Cicalese A, Piccinin S, Gasparini P, Luise C, Schurra C, Garre M, Nuciforo PG, Bensimon A, Maestro R, Pelicci PG and d'Adda di Fagagna F. (2006). Oncogene-induced senescence is a DNA damage response triggered by DNA hyper-replication. *Nature* **444(7119)**:638-642.
460. Szulc J, Wiznerowicz M, Sauvain MO, Trono D and Aebischer P. (2006). A versatile tool for conditional gene expression and knockdown. *Nature methods* **3(2)**:109-116.
461. Chicas A, Wang X, Zhang C, McCurrach M, Zhao Z, Mert O, Dickins RA, Narita M, Zhang M and Lowe SW. (2010). Dissecting the unique role of the retinoblastoma tumor suppressor during cellular senescence. *Cancer cell* **17(4)**:376-387.
462. Barde I, Salmon P and Trono D. (2010). Production and titration of lentiviral vectors. *Current protocols in neuroscience / editorial board, Jacqueline N Crawley [et al]* **Chapter 4**:Unit 4.21.
463. Stegmeier F, Hu G, Rickles RJ, Hannon GJ and Elledge SJ. (2005). A lentiviral microRNA-based system for single-copy polymerase II-regulated RNA interference in mammalian cells. *Proc Natl Acad Sci U S A* **102(37)**:13212-13217.
464. Darzynkiewicz Z and Juan G. (2001). Analysis of DNA content and BrdU incorporation. *Curr Protoc Cytom* **Chapter 7**:Unit 7.7.
465. Dai C, Whitesell L, Rogers AB and Lindquist S. (2007). Heat shock factor 1 is a powerful multifaceted modifier of carcinogenesis. *Cell* **130(6)**:1005-1018.
466. Sandberg R and Larsson O. (2007). Improved precision and accuracy for microarrays using updated probe set definitions. *BMC Bioinformatics* **8**:48.
467. Wright GW and Simon RM. (2003). A random variance model for detection of differential gene expression in small microarray experiments. *Bioinformatics* **19(18)**:2448-2455.
468. Benjamini Y and Hochberg Y. (1995). Controlling the False Discovery Rate - a Practical and Powerful Approach to Multiple Testing. *Journal of the Royal Statistical Society Series B-Methodological* **57(1)**:289-300.
469. Luo W, Friedman MS, Shedden K, Hankenson KD and Woolf PJ. (2009). GAGE: generally applicable gene set enrichment for pathway analysis. *BMC Bioinformatics* **10**:161.
470. Di Paola D, Price GB and Zannis-Hadjopoulos M. (2006). Differentially active origins of DNA replication in tumor versus normal cells. *Cancer Res* **66(10)**:5094-5103.
471. Di Paola D and Zannis-Hadjopoulos M. (2012). Comparative analysis of pre-replication complex proteins in transformed and normal cells. *J Cell Biochem* **113(4)**:1333-1347.
472. Wilson R, Ainscough R, Anderson K, Baynes C, Berks M, Bonfield J, Burton J, Connell M, Copsey T, Cooper J and et al. (1994). 2.2 Mb of contiguous nucleotide sequence from chromosome III of C. elegans. *Nature* **368(6466)**:32-38.
473. Lee T, Di Paola D, Malina A, Mills JR, Kreps A, Grosse F, Tang H, Zannis-Hadjopoulos M, Larsson O and Pelletier J. (2014). Suppression of the DHX9 helicase induces

premature senescence in human diploid fibroblasts in a p53-dependent manner. *J Biol Chem* **289(33)**:22798-22814.
474. Lin CJ, Nasr Z, Premsrirut PK, Porco JA, Jr., Hippo Y, Lowe SW and Pelletier J. (2012). Targeting synthetic lethal interactions between Myc and the eIF4F complex impedes tumorigenesis. *Cell Rep* **1(4)**:325-333.
475. Premsrirut PK, Dow LE, Kim SY, Camiolo M, Malone CD, Miething C, Scuoppo C, Zuber J, Dickins RA, Kogan SC, Shroyer KR, Sordella R, Hannon GJ and Lowe SW. (2011). A rapid and scalable system for studying gene function in mice using conditional RNA interference. *Cell* **145(1)**:145-158.
476. Hui L, Zheng Y, Yan Y, Bargonetti J and Foster DA. (2006). Mutant p53 in MDA-MB-231 breast cancer cells is stabilized by elevated phospholipase D activity and contributes to survival signals generated by phospholipase D. *Oncogene* **25(55)**:7305-7310.
477. Bae YH, Shin JM, Park HJ, Jang HO, Bae MK and Bae SK. (2014). Gain-of-function mutant p53-R280K mediates survival of breast cancer cells. *Genes & Genomics* **36(2)**:171-178.
478. Hoppe-Seyler F and Butz K. (1993). Repression of endogenous p53 transactivation function in HeLa cervical carcinoma cells by human papillomavirus type 16 E6, human mdm-2, and mutant p53. *J Virol* **67(6)**:3111-3117.
479. Robert F, Roman W, Bramoulle A, Fellmann C, Roulston A, Shustik C, Porco JA, Jr., Shore GC, Sebag M and Pelletier J. (2014). Translation initiation factor eIF4F modifies the dexamethasone response in multiple myeloma. *Proc Natl Acad Sci U S A* **111(37)**:13421-13426.
480. Wendel HG, De Stanchina E, Fridman JS, Malina A, Ray S, Kogan S, Cordon-Cardo C, Pelletier J and Lowe SW. (2004). Survival signalling by Akt and eIF4E in oncogenesis and cancer therapy. *Nature* **428(6980)**:332-337.
481. McJunkin K, Mazurek A, Premsrirut PK, Zuber J, Dow LE, Simon J, Stillman B and Lowe SW. (2011). Reversible suppression of an essential gene in adult mice using transgenic RNA interference. *Proc Natl Acad Sci U S A* **108(17)**:7113-7118.
482. Zuber J, McJunkin K, Fellmann C, Dow LE, Taylor MJ, Hannon GJ and Lowe SW. (2011). Toolkit for evaluating genes required for proliferation and survival using tetracycline-regulated RNAi. *Nat Biotechnol* **29(1)**:79-83.
483. Beard C, Hochedlinger K, Plath K, Wutz A and Jaenisch R. (2006). Efficient method to generate single-copy transgenic mice by site-specific integration in embryonic stem cells. *Genesis* **44(1)**:23-28.
484. Calcabrini A, Garcia-Martinez JM, Gonzalez L, Tendero MJ, Ortuno MT, Crateri P, Lopez-Rivas A, Arancia G, Gonzalez-Porque P and Martin-Perez J. (2006). Inhibition of proliferation and induction of apoptosis in human breast cancer cells by lauryl gallate. *Carcinogenesis* **27(8)**:1699-1712.
485. Trudel S, Stewart AK, Li Z, Shu Y, Liang SB, Trieu Y, Reece D, Paterson J, Wang D and Wen XY. (2007). The Bcl-2 family protein inhibitor, ABT-737, has substantial antimyeloma activity and shows synergistic effect with dexamethasone and melphalan. *Clin Cancer Res* **13(2 Pt 1)**:621-629.

486. Harper JW, Adami GR, Wei N, Keyomarsi K and Elledge SJ. (1993). The p21 Cdk-interacting protein Cip1 is a potent inhibitor of G1 cyclin-dependent kinases. *Cell* **75(4)**:805-816.
487. Tovar C, Rosinski J, Filipovic Z, Higgins B, Kolinsky K, Hilton H, Zhao X, Vu BT, Qing W, Packman K, Myklebost O, Heimbrook DC and Vassilev LT. (2006). Small-molecule MDM2 antagonists reveal aberrant p53 signaling in cancer: implications for therapy. *Proc Natl Acad Sci U S A* **103(6)**:1888-1893.
488. Parsyan A, Shahbazian D, Martineau Y, Petroulakis E, Alain T, Larsson O, Mathonnet G, Tettweiler G, Hellen CU, Pestova TV, Svitkin YV and Sonenberg N. (2009). The helicase protein DHX29 promotes translation initiation, cell proliferation, and tumorigenesis. *Proc Natl Acad Sci U S A* **106(52)**:22217-22222.
489. Sonenberg N and Hinnebusch AG. (2009). Regulation of translation initiation in eukaryotes: mechanisms and biological targets. *Cell* **136(4)**:731-745.
490. Dardenne E, Pierredon S, Driouch K, Gratadou L, Lacroix-Triki M, Espinoza MP, Zonta E, Germann S, Mortada H, Villemin JP, Dutertre M, Lidereau R, Vagner S and Auboeuf D. (2012). Splicing switch of an epigenetic regulator by RNA helicases promotes tumor-cell invasiveness. *Nat Struct Mol Biol* **19(11)**:1139-1146.
491. Davis BN, Hilyard AC, Lagna G and Hata A. (2008). SMAD proteins control DROSHA-mediated microRNA maturation. *Nature* **454(7200)**:56-61.
492. Fukuda T, Yamagata K, Fujiyama S, Matsumoto T, Koshida I, Yoshimura K, Mihara M, Naitou M, Endoh H, Nakamura T, Akimoto C, Yamamoto Y, Katagiri T, Foulds C, Takezawa S, Kitagawa H, et al. (2007). DEAD-box RNA helicase subunits of the Drosha complex are required for processing of rRNA and a subset of microRNAs. *Nat Cell Biol* **9(5)**:604-611.
493. Saporita AJ, Chang HC, Winkeler CL, Apicelli AJ, Kladney RD, Wang J, Townsend RR, Michel LS and Weber JD. (2011). RNA helicase DDX5 is a p53-independent target of ARF that participates in ribosome biogenesis. *Cancer Res* **71(21)**:6708-6717.
494. Mazurek A, Park Y, Miething C, Wilkinson JE, Gillis J, Lowe SW, Vakoc CR and Stillman B. (2014). Acquired dependence of acute myeloid leukemia on the DEAD-box RNA helicase DDX5. *Cell Rep* **7(6)**:1887-1899.
495. Soucek L, Whitfield J, Martins CP, Finch AJ, Murphy DJ, Sodir NM, Karnezis AN, Swigart LB, Nasi S and Evan GI. (2008). Modelling Myc inhibition as a cancer therapy. *Nature* **455(7213)**:679-683.
496. Malumbres M and Barbacid M. (2001). To cycle or not to cycle: a critical decision in cancer. *Nat Rev Cancer* **1(3)**:222-231.
497. Carvalho BS and Irizarry RA. (2010). A framework for oligonucleotide microarray preprocessing. *Bioinformatics* **26(19)**:2363-2367.
498. Gentleman RC, Carey VJ, Bates DM, Bolstad B, Dettling M, Dudoit S, Ellis B, Gautier L, Ge Y, Gentry J, Hornik K, Hothorn T, Huber W, Iacus S, Irizarry R, Leisch F, et al. (2004). Bioconductor: open software development for computational biology and bioinformatics. *Genome Biol* **5(10)**:R80.
499. Dai M, Wang P, Boyd AD, Kostov G, Athey B, Jones EG, Bunney WE, Myers RM, Speed TP, Akil H, Watson SJ and Meng F. (2005). Evolving gene/transcript definitions significantly alter the interpretation of GeneChip data. *Nucleic Acids Res* **33(20)**:e175.

500. Larsson O, Sonenberg N and Nadon R. (2011). anota: Analysis of differential translation in genome-wide studies. *Bioinformatics* **27(10)**:1440-1441.
501. Gene Ontology C. (2015). Gene Ontology Consortium: going forward. *Nucleic Acids Res* **43(Database issue)**:D1049-1056.
502. Lee T and Pelletier J. (2016). The biology of DHX9 and its potential as a therapeutic target. *Oncotarget*.
503. Lee T, Paquet M, Larsson O and Pelletier J. (2016). Tumor cell survival dependence on the DHX9 DExH-box helicase. *Oncogene* **35(39)**:5093-5105.
504. Mills JR, Hippo Y, Robert F, Chen SM, Malina A, Lin CJ, Trojahn U, Wendel HG, Charest A, Bronson RT, Kogan SC, Nadon R, Housman DE, Lowe SW and Pelletier J. (2008). mTORC1 promotes survival through translational control of Mcl-1. *Proc Natl Acad Sci U S A* **105(31)**:10853-10858.
505. Bunz F, Dutriaux A, Lengauer C, Waldman T, Zhou S, Brown JP, Sedivy JM, Kinzler KW and Vogelstein B. (1998). Requirement for p53 and p21 to sustain G2 arrest after DNA damage. *Science* **282(5393)**:1497-1501.
506. Brady CA, Jiang D, Mello SS, Johnson TM, Jarvis LA, Kozak MM, Kenzelmann Broz D, Basak S, Park EJ, McLaughlin ME, Karnezis AN and Attardi LD. (2011). Distinct p53 transcriptional programs dictate acute DNA-damage responses and tumor suppression. *Cell* **145(4)**:571-583.
507. el-Deiry WS, Tokino T, Velculescu VE, Levy DB, Parsons R, Trent JM, Lin D, Mercer WE, Kinzler KW and Vogelstein B. (1993). WAF1, a potential mediator of p53 tumor suppression. *Cell* **75(4)**:817-825.
508. Xiong Y, Hannon GJ, Zhang H, Casso D, Kobayashi R and Beach D. (1993). p21 is a universal inhibitor of cyclin kinases. *Nature* **366(6456)**:701-704.
509. Stambolic V, MacPherson D, Sas D, Lin Y, Snow B, Jang Y, Benchimol S and Mak TW. (2001). Regulation of PTEN transcription by p53. *Mol Cell* **8(2)**:317-325.
510. Budanov AV and Karin M. (2008). p53 target genes sestrin1 and sestrin2 connect genotoxic stress and mTOR signaling. *Cell* **134(3)**:451-460.
511. Giono LE and Manfredi JJ. (2007). Mdm2 is required for inhibition of Cdk2 activity by p21, thereby contributing to p53-dependent cell cycle arrest. *Mol Cell Biol* **27(11)**:4166-4178.
512. Craxton A, Draves KE and Clark EA. (2007). Bim regulates BCR-induced entry of B cells into the cell cycle. *Eur J Immunol* **37(10)**:2715-2722.
513. Kozuma Y, Ninomiya H, Murata S, Kono T, Mukai HY and Kojima H. (2010). The pro-apoptotic BH3-only protein Bim regulates cell cycle progression of hematopoietic progenitors during megakaryopoiesis. *J Thromb Haemost* **8(5)**:1088-1097.
514. Bai YQ, Miyake S, Iwai T and Yuasa Y. (2003). CDX2, a homeobox transcription factor, upregulates transcription of the p21/WAF1/CIP1 gene. *Oncogene* **22(39)**:7942-7949.
515. Rowland BD and Peeper DS. (2006). KLF4, p21 and context-dependent opposing forces in cancer. *Nat Rev Cancer* **6(1)**:11-23.
516. Li D, Yea S, Dolios G, Martignetti JA, Narla G, Wang R, Walsh MJ and Friedman SL. (2005). Regulation of Kruppel-like factor 6 tumor suppressor activity by acetylation. *Cancer Res* **65(20)**:9216-9225.

517. Narla G, Heath KE, Reeves HL, Li D, Giono LE, Kimmelman AC, Glucksman MJ, Narla J, Eng FJ, Chan AM, Ferrari AC, Martignetti JA and Friedman SL. (2001). KLF6, a candidate tumor suppressor gene mutated in prostate cancer. *Science* **294(5551)**:2563-2566.
518. Gartel AL and Tyner AL. (1999). Transcriptional regulation of the p21((WAF1/CIP1)) gene. *Exp Cell Res* **246(2)**:280-289.
519. Lee CW and La Thangue NB. (1999). Promoter specificity and stability control of the p53-related protein p73. *Oncogene* **18(29)**:4171-4181.
520. Yang A, Kaghad M, Caput D and McKeon F. (2002). On the shoulders of giants: p63, p73 and the rise of p53. *Trends Genet* **18(2)**:90-95.
521. Kaghad M, Bonnet H, Yang A, Creancier L, Biscan JC, Valent A, Minty A, Chalon P, Lelias JM, Dumont X, Ferrara P, McKeon F and Caput D. (1997). Monoallelically expressed gene related to p53 at 1p36, a region frequently deleted in neuroblastoma and other human cancers. *Cell* **90(4)**:809-819.
522. Flores ER, Tsai KY, Crowley D, Sengupta S, Yang A, McKeon F and Jacks T. (2002). p63 and p73 are required for p53-dependent apoptosis in response to DNA damage. *Nature* **416(6880)**:560-564.
523. Fricker M, Papadia S, Hardingham GE and Tolkovsky AM. (2010). Implication of TAp73 in the p53-independent pathway of Puma induction and Puma-dependent apoptosis in primary cortical neurons. *J Neurochem* **114(3)**:772-783.
524. Vayssade M, Haddada H, Faridoni-Laurens L, Tourpin S, Valent A, Benard J and Ahomadegbe JC. (2005). P73 functionally replaces p53 in Adriamycin-treated, p53-deficient breast cancer cells. *Int J Cancer* **116(6)**:860-869.
525. Martin AG, Trama J, Crighton D, Ryan KM and Fearnhead HO. (2009). Activation of p73 and induction of Noxa by DNA damage requires NF-kappa B. *Aging (Albany NY)* **1(3)**:335-349.
526. Hiyama H, Iavarone A and Reeves SA. (1998). Regulation of the cdk inhibitor p21 gene during cell cycle progression is under the control of the transcription factor E2F. *Oncogene* **16(12)**:1513-1523.
527. Gartel AL, Goufman E, Tevosian SG, Shih H, Yee AS and Tyner AL. (1998). Activation and repression of p21(WAF1/CIP1) transcription by RB binding proteins. *Oncogene* **17(26)**:3463-3469.
528. Gartel AL, Najmabadi F, Goufman E and Tyner AL. (2000). A role for E2F1 in Ras activation of p21(WAF1/CIP1) transcription. *Oncogene* **19(7)**:961-964.
529. Hershko T and Ginsberg D. (2004). Up-regulation of Bcl-2 homology 3 (BH3)-only proteins by E2F1 mediates apoptosis. *J Biol Chem* **279(10)**:8627-8634.
530. Hauck L, Harms C, Grothe D, An J, Gertz K, Kronenberg G, Dietz R, Endres M and von Harsdorf R. (2007). Critical role for FoxO3a-dependent regulation of p21CIP1/WAF1 in response to statin signaling in cardiac myocytes. *Circ Res* **100(1)**:50-60.
531. Sunters A, Fernandez de Mattos S, Stahl M, Brosens JJ, Zoumpoulidou G, Saunders CA, Coffer PJ, Medema RH, Coombes RC and Lam EW. (2003). FoxO3a transcriptional regulation of Bim controls apoptosis in paclitaxel-treated breast cancer cell lines. *J Biol Chem* **278(50)**:49795-49805.

532. Obexer P, Geiger K, Ambros PF, Meister B and Ausserlechner MJ. (2007). FKHRL1-mediated expression of Noxa and Bim induces apoptosis via the mitochondria in neuroblastoma cells. *Cell Death Differ* **14(3)**:534-547.
533. You H and Mak TW. (2005). Crosstalk between p53 and FOXO transcription factors. *Cell Cycle* **4(1)**:37-38.
534. Liu W, Swetzig WM, Medisetty R and Das GM. (2011). Estrogen-mediated upregulation of Noxa is associated with cell cycle progression in estrogen receptor-positive breast cancer cells. *PLoS One* **6(12)**:e29466.
535. Vaziri C, Stice L and Faller DV. (1998). Butyrate-induced G1 arrest results from p21-independent disruption of retinoblastoma protein-mediated signals. *Cell Growth Differ* **9(6)**:465-474.
536. Hotchkiss RS, Tinsley KW, Hui JJ, Chang KC, Swanson PE, Drewry AM, Buchman TG and Karl IE. (2000). p53-dependent and -independent pathways of apoptotic cell death in sepsis. *J Immunol* **164(7)**:3675-3680.
537. Lanni JS, Lowe SW, Licitra EJ, Liu JO and Jacks T. (1997). p53-independent apoptosis induced by paclitaxel through an indirect mechanism. *Proc Natl Acad Sci U S A* **94(18)**:9679-9683.
538. Bell SP and Dutta A. (2002). DNA replication in eukaryotic cells. *Annu Rev Biochem* **71(1)**:333-374.
539. Masai H, Matsumoto S, You Z, Yoshizawa-Sugata N and Oda M. (2010). Eukaryotic chromosome DNA replication: where, when, and how? *Annu Rev Biochem* **79**:89-130.
540. Sclafani RA and Holzen TM. (2007). Cell cycle regulation of DNA replication. *Annu Rev Genet* **41**:237-280.
541. Bell SP and Stillman B. (1992). ATP-dependent recognition of eukaryotic origins of DNA replication by a multiprotein complex. *Nature* **357(6374)**:128-134.
542. Sibani S, Price GB and Zannis-Hadjopoulos M. (2005). Decreased origin usage and initiation of DNA replication in haploinsufficient HCT116 Ku80+/- cells. *J Cell Sci* **118(Pt 15)**:3247-3261.
543. Sibani S, Price GB and Zannis-Hadjopoulos M. (2005). Ku80 binds to human replication origins prior to the assembly of the ORC complex. *Biochemistry* **44(21)**:7885-7896.
544. Carter T, Vancurova I, Sun I, Lou W and DeLeon S. (1990). A DNA-activated protein kinase from HeLa cell nuclei. *Mol Cell Biol* **10(12)**:6460-6471.
545. Giffin W, Gong W, Schild-Poulter C and Hache RJ. (1999). Ku antigen-DNA conformation determines the activation of DNA-dependent protein kinase and DNA sequence-directed repression of mouse mammary tumor virus transcription. *Mol Cell Biol* **19(6)**:4065-4078.
546. Giffin W, Torrance H, Rodda DJ, Prefontaine GG, Pope L and Hache RJ. (1996). Sequence-specific DNA binding by Ku autoantigen and its effects on transcription. *Nature* **380(6571)**:265-268.
547. Arosio D, Cui S, Ortega C, Chovanec M, Di Marco S, Baldini G, Falaschi A and Vindigni A. (2002). Studies on the mode of Ku interaction with DNA. *J Biol Chem* **277(12)**:9741-9748.
548. Torrance H, Giffin W, Rodda DJ, Pope L and Hache RJ. (1998). Sequence-specific binding of Ku autoantigen to single-stranded DNA. *J Biol Chem* **273(33)**:20810-20819.

549. Ruiz MT, Matheos D, Price GB and Zannis-Hadjopoulos M. (1999). OBA/Ku86: DNA binding specificity and involvement in mammalian DNA replication. *Mol Biol Cell* **10(3)**:567-580.
550. Cook JG, Chasse DA and Nevins JR. (2004). The regulated association of Cdt1 with minichromosome maintenance proteins and Cdc6 in mammalian cells. *J Biol Chem* **279(10)**:9625-9633.
551. Fragkos M, Ganier O, Coulombe P and Mechali M. (2015). DNA replication origin activation in space and time. *Nat Rev Mol Cell Biol* **16(6)**:360-374.
552. Fisher PA, Wang TS and Korn D. (1979). Enzymological characterization of DNA polymerase alpha. Basic catalytic properties processivity, and gap utilization of the homogeneous enzyme from human KB cells. *J Biol Chem* **254(13)**:6128-6137.
553. Leman AR and Noguchi E. (2013). The replication fork: understanding the eukaryotic replication machinery and the challenges to genome duplication. *Genes (Basel)* **4(1)**:1-32.
554. Garg P and Burgers PMJ. (2005). DNA polymerases that propagate the eukaryotic DNA replication fork. *Critical Reviews in Biochemistry and Molecular Biology* **40(2)**:115-128.
555. Pursell ZF, Isoz I, Lundstrom EB, Johansson E and Kunkel TA. (2007). Yeast DNA polymerase epsilon participates in leading-strand DNA replication. *Science* **317(5834)**:127-130.
556. McCulloch SD and Kunkel TA. (2008). The fidelity of DNA synthesis by eukaryotic replicative and translesion synthesis polymerases. *Cell Res* **18(1)**:148-161.
557. Podust VN, Tiwari N, Stephan S and Fanning E. (1998). Replication factor C disengages from proliferating cell nuclear antigen (PCNA) upon sliding clamp formation, and PCNA itself tethers DNA polymerase delta to DNA. *Journal of Biological Chemistry* **273(48)**:31992-31999.
558. Kamath-Loeb AS, Shen JC, Schmitt MW and Loeb LA. (2012). The Werner syndrome exonuclease facilitates DNA degradation and high fidelity DNA polymerization by human DNA polymerase delta. *J Biol Chem* **287(15)**:12480-12490.
559. Kamath-Loeb AS, Loeb LA, Johansson E, Burgers PMJ and Fry M. (2001). Interactions between the Werner syndrome helicase and DNA polymerase delta specifically facilitate copying of tetraplex and hairpin structures of the d(CGG)(n) trinucleotide repeat sequence. *J Biol Chem* **276(19)**:16439-16446.
560. Sidorova JM, Kehrli K, Mao F and Monnat R, Jr. (2013). Distinct functions of human RECQ helicases WRN and BLM in replication fork recovery and progression after hydroxyurea-induced stalling. *DNA Repair (Amst)* **12(2)**:128-139.
561. Karow JK, Constantinou A, Li JL, West SC and Hickson ID. (2000). The Bloom's syndrome gene product promotes branch migration of holliday junctions. *Proc Natl Acad Sci U S A* **97(12)**:6504-6508.
562. Constantinou A, Tarsounas M, Karow JK, Brosh RM, Bohr VA, Hickson ID and West SC. (2000). Werner's syndrome protein (WRN) migrates Holliday junctions and co-localizes with RPA upon replication arrest. *EMBO Rep* **1(1)**:80-84.
563. Sidorova JM, Li NZ, Folch A and Monnat RJ. (2008). The RecQ helicase WRN is required for normal replication fork progression after DNA damage or replication fork arrest. *Cell Cycle* **7(6)**:796-807.

564. Dewar JM, Budzowska M and Walter JC. (2015). The mechanism of DNA replication termination in vertebrates. *Nature* **525(7569)**:345-350.
565. Nevis KR, Cordeiro-Stone M and Cook JG. (2009). Origin licensing and p53 status regulate Cdk2 activity during G(1). *Cell Cycle* **8(12)**:1952-1963.
566. Bartkova J, Rezaei N, Liontos M, Karakaidos P, Kletsas D, Issaeva N, Vassiliou LV, Kolettas E, Niforou K, Zoumpourlis VC, Takaoka M, Nakagawa H, Tort F, Fugger K, Johansson F, Sehested M, et al. (2006). Oncogene-induced senescence is part of the tumorigenesis barrier imposed by DNA damage checkpoints. *Nature* **444(7119)**:633-637.
567. Srinivasan SV, Dominguez-Sola D, Wang LC, Hyrien O and Gautier J. (2013). Cdc45 is a critical effector of myc-dependent DNA replication stress. *Cell Rep* **3(5)**:1629-1639.
568. Reimann M, Loddenkemper C, Rudolph C, Schildhauer I, Teichmann B, Stein H, Schlegelberger B, Dorken B and Schmitt CA. (2007). The Myc-evoked DNA damage response accounts for treatment resistance in primary lymphomas in vivo. *Blood* **110(8)**:2996-3004.
569. Neiman PE, Kimmel R, Icreverzi A, Elsaesser K, Bowers SJ, Burnside J and Delrow J. (2006). Genomic instability during Myc-induced lymphomagenesis in the bursa of Fabricius. *Oncogene* **25(47)**:6325-6335.
570. Rohban S and Campaner S. (2015). Myc induced replicative stress response: How to cope with it and exploit it. *Biochim Biophys Acta* **1849(5)**:517-524.
571. Halazonetis TD, Gorgoulis VG and Bartek J. (2008). An oncogene-induced DNA damage model for cancer development. *Science* **319(5868)**:1352-1355.
572. Halazonetis TD. (2009). An Oncogene-Induced DNA Replication Stress Model for Cancer Development. The DNA Damage Response: Implications on Cancer Formation and Treatment: Springer Science + Business Media), pp. 47-63.
573. Kumar S, Dodson GE, Trinh A, Puchalski JR and Tibbetts RS. (2005). ATR activation necessary but not sufficient for p53 induction and apoptosis in hydroxyurea-hypersensitive myeloid leukemia cells. *Cell Cycle* **4(11)**:1667-1674.
574. Iizuka M, Sarmento OF, Sekiya T, Scrable H, Allis CD and Smith MM. (2008). Hbo1 Links p53-dependent stress signaling to DNA replication licensing. *Mol Cell Biol* **28(1)**:140-153.
575. Larizza L, Roversi G and Volpi L. (2010). Rothmund-Thomson syndrome. *Orphanet J Rare Dis* **5(1)**:2.
576. Ellis NA. (1995). The Bloom's syndrome gene product is homologous to RecQ helicases. *Cell* **83**:655-666.
577. Yu CE, Oshima J, Fu YH, Wijsman EM, Hisama F, Alisch R, Matthews S, Nakura J, Miki T, Ouais S, Martin GM, Mulligan J and Schellenberg GD. (1996). Positional cloning of the Werner's syndrome gene. *Science* **272(5259)**:258-262.
578. Kitao S, Shimamoto A, Goto M, Miller RW, Smithson WA, Lindor NM and Furuichi Y. (1999). Mutations in RECQL4 cause a subset of cases of Rothmund-Thomson syndrome. *Nat Genet* **22(1)**:82-84.
579. Mohaghegh P and Hickson ID. (2001). DNA helicase deficiencies associated with cancer predisposition and premature ageing disorders. *Hum Mol Genet* **10(7)**:741-746.

580. Muftuoglu M, Oshima J, von Kobbe C, Cheng WH, Leistritz DF and Bohr VA. (2008). The clinical characteristics of Werner syndrome: molecular and biochemical diagnosis. *Hum Genet* **124(4)**:369-377.
581. Oshima J. (2000). The Werner syndrome protein: an update. *Bioessays* **22(10)**:894-901.
582. Shen JC and Loeb LA. (2000). The Werner syndrome gene: the molecular basis of RecQ helicase-deficiency diseases. *Trends Genet* **16(5)**:213-220.
583. Vennos EM and James WD. (1995). Rothmund-Thomson syndrome. *Dermatol Clin* **13(1)**:143-150.
584. Wang LL, Levy ML, Lewis RA, Chintagumpala MM, Lev D, Rogers M and Plon SE. (2001). Clinical manifestations in a cohort of 41 Rothmund-Thomson syndrome patients. *Am J Med Genet* **102(1)**:11-17.
585. Faragher RGA, Kill IR, Hunter JAA, Pope FM, Tannock C and Shall S. (1993). The Gene Responsible for Werner Syndrome May Be a Cell-Division Counting Gene. *Proc Natl Acad Sci U S A* **90(24)**:12030-12034.
586. Hagelstrom RT, Blagoev KB, Niedernhofer LJ, Goodwin EH and Bailey SM. (2010). Hyper telomere recombination accelerates replicative senescence and may promote premature aging. *Proc Natl Acad Sci U S A* **107(36)**:15768-15773.
587. Lu H, Fang EF, Sykora P, Kulikowicz T, Zhang Y, Becker KG, Croteau DL and Bohr VA. (2014). Senescence induced by RECQL4 dysfunction contributes to Rothmund-Thomson syndrome features in mice. *Cell Death Dis* **5**:e1226.
588. Rossi ML, Ghosh AK, Kulikowicz T, Croteau DL and Bohr VA. (2010). Conserved helicase domain of human RecQ4 is required for strand annealing-independent DNA unwinding. *DNA Repair (Amst)* **9(7)**:796-804.
589. Chaganti RS, Schonberg S and German J. (1974). A manyfold increase in sister chromatid exchanges in Bloom's syndrome lymphocytes. *Proc Natl Acad Sci U S A* **71(11)**:4508-4512.
590. Lonn U, Lonn S, Nylen U, Winblad G and German J. (1990). An abnormal profile of DNA replication intermediates in Bloom's syndrome. *Cancer Res* **50(11)**:3141-3145.
591. Hickson ID. (2003). RecQ helicases: caretakers of the genome. *Nat Rev Cancer* **3(3)**:169-178.
592. Im JS, Ki SH, Farina A, Jung DS, Hurwitz J and Lee JK. (2009). Assembly of the Cdc45-Mcm2-7-GINS complex in human cells requires the Ctf4/And-1, RecQL4, and Mcm10 proteins. *Proc Natl Acad Sci U S A* **106(37)**:15628-15632.
593. Singh DK, Popuri V, Kulikowicz T, Shevelev I, Ghosh AK, Ramamoorthy M, Rossi ML, Janscak P, Croteau DL and Bohr VA. (2012). The human RecQ helicases BLM and RECQL4 cooperate to preserve genome stability. *Nucleic Acids Res* **40(14)**:6632-6648.
594. McCreath KJ, Howcroft J, Campbell KH, Colman A, Schnieke AE and Kind AJ. (2000). Production of gene-targeted sheep by nuclear transfer from cultured somatic cells. *Nature* **405(6790)**:1066-1069.
595. Dickins RA, McJunkin K, Hernando E, Premsrirut PK, Krizhanovsky V, Burgess DJ, Kim SY, Cordon-Cardo C, Zender L, Hannon GJ and Lowe SW. (2007). Tissue-specific and reversible RNA interference in transgenic mice. *Nat Genet* **39(7)**:914-921.

596. Dow LE, Nasr Z, Saborowski M, Ebbesen SH, Manchado E, Tasdemir N, Lee T, Pelletier J and Lowe SW. (2014). Conditional reverse tet-transactivator mouse strains for the efficient induction of TRE-regulated transgenes in mice. *PLoS One* **9(4)**:e95236.
597. Das AT, Zhou X, Vink M, Klaver B, Verhoef K, Marzio G and Berkhout B. (2004). Viral evolution as a tool to improve the tetracycline-regulated gene expression system. *J Biol Chem* **279(18)**:18776-18782.
598. Niwa H, Yamamura K and Miyazaki J. (1991). Efficient selection for high-expression transfectants with a novel eukaryotic vector. *Gene* **108(2)**:193-199.
599. Nasr Z, Dow LE, Paquet M, Chu J, Ravindar K, Somaiah R, Deslongchamps P, Porco JA, Jr., Lowe SW and Pelletier J. (2013). Suppression of eukaryotic initiation factor 4E prevents chemotherapy-induced alopecia. *BMC Pharmacol Toxicol* **14**:58.
600. Matthew EM, Hart LS, Astrinidis A, Navaraj A, Dolloff NG, Dicker DT, Henske EP and El-Deiry WS. (2009). The p53 target Plk2 interacts with TSC proteins impacting mTOR signaling, tumor growth and chemosensitivity under hypoxic conditions. *Cell Cycle* **8(24)**:4168-4175.
601. Miyake N, Chikumi H, Takata M, Nakamoto M, Igishi T and Shimizu E. (2012). Rapamycin induces p53-independent apoptosis through the mitochondrial pathway in non-small cell lung cancer cells. *Oncol Rep* **28(3)**:848-854.
602. Hosoi H, Dilling MB, Shikata T, Liu LN, Shu L, Ashmun RA, Germain GS, Abraham RT and Houghton PJ. (1999). Rapamycin causes poorly reversible inhibition of mTOR and induces p53-independent apoptosis in human rhabdomyosarcoma cells. *Cancer Res* **59(4)**:886-894.
603. Zaika AI, Kovalev S, Marchenko ND and Moll UM. (1999). Overexpression of the wild type p73 gene in breast cancer tissues and cell lines. *Cancer Res* **59(13)**:3257-3263.
604. Dominguez G, Silva JM, Silva J, Garcia JM, Sanchez A, Navarro A, Gallego I, Provencio M, Espana P and Bonilla F. (2001). Wild type p73 overexpression and high-grade malignancy in breast cancer. *Breast Cancer Res Treat* **66(3)**:183-190.
605. Yokomizo A, Mai M, Tindall DJ, Cheng L, Bostwick DG, Naito S, Smith DI and Liu W. (1999). Overexpression of the wild type p73 gene in human bladder cancer. *Oncogene* **18(8)**:1629-1633.
606. Guan M, Peng HX, Yu B and Lu Y. (2003). p73 Overexpression and angiogenesis in human colorectal carcinoma. *Jpn J Clin Oncol* **33(5)**:215-220.
607. Sun XF. (2002). p73 overexpression is a prognostic factor in patients with colorectal adenocarcinoma. *Clin Cancer Res* **8(1)**:165-170.
608. Li C-F, Chen L-T, Lin C-Y, Huang H-Y, Hsing C-H, Huang C-T and Shiue Y-L. (2013). E2F transcription factor 1 overexpression as a poor prognostic factor in patients with nasopharyngeal carcinomas. *Biomarkers and Genomic Medicine* **5(1-2)**:23-30.
609. Lee TI and Young RA. (2013). Transcriptional regulation and its misregulation in disease. *Cell* **152(6)**:1237-1251.
610. Bywater MJ, Pearson RB, McArthur GA and Hannan RD. (2013). Dysregulation of the basal RNA polymerase transcription apparatus in cancer. *Nat Rev Cancer* **13(5)**:299-314.
611. Pabst T and Mueller BU. (2007). Transcriptional dysregulation during myeloid transformation in AML. *Oncogene* **26(47)**:6829-6837.

612. Bjornsti MA and Houghton PJ. (2004). Lost in translation: dysregulation of cap-dependent translation and cancer. *Cancer cell* **5(6)**:519-523.
613. Bhat M, Robichaud N, Hulea L, Sonenberg N, Pelletier J and Topisirovic I. (2015). Targeting the translation machinery in cancer. *Nat Rev Drug Discov* **14(4)**:261-278.
614. Suzuki M and Takahashi T. (2013). Aberrant DNA replication in cancer. *Mutat Res* **743-744**:111-117.
615. Iorio MV and Croce CM. (2012). Causes and consequences of microRNA dysregulation. *Cancer J* **18(3)**:215-222.
616. Dykxhoorn DM. (2010). MicroRNAs and metastasis: little RNAs go a long way. *Cancer Res* **70(16)**:6401-6406.
617. Tsumuraya T, Ishikawa C, Machijima Y, Nakachi S, Senba M, Tanaka J and Mori N. (2011). Effects of hippuristanol, an inhibitor of eIF4A, on adult T-cell leukemia. *Biochem Pharmacol* **81(6)**:713-722.
618. Hood KA, West LM, Northcote PT, Berridge MV and Miller JH. (2001). Induction of apoptosis by the marine sponge (Mycale) metabolites, mycalamide A and pateamine. *Apoptosis : an international journal on programmed cell death* **6(3)**:207-219.
619. Kuznetsov G, Xu Q, Rudolph-Owen L, Tendyke K, Liu J, Towle M, Zhao N, Marsh J, Agoulnik S, Twine N, Parent L, Chen Z, Shie JL, Jiang Y, Zhang H, Du H, et al. (2009). Potent in vitro and in vivo anticancer activities of des-methyl, des-amino pateamine A, a synthetic analogue of marine natural product pateamine A. *Mol Cancer Ther* **8(5)**:1250-1260.
620. Cencic R, Carrier M, Galicia-Vazquez G, Bordeleau ME, Sukarieh R, Bourdeau A, Brem B, Teodoro JG, Greger H, Tremblay ML, Porco JA, Jr. and Pelletier J. (2009). Antitumor activity and mechanism of action of the cyclopenta[b]benzofuran, silvestrol. *PLoS One* **4(4)**:e5223.
621. Lucas DM, Edwards RB, Lozanski G, West DA, Shin JD, Vargo MA, Davis ME, Rozewski DM, Johnson AJ, Su BN, Goettl VM, Heerema NA, Lin TS, Lehman A, Zhang X, Jarjoura D, et al. (2009). The novel plant-derived agent silvestrol has B-cell selective activity in chronic lymphocytic leukemia and acute lymphoblastic leukemia in vitro and in vivo. *Blood* **113(19)**:4656-4666.
622. Cencic R, Robert F, Galicia-Vazquez G, Malina A, Ravindar K, Somaiah R, Pierre P, Tanaka J, Deslongchamps P and Pelletier J. (2013). Modifying chemotherapy response by targeted inhibition of eukaryotic initiation factor 4A. *Blood Cancer J* **3**:e128.
623. Aggarwal M, Sommers JA, Shoemaker RH and Brosh RM, Jr. (2011). Inhibition of helicase activity by a small molecule impairs Werner syndrome helicase (WRN) function in the cellular response to DNA damage or replication stress. *Proc Natl Acad Sci U S A* **108(4)**:1525-1530.
624. Liu W, Zhou M, Li Z, Li H, Polaczek P, Dai H, Wu Q, Liu C, Karanja KK, Popuri V, Shan SO, Schlacher K, Zheng L, Campbell JL and Shen B. (2016). A Selective Small Molecule DNA2 Inhibitor for Sensitization of Human Cancer Cells to Chemotherapy. *EBioMedicine* **6**:73-86.

THE APPENDICES

A.1 Supplementary figures and tables

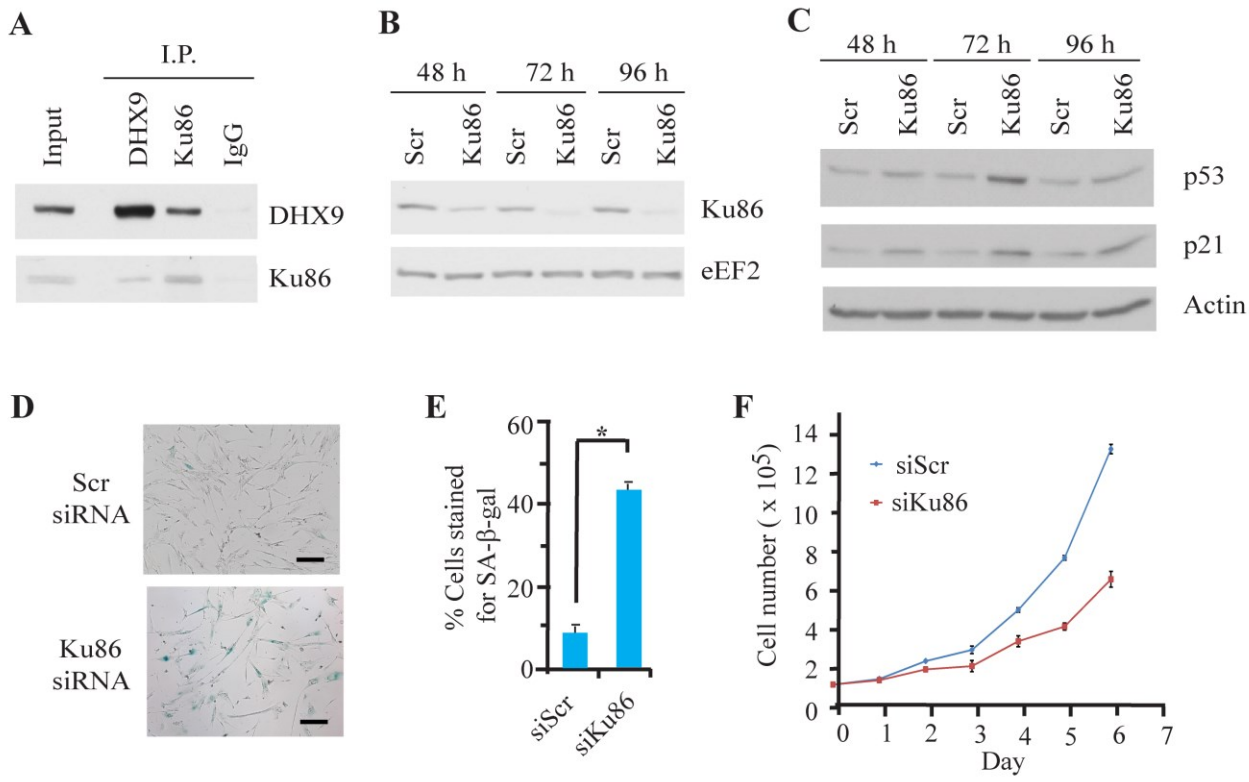

Figure A.1 Loss of Ku86 phenocopies the senescent phenotype observed upon DHX9 suppression.

(A) Western blot analysis of Ku86 following immunoprecipitation with the indicated antibodies from MRC-5 cells. Antibodies used in immunoprecipitations are indicated above the panel, IgG; rabbit immunoglobulin. **(B)** Western blot documenting knockdown of Ku86 using siRNAs and harvested at 48, 72 and 96 hours post-transfection. A scrambled (Scr) siRNA is used as a negative control. **(C)** Western blot showing the levels of p53 and p21 upon knockdown of Ku86 using siRNAs. Cells were harvested at 48, 72 and 96 hours post-transfection. A scrambled (Scr) siRNA is used as a negative control. **(D)** β-galactosidase staining of MRC-5 cells transfected with Scr or Ku86 siRNA. Staining was performed 8 days following transfection of siRNA. Bars represent 200 μm. **(E)** Quantitation of β-galactosidase staining from (D). Cells from at least 5 independent fields were quantitated. Error bars represent SEM, N=3. *$p<0.01$. **(F)** Growth curves for cells transduced with Scr or Ku86 siRNAs. Error bars represent SEM, N=3.

Table A.1 List of genes with at least 1.5 fold change in expression level upon DHX9 knockdown in MRC-5 cells

This table is too large to fit on a standard page. It is available at:
http://www.jbc.org/content/suppl/2014/07/02/M114.568535.DC1/jbc.M114.568535-1.xlsx

Table A.2 List of genes with at least 1.5 fold change in expression level upon DHX9 knockdown in mouse large intestine

Available at: http://www.nature.com/onc/journal/v35/n39/extref/onc201652x16.xls

Table A.3 GAGE analysis of biological processes upregulated in *DHX9.837/rtTA* (+DOX) vs *Fluc.1309/rtTA* (+DOX) mice

Available at: http://www.nature.com/onc/journal/v35/n39/extref/onc201652x17.xls

Table A.4 GAGE analysis of biological processes upregulated in *DHX9.1271/rtTA* (+DOX) vs *Fluc.1309/rtTA* (+DOX) mice

Available at: http://www.nature.com/onc/journal/v35/n39/extref/onc201652x18.xls